The Role of Complement and Monocytes in Antineutrophil Cytoplasmic Antibody Associated Vasculitis

Popat, Reena

Awarding institution:
King's College London

The Role of Complement and Monocytes in Antineutrophil Cytoplasmic Antibody Associated Vasculitis

Reena Popat

A dissertation submitted to the University of London in candidature of Doctor of Philosophy

MRC Centre for Transplantation

Division of Transplantation, Immunology and Mucosal Biology

King's College London, School of Medicine at Guy's, King's and St. Thomas' Hospitals

ERRATA CORRIGE

Page	Line	Note	ERRATA	CORRIGE
76	2		*Escherichia Coli* 0111 B4 from Enzo Life sciences, UK.	*Escherichia Coli R515* from Enzo Life sciences, UK – catalogue number. ALX-581-007-L002.
81	21		0.25 eU/250µg IgG	0.05 eU/250µg IgG
86	9		The text on the right should be inserted at the end of the text for 2.5.4 to clarify the cell numbers at the start and end of the experiment in the indicated data.	Initial culture volumes were 500µl at 1×10^6 cells/ml. Cells were counted after detaching with 5mM EDTA in PBS, washing and resuspending in a defined volume of PBS. Reported cell concentrations are from these raw counts in a final volume of 300 µl (Figure 4.16, 4.20) or 200 µl (Figure 4.21C, 4.22) of PBS respectively.

12/2/22 Date Signed by Reena Popat

Abstract

Antineutrophil cytoplasmic antibody (ANCA) associated vasculitis (AAV) is a multi-systemic disease with autoantibody generation to myeloperoxidase (MPO) and proteinase 3 (PR3), components of neutrophils and monocytes. It is widely believed that ANCA are pathogenic. The most convincing evidence for this comes from the ability to induce crescentic glomerulonephritis in mice with passive transfer of MPO-ANCA. Studies have also shown with limited numbers of ANCA, the autoantibodies can activate neutrophils *in vitro*. The role of monocytes in pathogenesis though is scarcely explored. The alternative pathway of complement has also been implicated as vital to the pathogenesis of AAV, but the activating factors of complement are unknown.

Contrary to previous studies we failed to consistently activate neutrophils with a large panel of randomly selected ANCA. We investigated the effect of these ANCA on peripheral blood monocytes. Interestingly, we found that MPO-ANCA derived from AAV patients cause a reduction in IL6 and IL10 production from lipopolysaccharide treated monocytes, which is Fc dependent and MPO enzyme dependent. Using gene expression microarrays we show that MPO-ANCA cause a widespread reduction in toll-like receptor (TLR) 4 signalling. We show using mass spectrometry analysis that MPO-ANCA leads to the production of a subset of oxidised phospholipids that can inhibit TLR4. We also demonstrate that MPO-ANCA lead to an increase in survival of macrophages differentiated *in vitro* from monocytes, which is dependent on colony stimulating factor-1. The differentiated macrophages have an M2-like phenotype that induce IL10 and TGFβ production from CD4 T cells, which would have a potential role in fibrosis.

Secondly, we address potential triggers for complement activation during disease and show that there is a redundancy between the classical and alternative pathway. C3 deficient mice are protected from disease, but factor B deficient and C4 deficient mice are not. We also demonstrate cross talk between the coagulation and complement cascade. Using bone marrow chimeras, we demonstrate a role for circulating and not bone marrow-derived C5 in disease pathogenesis, which may help refine complement-targeted therapy.

Acknowledgements

Firstly, I would like to express my sincere gratitude to my PhD supervisors Dr Michael Robson and Professor Claudia Kemper for providing me with the opportunity to work in their laboratories, their constant support as well as their continuing enthusiasm and encouragement especially when I had drifted into the abyss of negative results.

I would also like to thank Dr Simon Freeley and Dr Gaëlle Le Friec for their unwavering friendship, insightful discussions and support. I am grateful to Dr Simon Freeley for his incredible patience and teachings with regards to the *in vivo* work and Dr Gaëlle Le Friec for her breadth of knowledge and her ability to selflessly help with various *in vitro* techniques. I would like to thank Dr Ben Afzali, Dr Paul Lavender, Dr Kiran Parmar, Agnieszka Kuffel, Professor Beverley Hunt, Mr Alpesh Thakker and Dr Corinne Spickett for their collaborations.

Finally, I would like to thank the control subjects as well as patients and colleagues at Kent and Canterbury, Royal Sussex County, King's College, St Helier and Guy's and St Thomas' hospitals for help in obtaining samples.

The PhD was funded by the Medical Research Council and Kidney Research UK. The research was also supported by the Medical Research Council Centre for Transplantation, King's College London and the National Institute for Health Research Biomedical Research Centre based at Guy's and St Thomas' NHS Foundation Trust and King's College London.

Publications

Freeley SJ, Coughlan AM, **Popat RJ**, Dunn-Walters DK, Robson MG. Granulocyte colony stimulating factor exacerbates antineutrophil cytoplasmic antibody vasculitis. *Annals of the Rheumatic Diseases* (2013) 72: 1053-1058.

Freeley SJ, Giorgini A, **Popat RJ**, Horsfield C, Robson MG. Toll-like receptor 2 or Toll-like receptor 4 deficiency does not modify Lupus in MRLIpr mice. *PLoS One* (2013) 8: e74112.

Popat RJ, Robson MG. Review: Complement and glomerular diseases. *Nephron Clinical Practice* (2015) 128(3-4): 238-242.

Freeley SJ*, **Popat RJ*,** Parmar K, Hunt BJ, Stover CM, Schwaeble W, Kemper C, Robson MG. Experimentally induced anti-myeloperoxidase vasculitis does not require properdin, MASP2 or bone marrow derived C5. Journal of Pathology (2016) doi: 10.1002/path.4754 (* joint first authors).

Popat RJ, Thakker A, Spickett CM, Watson J, Afzali B, Lavender P, Kemper C, Robson MG. Anti-myeloperoxidase antibodies attenuate the monocyte response to LPS and shape macrophage development. Under review.

ERRATA CORRIGE

Page	Line	Note	ERRATA	CORRIGE
76	2		*Escherichia Coli* 0111 B4 from Enzo Life sciences, UK.	*Escherichia Coli R515* from Enzo Life sciences, UK – catalogue number. ALX-581-007-L002.
86	9		The text on the right should be inserted at the end of the text for 2.5.4 to clarify the cell numbers at the start and end of the experiment in the indicated data.	Initial culture volumes were 500ul at 1×10^6 cells/ml. Cells were counted after detaching with 5mM EDTA in PBS, washing and resuspending in a defined volume of PBS. Reported cell concentrations are from these raw counts in a final volume of 300 ul (Figure 4.16, 4.20) or 200 ul (Figure 4.21C, 4.22) of PBS respectively.

13 June 2021

Date Signed by

Contents

Index of figures and tables

Abbreviations

AAV	ANCA associated vasculitis
ANCA	Antineutrophil cytoplasmic antibody
ANOVA	Analysis of variance
APC	Antigen presenting cells
BSA	Bovine serum albumin
BVAS	Birmingham vasculitis activity score
CFA	Complete freund's adjuvant
cPR3	Complementary PR3
CR	Complement receptor
CSF1	Colony stimulating factor 1
CSF1R	CSF1 receptor
CTLA4	Cytotoxic T lymphocyte antigen 4
CXCL	Chemokine CXC motif ligand
DAF	Decay-accelerating factor
DAG	Diacylglycerol
DHR 123	Dihydrorhodamine 123
DPPI	Dipeptidyl peptidase I
EDTA	Ethylenediaminetetraacetic acid
EGPA	Eosinophilic granulomatosis with polyangiitis
ELISA	Enzyme linked immunosorbant assay
EMT	Epithelial to mesenchymal transition
ETP	Endogenous thrombin potential
$F(ab)_2$	Fragment antigen binding
FBS	Fetal bovine serum
Fc	Fragment crystallisable region
FcR	Fc receptor
fMLP	Formyl-methionyl-leucyl-phenylalanine
FoxP3	Forkhead winged helix transcription factor
GBM	Glomerular basement membrane
GCSF	Granulocyte colony stimulating factor
GMCSF	Granulocyte macrophage colony stimulating factor

GPA	Granulomatosis with polyangiitis
GPI	Glycosylphosphatidylinositol
GWAS	Genomewide association study
HBSS	Hanks balanced salt solution
HEPES	4-(2-hydroxyethyl)-1-piperazineethanesulfonic acid
HLA	Human leucocyte antigen
HOCl	Hypochlorous acid
HRP	Horseradish peroxidase
HUVEC	Human umbilical vein endothelial cells
iCFA	Incomplete freund’s adjuvant
ICAM	Intercellular adhesion molecule
IFN	Interferon
IL	Interleukin
IMDM	Iscove's modified dulbecco's media
iNOS	Inducible nitric oxide synthase
IP	Intraperitoneal
IP3	Inositol triphosphate
ITAM	Immunoreceptor tyrosine activation motif
IV	Intravenous
LAMP2	Lysosomal associated membrane protein 2
LFA	Lymphocyte function-associated antigen
LPS	Lipopolysaccharide
MAC	Membrane attack complex
MAPK	Mitogen activated protein kinase
MASP	MBL-associated serine protease
MBL	Mannose-binding lectin
MCP-1	Monocyte chemoattractant protein-1
MFI	Median fluorescence intensity
MHC	Major histocompatibility complex
MPA	Microscopic polyangiitis
MPO	Myeloperoxidase
MPRO	Mouse promyelocytic

NADPH	Nicotinomide adenine dinucleotide phosphate
NB1	Human neutrophil antigen B1
NET	Neutrophil extracellular trap
NOD	Non-obese diabetic
NOD-SCID	Non-obese diabetic severe combined immunodeficiency
NTN	Nephrotoxic serum nephritis
NZB/W	New Zealand Black / White
OCT	Optimal cutting temperature
OPD	O-Phenylenediamine dihydrochloride
PBMC	Peripheral blood mononuclear cells
PBS	Phosphate buffered saline
PC	Phosphatidylcholines
PCR	Polymerase chain reaction
PI3-K	Phosphoinositol 3-kinase
PIP2	Phosphatidylinositol (4,5) – bisphosphate
PIP3	Phosphatidylinositol (3,4,5) – triphosphate
PKC	Protein kinase C
PLCγ	Phospholipase Cγ
PLP	Phosphate-lysine-periodate
PMA	Phorbol myristate acetate
PMSF	Phenylmethanesulfonyl fluoride
PNPP	p-Nitrophenyl-phosphate
PR3	Proteinase 3
PRM	Pattern recognition molecule
RLU	Relative light units
ROS	Reactive oxygen species
RPMI	Roswell Park Memorial Institute
RT-qPCR	Reverse Transcription Quantitative PCR
RZ	Reinheit Zahl
SC	Subcutaneous
SNP	Single nucleotide polymorphism
TBS Tween	Tris-buffered saline – tween

TGFβ	Transforming growth factor β
TLR	Toll-like receptor
TNFα	Tumour necrosis factor α
UNG	Uracil-DNA glycosylase
VDI	Vasculitis damage index
WKY	Wistar Kyoto

Chapter 1 - Introduction

1.1 ANCA-Associated Vasculitis

Vasculitis is an inflammatory process of the blood vessels, which is histopathologically characterised by inflammation and fibrinoid necrosis of the vessel wall resulting in end organ injury. The pathogenesis of most cases of vasculitis is believed to be largely autoimmune, although infection, drugs, malignancy and other diseases can manifest as vasculitis. The clinical phenotype is heterogeneous and reflects the pattern of vessels affected. It often has cutaneous and systemic features.

The International Chapel Hill Consensus Conference 2012 revised the nomenclature and classification of vasculitides. Figure 1.1 below depicts the major categories of vasculitis in relation to vessel size and in particular highlights the broader spectrum of vessels affected in antineutrophil cytoplasmic antibody (ANCA) - associated vasculitis (AAV).

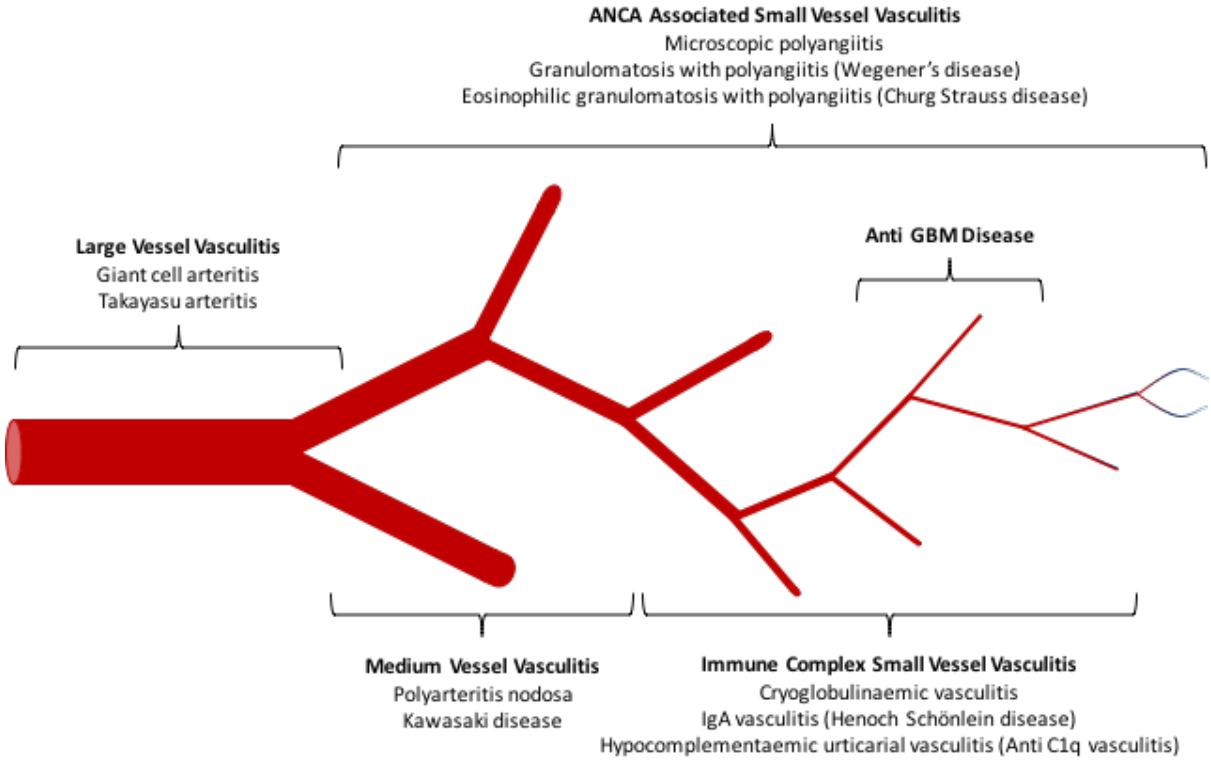

Figure 1.1 – Overview of the International Chapel Hill Consensus Conference 2012 nomenclature revision of vasculitides [1].

AAV is a life threatening vasculitis characterised by the presence of circulating autoantibodies (ANCA) targeted against antigens in the cytoplasm of neutrophils and monocytes, namely proteinase 3 (PR3) and myeloperoxidase (MPO). A small subgroup of patients are ANCA negative (discussed later). Figure 1.1 depicts the current sub-classification of ANCA vasculitides, however, there are proposals to categorise AAV based on autoantibody specificity rather than disease phenotype. This is due to fundamental differences between patients with MPO-ANCA and PR3-ANCA including distinct genetic associations, clinical as well as histopathological differences.

There is historically a lack of immune complex deposition, hence the associated name of pauci-immune vasculitis. However, a study by Haas *et al* examined renal sections of 126 cases of AAV and found that 54% of the biopsies showed evidence of immune complex deposits on electron microscopy [2]. The initial inflammatory lesion is characterised by segmental lytic necrosis, and neutrophil infiltration undergoing leucocytoclastic changes. Monocytes and macrophages become the predominant leucocytes within days, with macrophages persisting in vessels [3]. Fibrinoid necrosis is often noted, a consequence of activated coagulation factor spill over from necrotic vessels, with macrophages as the predominant cell type and T cells. With chronicity, the fibrinoid necrosis is replaced by collagenous material.

The first documented evidence of clinical disease in keeping with AAV was a description by Peter McBride in 1897 of necrotising vasculitis, respiratory tract granulomatous lesions and glomerulonephritis. Clinical manifestations of AAV are variable from organ-limited disease, for example renal limited vasculitis, to a multi-systemic disease affecting critical organs such as the skin, joints, lungs, kidneys and gastrointestinal system. The clinical features as alluded to above are dependent on organ involvement, disease stage, disease activity as well as the chronicity or extent of damage involved. Prodromal symptoms are often present which are non-specific and constitutional, common to the three types of AAV. Renal involvement, which is most commonly associated with microscopic polyangiitis (MPA) and granulomatosis with polyangiitis (GPA), is one of the most significant and often the most severe manifestation. It is associated with a worse outcome (see table 1.1). MPA and GPA possess similar clinical manifestations however MPA lacks the necrotising

granulomatous inflammation associated with GPA. Eosinophilic granulomatosis with polyangiitis (EGPA) is characterised by granulomatous eosinophil rich inflammation associated with asthma and eosinophilia. Classically GPA is associated with PR3 ANCA, whilst MPA and EGPA are associated with MPO ANCA.

It is difficult to evaluate the heterogeneous nature of AAV. The Birmingham vasculitis activity score (BVAS), now in its third version, can be used to assess disease activity. The BVAS is a checklist of 56 pertinent symptoms, signs and features of active vasculitis used to guide clinical activity and is applied as a research tool [4]. The vasculitis damage index (VDI) quantifies damage associated with vasculitis and is also a useful prognostic tool [5]. However, as the VDI does not indicate the full extent of damage in small and medium sized vasculitis, a revised combined damage assessment index is being developed.

The vasculitides are rare, AAV being the most common vasculitis in adults. A study looking at the Norfolk UK registry between 1998 and 2010 revealed an annual incidence of 11.3 per million for GPA and 5.9 per million for MPA cases, estimating the prevalence of AAV at 255 per million [6]. The peak age at diagnosis was 65 to 74 years with a male preponderance. There are geographical variations in disease incidence and presentation as shown by Fujimoto *et al*. The annual incidence of AAV between 2005 and 2009 was 21.8 per million in the UK with an average age of 60.5 years at presentation compared to 22.6 per million in Japan with a mean age of presentation at 69.7 years [7]. Furthermore, MPA was the predominant AAV subtype in Japan compared to GPA in the UK. A multi-centre European study revealed that 10-20% of patients diagnosed with MPA, GPA, EGPA or idiopathic rapidly progressive glomerulonephritis were ANCA negative [8].

The natural history of untreated AAV is a rapidly progressive fatal disease. If left untreated mortality approximates 80%, with a median survival of five months in multi-systemic disease [9]. The use of cyclophosphamide (introduces alkyl radicals into DNA strands which interferes with DNA replication) with steroids in the 1970s dramatically improved prognosis, with remission achieved in 79-93% of patients [10]. Modifications of the original management plan with the use of azathioprine (imidazolyl derivative of mercaptopurine whose metabolites are incorporated into replicating DNA inhibiting

replication and purine synthesis) and the introduction of rituximab (monoclonal antibody directed against the CD20 antigen on B lymphocytes) has improved outcomes, however, remission does not result in cure. Treatment limitations including limited efficacy, cumulative toxicity and infection risk persist. Table 1.1 below summarises the outcome of disease from selected prospective and retrospective studies.

Study	Disease (n)	Mortality risk factors	Survival	Cause of death
Sriskandarajah *et al* [11]	MPA GPA (455)	Age >60 years eGFR <15 Male Serum albumin <30g/L	82% at 1 year 85% at 1 year	Infection Cardiovascular Active disease
Lai *et al* [12]	MPA GPA Renal limited vasculitis (398)	Older age Pulmonary involvement Worse initial renal function	77.4% at 1 year 61.9% at 5 years	Infection Cardiovascular Active disease
Lee *et al* [13]	MPA GPA (155)	Older age No treatment response at 4 months	83% at 1 year 72% at 5 years	Cardiovascular Active disease Infection
De Joode *et al* [14]	MPA GPA Renal limited vasculitis (273)	Need for renal replacement therapy MPO-ANCA	83% at 5 years	Not declared
Flossmann *et al* [15]	MPA GPA (535)	Younger age eGFR <15 Higher BVAS MPO-ANCA Lower haemoglobin Higher white cell count	78% at 5 years	Infection Cardiovascular Active disease
Hilhorst *et al* [16]	MPO or PR3 positive (181)	Older age Worse initial serum creatinine Earlier year of diagnosis	77.2% at 1 year 65.8% at 5 years	Infection Cardiovascular Active disease and malignancy

Table 1.1 – Summary of select retrospective and prospective studies of AAV. Studies published between 2011 and 2015 were selected from Pubmed (http://www.ncbi.nlm.nih.gov/pubmed) searching for AAV associated mortality and prognosis.

A review of European trials data showed that 59% of deaths within the first year of diagnosis was associated with therapy compared to 14% due to active disease [17]. These studies highlight that although prognosis in AAV has improved, patients remain at risk of premature death, organ failure, a chronic relapsing disease and other adverse outcomes.

1.2 Pathogenesis

The precise aetiology of AAV remains elusive. However, several environmental and genetic factors are considered important.

1.2.1 Environmental factors

Case reports have shown that those with professional exposure to silica have a significantly higher risk of being ANCA positive and have a diagnosis of GPA [18, 19]. This may be due to the accelerated apoptosis of neutrophils and macrophages seen with silica exposure as demonstrated in an animal model of intratracheal instillation of silica [20]. Furthermore, several drugs including propylthiouracil, hydralazine and minocycline have been implicated in causing AAV [21-23]. There is also a link between AAV and ingestion of levamisole-contaminated cocaine [24].

There is a strong association between bacterial infections and the presentation or relapse of AAV. An infectious trigger may precipitate an autoimmune reaction by the formation of an inflammatory environment facilitating the exposure of auto-antigens or the generation of cross-reacting auto-antibodies. In comparison to healthy controls, GPA patients have a higher incidence of *Staphylococcus aureus* nasal carriage and colonised patients are more prone to relapses than non-colonised patients [25, 26]. Furthermore, treatment with co-trimoxazole has been shown to reduce relapses in GPA patients [27].

An interesting observation by Pendergraft *et al* revealed that GPA patients with PR3-ANCA also had antibodies targeting complementary PR3 (cPR3), the antisense peptide. In a mouse model the authors were able to induce antibodies to both sense PR3 and cPR3 following immunisation with cPR3. It is suggested that the PR3-ANCA are generated by an immune response against the anti-cPR3 antibody, an anti-idiotypic response. The cPR3 protein, in contrast to PR3, exhibits homology to a variety of microbial components, including *Staphylococcus aureus* and *Entamoeba histolytica*, supporting the role of infection in pathogenesis [28]. However, rodents immunized with *Staphylococcus aureus* do not develop vasculitis nor is there evidence that the anti-cPR3 antibodies cross-react with *Staphylococcus aureus*. Furthermore, a subsequent study found no difference in anti-cPR3 reactivity in PR3-AAV patients compared to healthy controls, challenging the theory of autoantigen complementarity in AAV [29].

AAV patients are often also positive for autoantibodies to lysosomal associated membrane protein 2 (LAMP2), a protein involved in cell adhesion, intracellular antigen presentation and maintenance of microbicidal activity of phagosomes [30]. LAMP2 is involved in regulating microbial clearance. Interestingly the LAMP2 epitope P41–49 is homologous to bacterial FimH present in various gram-negative bacteria species such as *Escherichia coli, Klebsiella pneumoniae* and *Proteus mirabilis*. Patients' autoantibodies cross-react with FimH and WKY rats immunised with FimH developed autoantibodies to LAMP2 and pauci-immune glomerulonephritis [31]. This suggests that FimH can induce disease by acting as a molecular mimic for LAMP2, implicating bacterial infection in pathogenesis.

Furthermore, lipopolysaccharide (LPS), a major component of the outer membrane of gram-negative bacteria, has been shown to exacerbate disease in a MPO-ANCA model of disease in mice (discussed later) [32]. LPS leads to increased circulating tumour necrosis factor α (TNFα) levels, which has been shown to prime neutrophils. Anti-TNFα antibody attenuated disease in the murine model. LPS promotes MPO-ANCA induced lymphocyte function-associated antigen (LFA) dependent glomerular leucocyte adhesion and increases endothelial toll-like receptor (TLR) 4, chemokine CXC motif

ligand (CXCL) 1 and 2 expression, which in turn increase neutrophil recruitment to the glomeruli [33, 34].

This suggests that infection has a role in MPO and PR3 expression, neutrophil recruitment and neutrophil adhesion in the glomeruli.

1.2.2 Genetic factors

Although familial cases of AAV have been described, evidence for familial clustering is poor. A study evaluating the Swedish register showed that GPA was present in 2 of 6,670 first degree relatives of patients compared to 13 of 68,994 first degree relatives of controls, with a relative risk of 1.56 (95% confidence interval of 0.35 to 6.9) [35], suggesting genetic risk factors for GPA.

A number of studies prior to the genomewide association study (GWAS) identified key genetic associations. Several small studies have suggested associations between major histocompatibility complex (MHC) loci including human leucocyte antigen (HLA) - DPB1*0401 as well as HLA-DR4 and risk of AAV [36, 37].

PRTN3, which encodes PR3, a target antigen in AAV, has also been implicated. The neutrophil membrane expression pattern of PR3 is bimodal in individuals, which remains constant over time. The pattern of expression correlates more closely in monozygotic twins rather than dizygotic twins suggesting that the neutrophil membrane expression pattern of PR3 is genetically predetermined [38]. In AAV patients there is a high membrane PR3 expression phenotype compared to healthy controls and elevated membrane bound PR3 expression is associated with an increased rate of relapse in GPA patients [38, 39]. Several single nucleotide polymorphisms (SNP) have been identified in the *PRTN3* sequence.

α1-antitrypsin, a serine protease (including PR3) inhibitor is encoded by *SERPINA1* gene, which is highly polymorphic. Both the Z and S alleles of the *SERPINA1* gene reduce the function of the protein and display associations with a higher risk of developing GPA than the general population [40]. The decreased activity of α1-antitrypsin may result in persistent PR3 presence in tissue leading to direct damage as well as resulting in the generation of ANCA.

Cytotoxic T lymphocyte antigen 4 (CTLA4) expressed by CD4 T cells, on binding to its ligands CD80 or CD86 on antigen presenting cells (APC) act as an immune off switch. CTLA4 has a role in the regulation of autoreactive T cells, hence CTLA4 polymorphisms have a role in autoimmunity. Zhou *et al* demonstrated that patients with GPA had significantly lower homozygosity frequency for the shortest allele 86 of CTLA4 microsatellite polymorphism (AT)n in the 3' region [41].

In 2012, the first GWAS of GPA and MPA performed in UK and Northern Europe cohorts was published. The combined data of AAV found associations of significance with the MHC (strongest in HLA-DPB1) and a SNP in the SERPINA1 locus. When sub-analysis was carried out differentiating between GPA and MPA or PR3-ANCA and MPO-ANCA, the HLA and SERPINA1 SNP differed significantly between the groups, with association related mainly to GPA and PR3-ANCA. The strongest association of the genetic polymorphisms was related to ANCA specificity rather than clinical groups [42].

1.3 ANCA and the Antigens

In 1982 Davies *et al* identified antibodies in the serum of 8 patients with segmental necrotising glomerulonephritis that stained the cytoplasm of neutrophils by indirect immunofluorescence [43]. This was confirmed by another group in 1984 in 4 patients with small vessel vasculitis [44]. Subsequently Van der Woude *et al* suggested that ANCA may well be pathogenic and that the detection of ANCA was an important diagnostic as well as prognostic marker in GPA [45]. Indirect immunofluorescence analyses of ethanol fixed neutrophils reveal a cytoplasmic staining pattern (c-ANCA) later shown to be associated with PR3-ANCA, while MPO-ANCA cause a perinuclear fluorescence pattern (p-ANCA) [46-48].

1.3.1 MPO

MPO, previously termed verdoperoxidase because of its intense green colour, was identified by Agner from purulent fluid of patients with tuberculous empyema [49]. MPO is a heme containing lysosomal enzyme present in the azurophilic granules of neutrophils and cells of monocyte lineage. It is a product of a single 11 kb gene located on chromosome 17 [50]. Its initial translated product is an 80 kDa protein which

undergoes proteolytic cleavage of a 41 amino acid peptide and N-linked glycosylation to generate an enzymatically inactive 90 kDa apoproMPO protein [51]. In the endoplasmic reticulum the apoproMPO product interacts with chaperones calreticulin and calnexin, with incorporation of the heme group by three covalent bonds on the backbone to generate the enzymatically active proMPO protein [52, 53].

The active proMPO undergoes several proteolytic events and is cleaved into a 75 kDa product with an approximately 57.5 kDa heavy (α) subunit and 14 kDa light (β) subunit by glucosidases. Two $\alpha\beta$ promoter units are linked by a disulfide bond between the heavy subunits to produce mature MPO of approximately 150 kDa [54, 55].

MPO oxidises chloride and other halides such as bromide and thiocyanate to generate hypohalous acids. The reactions involve two electron oxidation of the respective halide such as chloride by compound I with a net reaction of:

$$H_2O_2 + Cl^- \longrightarrow HOCl + OH^-$$

Hydrogen peroxide (H_2O_2) is formed during respiratory burst. Generation of H_2O_2 is NADPH oxidase dependent, which transfers electrons into phagosomes generating superoxide anion and H_2O_2 from molecular oxygen. HOCl itself has strong microbicidal effects [56].

MPO mediated damage is not limited to intraphagosomal microbes, the hypohalous acids and their derivatives can halogenate other cell constituents causing damage to surrounding tissue by modifying target molecules such as DNA, lipids and (lipo)proteins. HOCl reacts with pyrimidine derivatives leading to altered nucleotides. Cysteine and methionine residues are readily oxidised too. The derivatives are also capable of causing further damage by other mechanisms including free radical formation [57-59].

The oxidised and chlorinated lipids derived under inflammatory conditions have been implicated in specific disease pathogenesis including atherosclerosis, diabetes mellitus and multiple sclerosis. They are thought to mediate both pro- and anti- inflammatory roles through various mechanisms that will be discussed further in chapter 4.

MPO has also been shown to have non-enzymatic functions and has been implicated in neutrophil recruitment through electrostatic interactions *in vitro*. The same study showed that MPO knockout mice had less neutrophil recruitment to areas of inflammation in a hepatic ischaemia reperfusion model. Furthermore, injection of catalytically inactive MPO resulted in significant neutrophil recruitment in otherwise non-inflamed vessels [60].

MPO is usually not expressed on the surface of resting neutrophils. However, activation of neutrophils with TNFα results in increased membrane MPO expression, which is mitogen activated protein kinase (MAPK) dependent [61, 62]. This may well contribute to the pathogenesis of AAV by increasing exposure of the offending antigens to ANCA. Circulating MPO levels are higher in patients with MPO-ANCA vasculitis compared to healthy controls and soluble MPO released by activated neutrophils can make unprimed neutrophils reactive to MPO-ANCA [63, 64].

MPO is not a transmembrane protein, rather it is suggested that the cationic MPO is anchored to the negatively charged cell surface through electrostatic interactions. However, it has also been shown that MPO interacts with the CD11b/CD18 integrin complex (Mac-1 / CR3) leading to the activation of intracellular signalling, which may be a plausible method of specific antigen presentation on the cell surface and downstream signalling [65]. It is also possible that ANCA are internalised by neutrophils and monocytes and interact with their respective antigens intracellularly.

1.3.2 PR3

PR3 is a chymotrypsin-like serine protease found in the azurophilic and secretory granules of neutrophils as well as monocyte lysosomes. PR3 and other neutrophil proteases are multifunctional. They are directly involved in intracellular and extracellular pathogen destruction and also have a role in inflammatory process regulation [66].

The PR3 gene, *PRTN3* is located on chromosome 19 [67]. There are four post translational steps involved in the formation of the mature enzyme (29-32 kDa). Initially the signal peptide is cleaved, followed by glycosylation of the peptide. The N-

terminal dipeptide is cleaved by dipeptidyl peptidase I (DPPI) and subsequently the C-terminal propeptide cleavage occurs [68].

PR3 is directly involved in the killing of bacteria within phagolysosomes and neutrophil extracellular traps (NETs). In addition PR3 cleaves cathelicidin hCAP-18, an antibacterial protein, to its active form LL-37 upon exocytosis [69].

PR3 is also capable of modulating the immune response in other ways such as cleaving pro-form cytokines TNFα and interleukin (IL)-1β to their active forms, as well as the chemokine IL8, further perpetuating the immune response [70, 71]. PR3 has also been shown to increase expression of protease-activated receptor 2 (PAR2), a G protein coupled receptor that couples to $G_{\alpha q/11}$ and appears to have a role in inflammation as well as pain [72]. Furthermore, PR3 has been shown to induce human endothelial cell apoptosis. Human umbilical vein endothelial cells (HUVEC) internalise both MPO and PR3. PR3 cleaves p21 the major cell cycle inhibitor and induces apoptosis [73, 74].

Once secreted into the extracellular environment, a proportion of PR3 bind the cell membrane. As discussed earlier, PR3 is expressed in a bimodal fashion on neutrophils. Those with a higher expression of membrane PR3 on their neutrophils are at a higher risk of GPA and rheumatoid arthritis [75]. PR3 is present on the surface of resting monocytes and neutrophils, and is upregulated following neutrophil stimulation with formyl-methionyl-leucyl-phenylalanine (fMLP) and cytokines such as TNFα [76].

PR3 may be presented on the cell surface via direct insertion into the plasma membrane through basic and hydrophobic amino acids or presentation by a glycosylphosphatidylinositol (GPI) linked receptor, CD177 or human neutrophil antigen B1 (NB1) [77, 78]. However, NB1 does not possess an intracellular signalling domain, and therefore cannot propagate a signal by itself. Jerke *et al* have shown that NB1 interacts with the CD11b/CD18 complex and may induce intracellular signalling in this manner. They showed that neutrophils that co-express NB1 and PR3 have a higher level of membrane PR3 expression and undergo more robust degranulation as well as extracellular superoxide production upon PR3-ANCA induced activation compared to the NB1 negative neutrophils. Furthermore, CD11b blockade inhibited PR3-ANCA induced neutrophil activation [79].

Primed neutrophils and monocytes release serine proteases including PR3, elastase and cathepsin G. These other serine proteases, like PR3, are inactive proenzymes that are cleaved by DPPI. DPPI deficient mice lacking functionally active serine proteases are protected from disease in a model of MPO-ANCA induced necrotising crescentic glomerulonephritis. This was associated with reduced IL1β generation by DPPI deficient neutrophils and monocytes upon ANCA stimulation [80].

1.3.3 LAMP2

Kain *et al* in 1995 showed that 14 out of 16 patients with pauci-immune necrotising crescentic glomerulonephritis had antibodies to LAMP2 in addition to autoantibodies to MPO or PR3 [30]. LAMP2 is a heavily glycosylated type I transmembrane protein that is expressed by neutrophils and endothelial cells. It is a major lysosomal membrane component with three splice variants that is also found within intracellular vesicles and the cell plasma membrane itself. It has a polypeptide backbone of approximately 40 kDa, however the end product after glycosylation has a molecular weight of 120 kDa [81].

Deficiency of LAMP2 in mice resembles the human Danon disease, which is an X linked disorder of LAMP2 mutation characterised by hypertrophic cardiomyopathy, skeletal myopathy and mental retardation. The disease is characterised by late autophagic vacuole accumulation [82]. LAMP2 deficient mice have severe periodontitis early in life attributed to neutrophils that were unable to efficiently clear bacterial pathogens, because of reduced acidification and recruitment of proteins within phagosomes. Hence, LAMP2 appears to have an important role in phagosome maturation within neutrophils [83]. Furthermore, in LAMP2 deficient neutrophils, lysosomes appear clustered in the centre of the cell, suggesting a role in lysosome shuttling.

LAMP2 has also been implicated in the transport of cytosolic components across the lysosomal membrane (termed chaperone mediated autophagy), which is important for MHC class II presentation of cytoplasmic antigens. Cells with diminished expression of LAMP2, have a decreased display of cytoplasmic epitopes via class II molecules [84].

In follow up studies Kain *et al* showed a high prevalence of antibodies to LAMP2 in AAV patients, confirming the earlier data; 93% in a cohort of 84 patients in Vienna and Aberdeen, 89%, 91% and 80% in cohorts from Vienna, Cambridge and Groningen respectively [31, 85]. By contrast, in patients in remission following immunosuppression anti-LAMP2 remained positive in only 7%. Furthermore, anti-LAMP2 was shown to activate neutrophils and induce endothelial cell apoptosis *in vitro*. Passive immunisation of rats with polyclonal rabbit anti-LAMP2 antibodies precipitated a pauci-immune crescentic glomerulonephritis. The study also suggested the potential for molecular mimicry in breaking tolerance and the formation of anti-LAMP2 antibody [31].

A study by Roth *et al* appears to contradict the results of Kain *et al* [31, 86]. They found a substantially lower prevalence of anti-LAMP2 antibody of 21% in a cohort of 329 patients with AAV in North Carolina and Massachusetts, which was comparable to control groups [86]. In addition, Roth *et al* did not observe any disease in rats immunised with anti-LAMP2.

The discrepancies are likely to be due to the differences in patient population and assay designs. The BVAS scores for patients at presentation or in relapse in the Kain *et al* studies ranged from 10-15 whilst the BVAS score for the Roth *et al* study was >0. Kain *et al* showed that the highest anti-LAMP2 titres were consistently found in newly presented untreated patients. The majority of patients in the Roth *et al* study were on treatment. Kain *et al* tested the sera in triplicate using three independent methods; Enzyme linked immunosorbant assay (ELISA), Western blot and immunofluorescence, whilst this was not the case for the American cohorts. Furthermore, the antigen substrates used in the ELISA for both studies were not identical, another variable that may account for the differences.

The differences noted with passive immunisation of rats are more difficult to explain. Kain *et al* produced antibodies by injecting rabbits with complete recombinant human LAMP2 whilst Roth *et al* utilised a synthetic peptide corresponding to epitope $P_{41\text{-}49}$ as the immunogen in rabbits, which may offer a likely explanation.

The role of anti-LAMP2 in pathogenesis and clinical phenotype needs to be explored further.

1.4 Are ANCA pathogenic?

Clinical, *in vitro* and *in vivo* findings suggest that ANCA are pathogenic. However, there are several observations that suggest that not all ANCA are equally pathogenic and other factors are necessary for disease induction. A neonate developed pulmonary renal disease, which was thought to have occurred following transplacental transfer of MPO-ANCA IgG from the mother who had MPA [87]. However, no additional cases have been reported. Furthermore, a case whereby a neonate had acquired transplacental MPO-ANCA with no development of clinical features of the disease has been reported [88].

In clinical practice, remission is often associated with a reduction in ANCA titres and conversely a rise in ANCA levels can predict a relapse with a sensitivity of 79% and specificity of 68%. However, the period from change in titre levels to disease relapse is variable with a range of 0 to 20 months [89]. Other studies have failed to confirm these observations. In practice the relationship of ANCA titres to clinical outcome is questionable and treatment is based on clinical signs and symptoms rather than titres.

In the literature, there is reference to the indirect association in the efficacy of plasma exchange and ANCA pathogenicity, as plasma exchange therapy increases the rate of renal recovery in those with severe AAV compared to intravenous methylprednisolone [90]. However, it is important to note that plasma exchange removes several potentially pathogenic substances not only antibodies, such as cytokines, fibrinogen and complement components.

Natural autoantibodies against MPO and PR3 are found in healthy individuals, albeit at significantly lower levels than in AAV [91]. Furthermore, as mentioned, a subset of patients test negative for ANCA despite fulfilling the criteria for AAV, contesting the pathogenicity of ANCA. The pathogenicity of antibodies in AAV may be explained by the subclass or epitope specificity. The natural autoantibodies are mainly restricted to the IgG1 subclass [92]. In contrast, in AAV, ANCA are found as all four subclasses of

IgG, with IgG3 thought to be most pathogenic. But it is also important to highlight that the IgG1 subclass of ANCA are not benign and have been shown to activate neutrophils *in vitro* [93].

Epitope specificity may determine the pathogenicity of ANCA. Roth *et al* recently showed substantial MPO-ANCA epitope diversity using high sensitivity epitope excision and mass spectrometry. One linear epitope (aa447-459) was exclusive to active disease and reactivity to this epitope declined in remission. Purified IgG fractions from ANCA negative patients' serum, as tested by multiple laboratories, showed reactivity against this peptide, however serum did not. This discrepancy was due to masking of the epitope by a caeruloplasmin fragment [94].

Several *in vitro* studies have shown that monoclonal and limited numbers of patient derived polyclonal ANCA stimulate primed neutrophils to undergo respiratory burst and degranulation [61, 62, 64]. However, not all ANCA are equally effective in activating neutrophils. Franssen *et al* compared the release of reactive oxygen radicals as assessed by ferricytochrome C reduction and neutrophil degranulation upon stimulation with IgG fractions from 17 PR3-ANCA and 14 MPO-ANCA patients. They found no difference in respiratory burst or degranulation when neutrophils were incubated with IgG from MPO-ANCA positive patients as compared to IgG from healthy controls [95]. In this study, IgG from PR3-ANCA positive patients did induce an increased neutrophil respiratory burst and degranulation compared to controls, although there was a high degree of variability and overlap.

It has also been shown that activation of neutrophils with monoclonal ANCA and fragment antigen binding ($F(ab)_2$) fragments from a small number of donors with AAV results in endothelial cell injury [96]. Activation of neutrophils with ANCA from patients has been shown to result in the formation of NETs which harbour the antigens PR3 and MPO, suggesting that netosis is a form of antigen presentation [97].

As discussed earlier, neutrophil priming increases MPO and PR3 surface antigen expression. This would be a pre-requisite for ANCA binding. Furthermore higher membrane PR3 expression is a risk factor for GPA. MPO and PR3 gene expression is normally suppressed before mature neutrophils leave the bone marrow. However, in

AAV, patients have been shown to have abnormal epigenetic regulation of this suppression, leading to continued inappropriate expression of MPO and PR3 genes in circulating neutrophils [98]. The evidence does not necessarily suggest a direct role for ANCA in pathogenesis but is highly suggestive.

The *in vitro* evidence suggesting that ANCA are possibly pathogenic is reliant on TNFα priming of neutrophils. One could infer as a result that anti-TNF therapy would be beneficial in AAV. A randomised controlled trial using etanercept (human TNF receptor p75 Fc fusion protein that binds and inhibits TNF) did not show any favourable effect on the maintenance of remission [99]. This would suggest that the *in vitro* findings might not necessarily reflect *in vivo* mechanisms or other factors are capable of priming neutrophils *in vivo*.

In summary, it appears that not all ANCA are pathogenic, rather a distinct subset of ANCA against a specific repertoire of epitopes is required for the development of AAV. Furthermore, other factors as discussed in the following sections contribute to pathogenesis.

The most convincing evidence for the pathogenicity of ANCA to date has come from *in vivo* studies. Xiao *et al* raised MPO-ANCA by immunizing MPO deficient mice with murine MPO. Transfer of the MPO-ANCA into recipient mice led to the development of pauci-immune necrotising crescentic glomerulonephritis [100]. However, the development of an animal model of PR3-ANCA disease has been less successful and hence do not prove that PR3-ANCA are pathogenic (see section 1.11).

1.5 Potential ANCA signalling

Binding of ANCA to its respective antigen is thought to result in neutrophil activation. The precise intracellular cascade that leads to neutrophil activation has not been elucidated. Although there is conflicting data, it appears that both the fragment crystallisable (Fc) and the antigen binding regions are important.

Receptors to the Fc portion of antibodies are widely expressed by various cell types especially phagocytes. A variety of Fc receptor subtypes exist which display specificity

for different immunoglobulin subtypes. FcγR are either activating (FcγRIA, IIA, IIc, IIIA, IIIB in humans; FcγRI, III, IV in mice) or inhibitory (FcγRIIB) and bind IgG. Cross-linking of activating FcγR leads to the initiation of immunoreceptor tyrosine activation motif (ITAM) dependent tyrosine kinase recruitment and downstream activation of various targets including Src family protein Syk [101].

In one study, human ANCA $F(ab)_2$ or cross-linked Fab activated neutrophils to induce superoxide production, but mouse monoclonal $F(ab)_2$ fragments did not [102]. The ability of $F(ab)_2$ fragments to induce superoxide generation was confirmed in another study [103], but not by others [104-106].

The inability of $F(ab)_2$ fragments to induce neutrophil activation as shown by most studies suggests that Fc receptors are important and indeed blocking FcγRIIA reduced PR3-ANCA induced superoxide production [104]. Furthermore, *in vivo* data in FcγR knockout mice revealed that administration of MPO-ANCA IgG failed to induce a reduction in leucocyte rolling, or increase leucocyte adhesion and transmigration across cremasteric microvessels [107].

Other important factors in potential ANCA signalling include posttranslational modification of antibodies such as sialylation and glycosylation, which modify the capacity of ANCA to activate targets and potentially disease development [108].

As discussed MPO and PR3 are not transmembrane molecules, but interact with other molecules and the CD11b/CD18 integrin complex (Mac-1), resulting in ANCA induced signalling. Williams *et al* showed that both tyrosine kinase activation as well as the recruitment of G proteins are necessary for ANCA induced phosphoinositol 3-kinase (PI3-K) activation and subsequent superoxide generation. The generation of phosphatidylinositol (3,4,5) – triphosphate (PIP3) and superoxide generation was inhibited by pertussis toxin and a tyrosine kinase inhibitor, implicating Gi protein induced Ras GTP activation and the tyrosine kinase pathway [106].

Radford *et al* showed with the use of inhibitors that protein kinase C (PKC) and tyrosine kinases have a crucial role in ANCA induced superoxide generation too [109]. Subsequently it was demonstrated that p38 MAPK is important in antigen

translocation on priming of neutrophils with TNFα, whilst inhibition of p38 MAPK or ERK abrogates ANCA induced superoxide production [62].

Syk has been shown to be phosphorylated and hence activated upon ANCA IgG stimulation of TNFα primed neutrophils but not ANCA $F(ab)_2$ fragments. This was diminished by FcγRIIa and FcγRIIIb blockade, suggesting that FcγR engagement of ANCA IgG is necessary for Syk activation. Furthermore, inhibition of Syk attenuated ANCA induced superoxide release from primed neutrophils [110]. Syk is able to activate phospholipase Cγ (PLCγ) as well as PI3-K, with subsequent cleavage of phosphatidylinositol (4,5) – bisphosphate (PIP2) into diacylglycerol (DAG) which activates PKC and inositol triphosphate (IP3) which mediates calcium mobilisation.

PI3-K has a crucial role in ANCA signalling. LY294002 and wortmannin, both PI3-K inhibitors suppress ANCA induced superoxide release. Furthermore, pertussis toxin inhibits ANCA induced superoxide production suggesting that ANCA activate the p101/p110γ isoform of PI3-K [111]. The importance of PI3-Kγ was confirmed *in vivo* in a bone marrow transfer model of MPO-ANCA disease. Disease occurred in irradiated MPO deficient mice that had previously been immunised with MPO and reconstituted with wild type bone marrow but not PI3-Kγ deficient marrow. Furthermore, treatment with the PI3-Kγ inhibitor AS605240, also protected from disease in this model [112].

The proposed signaling mechanism is summarized in figure 1.2.

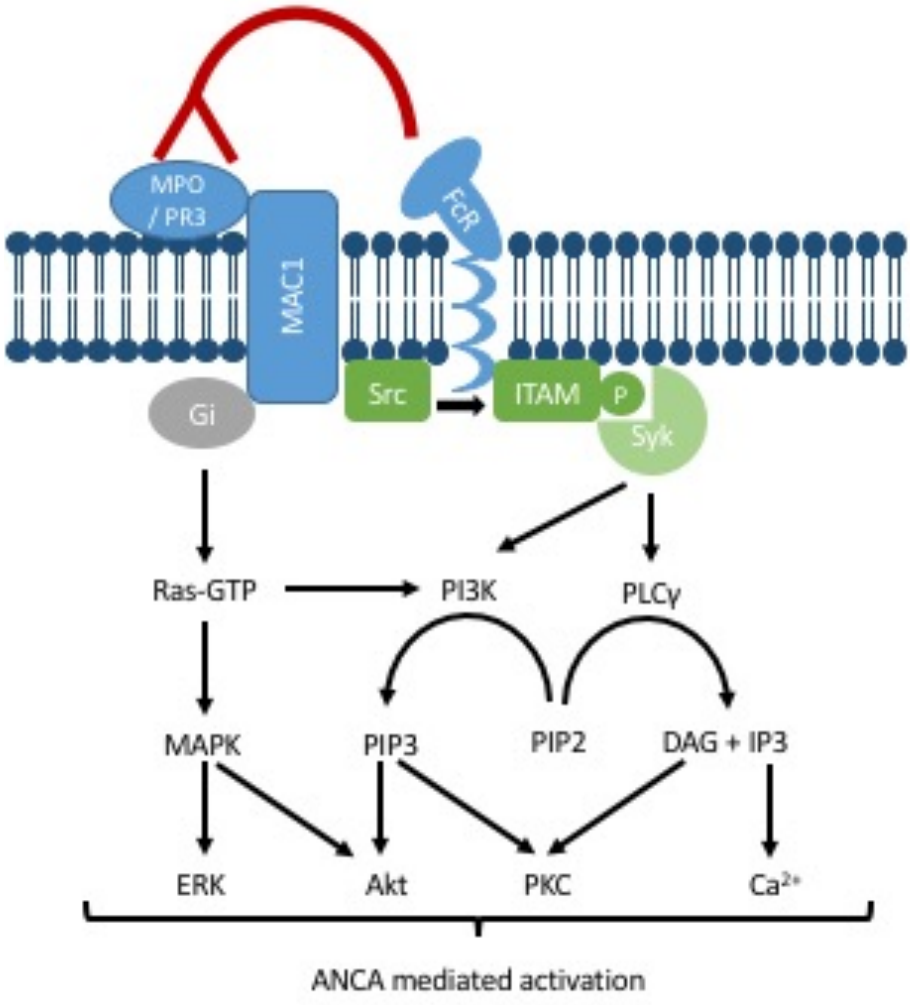

Figure 1.2 – A summary of the signalling molecules involved in ANCA mediated neutrophil activation. ANCA depicted in red binds to the respective antigen through the Fab segment and engages the Fc receptor activating G protein coupled pathways as well as tyrosine kinase pathways.

1.6 Neutrophils

As discussed the interactions between ANCA and neutrophils are thought to be pivotal to disease pathogenesis. Firstly, neutrophils house the antigenic stimuli necessary for the cascade of events that are thought to lead to disease induction. In healthy mature neutrophils MPO and PR3 transcription is silenced. In patients with AAV aberrant activation of transcription occurs [98]. MPO and PR3 are sequestered within neutrophil and monocyte granules. With neutrophil priming by inflammatory cytokines, complement components or bacterial products, membrane expression of MPO and

PR3 is induced. Subsequent binding of ANCA as reviewed, triggers neutrophil activation leading to degranulation and NETs formation exposing further antigen and potentiating the process of ANCA binding.

Neutrophil recruitment from the circulation to the site of inflammation involves a sequence of events namely rolling, high affinity binding and transmigration. Endothelial cells have a crucial role too. Endothelial cells respond to cytokines such as TNFα by producing granulocyte colony stimulating factor (GCSF) and upregulating local expression of P-selectin and E-selectin, which slow down neutrophil rolling. This induces changes in integrin adhesion molecules on neutrophils such as CD11b/CD18 complex and LFA-1, which bind to endothelial cell adhesion molecules intercellular adhesion molecule (ICAM) 1 and ICAM 2 resulting in high affinity binding and firm adhesion. Transmigration then occurs via two routes; paracellular in the majority of cases and transcellular. Neutrophils then follow a chemotactic gradient to the site of inflammation [113]. Intravital microscopy studies of cytokine pretreated mice cremasteric vasculature reveal that MPO-ANCA reduced leucocyte rolling and augmented firm adhesion and transmigration. Use of anti-CD18 blocking antibodies prevented these effects [107].

GCSF is central to the production of neutrophils. Mice lacking GCSF have chronic neutropaenia and impaired granulocyte mobilization [114]. GCSF also has other immunomodulatory roles including enhanced phagocytosis, superoxide generation as well as enhanced neutrophil responses to fMLP [115]. GCSF can be produced by a variety of cells including endothelial cells (as mentioned), epithelial cells, fibroblasts and immune cells such as monocytes, macrophages as well as neutrophils. GCSF mediates its effects by binding to a homodimer transmembrane receptor. Mobilization of neutrophils involves parallel but distinct mechanisms including; induction of proteases such as elastase as well as matrix metalloproteinases, attenuation of adhesion molecules such as integrins and disruption of signaling between CXCL12/CXCR4 [116].

It is thought that activated neutrophils undergo respiratory burst and degranulation releasing reactive oxygen species (ROS) and proteases, which cause local tissue destruction including endothelial cell necrosis and apoptosis ultimately leading to

fibrosis. Renal histology samples of patients with AAV support the role of neutrophils in tissue damage. The number of activated neutrophils in the renal biopsy samples of patients with GPA correlates with severity of renal impairment [117]. In addition, murine studies of the MPO-ANCA passive transfer model of AAV revealed that neutrophil depletion using the monoclonal antibody NIMP-R14 directed against Ly6G and Ly6C, protected mice from necrotising crescentic glomerulonephritis [118]. We have shown that GCSF primes neutrophils to induce respiratory burst in response to MPO-ANCA. Furthermore, patients with active AAV have higher serum GCSF levels compared to controls. *In vivo,* administration of GCSF exacerbated disease in the passive transfer model with an increment in peripheral blood neutrophil counts [119].

Neutrophils however are not just effector cells, they secrete cytokines and chemokines following appropriate stimulation instructing and interacting with other immune cells. For example neutrophils are a major source of B-cell activating factor, which is crucial for B cell survival, maturation and differentiation, hence neutrophils may have a role in sustained autoantibody production. They also have the ability to recruit Th1 and Th17 cells to sites of inflammation.

1.7 T cells

There is extensive evidence implicating T cells in AAV pathogenesis. Weidner *et al* demonstrated that the predominant interstitial infiltrating leucocytes in renal tissue from AAV patients were T cells [3]. T cell activation markers such as soluble IL2R and CD30 are elevated in the circulation of AAV patients and are associated with disease activity [120]. Moreover, ANCA are predominantly of the IgG1 and IgG4 subclass suggesting that antigen-driven T cell dependent class switching has occurred. ANCA antigen specific T cells are detectable in AAV patients. T cells from AAV patients proliferate in presence of MPO and PR3 to a greater extent than controls and these responses tend to persist with time, even in remission of disease [121]. Furthermore, anti-T cell therapy has been shown to induce remission in the clinical setting [122].

Further observations from animal models support the role of CD4 T cells. Ruth *et al* demonstrated a crucial role of CD4 T cells in an autoimmune mouse model of crescentic glomerulonephritis. They immunised wild type mice with human MPO and

subsequently challenged them with glomerular basement membrane (GBM) binding antibodies. Mice that were depleted of CD4 T cells at time of glomerular binding antibody administration developed significantly less disease compared to controls [123].

Further evidence for the pathogenic role of T cells emerged with the identification of an immunodominant MPO T cell epitope using a peptide composed of amino acids 409-428 of the MPO heavy chain [124]. Mice immunised with this peptide developed disease similar to that seen in mice immunised with whole MPO. MPO amino acids 409-428 were subsequently implanted by conjugation to an anti-GBM monoclonal antibody in the glomeruli of Rag-1 deficient mice. Transfer of MPO amino acids 409-428 specific CD4 T cell clones into these mice led to the development of focal necrotising glomerulonephritis.

Attempts to define the Th1 / Th2 paradigm in AAV have also been made, although there are concerns about the oversimplification of this distinction. Analysis of serum for markers of Th1 and Th2 cells reveal a shift toward a Th2 phenotype in patients with active generalised disease and a predominant Th1 response in those with localised disease [125, 126].

Th17 cells also play a role in AAV. Neutrophils activated by MPO ANCA secrete IL17 and IL23 both cytokines creating a milieu to promote Th17 differentiation [127]. IL17 in turn leads to inflammatory cytokine release including IL1β and TNFα from macrophages and induces local neutrophil recruitment. *In vivo* Th17 cells have been shown to be crucial to pathogenesis. Spleen cells from MPO immunised mice produce IL17 and low amounts of IFN-γ. Furthermore IL17 deficient mice were protected from disease induction in the autoimmune mouse model of crescentic glomerulonephritis [128].

Treg cells, characterised by their expression of forkhead winged helix transcription factor (FoxP3), have been implicated in autoimmunity. They regulate the immune response of effector memory T cells. In GPA patients the suppressive function of Treg cells has been shown to be defective compared to healthy controls [129]. Circulating CD4 effective memory T cells on the other hand are increased in AAV patients in

remission and reduced during active disease [130]. This is associated with an increase in CD4 effective memory T cells in the urinary sediment of patients with active renal involvement suggesting that in active disease these cells migrate to areas of inflammation [131].

Studies of CD8 T cells in AAV are sparse. During active AAV Iking-Konert *et al* showed that a distinct subset of CD8 T cells that are CD11b positive (a marker of activation) were found and these cells produced interferon (IFN)–γ [132]. Furthermore, AAV patients with poor prognosis have been shown to have an expanded CD8 T cell memory population [133].

1.8 B cells

B cells have an important role in pathogenesis as evidenced by the presence of autoantibodies in AAV. Not only do B cells differentiate into plasma cells that produce autoantibodies, they also have a role as APCs and produce pro-inflammatory cytokines.

In patients with AAV tertiary lymphoid structures containing dendritic cells as well as memory and non-memory B cells have been found in involved tissue including glomerulonephritis lesions [134]. However, there was no evidence of antibody production within the renal lesions, suggesting an antibody independent role in the tissue. Bunch *et al* compared the peripheral B cell subsets in either active or quiescent AAV to healthy controls and showed that those with active disease had a lower proportion of CD5 positive B cells to controls and those in remission [135]. Furthermore, normalisation of CD5 B cells after rituximab therapy correlated with more effective remission. CD5 is one of several surface markers that characterise regulatory B cells, which produce IL10.

Different subsets of B cells produce immunomodulatory cytokines that regulate immune responses. As mentioned regulatory B cells produce IL10. Other cytokines such as IL6 and TNFα can be produced upon stimulation, which can down-regulate the function of T regulatory cells and boost T effector cell differentiation. TNFα, as discussed, can also prime neutrophils to increase cell surface antigen presentation. B

cell depletion using rituximab has been shown to decrease serum IL6 and TNFα levels [136].

These findings have fostered the use of B cell depleting agents in the clinical setting. The effectiveness of B cell therapy further supports the role of B cells in pathogenesis.

1.9 Monocytes / Macrophages

Monocytes, like neutrophils, harbour the antigenic targets (MPO and PR3) for ANCA. The majority of AAV research has focused on neutrophils whilst the role of monocytes is less well examined.

Monocytes are circulating mononuclear phagocytes that can differentiate into tissue macrophages and dendritic cells. Circulating human monocytes can be subdivided into classical (CD14++CD16-, resemble mouse Ly6C high monocytes), intermediate (CD14++CD16+) and non-classical (CD14+CD16++, resemble mouse Ly6C low monocytes). Classical monocytes are the most prevalent subset and are considered pro-inflammatory.

During early myeloid differentiation, colony stimulating factor 1 (CSF1) in synergy with other growth factors produce mononuclear phagocyte progenitor cells and regulate the proliferation and differentiation into monocytes and macrophages. CSF1 exerts its effects through the receptor CSF1R, a homodimeric tyrosine kinase receptor. CSF1 also enhances monocyte and macrophage mediated cytotoxicity, phagocytosis as well as superoxide and cytokine production following appropriate stimulation. Thus CSF1 is strongly implicated in infection and autoimmunity. In an animal model of lupus using the MRL/lpr mice, Lenda *et al* showed that these mice have elevated CSF1 levels. CSF1 deficient MRL/lpr mice had reduced renal injury and systemic disease, fewer intrarenal macrophage and T cell infiltrates, as well as reduced circulating autoantibodies [137].

Attempts have been made to classify macrophage subsets based on cell surface markers, cytokine profile following various stimuli and the effects on adaptive immunity. Macrophages are often subdivided into M1 (cytotoxic) and M2 (healing).

The macrophage subsets were named M1 and M2 as they stimulate naïve T cells into Th1 or Th2 type responses respectively. M1 macrophages classically express inducible nitric oxide synthase, CD86 as well as MHC II and typically produce IL8, IL12 and CCL2. M2 macrophages express CD163 as well as CD206 and produce arginase, vascular endothelial growth factor and transforming growth factor (TGF) β [138]. *In vitro* the cell populations derived from culture with granulocyte macrophage colony stimulating factor (GMCSF) or CSF1 have been likened to M1 or M2 macrophages respectively. In tissue, there appears to be plasticity as macrophages mature in a dynamic manner to various stimuli and are thought to be adaptable, making a clear distinction between M1 and M2 macrophages challenging.

Normal human peripheral blood monocytes have well defined cytoplasmic staining with MPO and PR3 ANCA as shown by indirect immunofluorescence. *In vitro* these cells lose reactivity as they differentiate into macrophages, suggesting that ANCA can only interact with monocytes but not mature macrophages [139]. Limited *in vitro* studies show that ANCA can activate monocytes. Casselman *et al* showed that ANCA isolated from patients induced monocyte chemotaxis and induced monocyte chemoattractant protein-1 (MCP-1 / CCL2) secretion [140]. Ralston *et al* demonstrated that TNFα priming of monocytes led to increased surface PR3 expression on peripheral blood mononuclear cells. Monoclonal and polyclonal PR3-ANCA induced significantly more IL8 release from TNFα primed monocytes than control IgG, which was Fc dependent [141]. IL8 is a powerful neutrophil chemotactic factor that can amplify neutrophil induced injury, whilst MCP-1 regulates the migration of monocytes as well as memory T cells and natural killer cells. Hence, ANCA through its actions on monocytes may participate in the transition of neutrophil rich to monocyte / macrophage predominant inflammation in AAV.

Others have shown that monocytes from patients with PR3-ANCA disease had upregulated CD11b, although these monocytes had reduced oxygen radical production under basal conditions and in response to fMLP compared to healthy controls [142]. Weidner *et al* on the other hand showed that ANCA IgG isolated from patients induced healthy TNFα primed monocytes to produce oxygen radicals compared to control IgG. Interestingly, $F(ab)_2$ fragments of ANCA were also able to induce reactive oxygen

species production to an extent that was similar to ANCA IgG. But pre-incubation of monocytes with a FcγRII blocking antibody reduced the formation of oxygen radicals by ANCA IgG. A possible explanation for this inconsistency is that the $F(ab)_2$ fragments and whole IgG were used at identical concentrations at 50µg/ml yielding a higher molar concentration of the $F(ab)_2$ fragments making the results incomparable [143]. It has also been demonstrated that ANCA IgG induce *in vitro* upregulation of CD14 on unprimed monocytes, a co-receptor for LPS that contributes to monocyte adhesion to stimulated endothelial cells [144]. More recently, O'Brien *et al* showed that MPO-ANCA stimulated TNFα primed monocytes to produce IL1β, IL6 and IL8 [145]. So it appears from the limited studies ANCA are capable of activating monocytes.

Work by Weidner *et al* showed that in renal biopsies from patients with AAV related glomerulonephritis monocytes / macrophages were the predominant leucocytes in glomeruli [3]. These results are in accord with those reported by Zhao *et al*, who reported that monocytes / macrophages were the most frequent leucocytes in patients with ANCA glomerulonephritis [146]. They also demonstrated using electron microscopy that macrophages predominated at areas of perforations and attenuations of glomerular capillary basement membrane. Zhao *et al* attempted to characterise the macrophages in renal biopsies as M1 or M2 using CD68 and CD163 antibodies. They found that the majority of macrophages were CD163 positive at sites of segmental fibrinoid necrosis suggesting that M2 macrophages predominate [146]. Ohlsson *et al* reported that serum from AAV patients induced macrophage polarisation toward the M2c phenotype however it remains unclear if this was a direct result of ANCA or due to the cytokine milieu [147].

1.10 Complement and AAV

The complement system was first described in the late 19th century as a heat labile bactericidal factor initially termed alexin and later termed to its universally accepted nomenclature by Paul Ehrlich [148]. It consists of over fifty glycoproteins that are either soluble or membrane bound, functioning as activators, receptors and regulators. There are three known pathways of complement activation (figure 1.3), which culminate in the formation of the C3 and C5 convertase enzyme complexes that cleave

C3 and C5 into the anaphylatoxins C3a and C5a, the opsonin C3b and C5b. C5b deposition onto a target leads to the formation of the membrane attack complex (MAC) C5b-9, resulting in target lysis. The role of complement in innate immunity has been widely acknowledged, however a renewed interest since the 1970s has shown its involvement in many other effector systems including adaptive immunity.

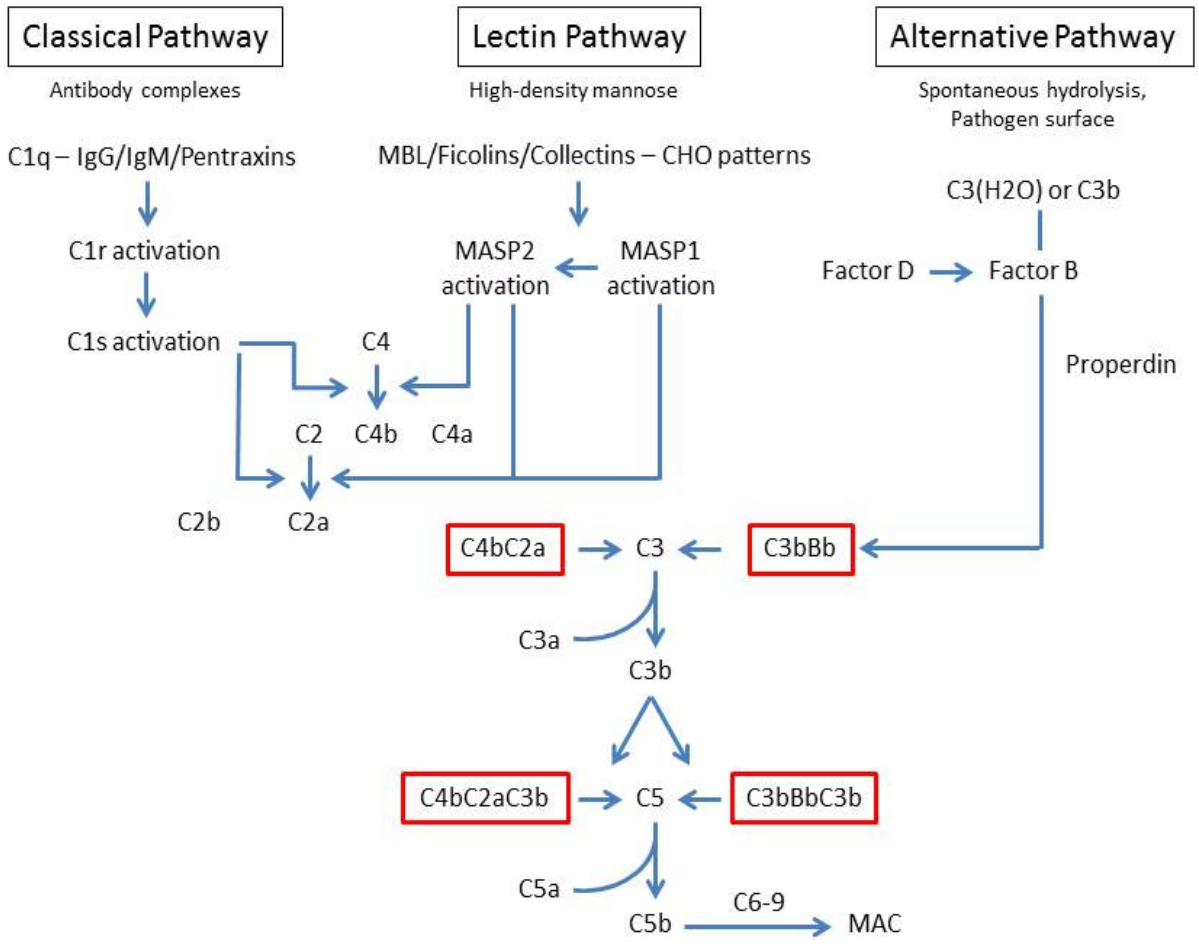

Figure 1.3 – The complement cascade. The three activation pathways of complement activation are depicted (MBL – mannose-binding lectin, CHO – carbohydrate, MAC – membrane attack complex). The C3 and C5 convertases are highlighted in red.

1.10.1 The classical pathway

The classical pathway is initiated when C1q (as part of the C1 complex composed of C1q, C1r and C1s) binds the Fc portion of IgG or IgM immune complexes, pentraxins such as C reactive protein or moieties on microbial and apoptotic cells [148, 149]. Binding of C1q leads to stepwise activation of C1r and C1s. C1s subsequently cleaves

C4 into C4a and C4b. The opsonin C4b deposits on the target surface and cleaves C2 to C2a and C2b, the former product binds to C4b, generating the classical pathway C3 convertase C4bC2a.

1.10.2 The lectin pathway

The lectin pathway has some functional similarities to the classical pathway. In this case, the mannose-binding lectin (MBL), ficolins and collectins act as pattern recognition molecules (PRMs) binding carbohydrate structures on pathogens or glycocalyx patterns on apoptotic cells (pathogen associated molecular patterns or damage associated molecular patterns). The PRMs associate with MBL-associated serine proteases (MASPs) 1-3 forming an enzyme complex. MASP2 cleaves C4 and C4b bound C2 to generate the classical C3 convertase C4bC2a, whilst MASP1 cleaves C2 but not C4, and C3 to a lesser extent [150].

1.10.3 The alternative pathway

Inert C3 is constantly hydrolysed to form C3(H_2O) which is similar to C3b and binds factor B. Bound factor B is cleaved by factor D to generate the C3 convertase $C3_{H2O}Bb$. Properdin has a role in stabilising the C3 convertase as well as PRM based activation. Properdin recognises pathogens and altered self cells through the detection of certain glycosaminoglycans propagating the complement cascade by attracting C3b onto surfaces, initiating further C3 convertase formation [151-153].

The C3 convertases cleave C3 into C3a and the opsonin C3b, leading to further amplification of the alternative pathway. In addition, C3b further complexes with the C3 convertases to form the C5 convertases C4bC2aC3b and C3bBbC3b, which in turn cleave C5 to form the anaphylatoxin C5a and C5b. C5b associates with C6-9 to form the MAC, composed of a pore like structure that disrupts the phospholipid bilayer of the target cell.

In addition to the conventional three activation pathways discussed, other factors are capable of initiating the complement cascade (see complement and coagulation).

1.10.4 Regulators of complement

Activation of complement can be deleterious leading to undesirable tissue damage and it is intuitive to perceive that C3b generated by the tick-over process described will bind non-specifically to healthy cells. Hence the complement system has key regulators in place to restrict unnecessary damage and activation.

The regulators can be divided into fluid phase and membrane-bound regulators [154]. The fluid-phase regulators are found in plasma and other bodily fluids such as synovial fluid. They include:

- C1 inhibitor - inhibits C1r and C1s as well as MASP1 and MASP2 [155, 156].
- C4bp - accelerates decay of the C3 convertase C4bC2a and facilitates factor I mediated C3b and C4b cleavage [157].
- Factor H – inhibits the alternative pathway C3 convertase C3bBb and acts as a cofactor for factor I, which inactivates C3b and C4b [158, 159].
- Carboxypeptidase N – cleave and partially inactivates the anaphylatoxins C3a and C5a to C3a-desArg and C5a-desArg [160].
- Clusterin and S protein (vitronectin) – regulate the MAC by inhibiting the membrane binding of the MAC [154].

The membrane bound regulators are found on the membrane of host cells and include:

- Complement receptor (CR) type 1 – accelerates decay of the C3 and C5 convertases and acts as a cofactor for factor I [161, 162].
- Membrane cofactor protein (CD46) – acts as a cofactor for factor I and induces C3b and C4b cleavage [163]. As discussed later the definition of CD46 as exclusively a complement regulator is not accurate.
- Decay-accelerating factor (DAF / CD55) – accelerates the decay of the classical and alternative pathway C3 convertases [164].

1.10.5 Effects of complement pathway activation

As discussed, complement pathway activation, regardless of the initiation pathway culminates in:

- Generation of pro-inflammatory anaphylatoxins C3a and C5a.

  C3a and C5a are approximately 10-15 kDa fragments that bind specific receptors to mediate their actions on immune and non-immune cells. They have been shown to increase vascular permeability and induce smooth muscle contraction [165]. They are powerful chemoattractants of macrophages, neutrophils, B cells as well as T cells and are capable of inducing neutrophil oxidative burst [166]. Both C3a and C5a are cleaved from the amino terminal region of the α chain of the respective parent molecule C3 or C5.

  The anaphylatoxins bind 7 transmembrane spanning receptors that belong to the G-protein family of receptors, C3aR for C3a, C5aR1 and C5L2 for C5a. Of note C5L2 is not coupled to G proteins. C5aR1 signalling is mediated by the G proteins Gαi and Gα16 with subsequent phosphorylation of G protein receptor kinases. C5L2 on the other hand may have a role as a decoy receptor making C5a and C5a-desArg inaccessible to C5aR1 or it may play a role in shuttling C5a / C5a-desArg to the intracellular compartment [167]. Of course G protein independent signalling pathways may play a role and certainly C5L2 has been shown to complex with β-arrestin [168].
- Clearance of target cells by the generation of opsonins such as C4b, C3b and iC3b. This is accomplished through the recognition of the complement fragments on cells by receptors CR1-4 and CRIg on phagocytic cells. CR1 binds C4b, C3b, iC3b, C3dg as well as C1q and MBL, mediating clearance of immune complexes as well as phagocytosis. CR1 also promotes proinflammatory cytokine release such as IL1β [169]. As discussed it also accelerates the C3 and C5 convertase decay and acts as a cofactor for factor I. CR2 has a key role in promoting B cell immunity, whilst CR3 and CR4 play a role in phagocytosis as well as leucocyte trafficking. CRIg is found in Kupfer cells and play a role in the clearance of C3 coated particles [170].
- Direct lysis of cells through MAC assembly. Cell lysis requires the presence of multiple MACs on the cell surface to overcome the elimination of C5b-9

components and repair process of the cell membrane. Sublytic C5b-9 can induce cell activation and proliferation as well as enhance synthesis of pro-inflammatory cytokines such as TNFα from certain cell types [171, 172].

1.10.6 Role of complement in adaptive immunity

B cell responses

The role of complement in adaptive immunity is now widely acknowledged. Pepys in 1972 showed that mice that were depleted of C3 using cobra venom factor had impaired humoral response against T cell dependent antigens [173]. It was subsequently shown that CR2 (CD21), which binds C3d, forms a receptor with CD19 and CD81 on B cells lowering the threshold of B cell activation [174, 175].

Others have demonstrated that B cells express the C3a receptor and that both C3a and C3a-desArg have an immunomodulatory effect on B cells. C3a and C3a-desArg supress a polyclonal immune response as well as B cell TNFα and IL6 secretion [176].

T cell responses

Complement plays a major role in T cell responses via two distinctive mechanisms; affecting the function of APCs modulating the T cell effector responses and by directly engaging complement receptors and regulators on T cells [177].

C3 deficient mice have impaired CD4 and CD8 T cell responses in models of viral infection and transplantation [178, 179]. Antigen uptake and presentation is suboptimal in the absence of C3, reducing the potency of APCs to stimulate T cell responses [180, 181]. The importance of the anaphylatoxins C3a and C5a in APC maturation has also been highlighted.

Two major complement regulators have been implicated in T cell biology and have led to interesting ideas about local complement function. DAF knockout mice have an enhanced Th1 response characterised by IFN-γ and IL2 hyper-secretion due to uncontrolled surface complement activation. The augmented response did not occur if DAF and factor D double knockout APCs were used and the response was reduced in

the presence of an anti-C5 monoclonal antibody whilst C5a addition amplified it [182]. This led to the hypothesis that locally produced complement products at the APC-T cell interface are crucially involved in T cell activation [183].

CD46 is critical in regulating T cell mediated inflammatory responses. CD46 functions as a co-stimulatory molecule with T cell receptor stimulation to induce CD4 cell activation and proliferation [184]. T cells isolated from CD46 deficient patients who suffer from recurrent infections are unable to produce IFN-γ, however Th2 responses are maintained [185]. Interestingly in the presence of high IL2, CD46 is involved in the switch of IFN-γ producing Th1 cells into an IL10 producing regulatory phenotype contracting the Th1 cell pool [186]. Furthermore, engagement of C3aR is necessary for Th1 IFN-γ production [183].

It appears that complement plays a vital role in orchestrating and bridging both the innate and adaptive immune system through complex interactions. However, complement has other roles including cell metabolism, in particular lipid synthesis and amino acid metabolism.

1.10.7 Local complement production

The liver is the established source of the majority of circulating complement components, excluding C1q, factor D, properdin and C7. C1q, properdin and C7 are mainly produced by monocytes and macrophages whilst factor D is sourced by adipocytes [187]. Several cell populations in diverse organs are capable of producing complement components, which can have paracrine and autocrine effects [188]. For example, resident renal cell types are capable of synthesising most if not all complement cascade components. Furthermore, studies have shown that local production of C3 is an important mediator of tissue damage in models of adriamycin induced injury and renal allograft rejection [189, 190]. As discussed above T cell produced C3 components have autocrine effects by engaging CD46 and C3aR.

It was assumed that local C3 and C5 generation was mediated by serum-derived convertases, however, T cells and APCs are capable of producing factor B and factor D, and hence the components necessary for C3 and C5 convertase formation [183].

Furthermore, it has been shown that various cell types have the capability of cleaving C3 intracellularly. Resting CD4 T cells harbour the protease cathepsin L, which cleaves C3 into C3a and C3b [191]. Intracellular derived C3 components may have a crucial role in cell metabolism and it has been demonstrated that cathepsin L inhibition as well as decreased intracellular C3aR expression reduces mTOR activity and induces T cell apoptosis, which cannot be rescued by serum derived C3a [191].

This suggests that intracellular derived complement and intracellular complement receptors have distinct functions compared to their extracellular counterparts.

1.10.8 Complement and coagulation

There is extensive cross-talk between the complement cascade and the coagulation pathway. It appears that the two pathways are able to regulate one another at various points (see figure 1.4) [192, 193].

The coagulation pathway is activated by two mechanisms; the intrinsic and extrinsic pathway on cell surfaces or micro-particles. It is believed that *in vivo*, tissue factor has a central role and is the main instigator of the cascade. Both initiation mechanisms lead to the activation of various serine proteases, which result in the release of activated factor X (Xa). Factor Xa converts prothrombin to thrombin, which generates fibrin that cross-link to generate a stable clot.

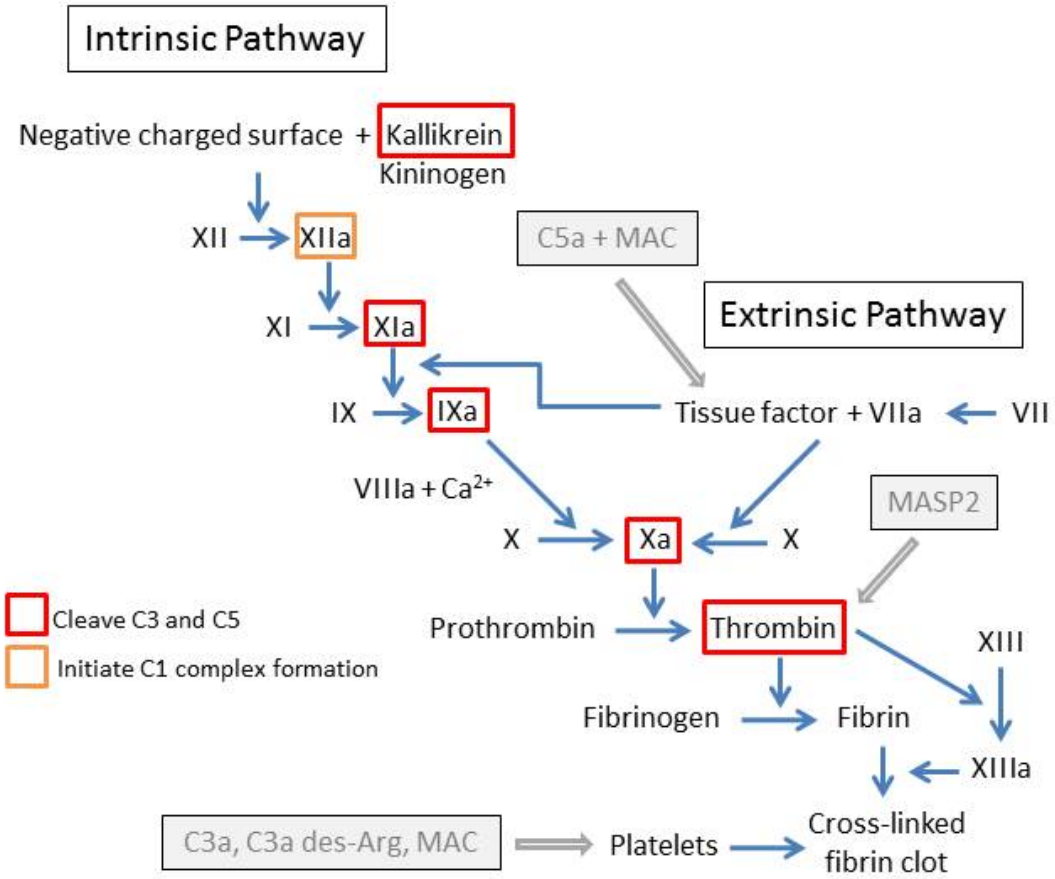

Figure 1.4 – The coagulation cascade and its interactions with complement components. Factors of the coagulation cascade that are known to interact with C1, C3 and C5 are highlighted in orange or red boxes, whilst the complement components that influence coagulation are highlighted in grey.

Various proteases activate the complement pathway. Factor XIIa has been shown to initiate the classical complement pathway by activating the C1 complex [194]. Thrombin is able to cleave C3 and C5 to produce active components of each [195, 196]. C3 and C5 can also be cleaved by factor IXa, factor Xa and factor XIa [196].

Similarly, complement components have the ability to initiate the coagulation cascade. MASP2 cleaves prothrombin into thrombin leading to fibrin clot formation [197]. MASP1 cleaves the two substrates of thrombin, namely factor XIII and fibrinogen although the catalytic activity is much lower than that of thrombin [198]. C3a, C3a des-Arg and the MAC can induce platelet adhesion and aggregation [199].

C5a has multiple effects and is regarded as a procoagulant. In combination with antibodies against endothelial cells, C5a triggers the shedding of endothelial surface

proteoglycan heparin sulfate, which is normally responsible for the regulation of an anticoagulant environment [200]. Both C5a and MAC can also induce tissue factor expression on human endothelial cells [201, 202].

1.10.9 Role of complement in AAV

The pauci-immune nature of AAV initially gave rise to the belief that complement may not play a role in pathogenesis. However, this dogma has since changed with numerous studies showing the importance of complement in AAV.

Xing *et al* reported the presence of complement components C3d, factor B, properdin and MAC in renal biopsies of 7 MPO-ANCA positive AAV patients, whilst MBL and C4d were not detected [203]. Furthermore, circulating levels of C3a, C5a, soluble C5b-9 and Bb have been reported to be significantly higher in patients with active AAV compared to those in remission and controls. Properdin levels were reduced possibly due to consumption. The plasma levels of Bb correlated with the degree of renal injury [204]. This suggested a potential role for the alternative pathway in pathogenesis. A further study by the same group on 12 patients with ANCA negative pauci-immune necrotising crescentic glomerulonephritis revealed the detection of C4d in 8 patients and MBL in 6 patients and this was thought to be associated with a poor renal outcome [205]. More recently Hilhorst *et al* analysed 187 renal biopsies of AAV patients and found C3d, C4d as well as C5b-9 staining in most of the samples [206].

The first experimental evidence suggesting that complement had a role in AAV pathogenesis was published in 2007. The administration of cobra venom factor to mice (a treatment that leads to the consumption and thus depletion of complement component C3) conferred protection against the development of MPO-ANCA induced disease [207]. The study showed that the alternative pathway played a crucial role in disease onset. After injection of MPO-ANCA IgG C4 deficient mice developed disease that was comparable to wild type mice. However, C5 deficient and factor B deficient mice developed no disease, implicating the alternative pathway in disease pathogenesis.

Subsequently Huugen *et al* showed that mice treated with an anti-C5 monoclonal antibody prior to disease induction in the passive transfer model were protected from disease [208]. If the anti-C5 monoclonal antibody was administered 1 day after disease induction, glomerular crescent formation in these mice was reduced by 80%.

Furthermore, *in vitro,* supernatant from TNFα primed and ANCA stimulated neutrophils has been shown to be sufficient to cause the generation of C3a and C5a in normal serum. The factors which are released by the activated neutrophils that result in the generation of C3a and C5a in normal serum were not identified [209]. However, neutrophils are capable of releasing C3, factor B and properdin, the machinery for convertase formation [187, 210]. Blockade of the C5a receptor C5aR1 (CD88) was shown to inhibit ANCA induced respiratory burst in neutrophils. The importance of the C5aR1 was then confirmed *in vivo* using the bone marrow transplant model of disease, with mice receiving C5aR1 deficient bone marrow developing relatively mild disease in response to MPO-ANCA when compared to mice receiving wild type bone marrow [209].

C5aR1 knockout mice were also shown to be protected from disease in the passive transfer model. However, C6 knockout mice were not protected in this model, suggesting that the MAC has no role in disease pathogenesis. Interestingly C5L2 knockout mice had the reverse effect, with more severe disease. The administration of CCX168, an antagonist of human C5aR1, showed dose dependent amelioration of disease in mice expressing the human C5aR1 (knock in mice) [211]. A phase II clinical multicentre trial (ChemoCentryx) to test the effectiveness of CCX168 in patients with AAV where the primary endpoint was to determine whether CCX168 could at least partially substitute for glucocorticoid treatment in inducing remission, showed that CCX168 achieved statistical significance in a test for non-inferiority in BVAS response compared to standard care (Jayne DR *et al* EULAR 2014 abstract, Ann Rheum Dis 73:148).

1.11 Animal models of ANCA vasculitis

Several animal models of glomerulonephritis exist. Glomerulonephritis encompasses a wide range of immune mediated disorders that result in inflammation of the glomeruli.

I will focus on animal models of ANCA vasculitis and also give a brief overview of other models of glomerulonephritis.

Since the 1990s there have been several attempts at developing robust rodent models of ANCA vasculitis. The following paragraphs describe the models in brief.

1.11.1 Models of MPO ANCA disease

The ability of susceptible rat strains such as the Brown Norway rat in developing an autoimmune syndrome mediated by T cell dependent polyclonal B cell activation upon exposure to mercuric chloride was utilised. The rats in this model developed several autoantibodies including antibodies to the glomerular basement membrane, collagen, DNA and MPO, making the contribution of each autoantibody difficult to judge. The rats had characteristic small to medium sized vessel fibrinoid necrosis in multiple organs, however, necrotising crescentic glomerulonephritis, a feature of human disease, was not a prominent sequela. [212, 213]

In 1993 Kinjoh *et al* described the spontaneous crescentic glomerulonephritis / Kinjoh (SCG/Kinjoh) mouse, derived from the selective mating of siblings of (BXSB/Mp x MRL/Mp-lpr/lpr) F1 hybrid mice [214]. These mice developed rapidly progressive crescentic glomerulonephritis with an incidence as high as 58% in females and 34% in males. They produced high titres of MPO-ANCA as well as other autoantibodies again making it difficult to define the pathophysiological role of specific autoantibodies. Furthermore, the disease was not pauci-immune, scanty deposits of immune complexes were noted on immunofluorescence.

Brouwer *et al* immunised Brown Norway rats with human MPO, which led to the generation of MPO-ANCA that cross-reacted with rat MPO. Unilateral perfusion of the kidney with extracts of activated neutrophils and hydrogen peroxide resulted in severe necrotising crescentic glomerulonephritis [215]. At 24 hours C3, IgG and MPO were present along the basement membrane, but not at 4 and 10 days.

Further work utilising the nephrotoxic nephritis model of glomerulonephritis showed that passive heterologous MPO-ANCA transfer or active immunisation of the rat with MPO exacerbated disease. Kobayashi *et al* showed that anti-GBM nephritis in rats is

aggravated by administration of rabbit anti rat MPO antibodies together with rabbit anti rat GBM antibodies. There was increased neutrophil infiltration and fibrin deposition but there was no evidence of crescentic disease [216]. Heeringa *et al* showed that rats immunised with human MPO and subsequently subnephritogenic rabbit anti rat anti-GBM antibodies developed more severe glomerulonephritis at day 10 with fibrinoid necrosis, macrophage infiltration and crescent formation compared to rats not immunised with MPO [217].

Although these models were very informative, they did not accurately model the pathology of ANCA vasculitis.

The key breakthrough in animal models of MPO-ANCA disease was published in 2002. Xiao *et al* offered a more definitive role *in vivo* for the pathogenic role of MPO-ANCA. MPO-ANCA derived by immunising MPO knockout mice, when injected intravenously into recombinase activating gene (RAG) 2 knockout or wild type mice caused a crescentic pauci-immune necrotising glomerulonephritis in 10.8% and 3.3% of glomeruli sampled respectively at day 6 [100]. This has been termed the passive transfer model. They showed more severe disease following the transfer of anti-MPO splenocytes into RAG2 knockout mice, with crescents and necrosis in approximately 80% glomeruli at day 13. However, there were significant glomerular immune deposits reported in these mice, making it a poor model of pauci-immune disease.

The disease severity in the passive transfer model was shown to be exacerbated by the use of systemic bacterial LPS in a dose dependent manner [32]. The crescent count was significantly increased with the use of 0.5 micrograms/g body weight LPS (5% crescents with no LPS and approximately 20% crescents with LPS use). LPS injection was accompanied by increased circulating TNFα and MPO levels. Furthermore, anti-TNFα therapy attenuated LPS aggravated disease.

Further work as already discussed revealed that neutrophils are crucial in the pathogenesis of disease induction in the passive transfer model, as depletion of neutrophils completely protected mice from development of disease [118].

The genetic background of the mouse has a profound effect on the development of disease in the passive transfer model. 129S6/SvEv and CAST/EiJ mice have a significantly higher crescent count compared to C57BL/6 mice, whilst DBA and PWK/PhJ mice amongst others were protected [218].

We recently showed that the administration of GCSF in addition to LPS exacerbates disease. In our experience mice administered GCSF with LPS had significantly more crescents (29.1% versus 5.8%), more glomerular macrophage infiltration and higher serum creatinine compared to those that received LPS alone [119].

Using a similar approach in immunising MPO deficient mice with MPO, Schreiber *et al* developed the bone marrow transfer model. The immunised knockout mice were lethally irradiated and reconstituted with wild type bone marrow. Antibody producing plasma cells survive the radiation dose and hence continue to produce MPO-ANCA. The antibody is exposed to MPO sufficient neutrophils and monocytes. At eight weeks these mice developed pauci-immune necrotising crescentic glomerulonephritis (7.3 to 80.4% crescents when exposed to 750 rad) [219]. They demonstrated the necessity of MPO positive bone marrow cells rather than resident tissue cells in the pathogenesis of disease and reinforced that ANCA are pathogenic.

Ruth *et al* demonstrated the importance of both cellular and humoral immunity using a different model [123]. Wild type mice were immunised with human MPO inducing MPO-ANCA and CD4 cell reactivity. However, MPO-ANCA levels were low and hence an additional stimulus in the form of sheep anti mouse glomerular binding antibody was used to induce disease. The glomerular binding antibody attracts neutrophils into the kidney leading to glomerular MPO deposition, planted autoantigen for MPO specific CD4+ cells. Depletion of CD4 cells attenuated crescentic glomerulonephritis without altering ANCA titres. Furthermore, μ chain deficient mice, which are unable to make antibody, remain susceptible to disease. The same group later demonstrated the importance of Th17 cells as discussed in section 1.7 [128].

Little *et al* immunised Wistar Kyoto (WKY) rats, a strain known to be susceptible to glomerulonephritis, with human MPO in complete Freund's adjuvant (CFA). These rats developed anti-human MPO, which cross-reacts with rat MPO at 2 weeks and 60%

develop a pauci immune crescentic glomerulonephritis at 6 to 8 weeks. Crescents were reported in 6-15% of glomeruli [220]. Subsequently the group showed that disease was inducible in all rats if a higher dose of MPO was used for immunisation [221]. WKY rats develop disease but Wistar Furth and Brown Norway rat strains do not despite similar antibody titres post immunisation. Once again this suggests a strong genetic component to disease susceptibility.

1.11.2 Models of PR3 ANCA disease

Unlike MPO ANCA disease, attempts to develop models of PR3 ANCA disease have remained unsuccessful. This is thought to be due to the difference in structure as well as expression pattern of PR3 in humans and rodents. PR3 is not detectable on the surface of murine neutrophils and hence the antigen availability to autoantibodies is restricted.

Pfister *et al* immunised PR3 and neutrophil elastase deficient mice with murine PR3 and transferred the antibody to LPS primed wild type mice. The mice did not develop renal or pulmonary pathology. However, a stronger subcutaneous panniculitis was noted following intradermal TNFα injection in the PR3 ANCA passive transfer group compared to controls [222]. This suggests that anti-PR3 antibody has an effect at sites of inflammation but does not cause histological or functional disease in murine kidneys. Subsequently Van der Geld *et al* generated autoantibodies in mice and rats to PR3 by immunisation with human PR3, murine PR3 or chimeric molecules, but again showed no evidence of disease [223].

Immunisation of non-obese diabetic (NOD) mice with murine PR3 led to the development of anti-PR3 antibody, but as with previous studies no evidence of pathology. However, transfer of splenocytes from the immunised NOD mice into immunodeficient NOD-severe combined immunodeficiency (NOD-SCID) mice resulted in severe segmental necrotising crescentic glomerulonephritis (15-31% crescent counts) leading to acute kidney injury. In contrast NOD-SCID mice that received splenocytes from non-immunised mice had no pathology. This suggests that PR3 immune responses are capable of inducing disease *in vivo*. No disease was observed when splenocytes from PR3 immunised C57BL/6 mice were transferred into

immunodeficient C57BL/6-RAG1 knockout mice, suggesting genetic factors play a role in pathogenesis [224]. It was unreported whether the disease observed was pauci-immune.

A more recent study used NOD-SCID-IL2Rγ knockout mice (lack native T, B and NK cells as well as the IL2 receptor), which enabled engraftment of primary human haematopoietic cells. This allowed the development a human mouse chimeric immune system potentially allowing the development of a model using ANCA derived from patients. These mice developed very mild glomerulonephritis and patchy areas of pulmonary haemorrhage following passive transfer of anti-PR3 antibody isolated from patients [225].

1.11.3 Models of LAMP2 ANCA disease

As previously discussed the significance of anti-LAMP2 antibody remains contentious. Kain *et al* showed that immunisation of WKY rats with rabbit anti-human LAMP2 antibody (cross-reacts with rat LAMP2) was sufficient to precipitate a pauci-immune crescentic glomerulonephritis [31]. In contrast Roth *et al* found no evidence of disease on injecting WKY rats with anti-LAMP2 IgG [86].

1.11.4 Other models of glomerulonephritis

There are various forms of animal models of glomerulonephritis. Here I will briefly discuss the more recognized and utilised models in the literature.

Nephrotoxic serum nephritis (NTN) is an established experimental model of antibody mediated glomerular injury. NTN was first developed in rabbits whereby guinea pig anti-rabbit kidney antibody was injected and subsequently other species including rats as well as mice have been used. It is induced by the binding of a foreign antibody to a crude glomerular preparation. The antibody is often raised in rabbit or sheep. NTN is composed of two distinct phases; the heterologous and autologous phases. The primary acute phase peaks approximately two hours after the nephrotoxic antibody administration, resulting in linear anti-GBM antibody deposition, neutrophil influx and proteinuria [226, 227]. This phase is exacerbated with the administration of LPS (or other TLR2 and TLR4 ligands), TNF or IL1β as judged by albuminuria and increasing

glomerular infiltrating neutrophils by almost six fold [228, 229]. This may explain why intercurrent infection often exacerbates disease or induces relapses clinically. TLR2 and TLR4 on circulating leucocytes as well as renal cells contribute to pathogenesis, with TLR4 deficiency on either cell groups leading to reduced neutrophil influx, however albuminuria was reduced to a greater extent when the TLR2 or TLR4 deficiency was on the circulating leucocytes [229, 230].

The autologous phase, which occurs as a result of the host adaptive immune response against foreign glomerular binding antibody, is encountered approximately five to seven days after disease induction [226, 231]. It is suggested that an autoantibody response to previously sequestered antigens contribute to pathogenesis. The host mounts a humoral and cell mediated response resulting in immune complex deposition and frank glomerulonephritis. The antibody mediated injury is reliant on Fc receptors. Fcγ receptor deficient mice are protected from disease [232, 233]. Bone marrow chimera models reveal that circulating leucocyte Fc receptors have the predominant effect in pathogenesis [234].

Interestingly μ chain deficient mice, which have no circulating mature B cells and hence no antibody production, are not protected from disease supporting a role for cell mediated mechanisms [235]. CD4 T cells have a crucial role in pathogenesis through activation of macrophages [236].

Serum sickness models are antibody-mediated glomerulonephritis as a result of immune complex production and deposition within glomeruli following repeated injections of foreign protein. Rabbits were initially injected with bovine serum albumin and subsequently BALB/c mice and Swiss mice were injected with horse spleen apoferritin [237]. Necrotising arteritis of medium sized vessels is a prominent feature. Studies using this model implicated neutrophils and complement in the pathogenesis of vasculitis.

Heymann nephritis is a model of membranous nephropathy in rats. Rats were immunised with antigens from the proximal tubule brush border. A glycoprotein named megalin gp330 located in clathrin-coated pits of glomerular and proximal tubular epithelia was identified as the target antigen [238, 239].

Spontaneous and induced murine models of ***lupus nephritis*** exist (as reviewed in [240]. The most commonly used mouse strains that develop spontaneous disease include the F1 cross between New Zealand Black and New Zealand White (NZB/W) mice, MRL/lpr mice and BXSB/Yaa mice. The NZB/W mice have a primary defect in the loss of tolerance to nuclear antigens resulting in autoreactive T and B cells. The MRL/lpr mice have a Fas gene mutation resulting in a defect in Fas induced T and B cell apoptosis. In the BXSB/Yaa model the telomeric end of the X chromosome is translocated onto the Y chromosome resulting in duplication of at least 16 genes including TLR7. Other susceptibility loci including BXS1-5 thought to be crucial to the phenotype have also been identified [240]. Induced models of lupus nephritis include intraperitoneal injection of pristane in most mice strains, injection of autoimmune sera or lymphocytes from spontaneous lupus prone mice, immunisation of archetypal lupus antigens such as DNA-protein complexes or genetically engineered mouse models of lupus bearing transgenes or knockouts.

1.12 Conclusions

As summarised AAV is a severe systemic disease with complex multi-faceted aspects to the underlying pathogenesis. Substantial progress in the last two decades have begun to unravel the key pathogenic features driving AAV, however, there are still unknowns that need to be explored to bridge the gap towards more patient targeted therapy. The factors that initiate the alternative pathway remain unknown. The roles of monocytes in pathogenesis have not been fully elucidated.

1.13 Aims

The aims of the present study have been summarised below.

- To set up a robust *in vitro* read out of polyclonal ANCA induced neutrophil activation with reduced variability.
- To establish the expression of complement components C3 and C5 by neutrophils and test the effect of ANCA on the expression pattern.

- To assess the impact of ANCA on human peripheral blood monocytes with regards to cytokine production and potentially the impact of ANCA on macrophage development *in vitro*.
- To further elucidate the role of complement in AAV using the passive transfer *in vivo* model of disease and in doing so explore potential activators of the alternative pathway.
- To differentiate the role of local and systemic complement in the disease model of AAV.

The following chapters detail the methods used and the results obtained as a consequence of the pursuit of these aims.

Chapter 2 - Materials and Methods

2.1 Reagents

All reagents were purchased from Sigma Aldrich, UK unless indicated otherwise.

PBS++

2.24mls of 7.5% Sodium Bicarbonate solution and 1.11mls 45% glucose in 500mls PBS (with Ca2+ and Mg2+).

HBSS++

1.25g low endotoxin BSA in 500mls HBSS (without Ca2+ and Mg2+), 19.75mls tissue culture grade sterile water (Thermo Fisher Scientific, UK) and 7.5mls 1M Hepes (final concentration 15mM).

500mM Bicarbonate buffer

160mM Na2CO3 and 330mM NaHCO3, pH 9.5.

20mM Sodium acetate buffer

2.72g sodium acetate trihydrate in 1L tissue culture grade water, pH 4.5.

MPO Purification buffer A

6.7mM sodium phosphate pH 6.0, 1mM MgCl2, 3mM NaCl and 0.5mM PMSF.

MPO Purification buffer B

100mM sodium acetate pH 6.3 and 100mM NaCl.

MPO Purification elution buffer

100mM sodium acetate pH 6.3, 100mM NaCl, 750mM methyl-D-mannopyranoside, 1mM CaCl2, 1mM MgCl2 and 1mM MnCl2.

0.1M Glycine

3.75g glycine in 500mls tissue culture grade water. pH 2.7 using 1M HCl.

1M Tris

24.23g Tris in 200mls tissue culture grade water. pH 9 using 1M HCl.

Formal Saline

1 in 4 dilution of 39% formaldehyde in PBS.

Bouin's Solution

Solution A - Saturated 1.2% w/v picric acid.

Solution B - Formaldehyde 40% w/v.

Bouin's stock solution is 3 volumes of A and 1 volume of B. 1ml/20mls of acetic acid is added immediately prior to use.

Phosphate-Lysine-Periodate (PLP) fixative

A lysine stock solution was prepared by adding 3.65g/100mls (0.2M) lysine monohydrochloride to an equal volume of disodium hydrogen orthophosphate (3.58g/100mls). The solution was adjusted to pH 7.4 and stored at 4^0C. Prior to use, 4g of paraformaldehyde was dissolved in 100mls distilled water while stirred at 60^0C in a fume hood. This milky solution was cleared using 1M NaOH. Immediately prior to use, 1 volume of paraformaldehyde was added to 3 volumes of lysine solution and 0.214g/100mls sodium metaperiodate was added (final concentration of 10mM).

1% Periodic Acid

5g of Periodic Acid in 500mls of tissue culture grade water.

Sucrose Solution

38mM sucrose dissolved in PBS (13g/100mls).

Anaesthetics

1.36mls vetalar - ketamine hydrochloride, 100mg/ml (Pharmacia, Animal Health Ltd, UK) was added to 2mls of domitor - medetomidine, 1mg/ml (Pfizer Ltd, UK) and 15.7mls of PBS. Mice were anaesthetized by IP injection of 200µls of this solution.

Red blood cell lysis buffer

4.17g NH_4Cl, 0.00185g EDTA and 0.5g $NaHCO_3$ in 500mls tissue culture grade water. Filter sterilized and stored in aliquots at -20^{0}C.

1X Tail buffer

50mM Tris-HCl pH 8 (5mls 1M/100mls), 100mM EDTA pH 8 (20mls 0.5M/100mls), 100mM NaCl (2mls 5M/100mls) and 1% SDS (5mls 20%/100mls). Immediately prior to use proteinase K was added to a final concentration of 0.5mg/ml.

1X TE Buffer

10mM Tris-HCl pH8 and 1mM EDTA.

Saturated ammonium sulphate

A saturated ammonium sulphate solution was prepared by dissolving 300g of ammonium sulphate in 500mls of tissue culture grade water. The solution was heated to 56-60^{0}C with frequent shaking. It was then cooled overnight with crystal formation indicating saturation.

Preparation of dialysis tubing

Dialysis tubing (Medicell, UK) was cut to an appropriate length and submerged in 200mls of tissue culture grade water with 2% sodium bicarbonate and 1mM EDTA. It was incubated at 80^{0}C for 30 minutes. It was then washed with 200mls tissue culture grade water. The tubing was kept wet until usage. Two knots were tied at the bottom end of the tubing and a clip was attached between them to prevent leaks.

Monoclonal antibodies

Target	Isotype	Clone	Supplier
Human MPO	IgG1 κ	266.6K2	IQ Products, Netherlands
Human PR3	IgG1 κ	WGM2	Hycult Biotech, Netherlands
TNP (control)	IgG1 κ	107.3	BD Biosciences, UK

Table 2.1 – Mouse anti human monoclonal antibodies used in assays.

Flow cytometry and Western Blot antibodies

Target	Isotype	Clone	Conjugate	Dilution	Supplier
Human C3a	Mouse IgG1	4H3	APC	1:1000	Abcam, UK
Human C3	Chicken IgG	Polyclonal	-	1:300	Sigma, UK
Human C5a	Mouse IgG1	2952	PE	1:200	Abcam, UK
Human C5	Rabbit IgG	Polyclonal	-	1:200	Abcam, UK
Human CD66b	Mouse IgM k	G10F5	FITC	1:12	BD Biosciences, UK
Human CD11b	Mouse IgG1 k	ICRF44	APC	1:6	BD Biosciences, UK
Human C3	Goat IgG	Polyclonal	-	1:1000	Calbiochem, UK
Human C3a	Mouse IgG1 k	013-16	-	1:5000	Abcam, UK
Rabbit IgG	Goat IgG	Polyclonal	Alexa Fluor 488	1:400	Invitrogen, Life Technologies, UK
Chicken IgG	Goat IgG	Polyclonal	Alexa Fluor 488	1:400	Invitrogen, Life Technologies, UK

Goat IgG	Donkey IgG	Polyclonal	HRP	1:1000	Santa Cruz, USA
Mouse IgG	Sheep IgG	Polyclonal	HRP	1:2000	GE Healthcare Life Sciences, UK
Mouse Ly6G	Rat IgG2b k	1A8	Alexafluor 700	1:200	BD Biosciences, UK
Mouse CD45.2	Mouse IgG2a	104	APC	1:200	eBioscience, UK
Human CD206	Mouse IgG1 k	15-2	APC	1:100	Biolegend, UK
Human CD80	Mouse IgG1 k	2D10	PE	1:100	Biolegend, UK

Table 2.2 – Antibodies used for flow cytometry and western blot analysis.

Immunohistochemistry antibodies

Target	**Isotype**	**Clone**	**Conjugate**	**Dilution**	**Supplier**
Mouse CD68	Rat IgG2a	FA11	-	1:200	AbD Serotec, UK
Mouse MBL	Rat IgG2a	16A8	-	1:50	Hycult Biotech, Netherlands
Mouse C3	Rat IgG2a	RMC11H9	-	1:200	Cedar lane, Canada
Rat IgG (H+L)	Mouse IgG	Polyclonal	DyLight488	1:200	Jackson Immunoresearch, USA

Table 2.3 – Antibodies used for immunohistochemistry.

ELISA kits

Target	Dilution of supernatant, serum or urine used	Supplier
Mouse albumin	1:200	Bethyl laboratories, USA
Mouse C5a	1:1000	R&D DuoSet ELISA, UK
Human Lactoferrin	1:500	Hycult Biotech, UK
Human IL1β	1:100	R&D DuoSet ELISA, UK
Human MPO	1:50	R&D DuoSet ELISA, UK
Human MIP1α	1:2000	R&D DuoSet ELISA, UK
Human IL8	1:1000	R&D DuoSet ELISA, UK
Human CSF1	1:2	R&D DuoSet ELISA, UK
Human TGFβ	1:1.4	R&D DuoSet ELISA, UK

Table 2.4– ELISA kits used.

2.2 Mouse promyelocytic (MPRO) cell culture and MPO purification

The MPRO cell line (clone 2.1 ATCC, LGC Standards, UK) is a murine granulocyte cell line derived from bone marrow cells of male BDF1 mice infected with the retroviral vector LRARalpha403SN. These cells differentiate in the presence of GMCSF into neutrophil granulocytes with promyelocyte characteristics such as azurophilic granules [241].

The medium used consisted of Iscove's Modified Dulbecco's Media (IMDM) (PAA / GE Healthcare Life Sciences, UK) with 20% foetal bovine serum (FBS), 1% Penicillin/Streptomycin (Thermo Fisher Scientific, UK) and 10ng/ml GMCSF (Peprotech Biotech, UK).

The cells were grown to a density of 2 x 10^6cells/ml. Upon harvesting, the cell pellets were resuspended in buffer A with 100mM PMSF and stored at -80^0C.

MPRO cell pellets were defrosted and centrifuged at 167xg for 10 minutes. The pellets were pooled in buffer A containing 100mM PMSF. The cells, while kept on ice, were homogenized using a probe sonicator. The cell lysate was then centrifuged at 20,000xg for 30 minutes using a J2-21MIE ultracentrifuge (Beckman Coulter, UK) with a JA-14 rotor. The cell pellet was resuspended in buffer A containing 100mM PMSF at a ratio of 10ml of buffer per 1ml of cell pellet. Cetyltrimethylammonium bromide was added to a final concentration of 1% and the mixture was stirred vigorously for 2 hours at 4^0C. The solution was subsequently centrifuged at 20,000xg for 20 minutes at 4^0C and the pellet was discarded. The sample has a distinct green colour by this stage (see figure 2.1).

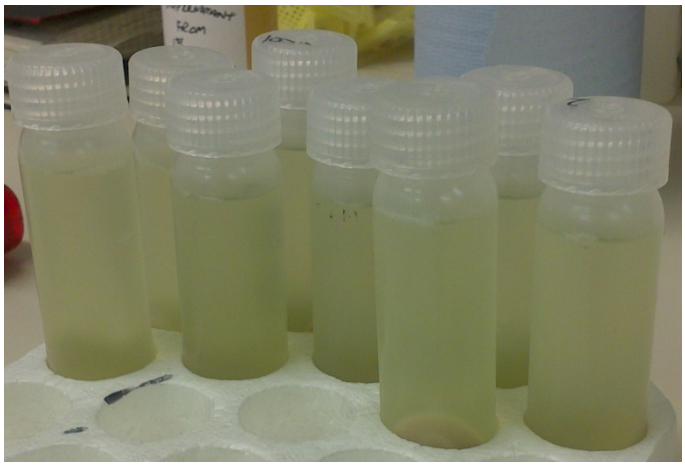

Figure 2.1 – MPRO cell pellet processing, revealing the green hue of the samples.

The sample was concentrated and buffer exchanged into buffer B using a Vivaflow 50 filtration device (Sartorius Stedim, UK) with a 30kDa molecular weight cut off, and stored at 4^0C overnight. $CaCl_2$, $MgCl_2$ and $MnCl_2$ were then added to a final concentration of 1mM of each.

A 1ml Concanavalin A Sepharose (GE Healthcare Life Sciences, UK) column was equilibrated with 50mls of 0.2µm filter sterilized buffer B containing 1mM of each of the ions $CaCl_2$, $MgCl_2$ and $MnCl_2$ at a flow rate of 60mls/hr. The sample was diluted in buffer B, containing the respective ions, filter sterilized, and run through the column at 12mls/hr. The column was washed with 7mls of buffer B containing ions at 12mls/hr. The MPO was eluted using elution buffer (750mM mannopyranoside diluted in buffer B with ions) at 60mls/hr and 1ml fractions were collected.

The absorbance was measured at 280nm and 430nm using a spectrophotometer (Beckman Coulter, DU-530). MPO containing fractions have a distinct green colour. The pooled aliquots containing MPO, as determined by absorbance measurements at 430nm, were dialysed against PBS at 4^0C (dialysis tubing was prepared as previously mentioned). After 4 hours the PBS was changed and the sample was left to dialyse overnight at 4^0C.

The purity of the MPO preparation in relation to total protein was determined by its Reinheit Zahl (RZ) value, the ratio of 430nm to 280nm absorbance (RZ = A430/A280). An RZ>0.84 is considered to be of high purity [242].

A 1ml HiTrap SP FF ion exchange column (GE Healthcare Life Sciences, UK) was equilibrated with 10mls of PBS at a flow rate of 60mls/hr. It was then washed with 10mls of 1M NaCl dissolved in PBS at 60mls/hr before being subjected to a final wash of 10mls PBS at 60mls/hr. The sample was passed through the column at 30mls/hr. The MPO, which is bound to the column, was eluted using stepwise increases of NaCl in PBS. A starting concentration of 0.075M NaCl was used to elute the majority of the MPO. The remainder of the MPO was eluted using 0.1M NaCl. 1ml fractions were collected and analysed at 280nm and 430nm using a spectrophotometer. The MPO containing fractions were pooled and buffer exchanged into PBS using PD10 columns (GE Healthcare Life Sciences, UK). Each PD10 column was first calibrated with 50mls PBS. After calibration, 2.5mls of sample was added to each column followed by 3mls of PBS and the follow through which contained the MPO was collected. The absorbance was then measured at 280 and 430nm and the concentration calculated using the following information.

Absorbance at 430nm of 0.19 = 125µg/ml MPO

The sample was adjusted to a final concentration of 1mg/ml using Vivaspin 20 ultrafiltration device with 30kDa molecular weight cut off (Sartorius Stedim, UK). After determination of the RZ value the MPO was stored in aliquots at -20^0C.

At this stage a 40 litres culture of MPRO cells will yield approximately 5mg of MPO (RZ approximately 0.6).

2.3 Animal experiments

The MPO deficient mice on a C57BL/6 background were purchased from Jackson Laboratories (Bar Arbour, Maine, USA) [243]. The C57BL/6 wild type mice were purchased from Harlan (Bicester, Oxon, UK). The C3 deficient mice were obtained from Professor Michael C Carroll [244], MASP2 deficient mice were obtained from Professor Wilhelm Schwaeble [245] and factor B deficient mice were obtained from Dr Harvey R Colten [246]. Naturally occurring DBA/J2 C5-deficient mice backcrossed on to the C57BL/6 genetic background were a generous gift from Professor Matthew Pickering [247]. These mice had all been backcrossed at least 10 generations to the C57BL/6 background and were then bred in house.

All animal experiments were performed in accordance with Home Office regulations.

2.3.1 Genotyping mice

Breeding mice from each strain were genotyped prior to *in vivo* experiments by polymerase chain reaction (PCR) from DNA acquired in ear clippings. The clippings were incubated overnight at 55^0C in 375µls of tail buffer with 20mg/ml proteinase K. The degraded ear tissue was vortexed thoroughly and 125µls of saturated NaCl was added. The solution was again mixed thoroughly and centrifuged at 9000rcf for 10 minutes. 375µls of this solution (taken from the top without disturbing the pellet) was placed into an empty eppendorf tube and 250µls of isopropanol was added. The DNA was precipitated out of solution by inverting the tube. It was then centrifuged at 9000xg for 4 minutes using a table-top microcentrifuge and the supernatant was discarded. The pellet was washed by adding 750µls of 70% ethanol. The ethanol was discarded and the pellet allowed to air dry. Finally it was resuspended in 150µls of TE buffer and stored at -20^0C.

The sequences of the primers used are as depicted below (forward primer first then reverse primer listed):

MPO wild type: 5'- CTGGACGCCAGGAGTCAATCG - 3', 5' - GTGAAGAAGGAGAAGCGGGTAG - 3'

MPO deficient: 5’ - TCCTCGTGCTTTACGGTATCG - 3’, 5’ - GTGAAGAAGGAGAAGCGGGTAG - 3’

Reaction conditions: 94^0C for 15 minutes, 35 cycles at 55^0C for 30 seconds, 72^0C for 1 minute, and then 72^0C for 10 minutes.

MASP2 wild type: 5’ - CATCTATCCAAGTTCCTCAGA - 3’, 5’ - AGCTGTAGTTGTCATTTGCTTGA - 3’

MASP2 deficient: 5’ - CTGATCAGCCTCGACTGTGC - 3’, 5’ - AGCTGTAGTTGTCATTTGCTTGA - 3’

Reaction conditions: 94^0C for 15 minutes, 35 cycles at 60^0C for 30 seconds, 72^0C for 1 minute, and then 72^0C for 10 minutes.

Factor B wild type: 5’ - CTTCTCAATCAAGTTGGTGAGGCACCGCTT - 3’, 5’ - GCAATACGCTGCCCACGACCGCAG - 3’

Factor B deficient: 5’ - TGCGTGCAATCCATCTTGTTCAATG - 3’, 5’ - GCAATACGCTGCCCACGACCGCAG - 3’

Reaction conditions: 94^0C for 15 minutes, 35 cycles at 64^0C for 30 seconds, 72^0C for 1 minute, and then 72^0C for 10 minutes.

Primers were diluted in sterile water to a concentration of 2µM. For each PCR reaction 1µl of template DNA was added to 11.5µls of primers and 12.5µls of HotStarTaq mastermix (Qiagen, UK) to give a final volume of 25µls and a final primer concentration of 1µM. PCR reactions were run on a PE Applied Biosystems GeneAmp PCR System 9700 under the respective conditions above. The samples were run on an agarose E-gel 2% (Life technologies, UK) using a self-contained power system for 15 minutes.

For C5 deficient mice we confirmed that mice used were C5 deficient by testing serum using a mouse C5 ELISA duoset (R&D Systems, UK). See general principles of ELISA studies in section 2.5.1.

2.3.2 Generating MPO-ANCA

MPO for immunization was prepared by mixing 50µls of MPO (1mg/ml) with 450µls PBS and 500µls of complete freund's adjuvant (CFA) for first immunisation or 500µls incomplete freund's adjuvant (iCFA) for subsequent boosts. The mixture was kept on ice and homogenized using a T-10 ultra-turrax homogenizer. The extent of homogenization was tested by aspirating a small drop of the solution onto water. If the sample remained intact and did not disperse in the water it was deemed ready for injection.

MPO deficient mice, approximately 6-8 weeks old, were immunized with 10µg (200µls of MPO preparation) of murine MPO (purity stated in results sections) using subcutaneous (SC) injection on day 0 in CFA. They received 100µls of this solution on either side of the flank.

To gain a higher yield of antibody per mouse and hence reduce the number of MPO deficient mice used as a whole (the three Rs principle), we injected mice with a sarcoma cell line to generate ascites. On day 14 wild type C57BL/6 mice were injected with $1x10^6$ (in 200µls PBS) Sarcoma 180 TIB-66 cells (ATCC, UK) by intraperitoneal (IP) injection. These mice were assessed twice a day and sacrificed 10 to 14 days later for ascitic fluid samples. The ascitic fluid samples were pooled and subsequently 100µls of the ascites was injected into each immunised MPO deficient mouse on days 24 to 28 (depending on development of ascites in the wild type mice) of the immunization protocol. The mice were examined twice a day

On days 21 and 35 of the immunization protocol the MPO deficient mice were boosted with 10µg MPO by IP injection in iCFA. On days 38 to 42 the mice were exsanguinated and the serum was pooled. The ascitic fluid was collected by paracentesis after sacrifice. MPO-ANCA titres in serum were measured by ELISA. Refer to section 2.4 for MPO-ANCA IgG purification methodology.

2.3.3 Generation of bone marrow chimera

Donor bone marrow cells were isolated from the tibia and femurs of mice. The muscle and tissue was stripped away and the bones were flushed with PBS. Repeated

pipetting dispersed the clumps of cells and the cell suspension was then centrifuged at 150xg for 10 minutes and the pellet resuspended in 1ml PBS. The total number of viable cells was counted using trypan blue viability stain and a haemocytometer. The cells were then resuspended at a final concentration of $25x10^6$ cells/ml. Recipient mice were lethally irradiated with 9 Gy in a single dose using a caesium source irradiator. They were then injected with 200µls of the cell suspension ($5x10^6$ cells) using the intravenous (IV) route immediately after irradiation.

A parallel cohort of chimeras were made between wild type C57BL/6 mice and C57BL/6 mice congenic for CD45.1 (B6.SJL-Ptprca Pepcb/BoyJ). Chimerism was determined by flow cytometry for CD45.2 on whole blood using anti mouse CD45.2 APC Clone 104 (eBioscience, UK) and chimerism was determined to be >90% in the animals (n=7).

2.3.4 Coagulation assays

100µls of trisodium citrate 3.2% was drawn into a 1 ml syringe and 900µls of blood was taken by intra-cardiac puncture under terminal anesthesia. Plasma was centrifuged twice at 800xg for 10 minutes, aliquoted and frozen at -20^0C until analysed.

The coagulation assays were performed by Kiran Parmar and Agnieszka Kuffel (Professor Beverley Hunt, Thrombosis & Vascular Biology, Guy's and St Thomas' NHS Foundation Trust, London, UK). Thrombin generation was monitored with a Fluoroskan Ascent Thrombinoscope (Thermo Electron Corporation, UK) and Thrombinoscope software version 5. Samples were run at a dilution of 1 in 3 and at 33^o C [248]. Clauss Fibrinogen was measured using the ACL300R analyser, and using the HemosIL Fibrinogen-C reagent by Werfen UK. Prothrombin fragment 1.2 was measured by ELISA using Enzygost F1+2 Micro kit from Sysmex UK Ltd.

2.3.5 Passive transfer model of ANCA associated vasculitis

On day -8 and -4 C57BL/6 mice were given 30µg of pegylated human GCSF (Neulasta®, Amgen, UK) by SC injection. On day -1, the mice were bled from the saphenous vein for baseline serum creatinine measurement. Baseline urines were also collected. On day 0, each mouse was given 2mg of the purified MPO-ANCA (refer to section 2.4 for IgG

purification methodology) via IV injection using the tail vein. They were also given 10µg of LPS (*Escherichia Coli* 0111 B4 from Enzo Life sciences, UK) on day 0 and day 3 by IP injection. Additionally they received doses of 30µg GCSF on days 0 and 4. Urine was collected on day 7. A terminal bleed was performed on day 7. In the C5 bone marrow chimera experiment, 2mg MPO-ANCA was given via IP injection and 30µg of pegylated GCSF was given by SC injection on day -4 and day 0. 2.5µg LPS was given IP on day 0 only.

Mouse kidneys were immediately dissected out and cut into half along the longitudinal axis. Two halves were fixed in Bouin's solution for 4 hours then transferred to formal saline. These kidneys were processed overnight using Leica ASP 300 S processor and embedded in hot wax. A single half was fixed in PLP at 4^0C for 4 hours then transferred into 13% sucrose solution overnight. The samples were subsequently frozen in cooled isopentane and fixed onto corkboards using OCT (Thermo Fisher Scientific, UK) and stored at -80^0C. The remaining half kidney was placed onto corkboards using OCT and immediately snap frozen in pre-cooled isopentane. The samples were stored at -80^0C.

2.3.6 Albuminuria measurement

Murine albuminuria was measured using a commercially available ELISA kit (Bethyl laboratories, USA). The technique is explained separately to section 2.5.1 in view of important differences in buffers.

ELISA plates were coated with 100µls/well of a 1 in 100 dilution of capture antibody diluted in 500mM bicarbonate buffer. Plates were coated for 1 hour at 37^0C and then washed 4 times using a wash buffer (0.05% Tween 20 in PBS). Plates were blocked using 100µls/well 1% bovine serum albumin (BSA) for 30 minutes. A standard curve ranging from 1000–7.8ng/ml was prepared from a murine albumin stock. Urines were diluted 1 in 200 in 1% BSA. After blocking for 30 minutes, 100µls of each standard and sample were added in duplicate to the plate for 1 hour at room temperature. The plate was then washed 4 times in PBS/0.05% Tween 20. The horseradish peroxidase (HRP) conjugated detection antibody was diluted 1 in 50,000 in 1% BSA and 100µls/well was added to the plate for 1 hour in the dark. The plate was washed as before. The HRP substrate, O-phenylenediamine dihydrochloride (OPD) was prepared by dissolving

each of two tablets in 20mls of deionized water. 100µls of OPD solution was added to each well and was allowed to develop in the dark for approximately 20 minutes. The reaction was stopped by the addition of 100µls 1N H_2SO_4. The reaction was analysed at 490nm using a SpectraMax Plus384 microplate reader (Molecular Devices, UK). The total albumin content of the urine was calculated from albumin concentration and the urine volume.

2.3.7 Haematuria

Haematuria was measured by dipstick (Combur-Test® from Roche, UK). Severity was measured on a scale ranging from 0 (none) to 4 (severe).

2.3.8 Serum and urine creatinine measurement

Serum and 24 hour urine creatinine concentrations were measured by Dr N Dalton and Dr C Turner by electrospray mass spectrometry in the Department of Paediatric Biochemistry at the Evelina Children's Hospital, Guy's and St Thomas' NHS Foundation Trust, London. A volume of 5µls of neat serum or urine was diluted into 250µls of D3 creatinine isotope and 250µls of acetonitrile containing 0.05% formic acid. Creatinine concentrations were measured using Applied Biosystems MDS Sciex API 4000 (Applied Biosystems, UK) and Applied Biosystems Analysis Version 1.4 software.

When assessing spot urine albumin creatinine ratios, the urine creatinine concentration was determined using a creatinine assay kit (Diazyme, Germany). Urine samples were diluted 1 in 20 in PBS and the provided standard was prepared to provide a range of concentrations from 39.6 to 0 µmol/L. 32µls of each sample or standard was added to a 96 well microplate in duplicates. 246µls of reagent 1 (sarcosine oxidase) was added to the sample and standard wells and incubated for 5 minutes at 37^0C. The plate was analysed at 550nm using a SpectraMax Plus384 microplate reader (Molecular Devices, UK). 90µls of reagent 2 (creatininase) was added to all samples and incubated in the dark for 5 minutes at 37^0C and analysed again at 550nm. The difference in optical density at the two time points was used to extrapolate the creatinine concentration from the standard curve.

2.3.9 Peripheral blood neutrophil counts

A volume of 100µls of heparin treated whole blood was added to each eppendorf. 25µls of a 1 in 125 pre-diluted Fc block (Becton Dickinson, Oxford, UK) was added for 20 minutes at room temperature. The appropriate Ly6G antibody (see table 2.2) was added and the blood was incubated at room temperature for 20 minutes in the dark. Erythroyctes were lysed using 2mls of a 1 in 10 dilution BD FACs Lysing solution (Becton Dickinson, Oxford, UK) in deionized water. The blood was then centrifuged at 280xg for 5 minutes. The supernatant was discarded and the cells resuspended in 2mls of PBS and centrifuged at 280xg for 5 minutes. Finally the cells were resuspended in 500µls of PBS with 0.1% sodium azide. FACs analysis was carried out immediately after staining using a FACS Canto flow cytometer (Becton Dickinson, Oxford, UK) and FACsDIVA software (Becton Dickinson, Oxford, UK). Neutrophils were identified based on their forward and side scatter profile. A minimum of 10,000 events were collected for each sample and data was analysed using FlowJo software (Treestar, Ashland, OR, USA). Total circulating neutrophil counts were determined from the percentage of Ly6G positive cells and total leucocyte numbers.

2.3.10 Periodic acid Schiff stain and Mayer's Haematoxylin

Paraffin embedded sections of 1µm thickness were cut using a microtome and placed onto microscope slides. The sections were baked onto the slides at 60^0C for a minimum of 30 minutes before staining. The slides were placed in xylene for 10 minutes in order to dissolve the wax. They were rehydrated by placing them in 100%, 90% and 70% alcohol for 10 seconds each. They were subsequently washed in running distilled water for 3 minutes before being put into 1% periodic acid for 10 minutes. They were washed for 3 minutes in running distilled water. Using a pasteur pipette each slide was covered in periodic acid schiff stain (Thermo Fisher Scientific, UK) for 20 minutes in the fume hood and again washed for 3 minutes. The slides were then treated with Mayer's haematoxylin (VWR, UK) for 5 minutes and washed for a further 5 minutes. They were then dehydrated by submerging the sections in 70%, 90% and 100% ethanol for 10 seconds each and were mounted in DPX (Thermo Fisher Scientific, UK).

These sections were used to score the number of glomerular crescents. Glomerular crescents were defined as the occurrence of two or more layers of cells in the Bowman's space. The numbers of crescents identified were expressed as a percentage of a total of 100 glomeruli per animal.

2.3.11 Immunofluorescent staining for glomerular macrophages

Sections of frozen kidney (PLP fixed) were cut to 5µm thickness using a cryostat and placed onto multispot slides (C.A Hendley, UK). The slides were allowed to air-dry overnight at room temperature. A 1 in 200 dilution (in PBS) of a 1mg/ml stock rat anti-mouse CD68 antibody, clone FA11 (AbD Serotec, UK) was prepared. 100µls of this staining solution was added to each kidney section and incubated in the dark in a humidity tray for 2 hours. The slides were washed in PBS for 5 minutes. 100µls of a 1 in 200 dilution (in PBS) of a 1.5mg/ml stock of a DyLight488 mouse-anti rat IgG (Jackson Immunoresearch, USA) was added to each section and incubated for 2 hours in the humidity tray. The slides were washed as before. The slides were mounted using permafluor (Thermo Fisher Scientific, UK) and scored within 48 hours. Individual macrophages infiltrating the glomeruli were counted and a mean number was calculated from a minimum of 20 glomeruli per section.

2.4 IgG purification

2.4.1 MPO-ANCA purification from mouse serum and ascites

IgG was purified from pooled mouse serum and ascites by ammonium sulphate precipitation and subsequent protein G chromatography.

Large clumps of fat and fibrin from the thawed ascites samples were removed manually. Cleanascite (Gentaur, USA) was added to the ascites sample at a ratio of 1:4 (1 part Cleanascite : 4 parts ascites) and incubated for 2 hours at 4^0C on a shaker plate. The sample was centrifuged at 1,000xg for 20 minutes the supernatant was decanted. The ascites sample was cooled to 4^0C and acetic acid was used to lower the pH to 4.9. At this pH the sample was left on ice for 1 hour to precipitate the fibrin. The sample was centrifuged at 9,000xg for 1 hour at 4^0C. The supernatant was collected and the

pH was increased back to 7 with the use of 1M sodium hydroxide. The serum sample was pooled with the ascites samples at this stage.

An equal volume of saturated ammonium sulphate was added to the pooled sample, in a drop-wise manner while gently shaking the tube, to a final concentration of 50%. The sample was left at 4^0C overnight for the antibody to precipitate out of solution. The sample was centrifuged at 1500xg for 20 minutes and the pellet resuspended in PBS and aspirated until completely dissolved. The sample was dialysed against PBS overnight, with the PBS being replaced after 4 hours.

The dialysed sample was diluted 1 in 3 in PBS in preparation for protein G chromatography. A 5ml HiTrap protein G column (GE Healthcare Life Sciences, UK) was equilibrated with 50mls of PBS at a flow rate of 60mls/hr. The sample was filter sterilized through a 0.2µm filter (Sartorius Stedim, UK) and run through the column at a flow rate of 10mls/hr. The column was washed with 40ml of PBS at 60mls/hr. The IgG was eluted using 0.1M glycine-HCl solution, pH 2.7, into eppendorfs containing 150µls of Tris pH 9. 1.5ml fractions were collected. The absorbance at 280nm of each fraction was measured using a spectrophotometer (Beckmann Coulter DU-530). Selected fractions were pooled and buffer exchanged into PBS using PD10 desalting columns (GE Healthcare Life Sciences, UK). The absorbance at 280nm of the pooled sample was determined using the following information.

Absorbance at 280nm of 1.4 = 1mg/ml.

The concentration of the antibody was adjusted to 10mg/ml using a Vivaspin 20 ultrafiltration device with 30kDa molecular weight cut off (Sartorius Stedim, UK). The antibody was stored in 1ml aliquots at -20^0C.

2.4.2 IgG Purification from patient and control plasma samples – Sodium chloride precipitation

Plasma stored at -80^0C was defrosted in a water bath at 37^0C. Solid sodium chloride was added at 18g/100mls of plasma to remove fibrin. I had previously compared the use of sodium chloride and ammonium sulphate precipitation for the removal of fibrin with Dr Alice Coughlan (Coughlan A. 2012 The development of a humanised mouse

model of ANCA associated vasculitis, King's College London) prior to starting my PhD. The two techniques were similar in yield, with the sodium chloride precipitation method not requiring an extra dialysis step; hence this was the method of choice for the PhD. The plasma was left to precipitate overnight at 4^0C. The sample was centrifuged at 1000xg for 30 minutes and the supernatant was removed and diluted 1 in 5 in endotoxin free, tissue culture water before being passed through a 0.2µm filter for purification using a Protein G column (GE Healthcare Life Sciences, UK). 1ml Protein G columns were first equilibrated with 10mls 0.2µm filtered PBS using a syringe pump set at 20mls/hr before the filtered sample was run through the column at 10mls/hr. The column was washed with 5mls sterile filtered PBS and the bound IgG was eluted by passing 0.2µm filtered 0.1M glycine, pH 2.7, through the column at 20mls/hr. The eluate was collected in 1.5ml fractions into eppendorf tubes containing 150µls 1M Tris, pH 9. The wavelength of each fraction of the eluted antibody was measured at 280nm using a spectrophotometer and samples with an OD greater than 1.5 were pooled and buffer exchanged into PBS using a PD10 desalting column (GE Healthcare Life Sciences, UK). The final concentration of antibody was calculated and the antibody was aliquoted and stored at -20^0C.

The endotoxin concentration in the final IgG preparations was measured externally by Lonza Company (Vervier, Netherlands) using a limulus amebocyte lysate kinetic chromogenic assay. For all 30 polyclonal IgG preparations used, the endotoxin level was less than 0.25 eU/250ug IgG.

2.4.3 Generation of $F(ab)_2$ fragments

Whole IgG (>5mg/ml) was buffer exchanged using PD10 columns (GE Healthcare Life Sciences, UK) into 20mM sodium acetate buffer. The pepsin preparation (Thermo Fisher Scientific, UK) was prepared as follows; 0.25mls of the 50% slurry of immobilised pepsin was added to the 20mM sodium acetate buffer, centrifuged at 1000xg for 5 minutes and the buffer was decanted and discarded. This step was repeated once more and the immobilised pepsin was resuspended in 0.5mls of the 20mM sodium acetate buffer. 1ml of IgG was added to the immobilised pepsin and incubated for 4 hours at 37^0C in a high speed shaking water-bath. The contents were centrifuged at 1000xg for 5 minutes and the crude digest was aspirated into a new eppendorf tube.

The $F(ab)_2$ fragments were separated from undigested IgG using protein A affinity columns (GE Healthcare Life Sciences, UK). 1ml protein A columns were utilised. The column was first washed with 10mls of the sodium acetate buffer at 30mls/hr and then the sample was run through the column at 10mls/hr. 1ml aliquots were collected. The wavelength of each fraction of $F(ab)_2$ (diluted at 1:20) was measured at 280nm using a spectrophotometer and samples with an OD greater than 0.1 were pooled.

Sodium dodecyl sulphate polyacrylamide gel electrophoresis (SDS-PAGE) chromatography was performed to demonstrate the purity of whole IgG and the $F(ab)_2$ fragments for all preparations. 5µg of each antibody or $F(ab)_2$ fragment was mixed with a LDS loading buffer 4X (Life Technologies, UK) and a volume of 20µls was loaded onto a 4-12% NuPage Bis Tris gel (Life Technologies, UK). A volume of 10µls of SeeBlue Plus 2 pre-stained standard (Life Technologies, UK) was added in a separate well. The gel was run using a PowerEase500 power supply (Life Technologies, UK) at 200V for 30 minutes. The gel was removed from the cassette and washed 3 times in deionized water for 5 minutes each time on a shaker plate. 20mls of SimplyBlue SafeStain (Life Technologies, UK) was added to cover the gel and the manufacturer's microwave procedure was used. The gel was scanned.

2.4.4 Use of polyclonal IgG or $F(ab)_2$ fragments

For all *in vitro* assays when patient ANCA were used to stimulate the neutrophils or monocytes, the polyclonal ANCA samples were thawed out from -20^0C and centrifuged at 16,000xg at 4^0C using a microcentrifuge to remove aggregates. Patient derived polyclonal ANCA were used at a final concentration of 250µg/ml. $F(ab)_2$ fragments were used at the same molarity as the corresponding polyclonal antibodies.

2.5 *In vitro* studies

2.5.1 General principles of ELISA studies

The ELISA kits used are highlighted in table 2.4. The general ELISA protocol involved the use of a 96 well microplate that was coated with the respective capture antibody (100µls/well) diluted to the manufacturer's recommendation in PBS. The plate was

sealed and incubated overnight at room temperature. The following day the plate was washed using 0.05% Tween 20 in PBS and blotted against clean paper towels. The plates were blocked using 300µls/well 1% BSA in PBS for all ELISAs except the TGFβ ELISA where 5% Tween 20 was used instead as recommended. The plate was incubated for 1 hour at room temperature. The wash was repeated. 100µls/well of the respective prepared standards or samples were added in duplicates, the plate was sealed and incubated for 2 hours at room temperature. For the TGFβ ELISA, the samples were initially activated in polypropylene tubes with the addition of 1N HCl (20µls 1N HCl to 100µls supernatant), incubation at room temperature for 10 minutes then neutralisation with 1.2N NaOH/0.5M HEPES at the same volume as the 1N HCl used.

The wash step was repeated and 100µls/well of the detection antibody was added at the recommended dilution. The plate was again incubated for 2 hours at room temperature. The wash was repeated and 100µls/well of streptavidin-HRP was added to each well. The plate was covered and incubated in the dark for 20 minutes. The wash step was repeated for the final time and 100µls/well of the substrate OPD solution was added to each well and was allowed to develop in the dark for approximately 20 minutes. The reaction was stopped by the addition of 100µl 1N H_2SO_4. The reaction was analysed at 490nm using a SpectraMax Plus384 microplate reader (Molecular Devices, UK). The average of the duplicate readings for each standard or sample was calculated and the average zero standard optical density was subtracted. A standard curve was created using Graphpad Prism software (Graphpad Software Inc, USA) and the concentrations of the measured samples were extrapolated and multiplied by the dilution factor used.

Other modifications to the ELISA techniques are described in detail in the respective sub-sections.

2.5.2 Human neutrophil isolation from blood

Heparinised blood from healthy controls was diluted 1:1 with Hanks Balanced Salt Solution (HBSS). In 15ml tubes, 8mls of the blood/HBSS mixture was carefully layered

on top of 4mls Ficoll-Paque™ PLUS (GE Healthcare Life Sciences, UK). This was centrifuged for 20 minutes at 380xg, 20^{0}C and with zero deceleration (see figure 2.2).

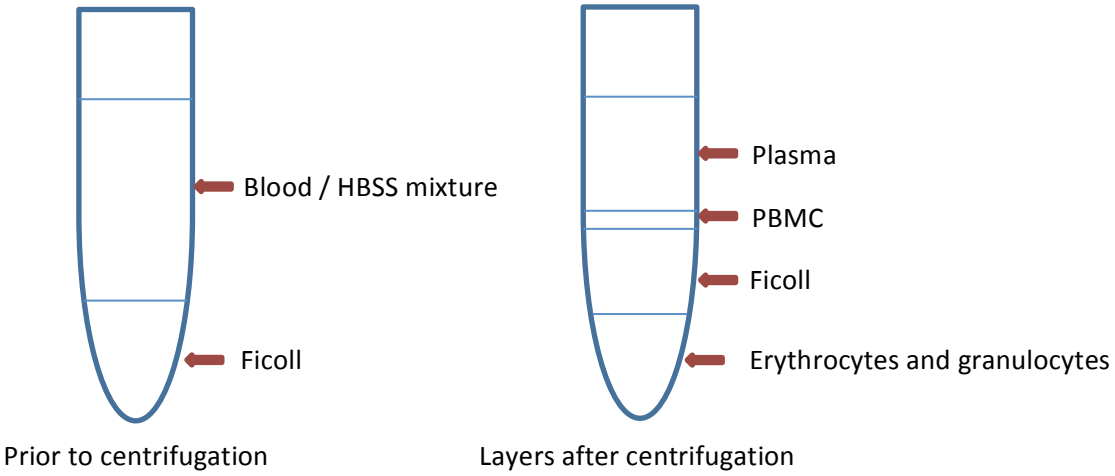

Figure 2.2 – Diagrammatic representation of layers of blood and respective constituents prior to and after centrifugation following Ficoll layering.

The upper layer including the lymphoctyes was aspirated with circular movement. Gentle tapping loosened the sedimented pellet and 10mls red blood cell lysis buffer was added to lyse the erythrocytes. The tube was inverted several times and incubated on ice for 5 minutes, with occasional mixing. This was centrifuged at 380xg, 20^{0}C for 5 minutes. The supernatant was aspirated, being careful not to disturb the cell pellet, which was then resuspended in 10mls red blood cell lysis buffer and incubated on ice for 5 minutes. This was spun at 280xg, 20^{0}C for 5 minutes. The supernatant was removed and the pellet was washed with ice-cold HBSS and centrifuged at 200xg for 5 minutes. The cells were resuspended in HBH (500mls HBSS + 5mls 1M HEPES) or PBS++.

The cells were counted using a 1 in 10 dilution of Turk's Solution. An Olympus BX51 microscope (Olympus Microscopy, UK) set to phase contrast and a counting chamber (improved Neubauer haemocytometer) was used for calculating cells numbers. Turk's solution is a mixture of acetic acid and gentian violet that haemolyses red blood cells and stains the nuclei of white cells purple. The total number of cells within the 25 grid square was counted. This was multiplied by the dilution factor and 10^4 to obtain the number of cells/ml of medium i.e. cell concentration. The cell concentration was multiplied by the volume of the cell suspension to obtain the total cell yield.

2.5.3 Mouse neutrophil isolation from bone marrow

Bone marrow cells were isolated from the tibia and femurs of mice. The muscle and tissue was stripped away and the bones were flushed with HBSS++ using a 27G needle. Clumps of cells were dispersed by repeated pipetting. The cells were centrifuged at 385xg for 10 minutes. In the meantime 62% and 55% Percoll were prepared using HBSS for dilution of sterile Percoll. 6mls of 62% Percoll was gently underlayed beneath 3mls of 55% Percoll to create a gradient. The cell pellet was resuspended in HBSS++, gently placed onto the Percoll gradient and centrifuged at 1256xg for 30 minutes at low deceleration. The neutrophil layer was harvested from the gradient and resuspended in HBSS++. The cell pellet was washed in HBSS++ and resuspended for 1 minute in Geyes solution then in HBSS++ and centrifuged at 385xg for 10 minutes. Finally the cell pellet was resuspended in PBS++ and a cell count was performed as above using Turk's solution. When using mice neutrophils for assays, the cells were primed with 5ng/ml TNFα (Peprotech, UK) and 200ng/ml GMCSF for 1 hour at 37^0C.

2.5.4 Human monocyte isolation from blood

As for neutrophil isolation, the blood/HBSS mixture was centrifuged after layering on Ficoll. This time the peripheral blood mononuclear cell layer (PBMC) was gently aspirated and isolated for use (see figure 2.2).

The PBMC layer was washed with PBS/FBS buffer. CD14 microbeads (Miltenyi Biotec, UK) were added and the suspension was incubated at 4^0C for 15 minutes. The suspension was washed with the PBS/FBS buffer and applied to a magnetic 25LS column (Miltenyi Biotec, UK) after the column was prepped with the buffer. The column was washed three times with PBS/FBS buffer to limit contamination. The column was then removed from the magnetic separator and the buffer was added onto the column to flush out magnetically labelled cells with a plunger. The cells were washed and counted.

Monocytes were resuspended at $1x10^6$ cells/ml in RPMI 1640 media containing 10% foetal bovine serum or human AB serum for the monocyte to macrophage differentiation (PAA labs, UK), and 1% Penicillin/Streptomycin (Thermo Fisher

Scientific, UK). Monocytes were cultured in 48 well plates for selective time periods with or without 100ng/ml LPS (from *Escherichia Coli* 055:B5, γ-irradiated) and polyclonal ANCA or control IgG at a final concentration of 250µg/ml. The cells were incubated at 37^0C for varying time points, after which supernatants were collected and cell counts were performed. When used, inhibitors were added 30 minutes prior to the addition of ANCA or control IgG and the cells were incubated at 37^0C (MPO inhibitor AZD5904 Astra Zeneca, UK variable concentration [249], CSF1R inhibitor GW2580 BioVision, UK variable concentration, anti CD11b clone ICRF44 Biolegend, UK 10µg/ml and anti CD18 clone TS1/18 Biolegend, UK 10µg/ml).

2.5.5 Human CD4 T cell isolation from blood

PBMC were isolated and processed as described above. CD4 microbeads (Miltenyi Biotec, UK) were used to isolate CD4 T cells instead of CD14 beads. The T cells were resuspended in complete RPMI medium.

2.5.6 Human monocyte to macrophage differentiation

There are protocols in the literature detailing skewing of naïve monocytes into M1 or M2 macrophages using growth factors and cytokines. However, we wanted to analyse how MPO-ANCA skew the macrophages, if at all, into a specific phenotype. As a result we cultured monocytes in complete RPMI using 10% AB serum instead of FBS to mirror physiological conditions without influencing differentiation into a certain phenotype. Cells were incubated with MPO-ANCA or control IgG for 6 days after which cells and supernatant were collected. The cells were stained with anti CD80 (PE clone 2D10) and anti CD206 (APC clone 15-2). Samples were analysed using a FACS Canto flow cytometer (Becton Dickinson, UK) using FACSDiva software (Becton Dickinson, UK). At least 10,000 events were collected per sample and data was analysed using FlowJo software (Treestar, USA).

The supernatant collected from the macrophage cultures described above were co-incubated with activated CD4 T cells. T cells were activated in 48 well plates coated with antibodies to CD3 (2µg/ml OKT-3 in-house from a hybridoma line) and CD28 (2µg/ml BD Biosciences). A final concentration of 10U/ml recombinant IL2 was added.

Supernatants from the monocyte to macrophage-differentiated cells were used at a ratio of 2:1 with the T cells. Supernatants from the T cell cultures were harvested at day 3 and 5 to assay the cytokine profile.

2.5.7 Respiratory burst assays

- ***Dihydrorhodamine (DHR) 123 assay***

DHR 123 is a non-reduced non-fluorescent molecule that in the presence of hydrogen peroxide is converted to rhodamine 123, which fluoresces at a wavelength of approximately 534nm, and can therefore be detected in the FITC (FL-1)-light channel on flow cytometry. Neutrophils were isolated as described in section 2.5.2 and used at a concentration of 2.5 x 10^6 cells/ml resuspended in HBH. The cells were loaded with 17µg/ml DHR123 (Calbiochem, UK) together with 5µg/ml Cytochalasin B as well as 2 mM sodium azide and incubated in the dark for 10 minutes at 37^0C. Cells were primed by incubation with 2ng/ml TNFα for 15 minutes at 37^0C with gentle mixing at 5 minute intervals. They were subsequently incubated with a respective stimulant. fMLP at 100ng/ml was used as the positive control. The reaction was stopped by the addition of a 30-fold volume of cold HBSS containing 1% BSA. This was spun at 280xg and 4^0C for 5 minutes. The cells were resuspended in 300µls HBSS. Flow cytometry was performed on a FACS Canto flow cytometer (Becton Dickinson, UK) using FACSDiva software (Becton Dickinson, UK). At least 10,000 events were collected per sample and data was analysed using FlowJo software (Treestar, USA).

- ***Luminometer assay***

Luminol and isoluminol are chemicals that exhibit chemiluminescence in the presence of an oxidant such as hydrogen peroxide. Luminol measures intacellular and extracellular reactive oxygen species (ROS), whilst isoluminol, a hydrophilic molecule that cannot enter the cell and therefore can be used to measure extracellular ROS production.

A luminometer plate (PAA labs, UK) was coated with 200µls of FBS per well for 12 hours prior to use. Neutrophils were isolated as described in section 2.5.2 and used at a concentration of 6.25x10^6 cells/ml resuspended in PBS++. Luminol / HRP (3mls PBS++

add 1µl of 1M luminol and 200µls of 0.8U/µl HRP) or isoluminol / HRP (3mls PBS++ add 1µl of 1M isoluminol and 200µls of 0.8U/µl HRP) was prepared. The cell suspension was mixed with 1.25 times the volume of (iso)luminol / HRP. Cells were primed by incubation with 2ng/ml TNFα for 15 minutes at 37^0C with gentle mixing at 5 minute intervals. In the meantime the unbound FBS was discarded from the luminometer plate and the plate was washed with PBS. The appropriate stimulant was placed into the appropriate well and prewarmed to 37^0C in the luminometer (Mithras LB940, Berthold Technologies, UK). fMLP at 100ng/ml was used as the positive control. Finally 200µls of cells per well were transferred to the luminometer plate swiftly using a multi-pipette and the reaction was recorded.

2.5.8 Degranulation assays

Degranulation of neutrophils is frequently measured by the release of granular contents such as MPO (azurophilic granules), lysozyme (azurophilic and specific granules), neutrophil elastase (azurophilic granules), lactoferrin (specific granules), CD63 (azurophilic granules), CD66b (specific granules) and CD11b (secretory, gelatinase and specific granules).

Neutrophils were isolated as described in section 2.5.2 and used at a concentration of $2.5x10^6$ cells/ml resuspended in HBH. The cells were primed and stimulated as stated in the results section. fMLP at 100ng/ml was used as the positive control activating agent.

- ***Lactoferrin ELISA***

Once the neutrophils were primed and stimulated, the cell suspension was centrifuged at 380xg for 5 minutes at 4^0C and the supernatant was collected and stored at -20^0C. A human lactoferrin ELISA kit (Hycult Biotech, UK) was used. 100µls/well standard or sample was added to an antibody pre-coated plate. The plate was incubated at 37^0C for 1 hour. The plate was washed 4 times with the provided wash buffer. A diluted tracer (100µls/well) was added and the tray was incubated for 1 hour at room temperature. The wash procedure was repeated. 100µls/well of streptavidin-peroxidase was pipetted and the tray was incubated for 1 hour. Following a wash, the

provided TMB substrate was added (100µls/well) and the plate was incubated in the dark for 30 minutes. The reaction was stopped with the provided solution and the plate was read at 450nm using a SpectraMax Plus384 microplate reader (Molecular Devices, UK).

- ***MPO Detection***

The supernatant from neutrophils primed and stimulated were collected as for the Lactoferrin ELISA. 75µls/well of the supernatant was pipetted into respective ELISA plate wells and as a positive control 75µls of $2.5x10^6$ neutrophils/ml was used. 100µls/well of OPD solution was added and incubated in the dark at room temperature for 30 minutes. The reaction was stopped by adding 100µls/well of 100% acetic acid. The plate was read at 450nm using a SpectraMax Plus384 microplate reader (Molecular Devices, UK).

- ***CD66b and CD11b Flow cytometry***

Neutrophil activation was stopped by adding cold 1% BSA/HBSS and the cell suspension was then centrifuged at 380xg for 5 minutes at 4^0C. The neutrophils were stained with anti-human antibodies CD66b FITC and CD11b APC. The respective antibodies were added and incubated for 20 minutes at room temperature in the dark. The suspension was later centrifuged at 280xg for 5 minutes. The supernatant was discarded and the cells resuspended in 2mls of PBS and centrifuged at 280xg for 5 minutes. Finally the cells were resuspended in 500µls of PBS with 0.1% sodium azide. FACs analysis was carried out immediately after staining using a FACS Canto flow cytometer (Becton Dickinson, UK) and FACsDIVA software (Becton Dickinson, UK).

2.5.9 Intracellular and extracellular staining of C3, C5, C3a and C5a

Neutrophils were isolated, primed and stimulated as described in section 2.5.2 and 2.5.7. Neutrophil activation was stopped with cold 1% BSA/HBSS and cells were resuspended in FACS buffer (PBS, 0.5% BSA and 2mM EDTA). Fc receptor block (Miltenyi Biotec, UK) was added at 20µls per 10^7 total cells in 60µls buffer and incubated or 10 minutes on ice. The cell suspension was washed with the FACS buffer. A fixation / permeabilization kit (Becton Dickinson (BD), UK) was used. For extracellular

staining, the cells were washed using BD permwash solution. The relevant primary antibody (see table of antibodies) was added and incubated for 20 minutes at 4^0C. The suspension was washed twice and if needed the secondary antibody was added and incubated for 20 minutes at 4^0C. Excess unbound antibody was washed off and the cells were resuspended in FACS buffer. For intracellular staining, the cells were treated similarly, however, prior to the use of the primary antibody, the cells were permeabilised by incubation with BD cytofix/cytoperm plus for 20 minutes at 4^0C.

FACs analysis was carried out immediately after staining using a FACS Canto flow cytometer (Becton Dickinson, UK) and FACsDIVA software (Becton Dickinson, UK).

2.5.10 Cytometric bead assay (CBA) – Human anaphylatoxins

Neutrophils were isolated as described and used at a concentration of $2.5x10^6$ cells/ml resuspended in HBH. The cells were primed and stimulated as appropriate. fMLP at 100ng/ml was used as the positive control. The cells were centrifuged at 380xg for 5 minutes to attain the supernatants. The supernatant was divided into aliquots and stored at -20^0C.

A BD anaphylatoxin CBA kit was used (Becton Dickinson, UK). The standards were prepared at different concentrations using the assay diluent. The samples were diluted either 1:2 or 1:5. The capture bead suspension, which consisted of three detection beads (one for each of the anaphylatoxins, C3a, C4a and C5a), was added to the samples and standards. The samples were incubated for 2 hours in the dark at room temperature. The suspensions were washed to eradicate unbound beads and the human anaphylatoxin PE detection antibody mixture was added and incubated for 1 hour in the dark. The suspension was washed and resuspended in FACS buffer.

FACS analysis was carried out immediately using a FACS calibur (Becton Dickinson, UK) and analysed using CellQuest Pro.

2.5.11 CBA – Th1, Th2 and Th17 cytokines

Monocytes were isolated as described in section 2.5.4 and subsequently stimulated with or without LPS (100ng/ml) and respective patient ANCA or control IgG at

250µg/ml for 18 hours at 37^0C. The cells were harvested and centrifuged at 380xg for 5 minutes to attain the supernatants, which were stored at -20^0C.

A BD Th1, Th2 and Th17 cytokine CBA kit was used (Becton Dickinson, UK). The standards were prepared and samples were thawed out. The capture bead suspension was added to the samples (used at 1:40 dilution) and standards, as was the PE detection antibody mixture. The samples were incubated for 3 hours in the dark at room temperature. The suspensions were washed to remove unbound beads and excess PE detection antibody and resuspended in FACS buffer.

FACS analysis was carried out immediately using a FACS calibur (Becton Dickinson, UK) and analysed using CellQuest Pro.

2.5.12 Reverse Transcription Quantitative PCR (RT-qPCR)

RNA was isolated from monocytes incubated with MPO-ANCA or control IgG +/- LPS for 18 hours using a Qiagen RNeasy mini kit (Qiagen, UK) according to manufacturer's instructions. Cells were lysed using 350µls RLT buffer provided and vortexing. The samples were transferred to the QIAshredder spin column and centrifuged at 13,000xg for 4 minutes. 350µls of 70% ethanol was added to the homogenised lysate and mixed well by pipetting. 700µls of the sample was transferred to the RNeasy spin column and centrifuged at 8,000xg for 30 seconds. The supernatant was discarded and 700µls of the RW1 wash buffer (removes biomolecules such as carbohydrates, proteins and fatty acids that are non-specifically bound to the silica membrane) added to the column, centrifuged at 8,000xg for 30 seconds and once again the supernatant was discarded. 500µls of the RPE wash buffer (removes salts from previous buffers adherent to the column) was added to the column and centrifuged at 8,000xg for 30 seconds. The supernatant was discarded and the wash step repeated. The RNeasy column was placed into a new collection tube. 35µls of RNase free water was added to the column and centrifuged at 8,000xg for 1 minute. The eluted RNA was immediately placed on ice.

The RNA concentration and purity was quantified using a Nanodrop ND-1000 spectrophotometer (Thermo Fisher Scientific, Wilmington, USA). RNA purity and

integrity was screened by analysing the ratio of absorbance A260/280 with a value equal or great than 2 indicating high purity of RNA. RNA was stored at -80^{0}C.

200ng RNA was converted to cDNA using a RevertAid H Minus kit (Thermo Fisher Scientific). The mastermix was generated using 1µl of primer, 4µls of reaction buffer (5x), 1µl of RiboLock RNase inhibitor, 2µls of 10mM dNTP mix, 1µls of RevertAid H Minus M-MuLV Reverse Transcriptase and 11µls of RNA sample (total volume 20µls). The reverse transcription reaction was carried out by incubating the samples at 25^{0}C for 5 minutes, followed by a step of 30 minutes at 42^{0}C and a final incubation of 5 minutes at 85^{0}C. The cDNA was stored at -80^{0}C and used for RT-qPCR.

Hydrolysis probes (TaqMan) were used for CSF1 (Hs00174164_M1) and CSF1R (Hs00911250_M1) labelled with a fluorescent reporter dye FAM (Thermo Fisher Scientific, UK), which is covalently bound to its 5' end and a dark quencher dye at the 3' end. During the PCR reaction, the polymerase will degrade the probe releasing the reporter dye from its quencher and allowing it to fluoresce. The fluorescent dye release corresponds to amplification of the specific target sequence. The reaction mastermix was created using 1µl of the 20x Taqman assay probe including primers, 10µls Taqman universal mastermix II with Uracil-DNA glycosylase (UNG), 5µls RNase free water and 4µls cDNA. The reference gene beta glucuronidase (bGUS) was used as an endogenous control (forward primer 5'-GAAAATATGTGGTTGGAGAGCTCATT-3', reverse primer 5'-CCGAGTGAAGATCCCCTTTTTA-3' and Taqman probe 5'-CCAGCACTCTCGTCGGTGACTGTTCA-3'). The reference gene mastermix was set up using 0.6µl of the forward primer, 0.6µl of the reverse primer, 0.664µl of the probe, 10µls Taqman universal mastermix II with UNG, 4.136µls of RNase free water and 4µls cDNA. For each set of primers a water control was used to control for contamination.

The cDNA was amplified in 384 well plates using ABI Prism 7900 HT Sequence Detection System (Applied Biosystems, Foster City, CA) in duplicates. The thermal cycling conditions used were hold at 50^{0}C for 2 minutes, hold at 95^{0}C for 10 minutes, 45 cycles of 15 seconds at 95^{0}C and 1 minute for 60^{0}C. Results of individual samples were normalized to that of human bGUS. The sequence detector SDS 2.4 software (Applied Biosystems) was used to export the Ct values. The Ct value is the PCR cycle at which the fluorescent signal of the reporter dye surpasses an arbitrary threshold.

Hence, the lower the Ct value the greater the amount of amplification. ΔCt was obtained by normalising the data through subtraction of the Ct value of the endogenous reference gene control from the gene of interest Ct. The ΔCt of the control sample was next subtracted from the ΔCt of the other samples to give the ΔΔCt. Subsequently, the relative quantity of target gene mRNA expression was calculated using the equation of the comparative Ct method ($2^{-\Delta\Delta Ct}$) for quantification allowing presentation of data as a fold change in expression [250].

2.5.13 Microarray experiments

The microarray experiments were performed with Julie Watson and Dr Paul Lavender (MRC and Asthma UK Centre in Allergic Mechanisms of Asthma, King's College London, Guy's Hospital, UK). RNA was isolated from $5X10^5$ monocytes incubated with 100ng/ml LPS and MPO-ANCA or control IgG (250µg/ml) for 6 hours using a Qiagen Allprep kit (Qiagen, UK) according to manufacturer's instructions (see above).

Potential genomic DNA contamination was removed by Turbo DNase treatment (Ambion/Life Technologies, UK). 0.1 volume 10xTURBO DNase Buffer and 1µL TURBO DNase was added to the RNA, mixed gently and incubated at 37^0C for 45 minutes. A DNase inactivating reagent was added at 0.1 volume and incubated for 5 minutes at room temperature with gentle mixing. The samples were centrifuged at 10,000xg for 90 seconds and the RNA was transferred to a fresh tube. 100% ethanol was added at 2.5x the volume, the sample was mixed well, transferred to the RNeasy MinElute column (Qiagen, UK) and centrifuged at 8,000xg for 15 seconds. The flow through was discarded, 500µls of RPE wash buffer was added and centrifuged at 8,000xg for 30 seconds. The flow through was discarded and 500µls of 80% ethanol was added and again the column was centrifuged, this time at 10,000xg for 2 minutes. The flow through was discarded, the column was left open to dry the membrane and transferred to a new collection tube. The RNA was eluted by adding 14µls RNase free water to the column membrane and centrifugation at 8,000xg for 1 minute.

As for the RT-qPCR, a nanodrop was used to quantify the purity and concentration of the RNA. 5ng total RNA per sample (5µls volume) was reverse transcribed and labeled using Ovation Pico WTA System V2 and Encore BiotinIL Kits (NuGen Inc., USA). For

each sample, 2µls of the first strand primer mix was added to the RNA and mixed. The tubes were heated to 65^0C for 2 minutes then cooled at 4^0C. 2.5µls of the first strand buffer mix and 0.5µl of the enzyme mix were added to each sample and pipetted gently. The samples were placed in a thermal cycler (Bio-Rad S1000 Thermal Cycler, UK) at 4^0C for 2 minutes, 25^0C for 30 minutes, 42^0C for 15 minutes, 70^0C for 15 minutes and held at 4^0C.

The second strand reagents were thawed; 9.7µls of the buffer mix and 0.3µl of the enzyme mix were added to each first strand reaction tube and mixed. The tubes were again placed in a thermal cycler at 4^0C for 1 minute, 25^0C for 10 minutes, 50^0C for 30 minutes, 80^0C for 20 minutes and held at 4^0C.

The double stranded cDNA was purified using RNAClean XP beads (NuGen Inc., USA). 32µls of the beads were added to each reaction, mixed and incubated for 10 minutes at room temperature. The tubes were placed on a magnet for 5 minutes to completely clear the beads. 45µls of the buffer was carefully removed and discarded. The beads were washed while still on the magnet for 30 seconds with 200µls of freshly prepared 70% ethanol three times and dried for 20 minutes.

Next, the single primer isothermal amplification (SPIA) protocol was used. 100µls of the SPIA master mix provided was added to each second strand reaction tube containing the dried beads. They were gently mixed and centrifuged at 8,000xg for 10 seconds. The tubes were again placed in a thermal cycler at 4^0C for 1 minute, 47^0C for 75 minutes, 95^0C for 5 minutes and held at 4^0C. The tubes were centrifuged at 8,000xg for 10 seconds, transferred to the magnet and allowed to stand for 5 minutes and the eluted SPIA cDNA was pipetted into a new tube.

The MinElute reaction Cleanup kit (Qiagen, UK) was used for DNA purification following enzymatic reactions. 300µls of the ERC buffer provided was added to the samples, vortexed and transferred to the MinElute spin columns, which were centrifuged at 8,000xg for 1 minute. The flow through was discarded and 750µls of the PE buffer was added and similarly centrifuged twice to remove any remaining buffers. The columns were blotted gently and placed onto new collection tubes. To elute the cDNA 20µls of nuclease free water was added, the columns were allowed to stand for

1 minute then centrifuged at 10,000xg for 1 minute. The cDNA was quantified using a nanodrop (see RNA quantification).

The Encore BiotinIL kit (NuGen Inc., USA) was used. UNG was added first to remove the uracil base incorporated during the cDNA amplification process. This creates an abasic site in the cDNA strand, which is subsequently labelled with a biotin moiety. 5µls of the UNG buffer then 5µls of the UNG enzyme was added per sample, vortexed and centrifuged briefly to ensure mixing. The samples were heated to 50^0C for 30 minutes then cooled to 4^0C. Next, 5µls of the labelling buffer was added to each sample, mixed then 5µls of the labelling reagent was added and mixed by pipetting and brief centrifugation. The samples were heated to 50^0C for 60 minutes then cooled to 4^0C. The MinElute reaction Cleanup kit (Qiagen, UK) was used as in described in the previous paragraph and the labelled cDNA samples were eluted and quantified using the nanodrop.

The cDNA was hybridized to Illumina HT12V4 Microarrays, scanned using an Illumina iScan System and subjected to quantile normalization within the Genome Studio Suite v1.0 (Illumina). Expression data were analysed using Partek Genomics Suite (Partek Inc., USA) version 6.6, Ingenuity Pathway Analysis (Qiagen, UK) and Gene Set Enrichment Analysis, GSEA (Broad Institute of MIT and Harvard, USA) by Dr Ben Afzali (Division of Transplant Immunology and Mucosal Biology, MRC Centre for Transplantation, King's College London, Guy's Hospital, UK) and Dr Paul Lavender (MRC and Asthma UK Centre in Allergic Mechanisms of Asthma, King's College London, Guy's Hospital, UK).

2.5.14 Cellular lipid extraction and mass spectrometry

The cellular lipid extraction and mass spectrometry was performed in collaboration with Dr Corinne M Spickett and Alpesh Thakker (School of Life & Health Sciences, Aston University, Aston Triangle, Birmingham, UK). These experiments were performed in their laboratory under their supervision. The mass spectrometry was run with the help of Alpesh Thakker and the analyses was performed by Dr Corinne M Spickett.

Monocytes from a healthy donor were incubated with MPO-ANCA or control IgG for 18 hours as described before ($3X10^6$ cells/condition). The cell pellets were washed and stored at -80^0C. All organic solvents used for lipid extraction and mass spectrometry were of high performance liquid chromatography grade.

The extraction of phospholipids were performed using a double extraction technique by addition of ice cold 500µls methanol containing 0.005% butylated hydroxytoluene and 500µls deionised water to each cell pellet sample. The sample was vortexed and 100µls of a 1µg/ml solution of 1,2-ditridecanoyl-sn-glycero-3-phosphocholine (13:0, 13:0 PC) in methanol containing 0.005% butylated hydroxytoluene was added to each sample (used as an internal standard). The samples were sonicated at 4^0C for 15 minutes in a waterbath. 500µls of chloroform was added and the samples were sonicated further as described. The samples were then centrifuged for 5 minutes at 5000xg and the upper aqueous phase was removed and the extraction procedure was repeated as above. Both organic phases (bottom layer) were combined and dried under a stream of oxygen-free nitrogen and stored at -80^0C.

Before analysis the extracts were reconstituted in 200µls methanol:chloroform (1:1). Two solvents A and B were used at a ratio of 3:7; solvent A was made of water, 0.1% formic acid and 5mM ammonium formate whilst solvent B was made of methanol, 0.1% formic acid and 5mM ammonium formate. The extracts were diluted in the solvent A:B mixture at 1:5 or 1:10.

Phospholipids were separated by reverse phase chromatography on an HPLC system (Dionex Ultimate 3000 system) controlled by Chromoleon software, using a Proswift RP-4H column (1mm x 250mm) at room temperature. The eluents used were (A) aqueous 0.1% formic acid containing 5 mM ammonium formate and (B) methanol containing 0.1% formic acid and 5 mM ammonium formate. The LCMS run time was 50 minutes with a chromatographic gradient of 70% B at 0 – 4, followed by 3-step gradient increase to 80% B at 8 minutes, 90% B at 15 and 100% B at 20 minutes. The gradient was maintained at 100% B until 38 minutes and then decreased back to 70% B by 50 minutes. The flow of the mobile phase was set to 50µls/minute. Samples were diluted 1:5 or 1:10 as described above in the starting solvent and 10µls were loaded onto the column.

The phospholipids were detected using targeted and data dependent scanning routines performed on a Absciex 5500 QTrap mass spectrometer controlled by Analyst software. Precursor ion scanning (PIS) of 184 Da was carried out over the mass range 400 Da - 1000 Da to identify phosphatidylcholines and oxidised phosphatidylcholines. The declustering potential was set to 50V for all scans and collision energy for PIS was set to 45eV. Information dependent data acquisition (IDA) was used to collect MS/MS data based on following criteria: the most intense ion with +1 charge and minimum intensity of 1000cps was chosen for analysis, using dynamic exclusion for 20 seconds after 2 occurrences and a fixed collision energy setting of 47eV. Other source parameters were adjusted to give optimal response from the direct infusion of a dilute solution of standards.

Data analysis was performed manually using Peakview 2.0 software by generating extracted ion chromatograms for individual mass to charge ratios corresponding to different modified and unmodified phospholipid species and calculating peak area. The peak area was normalised to the peak area of the internal standard to check for extraction variability, but subsequently the signal intensities were expressed as a percentage of the intensity of the dipalmitoyl phosphatidylcholine at *m/z* 734 to take into account variability in the total phospholipid present in the samples.

2.5.15 PR3 Cleaving C3 Assay - Sodium dodecyl sulphate polyacrylamide gel electrophoresis (SDS-PAGE) and Western blot

Human PR3 (Calbiochem, UK) was incubated with purified human C3 (10µg/ml) and C3b (10µg/ml) (from Complement Technologies Inc. USA) to help determine the potential of C3 cleavage by PR3 for 15 minutes or 60 minutes at 37^0C. Different concentrations of PR3 were used (5-15µg/ml). A reducing sample buffer was added and the eppendorfs containing the proteins were placed on a thermomixer for 3 minutes at 100^0C. The samples were then loaded onto a 4% NuPage Bis Tris gel (Life Technologies, UK), at a volume of 25µls sample per well. A volume of 12µls of SeeBlue Plus 2 pre-stained standard (Life Technologies, UK) was added too. The gel was run using a PowerEase500 power supply (Life Technologies, UK) at 200V for 30 minutes. The gel was removed from the cassette and washed 3 times in deionized water for 5 minutes each time on a shaker plate. The gel was fixed using deionized water (90mls) /

methanol (100mls) / acetic acid (20mls), sensitized using deionized water (105mls) / methanol (100mls) / sensitizer (5mls) and washed again. The gel was stained with stainer A and B (Life Technologies, UK), and washed again as above. 5mls of the developer was added to 95mls of deionized water and the gel was soaked in this diluted developer. The reaction was stopped and the gel washed. The gel was scanned.

The samples were also analysed by western blotting technique. Western blots were carried out using the iBlot gel transfer device as per the manufacturer's instructions (Life Technologies, UK). The iBlot NC anode stack bottom (Life Technologies, UK) was placed onto the blotting surface of the iBlot machine at 20 volts. After completion, the SDS-PAGE gel was removed from the cassette and placed directly onto the transfer membrane of the anode stack. iBlot filter paper that had been pre-soaked in deionized water was placed over the gel and air bubbles were removed using the iBlot roller. The iBlot cathode stack top (Life Technologies, UK) was placed over the filter paper with the electrode side facing up and aligned to the right edge. The disposable sponge was placed with the metal contact on the upper right corner of the lid. The lid was closed and the gel was transferred in seven minutes. The completed blot was blocked for 1 hour in 1xTBS tween/5% powdered milk (shaking vigorously) after which it was washed in 1xTBS tween three times for 15 minutes each time whilst being shaken vigorously.

A volume of 15mls of the appropriately diluted (in 1xTBS tween/5% powdered milk) primary antibody (see table of antibodies) was added to the blot and incubated at 4^0C overnight (shaking gently). The blot was washed as before. A horseradish peroxidase (HRP) secondary antibody was diluted appropriately (in 1xTBS tween/5% powdered milk) and 15mls was added to the blot for 2 hours at room temperature (with gentle shaking). The blot was washed as before. The HRP substrate was prepared by mixing equal volumes of Supersignal west pico chemiluminescent substrates (Thermo Fisher Scientific, UK) (7.5ml + 7.5ml) and was added to the blot (shaking gently) for 5 minutes. The blot was put into a polythene pocket and secured into a Kodak BioMax cassette (Anachem, UK). In a dark room the Kodak BioMax Light film (Anachem, UK) was placed inside and the cassette was closed for the appropriate exposure time. The film was developed.

2.6 Statistics

Data was analysed using Graphpad Prism version 6 software (Graphpad Software Inc, La Jolla, CA, USA). The specific tests used in each experiment are stated in the results sections. P values <0.05 were considered to be statistically significant.

Chapter 3 – Activation of neutrophils by ANCA

3.1 Introduction

ANCA recognise antigens that are present in primary granules of neutrophils and lysosomes of monocytes, namely PR3 and MPO. ANCA were first thought to represent a serological marker of disease but subsequent studies have shown that they have a more significant role in pathogenesis. Initial studies of the potential pathogenic role of ANCA were performed *in vitro* and revealed that primed neutrophils can be activated to undergo respiratory burst and degranulation [61]. They showed that ANCA IgG increased ROS release from primed neutrophils in comparison to control IgG as measured by a chemiluminescence assay and a ferricytochrome C reduction assay. They also assessed primary granule degranulation as measured by β-glucuronidase and N-acetylglucosaminidase release and showed that ANCA IgG in the presence of TNFα led to increased degranulation in comparison to control IgG [61]. Since then other published literature has corroborated that monoclonal and polyclonal patient derived ANCA in the presence of TNFα leads to neutrophil respiratory burst [62, 64, 111, 251]. However, they had relatively small numbers of patient ANCA and control IgG, as well as often a single donor for neutrophils. Furthermore, it is not apparent in the literature how the ANCA or control IgG samples were selected. Anecdotally, it has been reported that the neutrophil activating capacity of different IgG preparations from different AAV patients vary in their ability to activate neutrophils.

The role of neutrophils in AAV has been discussed in chapter 1, there is convincing *in vivo* evidence to support the *in vitro* data that neutrophils have a crucial role in AAV pathogenesis. The contribution of neutrophils to pathogenesis seems to be multifaceted. As reviewed in section 1.6, the damage mediated by neutrophils appears to be dependent on generation of ROS, degranulation, generation of NETs and subsequent complement activation. Neutrophils are capable of other functions including release of cytokines, chemokines, leucotrienes, prostaglandins as well as proteases and antigen presentation via MHC class II, which all contribute to pathogenesis.

The generation of oxidants by neutrophils results from the activation of the multi-protein enzyme complex NADPH oxidase, an electron transporting system, which is formed by four oxidase specific proteins ($p22^{phox}$, $p47^{phox}$, $p67^{phox}$ and $gp91^{phox}$) as well as a GTPase (Rac1/2) component [252]. Upon cell activation the cytosolic proteins translocate to the membrane bound component ($gp91^{phox}$) and catalyse the formation of superoxide anions through oxygen reduction. This occurs once the electrons are ferried from NADPH in the cytosol over the membrane in question and is delivered to the oxygen molecule in the intracellular or extracellular milieu. Other ROS species such as hydrogen peroxide (H_2O_2), hydroxyl radicals and hypochlorous acid are derived. A number of techniques have been developed to assess respiratory burst activity and the work shown in this chapter describes two methods we utilised.

DHR 123, a non-fluorescent molecule is taken up by phagocytes and oxidised to its fluorescent derivative rhodamine 123 by reactive oxygen intermediates, primarily H_2O_2, produced during the respiratory burst response. This assay primarily measures intracellular ROS production. Several dyes release energy in the form of light (chemiluminescence) following excitation by ROS. Luminol is an example and the most commonly investigated. It is an activity amplifier, which reduces the detection limits making the respiratory burst assay technique sensitive. Luminol measures both intracellular and extracellular ROS production. Isoluminol is another chemiluminescent molecule that is used to exclusively measure extracellular ROS released by the cell. By moving the amino group away from the first carbon atom in the phthalate ring of luminol, isoluminol is more hydrophilic and less able to transverse the cell membrane (see figure 3.1) [253].

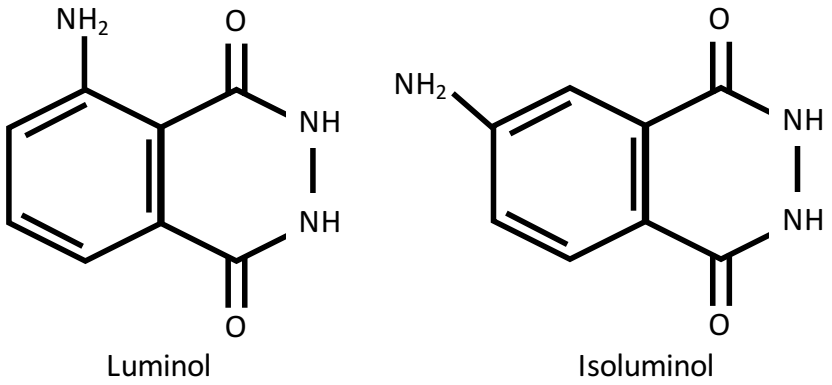

Figure 3.1 – The molecular structure of luminol and isoluminol.

Upon stimulation neutrophil granules translocate to the cell surface or phagosomal membrane where they fuse with the membrane to release their contents (degranulation). Neutrophils contain at least four different granule types [254]:

- Azurophilic (primary) granules, which contain CD63, MPO, PR3, elastase, cathepsins and α1-antitrypsin amongst other constituents.
- Specific (secondary) granules, which contain CD11b/CD18, CD66, lactoferrin, lysozyme, collagenase and TNF-receptors.
- Gelatinase (tertiary) granules contain CD11b/CD18, fMLP-receptors, lysozyme and gelatinase.
- Secretory vesicles, which contain CD11b/CD18, fMLP-receptors, DAF and other plasma proteins.

Degranulation of neutrophils can be quantified by measuring granule contents in the supernatant. Other methods include measuring surface expression of granule membrane components with flow cytometry. In this chapter we measured MPO activity and lactoferrin in the neutrophil supernatant, and cell surface CD66 and CD11b as markers of degranulation.

The role of complement in AAV has been discussed extensively in chapter 1, section 1.10. Most studies have centred on *in vivo* models to demonstrate the pathogenic role of complement components. Camous *et al* showed that human neutrophils stimulated by cytokines or coagulation system derived factors activate exogenous complement (from serum) with the consequence that C3 activation fragments, C5a and C5b-9 complexes are detectable on the neutrophil surface [255]. Neutrophils are capable of releasing C3, factor B and properdin, the machinery for convertase formation [187, 210] and hence like other leukocytes such as T cells, may be able to generate the complement components C5a and C5b.

3.2 Aims

In this chapter we aimed to set up a robust *in vitro* read out of polyclonal ANCA induced neutrophil activation with reduced variability and in doing so show the impact of ANCA on neutrophil respiratory burst and degranulation. We also aimed to examine

the expression of complement components C3 and C5 by neutrophils and the effect of ANCA on C3 and C5.

3.3 Polyclonal ANCA are not consistently able to activate neutrophils to produce ROS in comparison to control IgG

We began by investigating the activation of neutrophils isolated from healthy donors in response to ANCA. To obtain a non-biased and objective measure of this effect, we examined the responses of unselected IgG purified from the blood of 10 healthy donors, 11 patients with MPO-ANCA disease and 9 patients with PR3-ANCA disease. The clinical characteristics of the patients and controls are shown in table 3.1 and table 3.2.

Age	Sex	ANCA	Renal BVAS	Total BVAS	Extra renal disease	Treatment at time of sample collection
68	F	MPO	12	22	ENT, Chest	MP day 3
72	F	MPO	12	18	Chest	MP day 1
55	F	MPO	12	15	No	Nil
77	F	MPO	12	18	ENT, Chest	LDOP
38	M	MPO	6	10	Eyes, Skin	Nil
66	M	MPO	12	18	Chest	Nil
82	F	MPO	12	15	No	LDOP
74	F	MPO	12	12	No	MP day 3
73	F	MPO	12	12	No	Nil
74	F	MPO	12	15	No	MP day 1
63	M	MPO	12	25	ENT, Eyes, Skin	Nil
42	M	PR3	12	35	ENT, NS, Eyes, Chest	Oral cyclo, high dose oral pred
74	M	PR3	12	31	ENT, NS, Skin, Chest	Nil
75	M	PR3	12	19	NS, Eyes, Skin	Nil
59	M	PR3	12	27	ENT, Eyes, Chest	Methotrexate
76	M	PR3	12	19	Skin	Nil
51	M	PR3	12	23	Eyes, Chest	Oral cyclo, MP day 2
51	M	PR3	10	14	ENT, Eyes	Nil
73	M	PR3	12	19	Eyes, Skin	Nil
72	F	PR3	12	18	ENT	Nil

Table 3.1 - Characteristics of the 20 patients from who samples were collected for ANCA isolation. Samples were attained from patients in a number of renal units in Southeast England. All patients had active ANCA vasculitis and all were new presentations of ANCA vasculitis. (BVAS = Birmingham vasculitis activity score, ENT = ear, nose or throat, NS = nervous system, MP = methylprednisolone, LDOP = low dose oral prednisolone, Cyclo = cyclophosphamide).

Age	Sex
27	M
27	F
50	M
52	M
41	M
35	M
33	F
24	F
36	F
40	M

Table 3.2 - Characteristics of 10 healthy controls used for control IgG purification.

The antibodies were purified as described in section 2.4.2 using sodium chloride precipitation. The purity of the antibodies were tested using SDS-PAGE chromatography (reducing conditions).

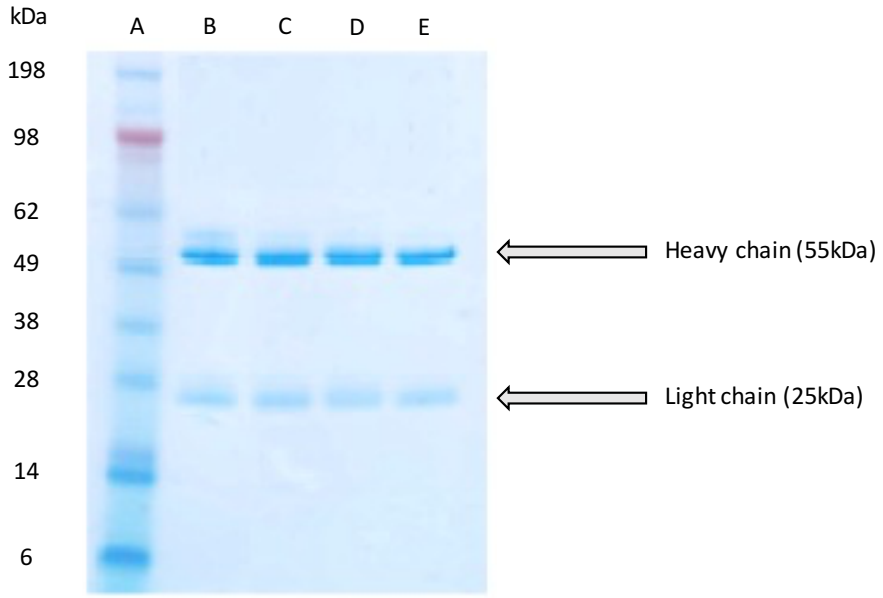

Figure 3.2 – SDS-PAGE gel of IgG preparations. Example of reducing SDS-PAGE gel showing in A the standard ladder, whilst B-E reveal the separation of 2 control and 2 ANCA IgG preparations.

3.3.1 DHR 123 assays

The DHR 123 assay was initially performed using TNFα primed neutrophils from control donors, which were subsequently stimulated with fMLP, monoclonal MPO-ANCA (clone 266.6K2), monoclonal PR3-ANCA (WGM2) or an equivalent isotype control (clone 107.3) to discount non-specific rhodamine 123 production (see section 2.5.7 for methodology). Figure 3.3 below shows typical FACS histogram plots using one donor's TNFα primed neutrophils.

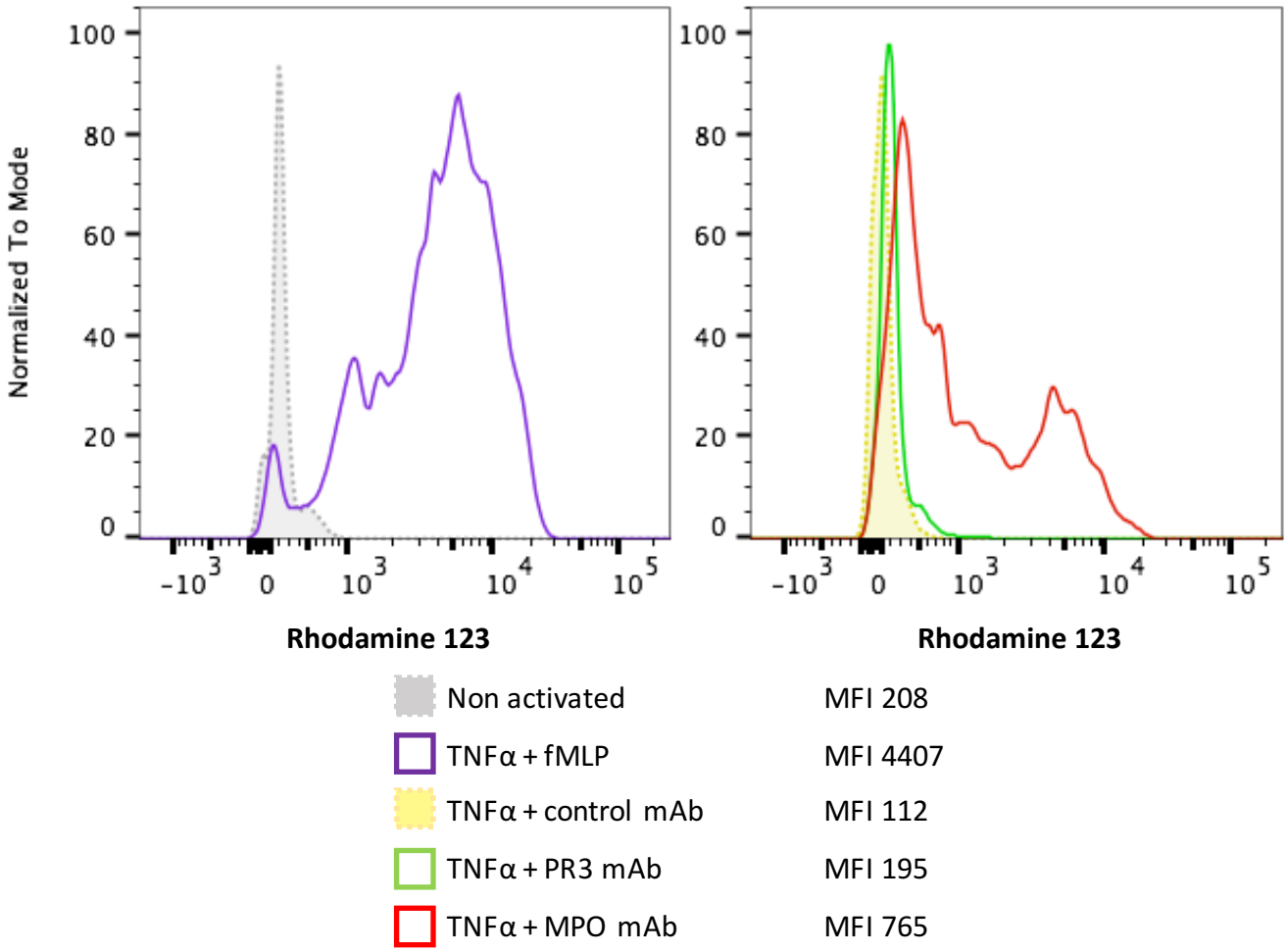

Figure 3.3 – Representative DHR 123 FACS histogram plots and MFI values of TNFα primed neutrophils stimulated with monoclonal antibodies. The primed neutrophils were stimulated with fMLP (100ng/ml) or monoclonal ANCA (PR3 mAb and MPO mAb) (5µg/ml) or monoclonal isotype control (control mAb) (5µg/ml). Non activated cells were not primed or stimulated.

Primed neutrophils exposed to fMLP were used as a positive control. There was a response in rhodamine 123 production to monoclonal MPO-ANCA. There was a slight increase in median fluorescence intensity (MFI) with monoclonal PR3-ANCA compared to the monoclonal isotype control.

TNFα primed neutrophils from two donors (27 year old male and 50 year old male) were then stimulated with unselected polyclonal antibodies highlighted in table 3.1 and table 3.2 from patients (11 patients with MPO-ANCA disease and 9 patients with PR3-ANCA disease) and 10 control subjects. Surprisingly, we found no significant difference in DHR 123 plot MFI between polyclonal ANCA samples and control IgG samples as shown in figure 3.4 and figure 3.5.

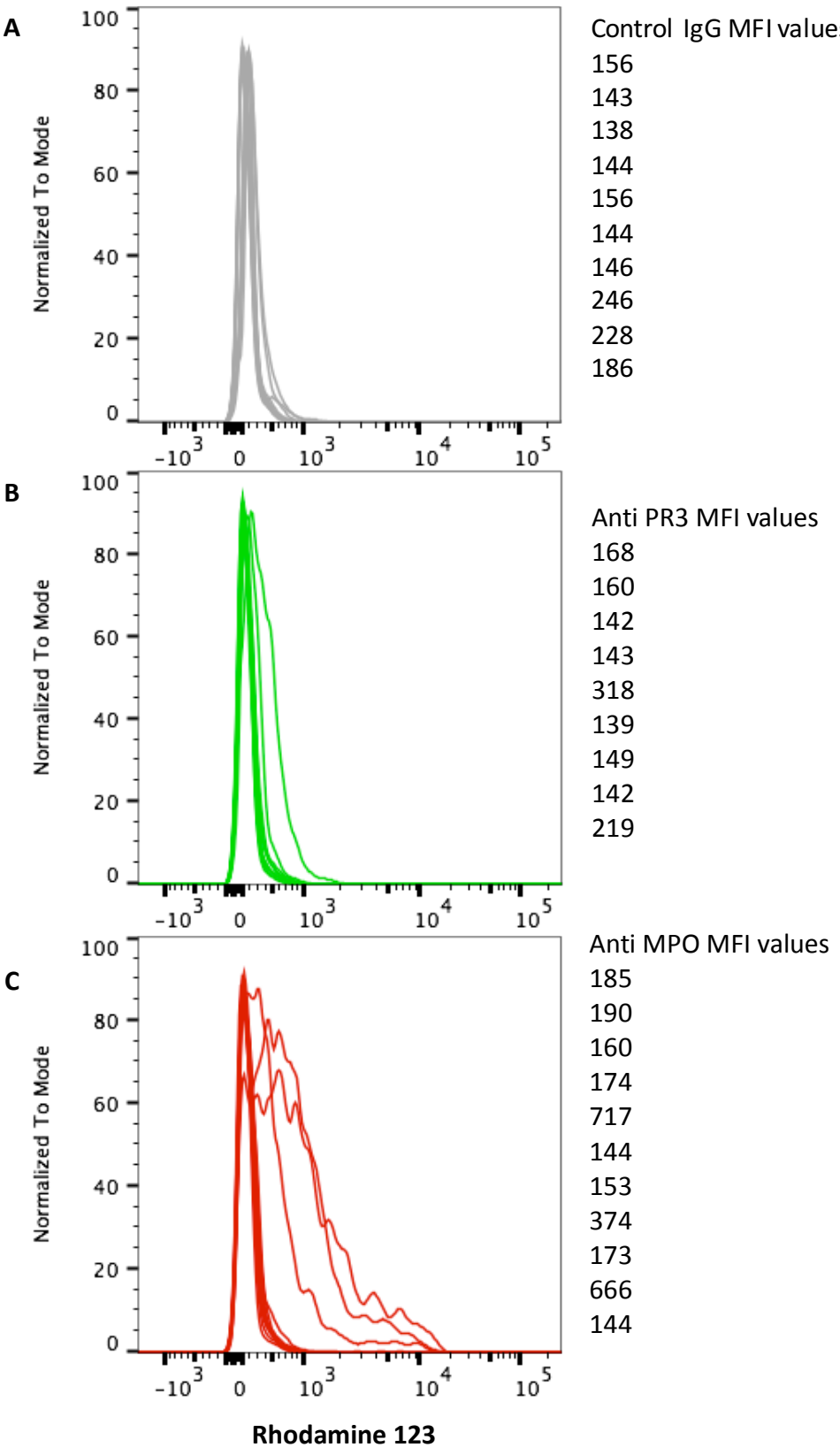

Figure 3.4 – Representative DHR 123 FACS histogram plots and MFI values of TNFα primed neutrophils from one donor stimulated with polyclonal antibodies. The primed neutrophil were stimulated with polyclonal control IgG (A), patient derived MPO-ANCA (B) or patient derived PR3-ANCA (C).

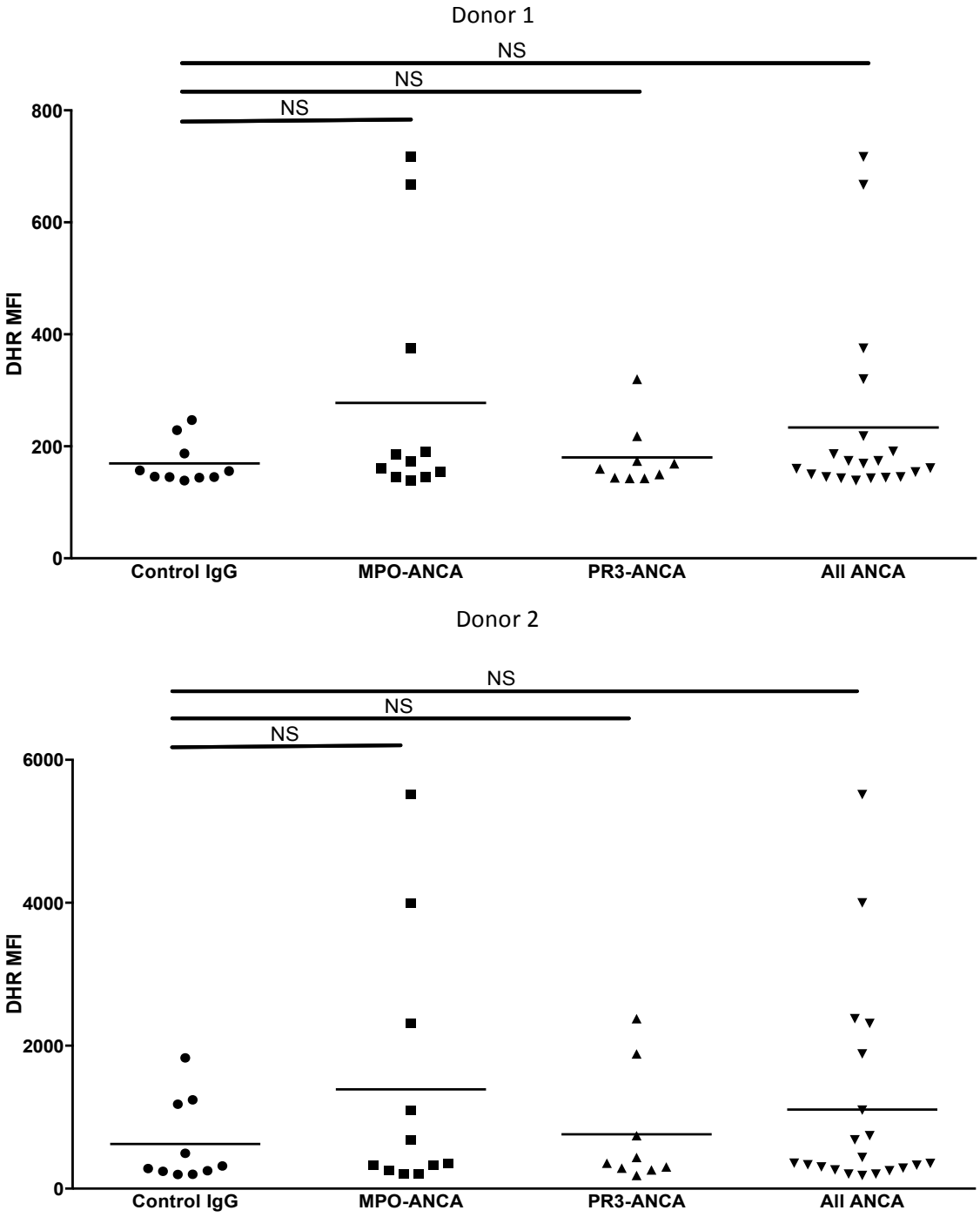

Figure 3.5 – Summary of the MFI of TNFα primed neutrophils DHR 123 responses to polyclonal antibodies. TNFα primed neutrophils from two healthy donors were stimulated with control IgG (n=10), MPO-ANCA (n=11) or PR3-ANCA (n=9). All ANCA represents the combined results for MPO-ANCA and PR3-ANCA (n=20). Data was analysed using one-way ANOVA with Dunnett's post test (NS = non significant). Data for all ANCA was compared to control IgG samples using a student's t test.

3.3.2 Luminometer assays

The luminol neutrophil respiratory burst assay was initially set up as described in section 2.5.7 using the positive control fMLP, in varying concentrations as shown in a typical plot in figure 3.6. Increasing concentrations of fMLP led to a stronger response in TNFα primed neutrophils as expected.

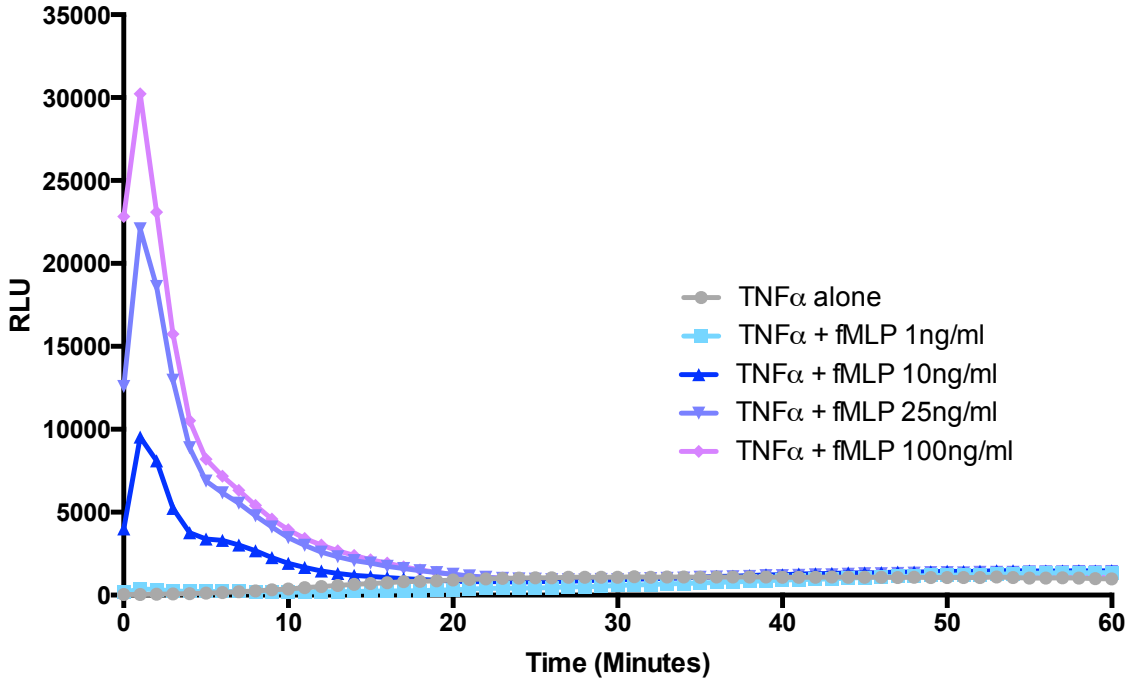

Figure 3.6 – Representative luminol assay plot of human neutrophils primed with TNFα and stimulated with different concentrations of fMLP. RLU = Relative light units.

The response of TNFα primed neutrophils to monoclonal ANCA were also tested in comparison to a monoclonal isotype control antibody. Figure 3.7 is a representative plot of the luminol assay response and as depicted the response is different to the typical fMLP response seen in timing and duration. The response of monoclonal ANCA is also relatively muted in comparison. Isoluminol (extracellular ROS measure) traces were similar to the luminol (intracellular and extracellular ROS measure) traces displayed but with a lower RLU as anticipated.

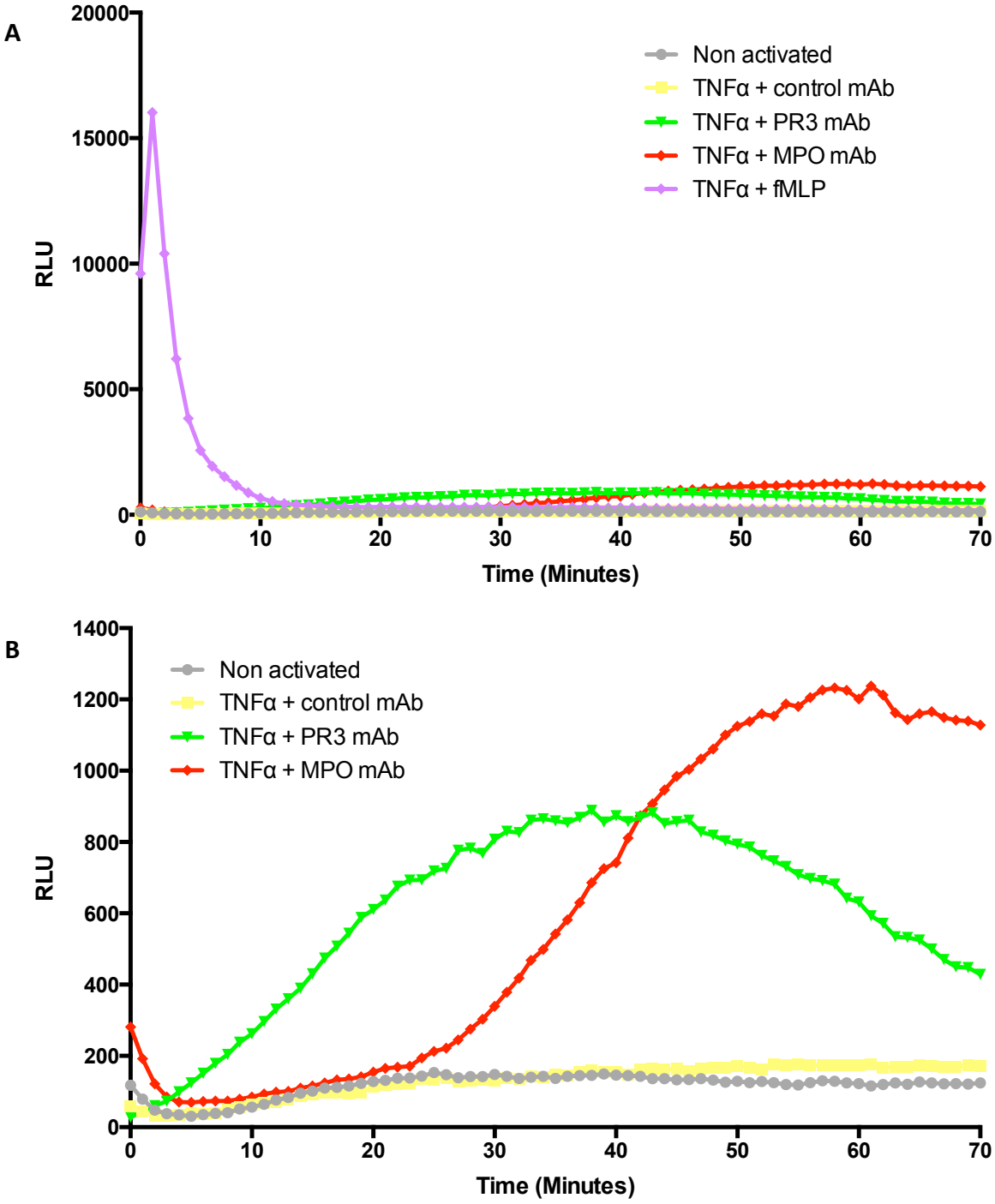

Figure 3.7 – Representative luminol assay plot of one donor's neutrophils primed with TNFα and stimulated with monoclonal antibodies. fMLP was used as a positive control (A). The second plot is a replica of plot A without the fMLP trace detailing the activation of TNFα primed neutrophils with monoclonal MPO-ANCA, PR3-ANCA or monoclonal isotype control (B).

Isoluminol and luminol assays were next performed using TNFα primed neutrophils from two donors (same donors as for the DHR assays) and polyclonal control IgG (n=10) or patient derived ANCA (11 MPO-ANCA and 9 PR3-ANCA).

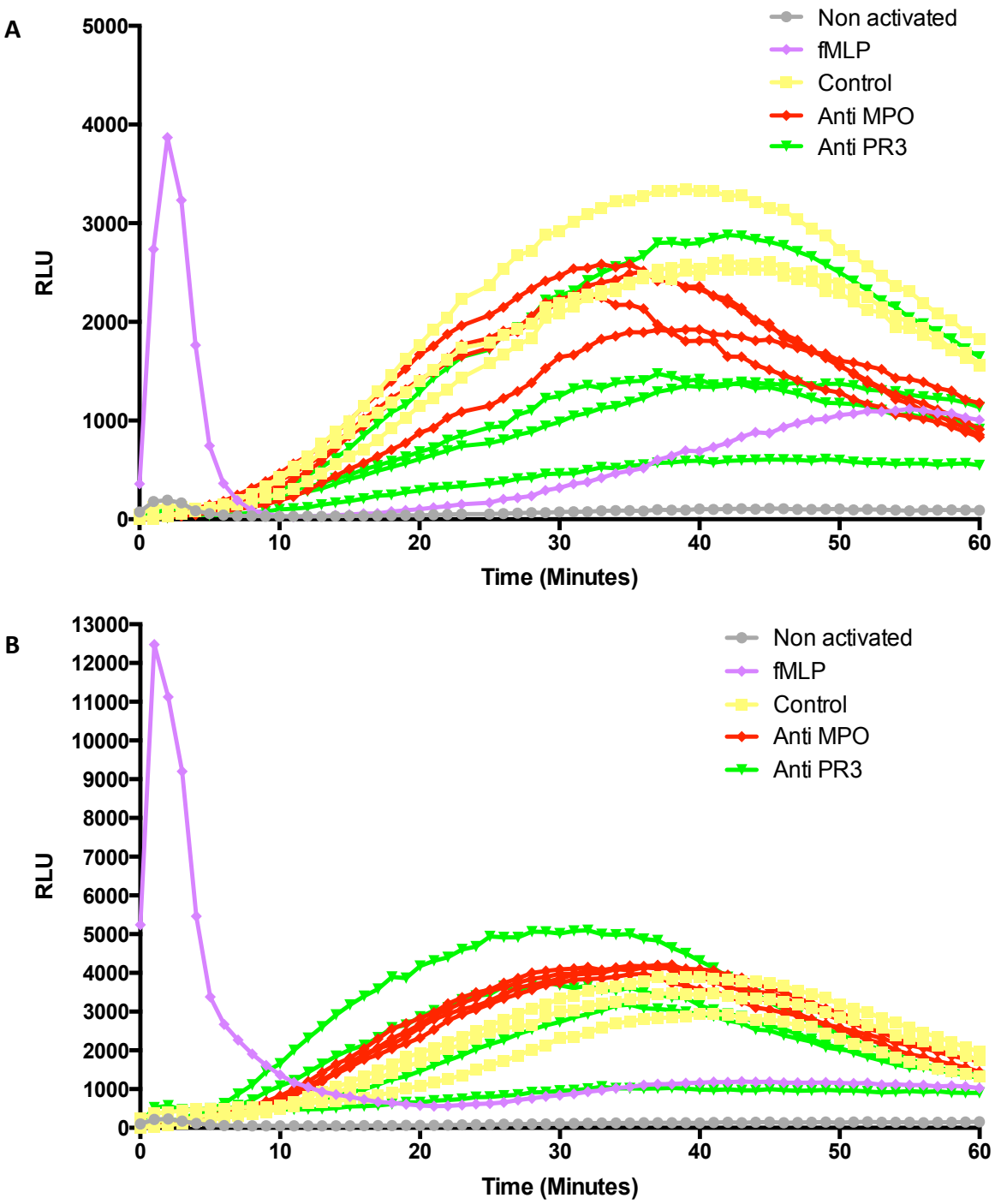

Figure 3.8 – Representative isoluminol and luminol assay plots of one donor's neutrophils primed with TNFα and stimulated with polyclonal antibodies. Plot A represents the Isoluminol traces whilst plot B demonstrates the luminol traces of TNFα primed neutrophils activated with fMLP (positive control), polyclonal control IgG, polyclonal patient derived MPO-ANCA or PR3-ANCA.

Due to logistical reasons, the 30 polyclonal antibody samples had to be analysed over 3 separate experiments for each of the two neutrophil donors. The highest RLU for each experiment was plotted and compared (figure 3.9 isoluminol assays and figure 3.10 luminol assays).

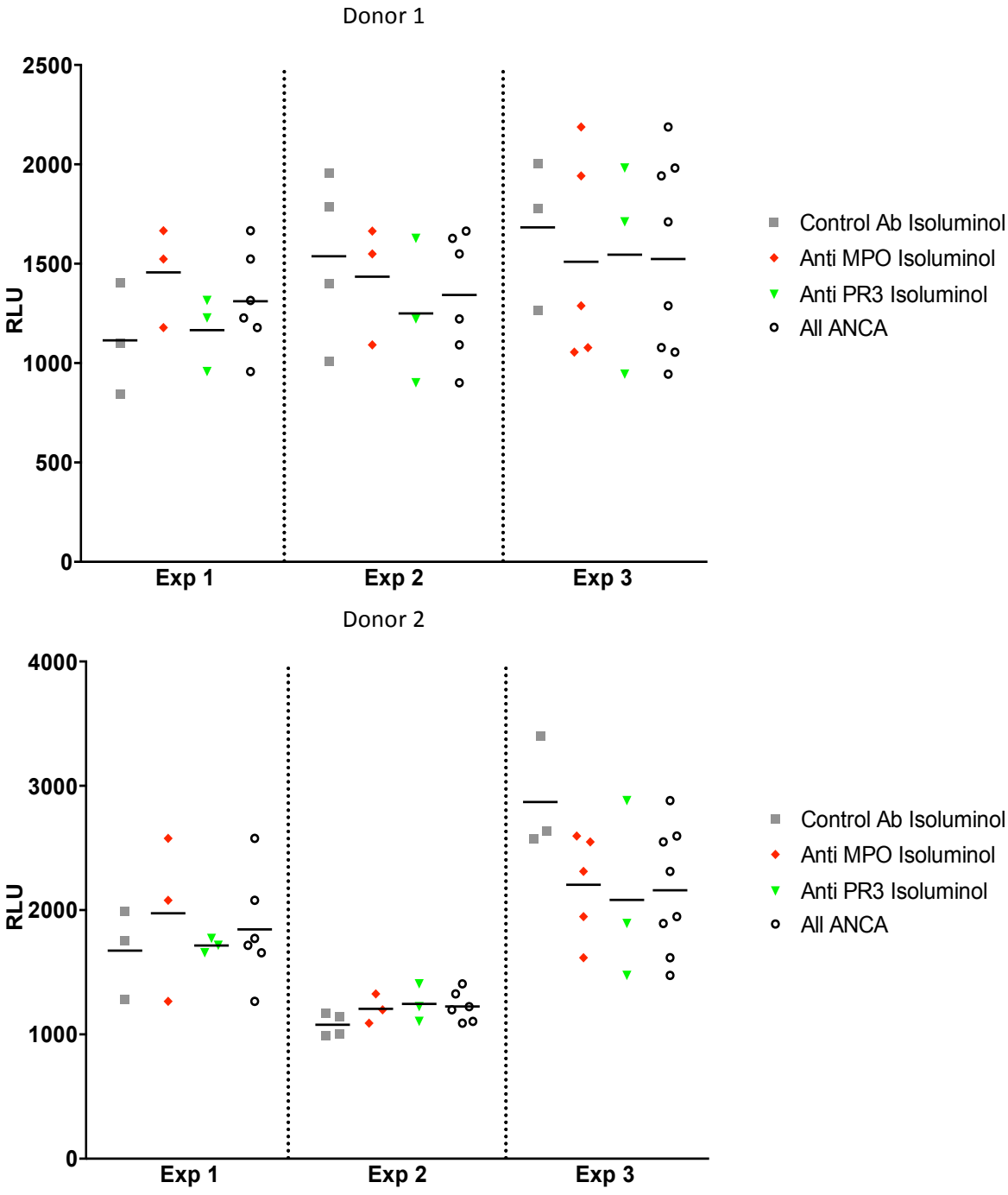

Figure 3.9 - Highest RLU values from isoluminol assay plots in two different donors. TNFα primed neutrophils were activated with control IgG (n=10) or ANCA (MPO-ANCA n=11, PR3-ANCA n=9). Data analysed using a two-way ANOVA (all p values > 0.05).

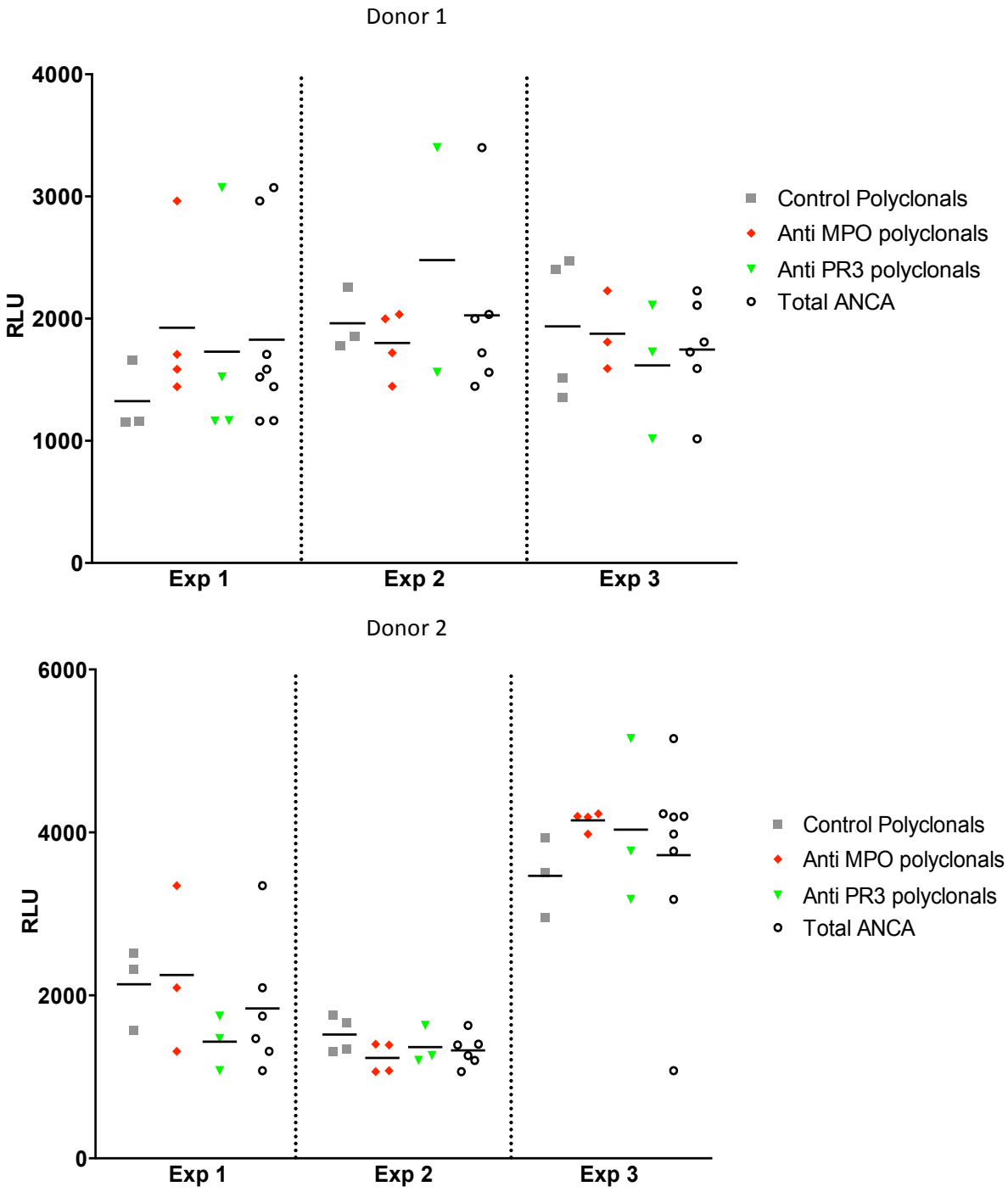

Figure 3.10 - Highest RLU values from luminol assay plots in two different donors. TNFα primed neutrophils were activated with control IgG (n=10) or ANCA (MPO-ANCA n=11, PR3-ANCA n=9). Data analysed using a two-way ANOVA (all p values > 0.05).

There was no significant difference in ROS production in either human donor's TNFα primed neutrophils activated with MPO-ANCA or PR3-ANCA compared to control IgG with both the isoluminol and luminol assays.

We then used bone marrow-derived TNFα primed mouse neutrophils to assess if there was a difference in comparison to human neutrophils. The luminometer assay (luminol based) was used with polyclonal mouse derived MPO-ANCA in comparison to polyclonal mouse control IgG (figure 3.11).

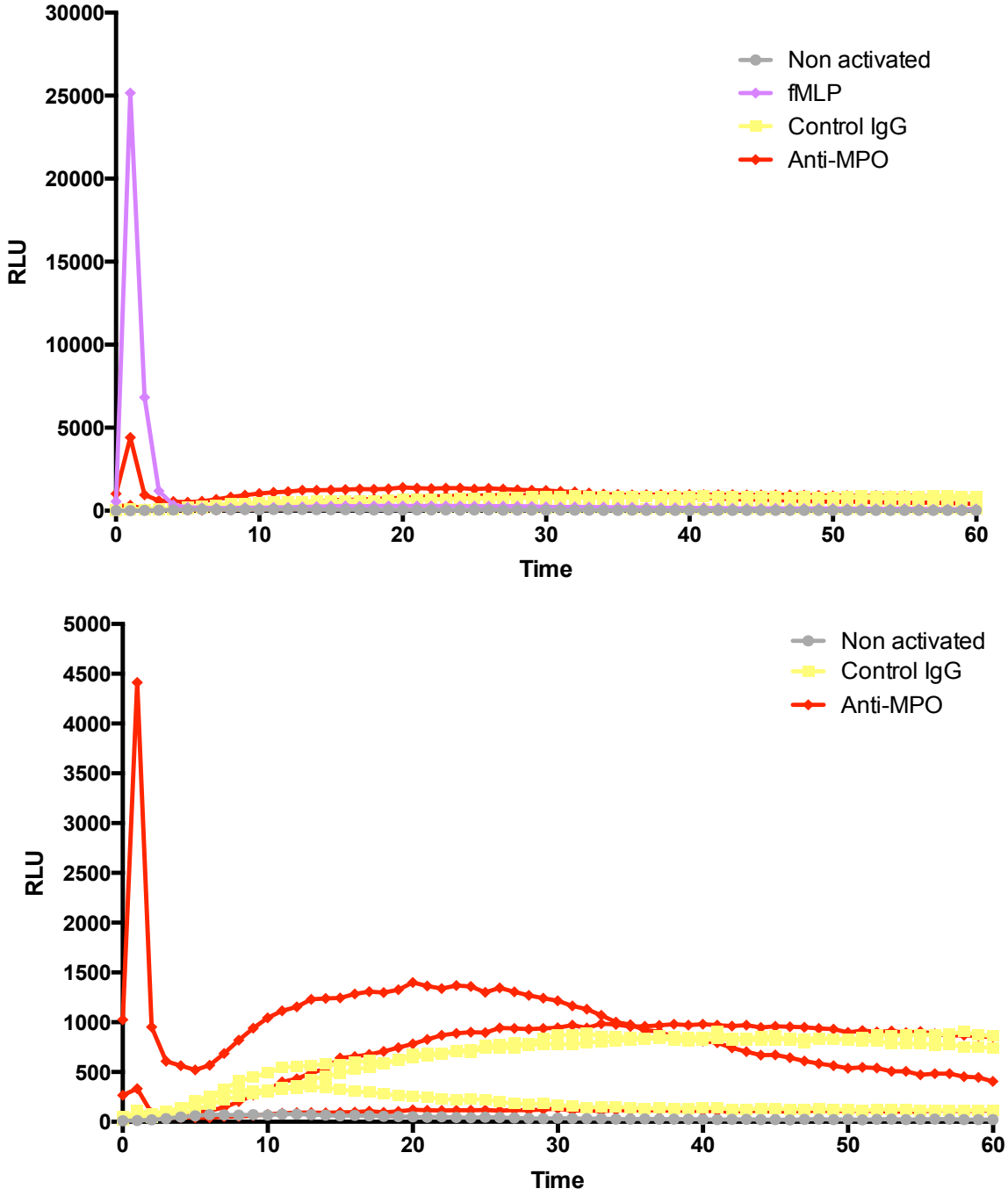

Figure 3.11 – Representative traces of mouse neutrophil activation by luminol assay. Non activated or TNFα primed bone marrow-derived neutrophils from three different mice were stimulated with fMLP (10mM), polyclonal MPO-ANCA (500µg/ml) or control IgG (500µg/ml). The second graph is a copy of the top one with the omission of the fMLP trace.

The mouse luminol assays showed that out of the three different batches of murine generated polyclonal MPO-ANCA only one significantly stimulated mouse neutrophils compared to control polyclonal IgG.

The capacity of ANCA to activate TNFα primed human or mouse neutrophils to undergo respiratory burst is variable and certainly not significantly different to control IgG in our experiments. We also observed that the ANCA that led to higher respiratory burst read-outs in one donor were not necessarily the same ANCA that led to the high read-outs in the second donor. Furthermore, repeating the assays on the same individual neutrophil donor on different days did not always lead to reproducible data with the same ANCA (data not shown).

3.4 Polyclonal ANCA do not consistently induce neutrophil degranulation

We next assessed if patient derived polyclonal ANCA affects neutrophil degranulation. The 20 ANCA and 10 control IgG used for the respiratory burst assays were also used to assess degranulation *in vitro* in two donors. Two different degranulation assays, lactoferrin release and MPO release assays were used as well as neutrophil surface CD66b and CD11b FACS staining to potentially assess all four types of vesicle degranulation (see section 2.5.8 for methodology).

3.4.1 Lactoferrin ELISA

The Lactoferrin ELISA was set up as described in section 2.5.8. As shown in figure 3.12 there was no significant difference in the concentration of lactoferrin in either donor's TNFα primed and ANCA stimulated neutrophil supernatant compared to control IgG from healthy donors.

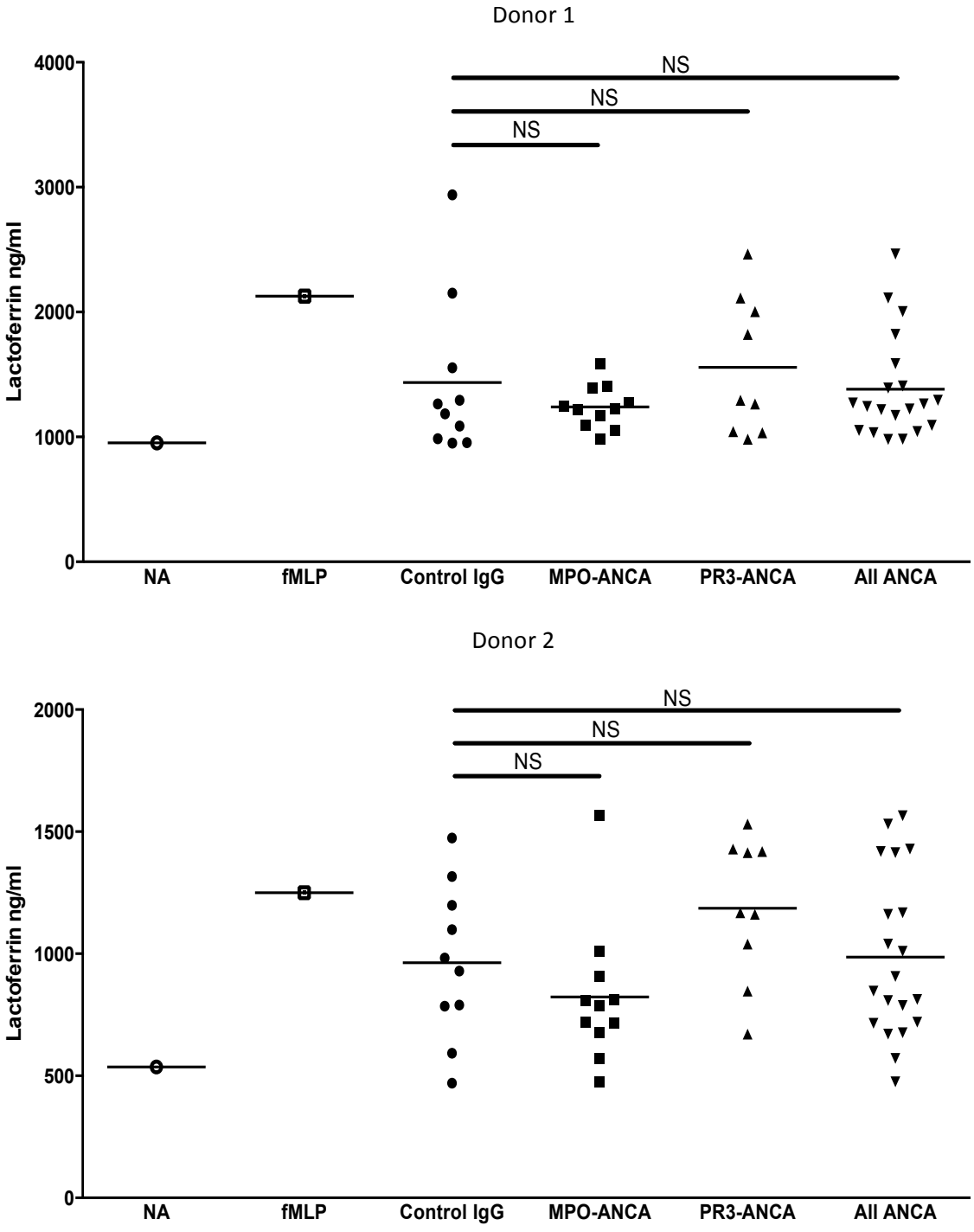

Figure 3.12 - Concentration of lactoferrin in the supernatant of TNFα primed and activated neutrophils from two donors. The NA (non activated) sample serves as a negative control whilst the fMLP stimulated sample serves as a positive control. Data was analysed using one-way ANOVA with Dunnett's post test (NS = non significant). Data for all ANCA was compared to control IgG samples using a student's t test.

3.4.2 MPO assay

Similarly, the MPO assay showed no significant difference in degranulation in either donor's TNFα primed and ANCA stimulated neutrophil supernatant compared to control IgG (see figure 3.13).

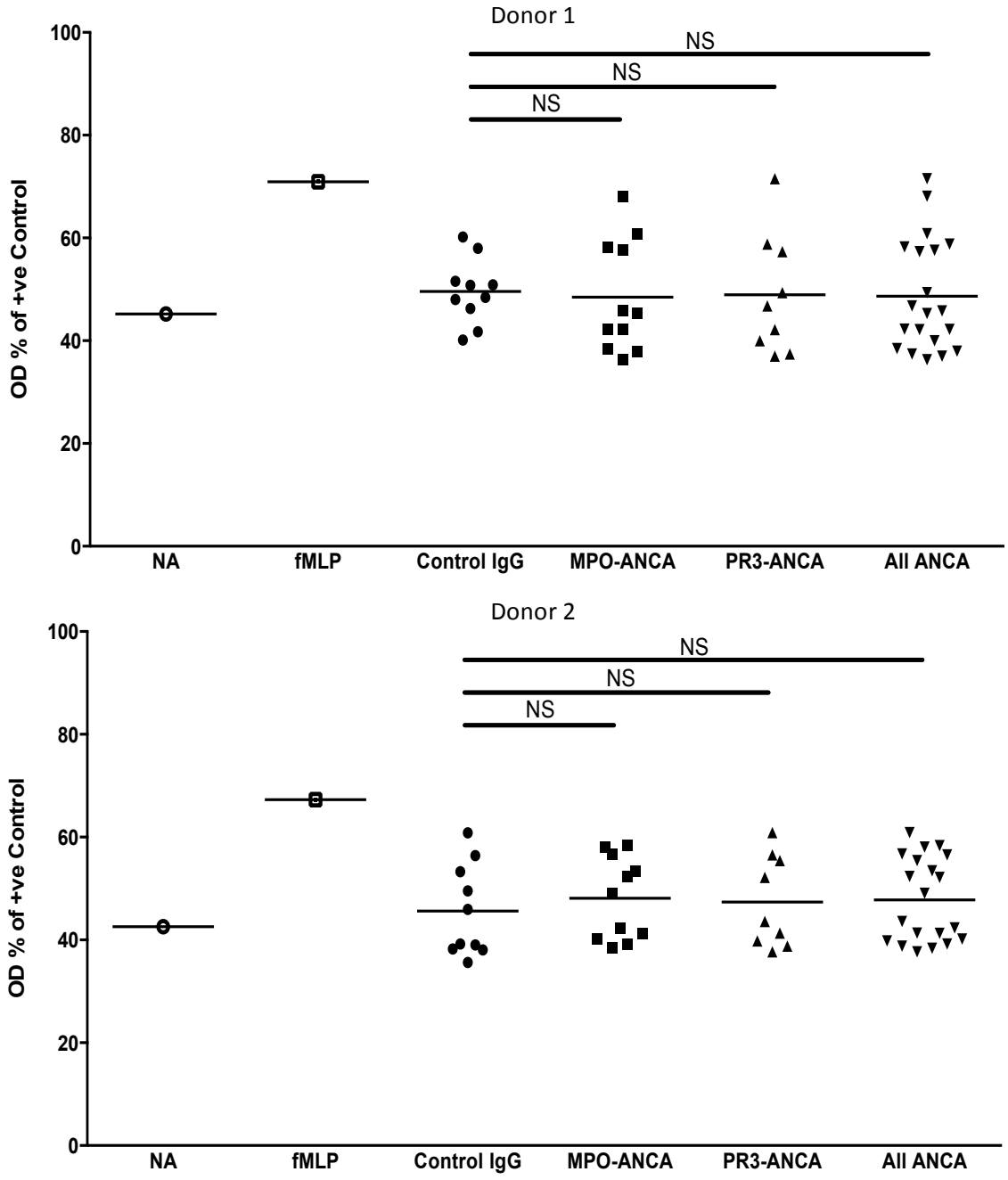

Figure 3.13 - MPO degranulation assay using TNFα primed and ANCA / control IgG activated neutrophil supernatant. The data is presented as a percentage of the positive control (2.5 x 10^6 neutrophils/ml) OD. Data was analysed using one-way ANOVA with Dunnett's post test (NS = non significant).

3.4.3 CD66b neutrophil staining

As described in section 2.5.8, the treated neutrophils were stained for CD66b. Figure 3.14 shows no significant difference in MPO-ANCA or PR3-ANCA treated TNFα primed neutrophils CD66b expression compared to control IgG treated neutrophils.

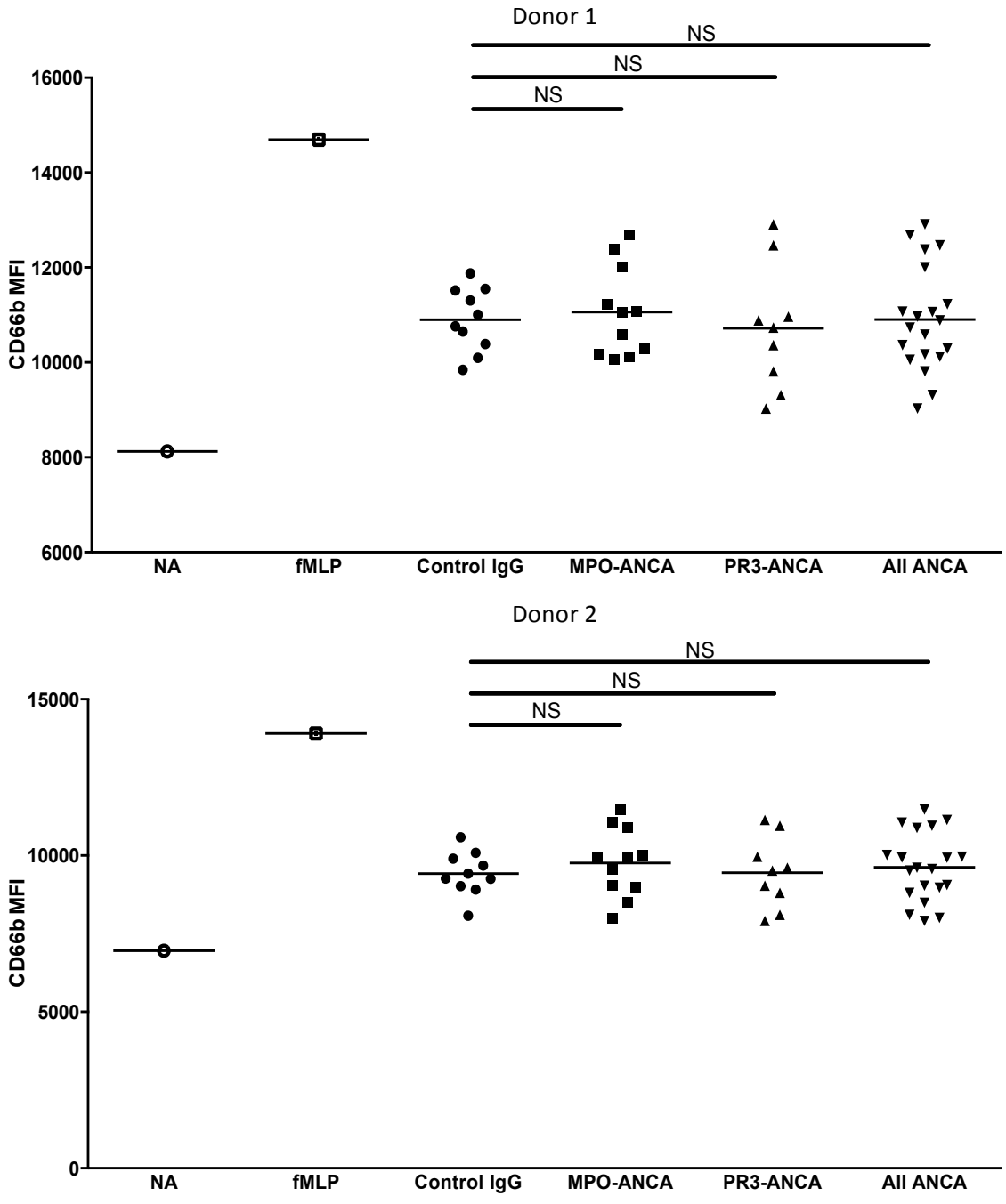

Figure 3.14 – CD66b expression on neutrophil cell surface. The MFI for neutrophil cell surface CD66b expression for each treated condition using either non-activated (NA) neutrophils or TNFα primed and fMLP / control IgG / ANCA stimulated neutrophils from two donors. Data was analysed using one-way ANOVA with Dunnett's post test (NS = non significant).

3.4.4 CD11b neutrophil staining

As for the CD66b staining, neutrophils from the different treatment groups were stained for CD11b on the cell surface (figure 3.15).

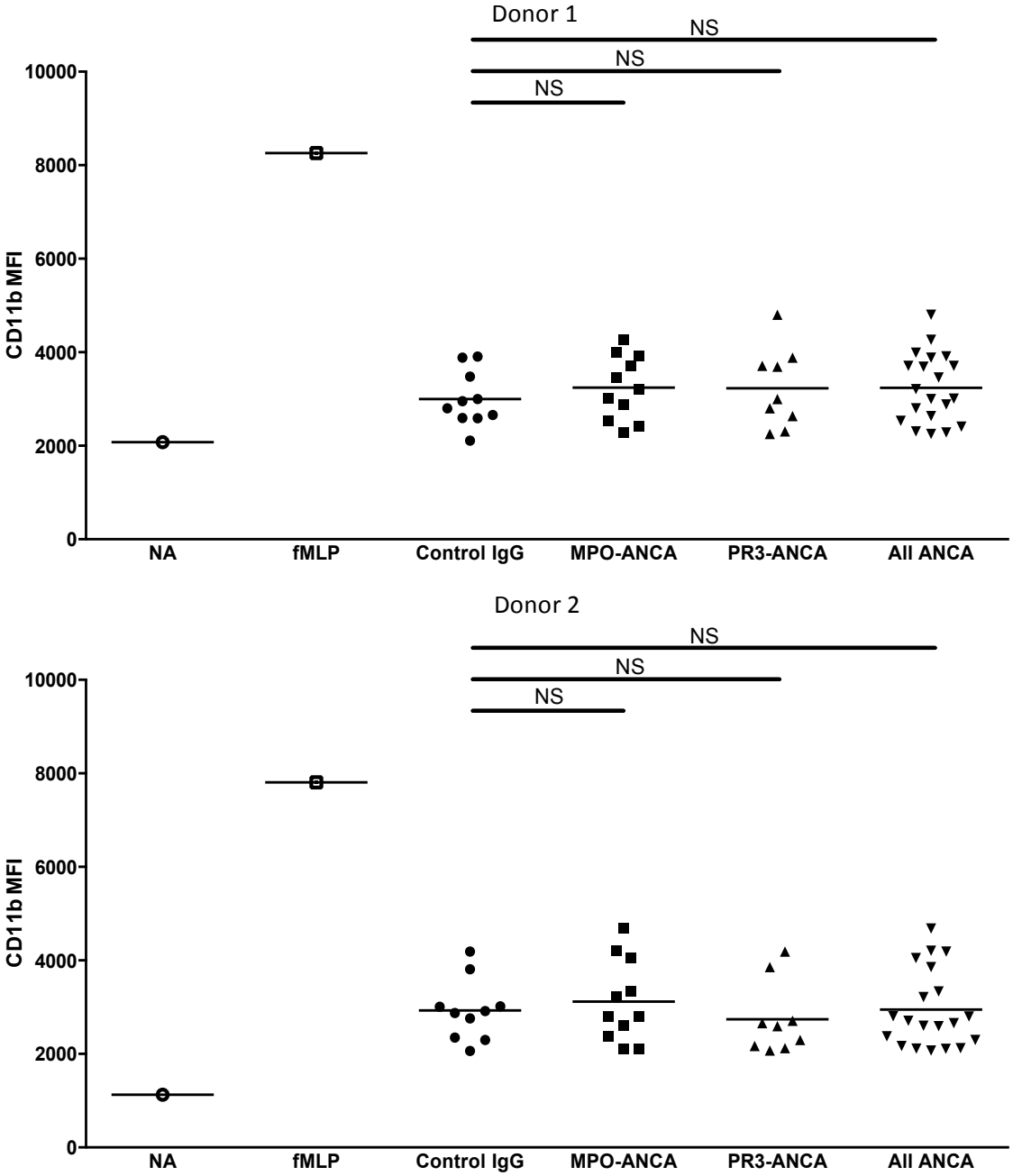

Figure 3.15 – CD11b expression on neutrophil cell surface. The MFI for neutrophil cell surface CD11b expression for each treated condition using either non-activated (NA) neutrophils or TNFα primed and fMLP / control IgG / ANCA stimulated neutrophils from two donors. Data was analysed using one-way ANOVA with Dunnett's post test (NS = non significant).

3.5 Human neutrophils express C3, C5 and the respective anaphylatoxins

In our experience, unselected patient derived polyclonal ANCA do not affect neutrophil respiratory burst or degranulation consistently. However, ANCA may alter other functions. We were interested in not only assessing this but also investigating if like other cell types, neutrophils are capable of generating complement components, and if so how ANCA may affect this. These experiments were performed in the absence of serum and the anti-C3a FACs antibody recognises the neo-epitope.

We first demonstrate using permeabilisation of primed and activated neutrophils (as described in section 2.5.9) that neutrophils, even in the resting state contain C3a and C3 / C3b (figure 3.16) as well as C5a and C5 / C5b (figure 3.17).

The neutrophil cell surface also appears to express C3a, whole C3 / C3b and C5 / C5b and to some extent C5a in the resting, non-activated state (figures 3.18 and 3.19) as shown by FACS. It is unclear why the non-permeabilised cells express high levels of C3a on the cell surface. We did not expect to see the marked shift in MFI noted (see figure 3.18). One would assume that on binding the C3a receptor the complex would be internalised. It is possible that there is non-specific binding of the staining antibody, hence the results need to be interpreted with caution.

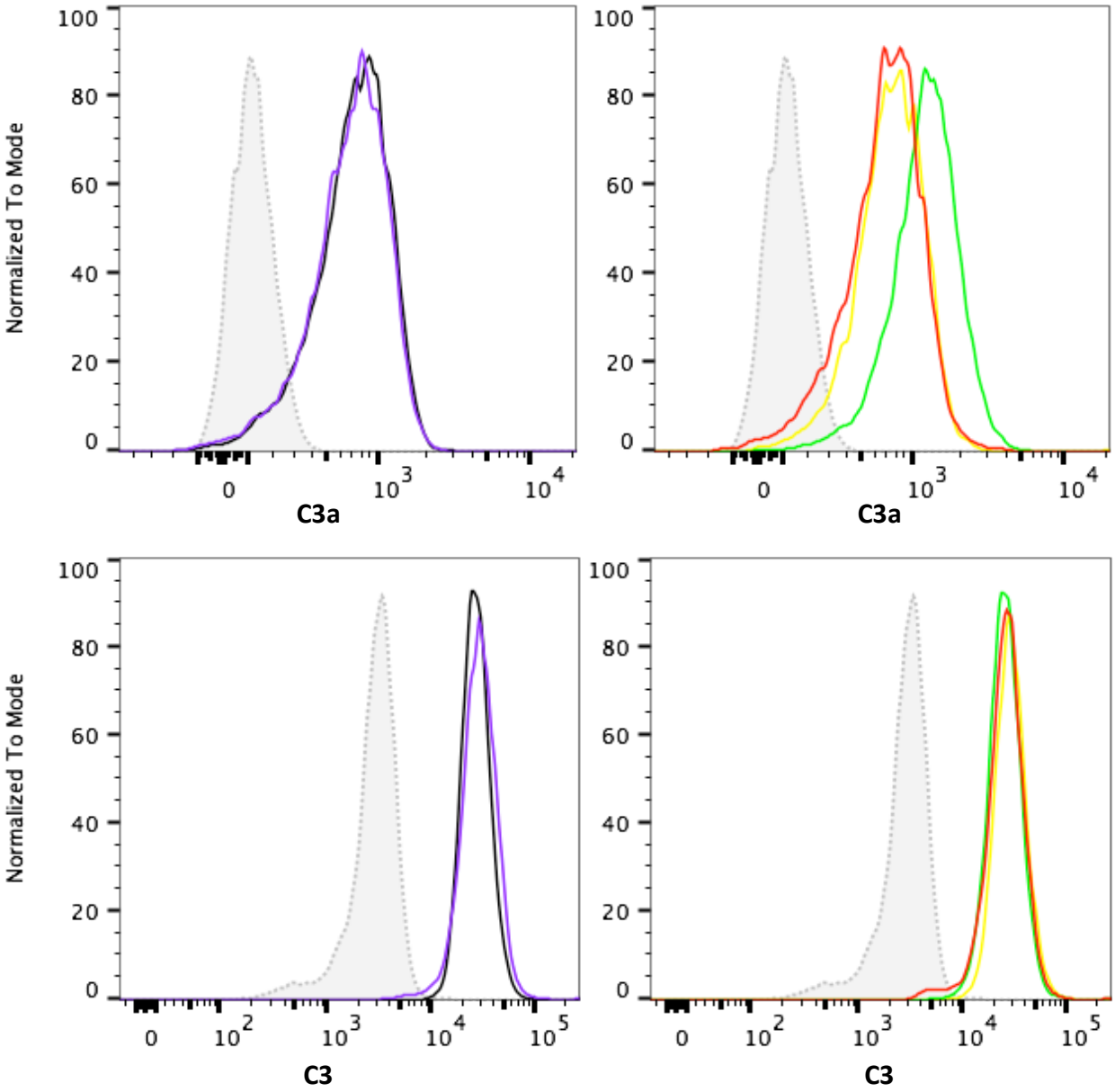

	C3a	C3
Control fluorescent Ab	MFI 113	MFI 2998
Non activated	MFI 745	MFI 26637
TNFα + fMLP	MFI 723	MFI 28751
TNFα + control mAb	MFI 762	MFI 28410
TNFα + PR3 mAb	MFI 1225	MFI 25157
TNFα + MPO mAb	MFI 713	MFI 26010

Figure 3.16 – C3a and C3 FACS histogram plots of permeabilised neutrophils. Non activated or TNFα primed neutrophils stimulated with monoclonal ANCA or control IgG were permeabilised and stained for C3a and C3. MFI for each condition listed.

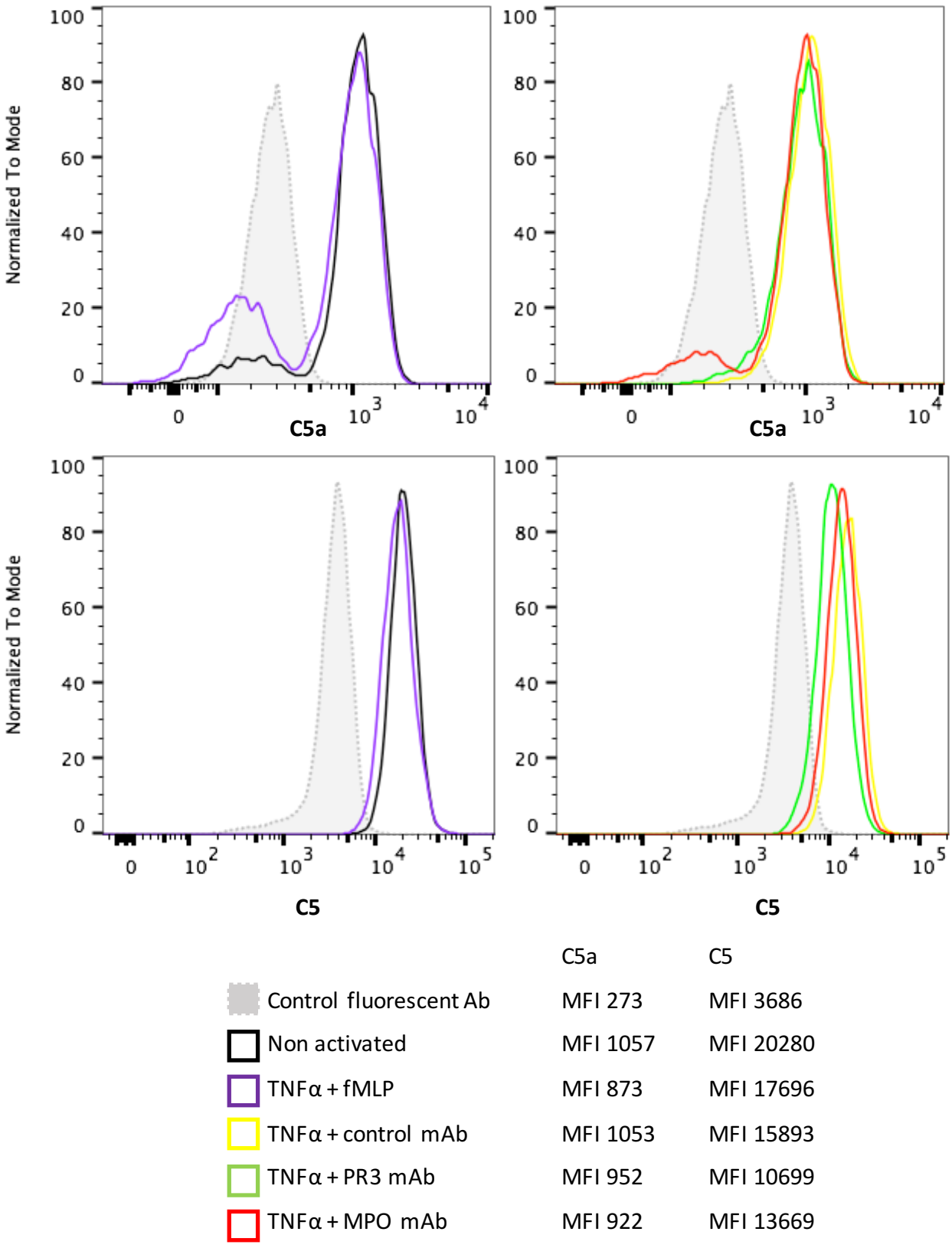

	C5a	C5
Control fluorescent Ab	MFI 273	MFI 3686
Non activated	MFI 1057	MFI 20280
TNFα + fMLP	MFI 873	MFI 17696
TNFα + control mAb	MFI 1053	MFI 15893
TNFα + PR3 mAb	MFI 952	MFI 10699
TNFα + MPO mAb	MFI 922	MFI 13669

Figure 3.17 – C5a and C5 FACS histogram plots of permeabilised neutrophils. FACS plots of permeabilised neutrophils either non activated or primed with TNFα and stimulated with monoclonal ANCA or control IgG stained for C5a and C5. MFI for each condition listed.

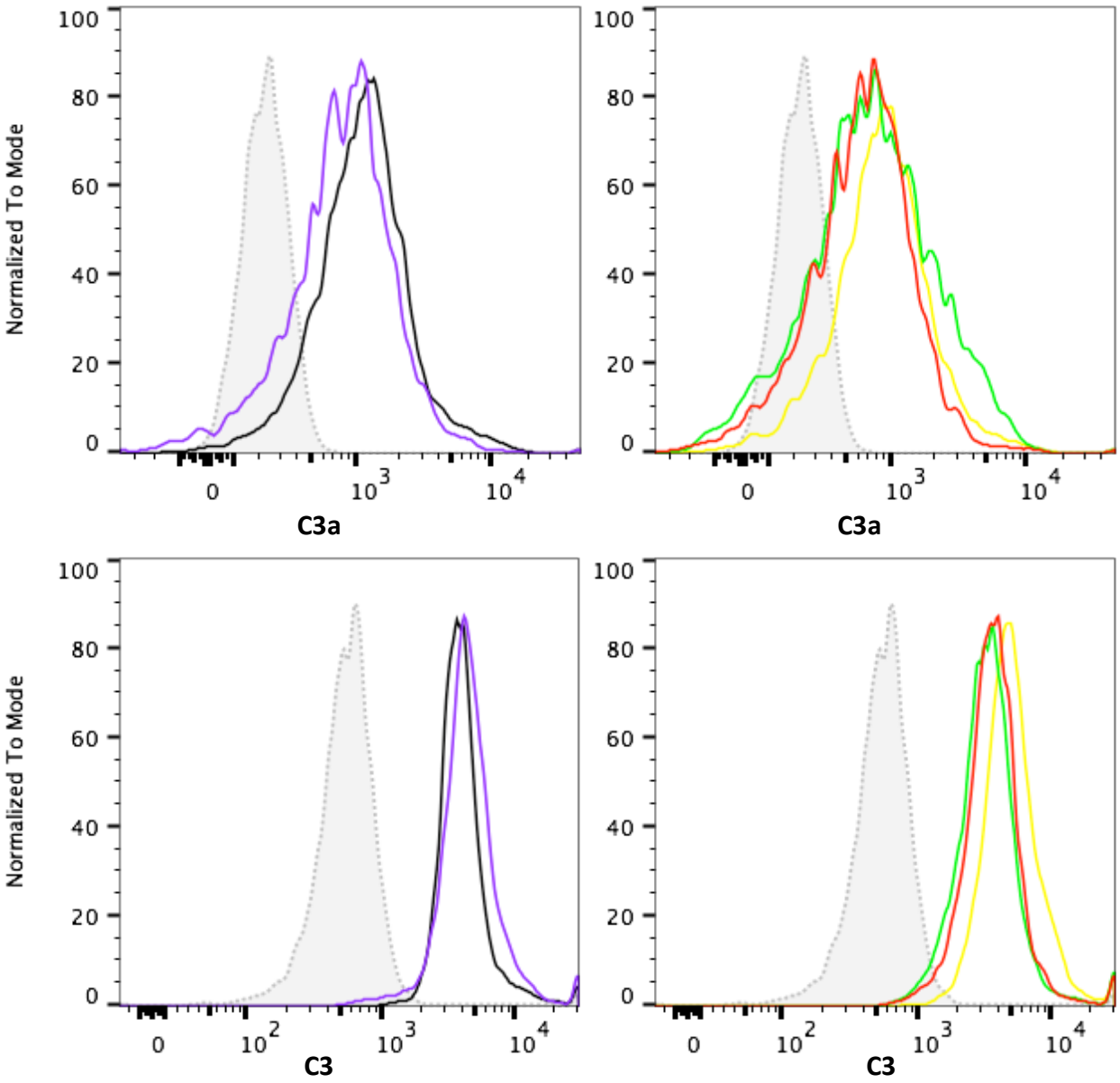

	C3a	C3
Control fluorescent Ab	MFI 232	MFI 559
Non activated	MFI 1136	MFI 3816
TNFα + fMLP	MFI 853	MFI 4325
TNFα + control mAb	MFI 892	MFI 4841
TNFα + PR3 mAb	MFI 753	MFI 3286
TNFα + MPO mAb	MFI 668	MFI 3590

Figure 3.18 – Neutrophil cell surface C3a and C3 expression. FACS histogram plots of neutrophils either non activated or primed with TNFα and stimulated with monoclonal ANCA or control IgG stained for C3a and C3 (cell surface expression). MFI for each condition listed.

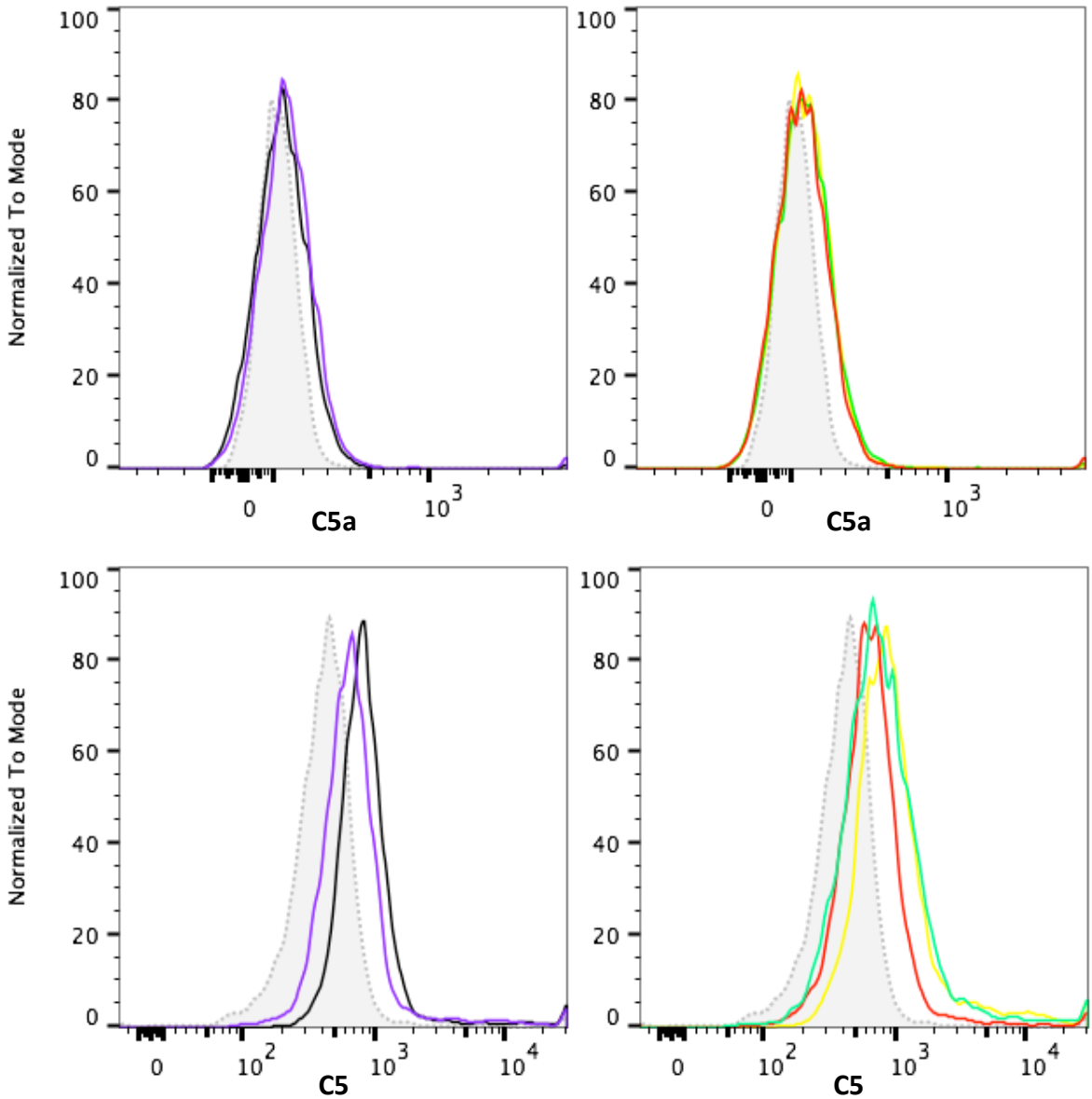

	C5a	C5
Control fluorescent Ab	MFI 111	MFI 417
Non activated	MFI 125	MFI 801
TNFα + fMLP	MFI 139	MFI 641
TNFα + control mAb	MFI 139	MFI 853
TNFα + PR3 mAb	MFI 140	MFI 628
TNFα + MPO mAb	MFI 134	MFI 730

Figure 3.19 - Neutrophil cell surface C5a and C5 expression. FACS histogram plots of neutrophils either non activated or primed with TNFα and stimulated with monoclonal ANCA or control IgG stained for C5a and C5 (cell surface expression). MFI for each condition listed.

We next assessed expression of the anaphylatoxins C3a and C5a in TNFα primed neutrophils (permeabilised in figure 3.20 and cell surface in figure 3.21) incubated with polyclonal control IgG or patient ANCA.

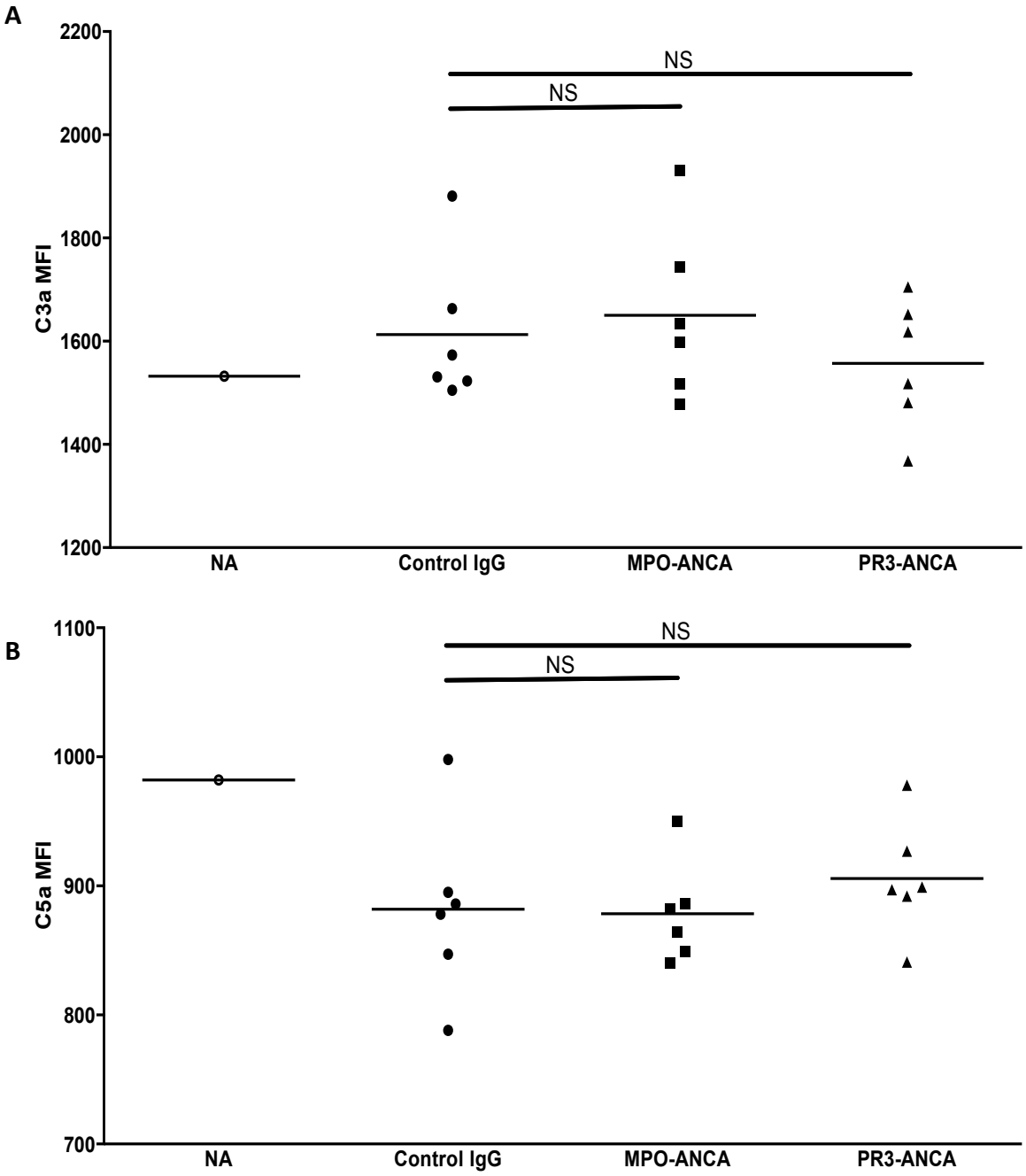

Figure 3.20 – C3a and C5a expression in permeabilised neutrophils. MFI for permeabilised neutrophil C3a (A) and C5a (B) expression for each treated condition using either non-activated (NA) neutrophils or TNFα primed and polyclonal control IgG or patient derived ANCA stimulated neutrophils. Data analysed using one-way ANOVA with Dunnett's post test.

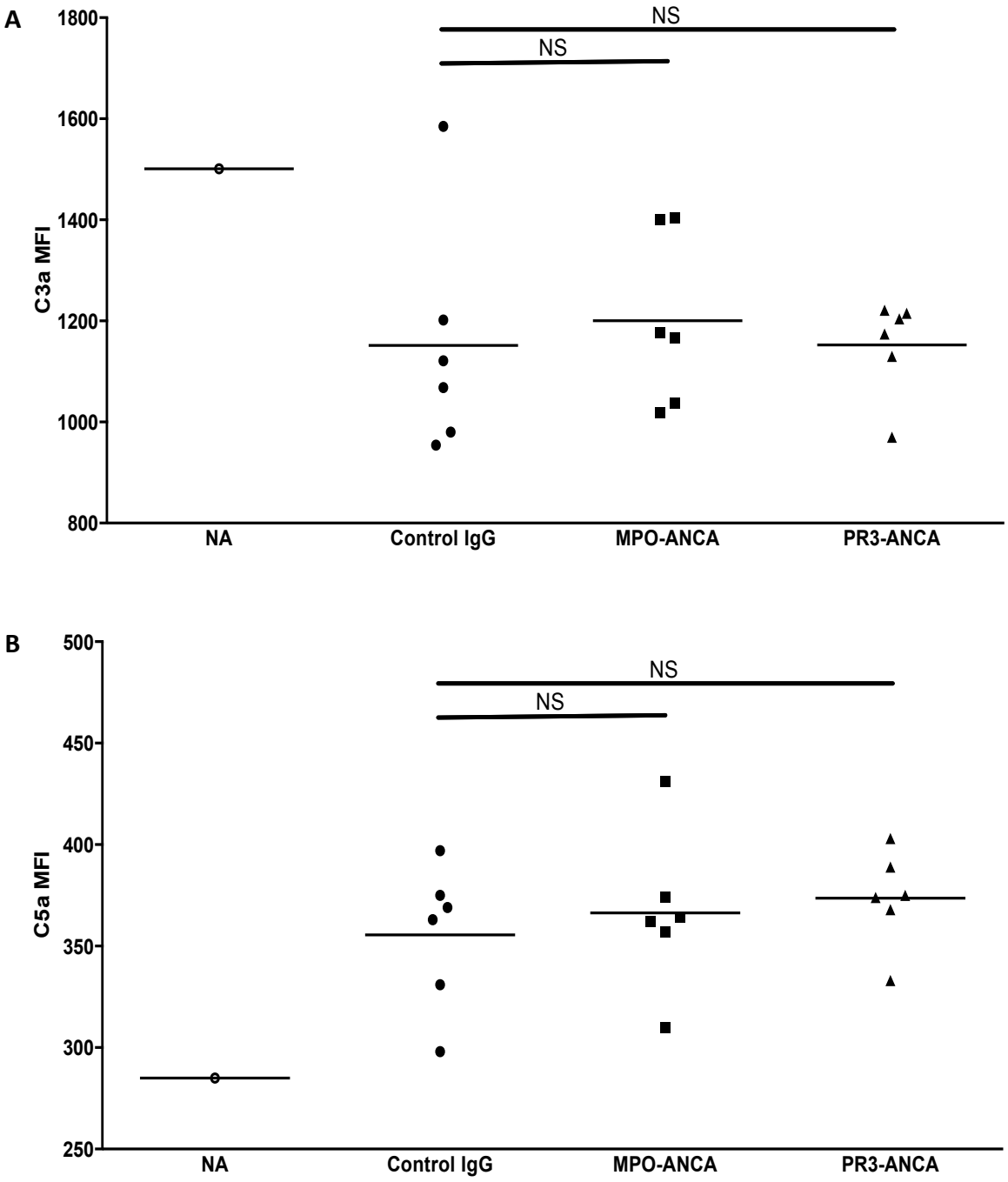

Figure 3.21 - C3a and C5a expression on neutrophil cell surface. MFI for neutrophil cell surface C3a (A) and C5a (B) expression for each treated condition using either non-activated (NA) neutrophils or TNFα primed and polyclonal control IgG or patient derived ANCA stimulated neutrophils. Data were analysed using a one-way ANOVA with Dunnett's post test.

There was no significant difference in C3a or C5a expression in permeabilised and non-permeabilised TNFα primed neutrophils treated with polyclonal ANCA compared to control IgG. The resulting question was whether the anaphylatoxins observed by FACS within neutrophils were expelled by the TNFα primed neutrophils incubated with polyclonal ANCA into the supernatant. The supernatant of the activated neutrophils were acquired as described in section 2.5.10 and analysed using a CBA anaphylatoxin kit (see figure 3.22 for C3a and figure 3.23 for C5a levels).

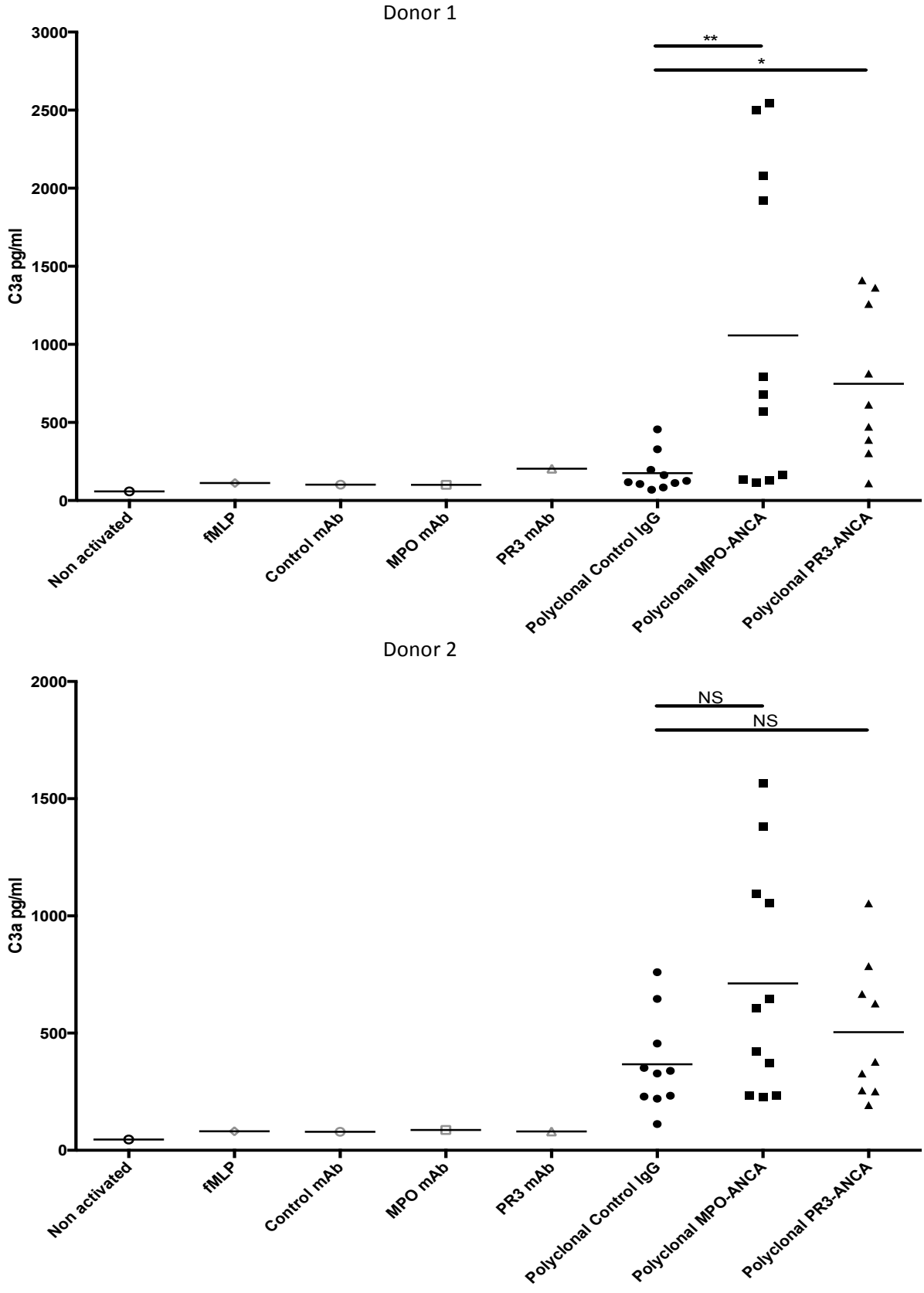

Figure 3.22 – C3a levels in the supernatant of non activated or TNFα primed neutrophils from two separate donors. The primed neutrophils were stimulated with monoclonal (mAb) or polyclonal antibodies from controls or patients. Data were logarithmically transformed and analysed using a one way ANOVA with Dunnett's post test (NS = non significant, * = $p < 0.05$, ** = $p < 0.01$).

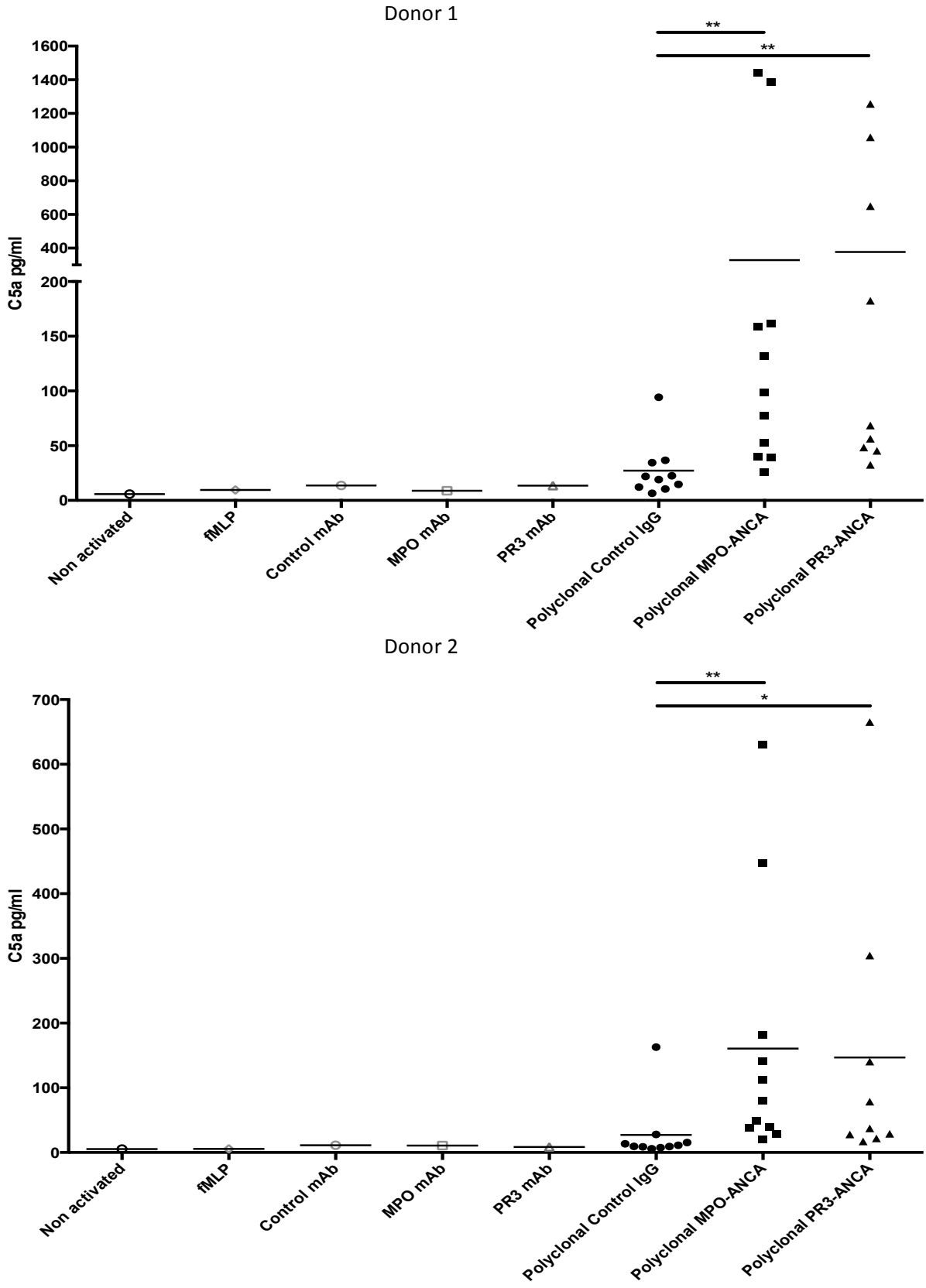

Figure 3.23 – C5a levels in the supernatant of non activated or TNFα primed neutrophils from two separate donors. The primed neutrophils were stimulated with monoclonal (mAb) or polyclonal antibodies from controls (n=10) or patients (MPO-ANCA n=11, PR3-ANCA n=9). Data were logarithmically transformed and analysed using a one way ANOVA with Dunnett's post test (* = $p < 0.05$, ** = $p < 0.01$).

The level of C5a in the supernatant of TNFα primed neutrophils from two separate donors was significantly increased following incubation with polyclonal antibody from patients with MPO-ANCA or PR3-ANCA disease. The level of C3a in the supernatant was variable amongst the two neutrophil donors under similar treatment conditions.

The concern was that the anaphylatoxins might be carried through in our antibody preparations upon isolation from human serum samples. Hence the measured rise in C5a noted after incubation with MPO-ANCA and PR3-ANCA polyclonal antibodies might well be an artefact. As a result we measured the levels of C3a and C5a in our antibody preparations and in the supernatants of TNFα primed neutrophils incubated with the respective polyclonal antibodies in one donor (figure 3.24).

The levels of C3a and C5a were significantly higher in the supernatants of the TNFα primed neutrophils following incubation with the polyclonal MPO-ANCA preparations compared to the antibody preparations alone suggesting that indeed the neutrophils release the anaphylatoxins on exposure to MPO-ANCA. C3a levels were elevated in the supernatants of all polyclonal treated TNFα primed neutrophils including control IgG and PR3-ANCA. When C3a and C5a levels were compared in the baseline antibody samples there was no statistically significant difference in the anaphylatoxin levels between control IgG samples and MPO-ANCA samples or PR3-ANCA samples (student's t test).

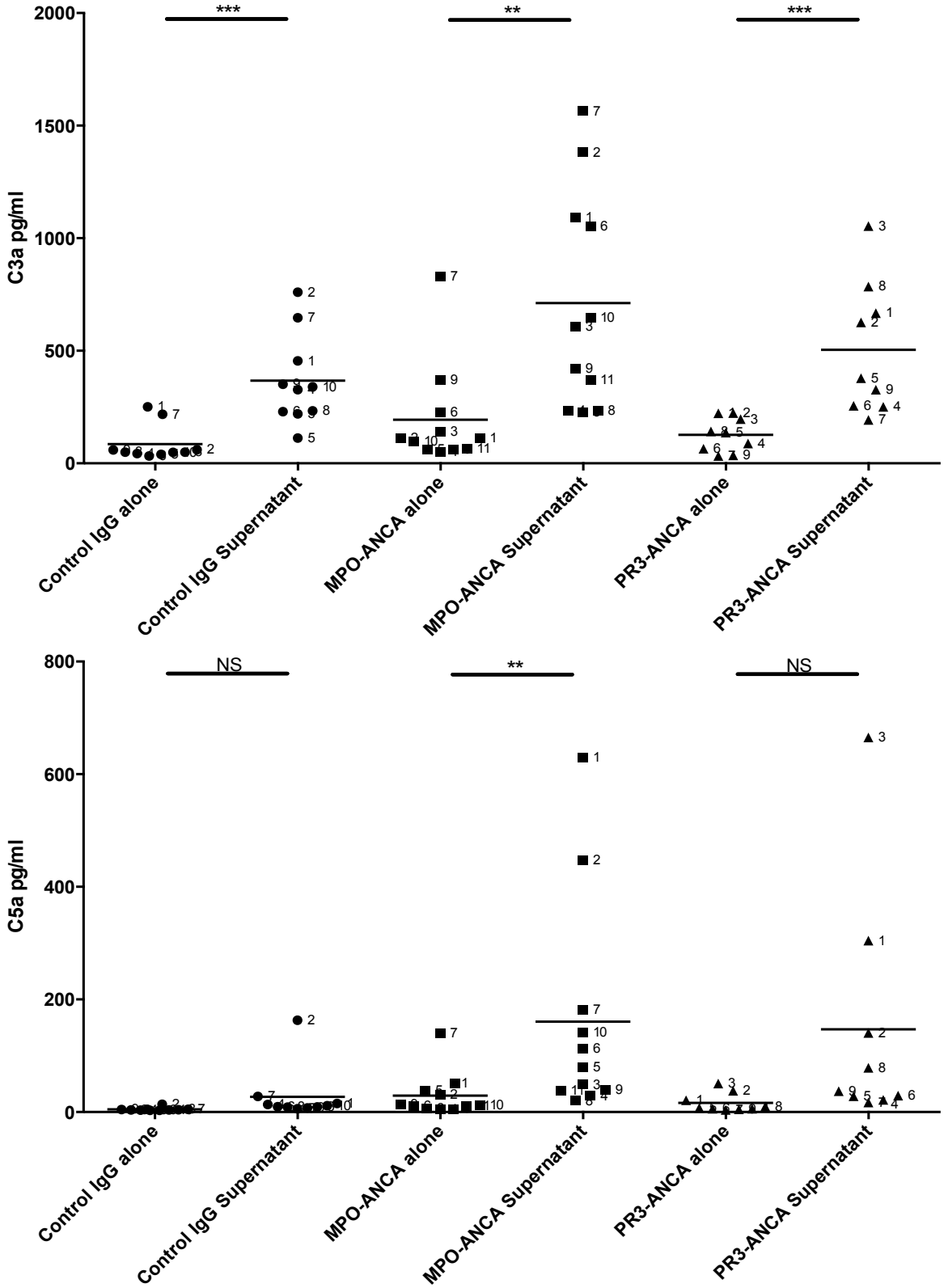

Figure 3.24 – C3a and C5a levels in the antibody preparations and activated neutrophil supernatant. Anaphylatoxin levels measured in antibody preparations alone and in the supernatant of TNFα primed neutrophils stimulated with polyclonal antibodies from controls (n=10) or patients (MPO-ANCA n=11, PR3-ANCA n=9). Each antibody in each group is numbered with corresponding supernatant. Data were analysed using a student's t test (NS = non significant, ** = $p < 0.01$, *** = $p < 0.001$).

As discussed neutrophils are capable of expressing all the components that make up the C5 convertase and hence C5a may well be produced locally by the neutrophils. C3 has been previously shown to be enzymatically cleaved in a non-convertase dependent manner by cathepsin L [191]. Neutrophils harbour a range of serine proteases that are possibly able to cleave C3. As a result, we tested whether PR3 was able to cleave C3 as desc ribed in section 2.5.15, by incubating purified human C3 with PR3 and performing SDS-PAGE (figure 3.25).

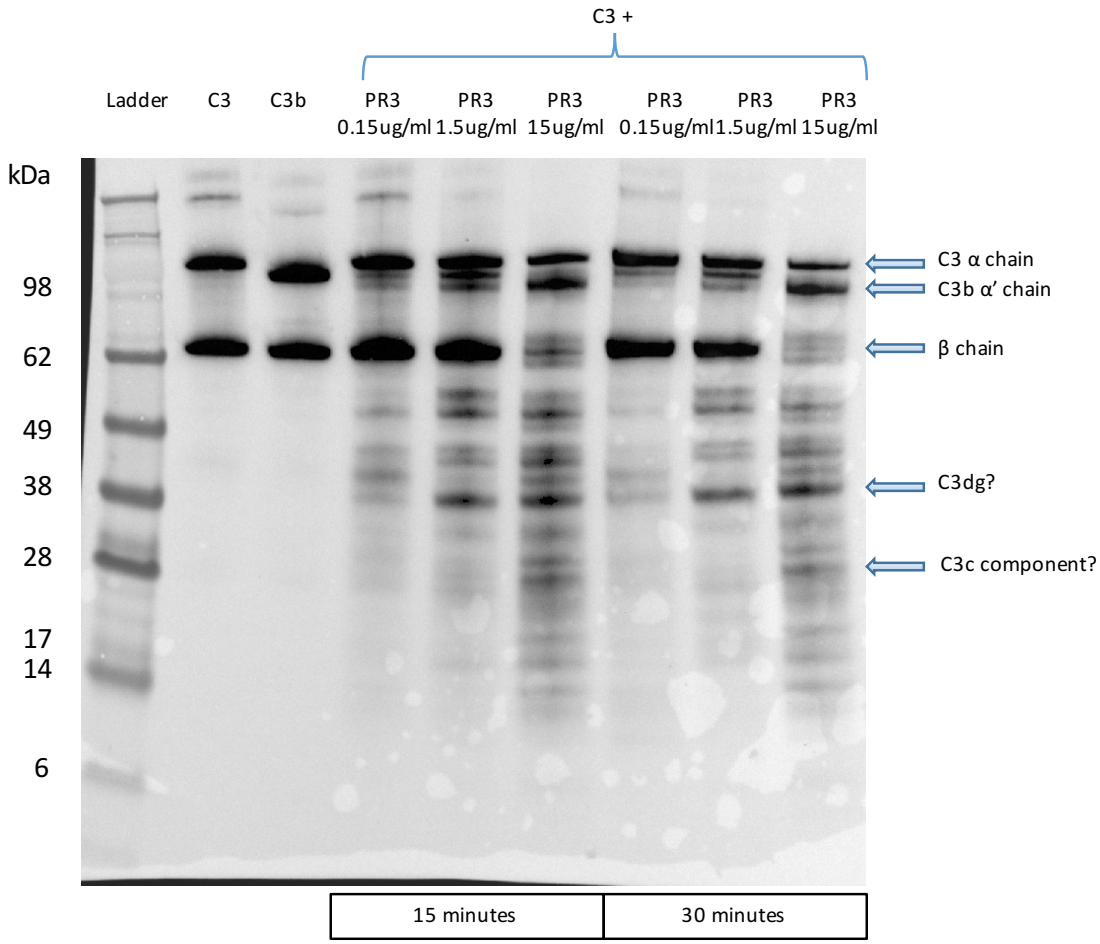

Figure 3.25 – Representative Western blot of C3 product breakdown by PR3. Serum purified C3 was incubated with differing concentrations of PR3 for 15 or 30 minutes and analysed by Western blot with the use of an anti-C3 antibody. Serum purified C3 and C3b were used as controls. The possible components of C3 are listed.

A silver stain of the blot was also run to assess the presence of C3a (figure 3.26).

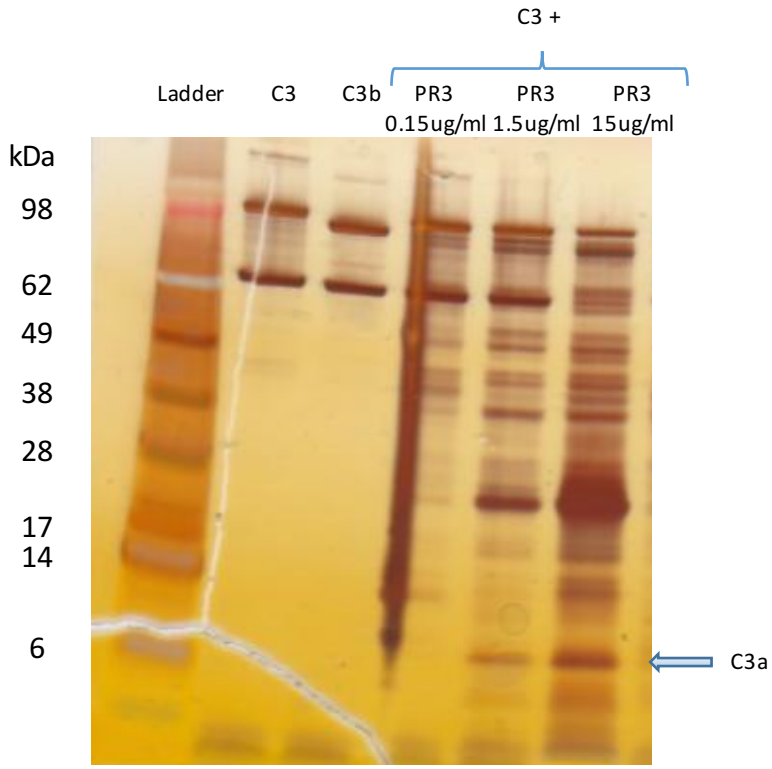

Figure 3.26 – Representative silver stain of C3 product breakdown by PR3. Serum purified C3 was incubated with differing concentrations of PR3 and analysed by silver stain blot. Serum purified C3 and C3b were used as controls. The possible C3a component is highlighted.

It seems that PR3 is capable of cleaving C3 into various identifiable but also non-specific components as shown by the blots.

3.6 Discussion

Since the first report of ANCA in 1982, advances have been made in the understanding of the pathogenesis of AAV. However, plenty of unknowns remain. The use of *in vitro* assays and *in vivo* models has advanced the field, but inconsistencies remain.

It is widely accepted in the field that ANCA are pathogenic, although cell-mediated immunity to MPO and PR3 probably plays a role as well. The most convincing evidence for the pathogenicity of ANCA, as discussed, comes from the passive transfer *in vivo* model, whereby injecting MPO-ANCA causes a crescentic glomerulonephritis [100]. *In vitro* studies, as discussed, have shown with often limited neutrophil donors and numbers of IgG preparations from control subjects and patients that ANCA stimulate primed neutrophils to undergo respiratory burst and degranulation.

There are a few reports in the literature where investigators have studied large panels of MPO-ANCA or PR3-ANCA. Franssen *et al* purified ANCA IgG from 17 PR3-ANCA and 14 MPO-ANCA positive patients with pauci-immune necrotising crescentic glomerulonephritis who presented to the hospital consecutively, thus reducing selection bias. Control IgG from 16 healthy volunteers was used for comparison. Two different healthy donors were used to isolate neutrophils. They showed that PR3-ANCA significantly increased TNFα primed neutrophil ROS production (using the ferricytochrome C reduction assay and DHR 123 assay) and degranulation (β-glucuronidase release) compared to control IgG but MPO-ANCA did not. Most but not all PR3-ANCA IgG fractions were capable of inducing respiratory burst or degranulation to an extent that was greater than that observed with control IgG [95]. Furthermore, they found no significant correlation between *in vitro* capacity of the IgG fractions to activate neutrophils and disease severity parameters such as creatinine level and BVAS.

Harper *et al* used 23 MPO-ANCA and 15 PR3-ANCA fractions from patients with pauci-immune necrotising crescentic glomerulonephritis, as well as 8 control IgG. At least five different donor neutrophils were used. In contrast they showed that MPO-ANCA fractions were significantly more potent at causing respiratory burst (ferricytochrome

C reduction assay) and degranulation (MPO assay) of TNFα primed neutrophils compared to PR3-ANCA or control IgG [256].

We found that our group of randomly selected twenty polyclonal patient samples (11 MPO-ANCA and 9 PR3-ANCA) did not significantly lead to a greater level of respiratory burst or degranulation of TNFα primed human neutrophils from two separate donors compared to randomly selected 10 control IgG fractions. This was corroborated by the mouse neutrophil luminol assays. Polyclonal mouse MPO-ANCA did not cause a significant rise in ROS production as measured by the luminometer assay in comparison to polyclonal control IgG.

The data are highly inconsistent and it is not entirely apparent why. The ferricytochrome C reduction assays measure extracellular ROS production and can be very variable and inconsistent in our experience. Hence, we assessed ROS production by chemiluminescence using luminol, which measures both extracellular and intracellular ROS production as well as the isoluminol assay, which measures extracellular ROS only. We also used the DHR 123 assay, which primarily measures intracellular ROS production.

There are several compounding factors. The use of whole non-affinity purified IgG fractions means that the percentage of MPO-ANCA or PR3-ANCA in the samples is unknown. It may be that ANCA that induce strong neutrophil responses do so simply because they are composed of a higher proportion of PR3-ANCA or MPO-ANCA IgG as opposed to other contaminating IgG. However, we found no significant correlation between ANCA titres and neutrophil respiratory burst or degranulation read-outs in our studies.

Furthermore, other IgG in the samples may bind to neutrophil Fc receptors required for ANCA activation thus inhibiting ANCA induced responses. The polyclonal IgG purified from patients may also differ in regards to subclass, which has been shown to influence the ability of ANCA to cause respiratory burst [257].

The ANCA preparations will also differ in epitope specificity and affinity, which may account for differences in neutrophil activation. Roth *et al* recently showed substantial

MPO-ANCA epitope diversity. They used high sensitivity epitope excision and mass spectrometry investigating patients in remission, those with active disease, ANCA-negative patients and healthy controls. They identified a total of 25 different epitopes, 12 of which were exclusive to active disease and 8 were also present in healthy subjects. One epitope (aa447-459) was exclusive to active disease and reactivity to this epitope declined in remission. Interestingly, anti-MPO447–459 antibodies could induce the release of ROS from neutrophils, whereas antibodies specific for natural epitopes barely induced ROS release. Furthermore transfer of IgG from mice immunized with a murine MPO peptide that overlaps with peptide aa447–459, induced glomerular injury and neutrophil accumulation in recipient mice. This study suggests that epitope specificity defines the pathogenicity of ANCA [94].

It is also possible that the role of ANCA in disease pathogenesis is not related to its ability to activate neutrophil respiratory burst or degranulation. In support of this a recent article showed mice deficient in NADPH oxidase (and hence have an inability to produce ROS) have more severe disease compared to wild type controls [258].

Lastly, extrapolating results from *in vitro* assays to the *in vivo* situation must be done with caution. *In vitro* assays may not necessarily reflect *in vivo* mechanisms. The cells are treated outside their normal milieu, not accounting for exposure to other cells as well as factors such as systemic or local complement, cytokines and chemokines. It is highly likely that isolated neutrophils behave differently to *in vivo* neutrophils. The interaction of neutrophils and the endothelium *in vivo* may be crucial to the way ANCA interacts with its antigens. Further efforts could be made to more closely mirror these conditions *in vitro*. Endothelial cell and neutrophil co-cultures could be employed for example, or even a more simple measure such as plate-bound ANCA rather than ANCA in solution. Furthermore, we did not assess nor control for MPO or PR3 surface expression in response to TNFα priming in our neutrophil donors, which may be a confounding factor. Another factor that we have not accounted for is the ages of the control IgG donors. The control IgG donors were not age matched to the ANCA donors which may lead to a discrepancy in the read-outs as IgG glycoform structure and function varies with age.

So, although we have not shown *in vitro* that ANCA activate TNFα primed neutrophils in terms of respiratory burst or degranulation they may do so *in vivo*.

Although we did not find a difference in the classical functional roles of neutrophils with ANCA, we show that neutrophils express C3 and C5 and have the ability to process these complement components to their respective anaphylatoxins. Furthermore, it seems ANCA alter the processing of the anaphylatoxins.

C5a is a potent inflammatory mediator that acts as a chemoattractant for myeloid cells and can elicit superoxide generation in neutrophils. Plasma levels of C5a are raised in patients with active AAV than those in remission [204]. It has been shown *in vitro* that recombinant C5a dose dependently primes neutrophils for ANCA induced respiratory burst [209]. Furthermore, C5a is able to prime neutrophils resulting in the expression of PR3 on the neutrophil membrane and leading to degranulation as measured by the release of lactoferrin. The use of p38 MAPK, ERK, and PI3K inhibitors decrease C5a induced membrane expression of PR3 and lactoferrin release from neutrophils activated by PR3-ANCA following C5a priming [259].

We have shown that resting neutrophils have intracellular C3, C5, C3a and C5a, as well as extracellular C3 and C5. The expression of these complement components was not altered by polyclonal ANCA or fMLP induced activation either within the intracellular compartment or on the cell surface. However, upon incubation with patient polyclonal ANCA, the TNFα primed neutrophils expel C5a into their supernatants at a significantly higher level than that seen with control IgG. This suggests that upon ANCA mediated activation neutrophils may well be more capable of readily breaking down C5 into its anaphylatoxin and possibly C5b components. This may have effects on the donor cell and act in an autocrine fashion or contribute to paracrine functions of C5a. It appears that neutrophils have the innate ability to cleave C3 and C5 into its respective components and the mechanism of this still remains to be elucidated. The process may occur with the use of conventional C3 and C5 convertases or may be convertase independent using local proteases such as PR3.

Chapter 4 – The role of monocytes in AAV

4.1 Introduction

The term ANCA is a misnomer as the autoantibodies recognise antigens that are not specific solely to neutrophils. Monocytes are the other subset of leucocytes that express the classical antigens to ANCA, namely MPO and PR3, as described in chapter 1. Whilst the pathological effects of ANCA on neutrophils are broadly explored, the impact of ANCA on monocyte function is less well understood.

Monocytes and macrophages are present within early segmental lesions seen on renal biopsies from patients with AAV and have been shown to be the predominant glomeruli infiltrating leucocytes [3, 146]. This certainly implicates monocytes in addition to neutrophils in the tissue damage associated with AAV. As discussed in section 1.9, some *in vitro* studies have shown that ANCA can modulate monocyte function. Ralston *et al* described the production of IL8 in response to PR3-ANCA and O'Brien *et al* recently described the production of IL1β, IL6 and IL8 by TNFα primed monocytes in response to MPO-ANCA but not to PR3-ANCA [141, 145]. In addition, the production of oxygen radicals by TNFα-primed monocytes in response to ANCA has been described [143].

Monocytes are circulating leucocytes that are present in the bloodstream for 3 to 5 days and have the potential to differentiate into and replenish tissue macrophages and dendritic cells. Monocytes as a result have a key role in inflammation and tissue repair. Human monocytes are divided into subsets on the basis of CD14 and CD16 expression as discussed in chapter 1. Classical monocytes (CD14++CD16-), which account for approximately 90% of the total monocyte population, are thought to have a role in phagocytosis, produce high levels of IL10 and low-grade levels of TNFα in response to LPS. Intermediate monocytes (CD14++CD16+) have a higher capacity to release TNFα and IL1β in response to LPS. Non-classical monocytes (CD14+CD16++) release TNFα and IL1β in response to DNA and RNA particles [260, 261].

Macrophages were classically thought to only originate from blood monocytes. More recent understanding of macrophage biology has revealed that tissue macrophages

can in fact be established during embryology and persist into adulthood [262]. During an inflammatory insult, circulating monocytes are recruited and thought to undergo differentiation into two subsets of macrophages M1 and M2 depending on environmental cues.

M1 macrophages are classically pro inflammatory whilst M2 macrophages are thought to stimulate tissue repair and fibrosis. M2 macrophages are further subdivided into M2a (induced by IL4 or IL13), M2b (upon exposure to immune complexes and IL1β or LPS) or M2c (stimulated by IL10 or TGFβ). M1 macrophages are induced by IFN–γ and LPS or TNFα [263]. GMCSF polarises macrophages to the M1 phenotype whilst CSF1 promotes a M2 phenotype [264]. There are various markers used to differentiate M1 and M2 macrophages. M1 macrophages typically express inducible nitric oxide synthase (iNOS), CD80 and CD86, whilst M2 macrophages express arginase 1, CD163 and CD206 [265]. Furthermore, macrophages have a role in directing Th1 and Th2 responses as well as being influenced by the CD4 T cell cytokines themselves [266].

Nonetheless, macrophages are highly plastic and heterogeneous, it is felt that classification into the M1 and M2 subsets is relatively simplistic. Instead macrophages display a continuum of phenotypes and co-exist with the resulting phenotype depending on the local milieu. Hence clear distinctions are often not possible.

Inflammation is a normal response to tissue injury and is highly regulated with both pro- and anti- inflammatory events in place to ensure prompt restoration of tissue homeostasis. Macrophages are vital in inflammation as well as tissue repair and remodelling. However, persistent macrophage presence is associated with tissue destruction and fibrosis. Fibrosis, the excessive accumulation of fibrous connective tissue, is a common pathological sequela of many chronic inflammatory diseases and is often linked to outcome. In AAV, a greater degree of renal glomerulosclerosis on biopsies has been shown to be a predictor of poor prognosis [267]. In the kidney, an accumulation of the extracellular matrix is thought to result from proliferation of resident fibroblasts and epithelial to mesenchymal transition (EMT) of tubular cells. TGFβ1 is thought to be an important inducer of EMT [268].

The importance of monocyte / macrophage influx in renal injury has been highlighted by various groups. Kitagawa *et al* induced renal fibrosis using a unilateral ureteric obstruction model in mice. Administration of a CCR2 (MCP-1 receptor) inhibitor led to a reduction in cellular infiltrate and an amelioration of interstitial renal fibrosis. This was confirmed in CCR2 knockout mice. There was an associated reduction in TGFβ expression in the CCR2 knockout mice [269]. Using the same model of injury, Pan *et al* showed that the recruited macrophages were of an M2 phenotype. This was associated with increased expression of TGFβ1 and alpha smooth muscle actin (a marker of myofibroblasts) in the affected kidney and reduced levels of bone morphogenic protein 7 (inhibitor of TGFβ1) and E-cadherin, suggesting increased drive for EMT [270]. Lloyd *et al* showed that blockade of MCP-1 in the nephrotoxic nephritis model led to a reduction in infiltrating leucocytes as well as reduced glomerular crescent formation and type 1 collagen deposition [271]. In renal pathology, macrophages, a source of TGFβ has a crucial role in fibrosis and potentially development of chronic kidney disease.

4.2 Aims

As a result, we set out to assess the impact of ANCA on human peripheral blood monocytes with regards to cytokine production and potentially the impact of ANCA on macrophage development *in vitro*, which to our knowledge has not been investigated.

4.3 MPO-ANCA decreases IL10 and IL6 production from monocytes in response to LPS

We examined the effect of the same panel of unselected MPO-ANCA, PR3-ANCA, and control IgGs (see table 3.1 and 3.2) on peripheral blood monocytes isolated from three healthy donors as described in section 2.5.4. The purity of CD14 cells was measured to be >95% using FACS analysis in the experiments described in the following sections. To mirror the *in vivo* situation where ANCA bind monocytes in the context of an inflammatory response, we stimulated monocytes with LPS and explored whether ANCA modulated the response to LPS. The stimulated monocytes were incubated with ANCA or control IgG for 18 hours and the supernatants were harvested.

The Th1, Th2 and Th17 CBA kit (described in section 2.5.11) as well as IL1β, IL8 and MIP1α ELISA kits were used to measure cytokines in the supernatants (see figure 4.1).

After incubation of monocytes with MPO-ANCA, PR3-ANCA or control IgG without LPS, none of the indicated cytokines were detectable (data not shown).

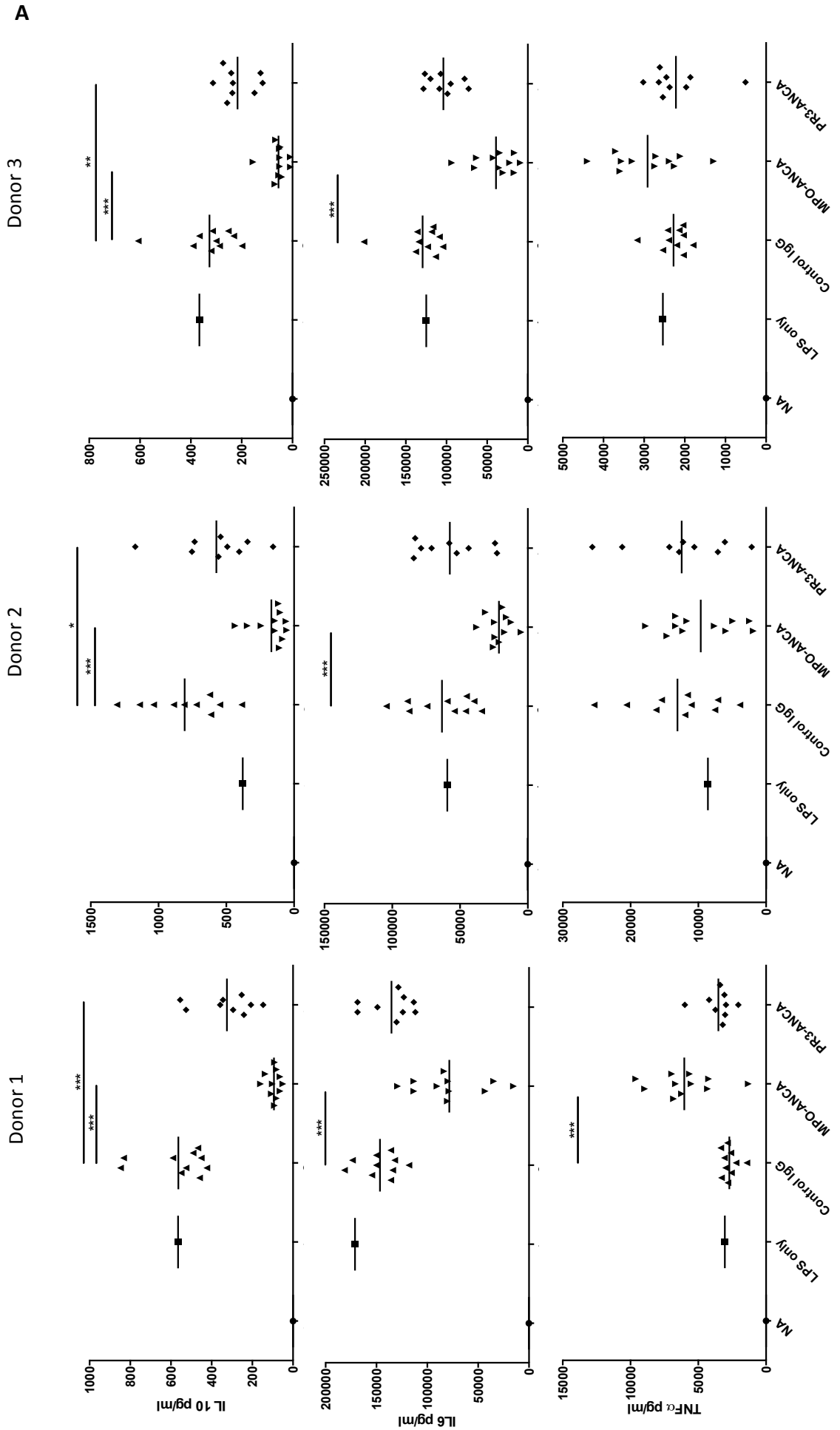
A
Donor 1
Donor 2
Donor 3
IL 10 pg/ml
IL6 pg/ml
TNFα pg/ml
NA
LPS only
Control IgG
MPO-ANCA
PR3-ANCA

B

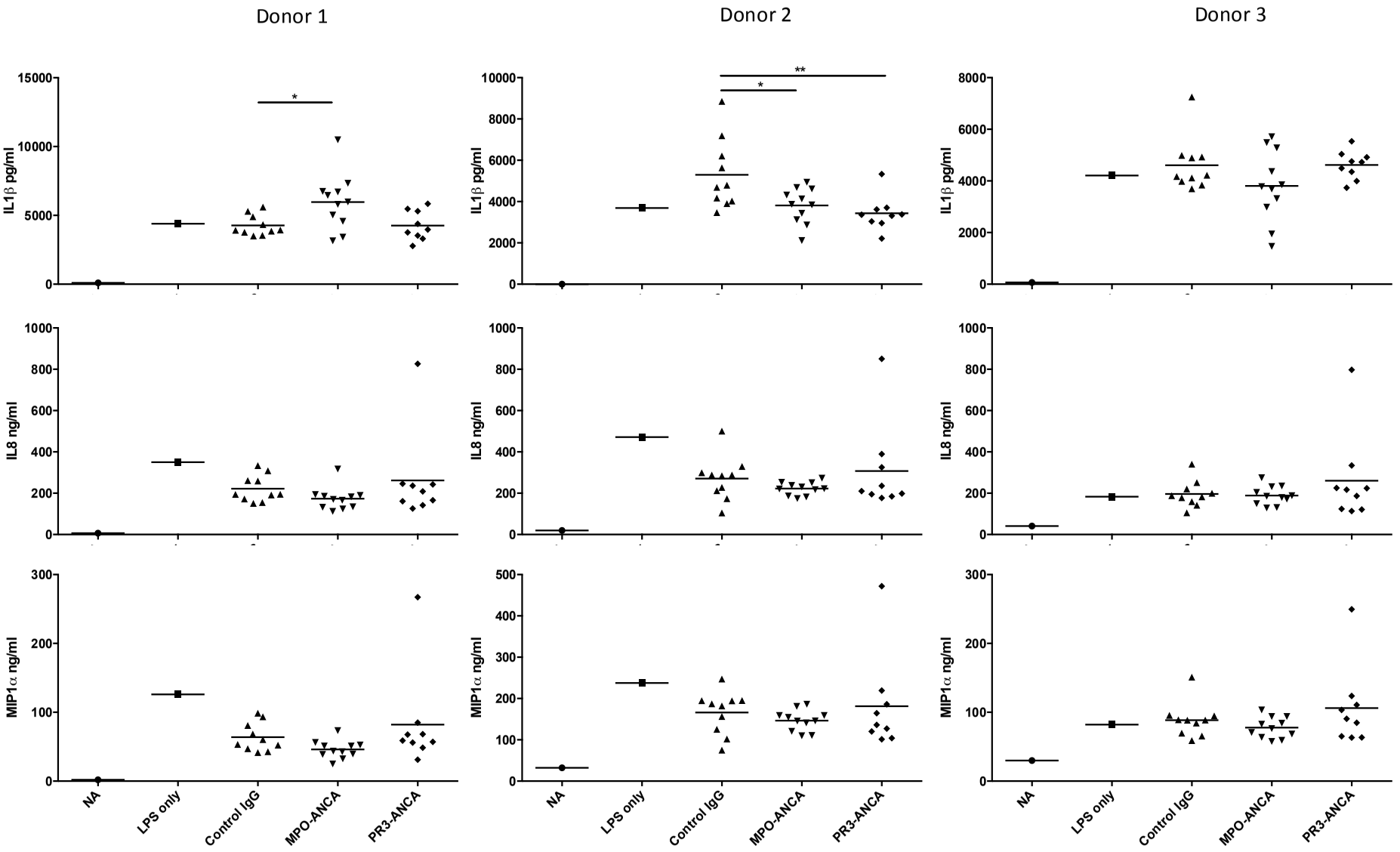
Donor 1
Donor 2
Donor 3
IL1β pg/ml
IL8 ng/ml
MIP1α ng/ml
NA
LPS only
Control IgG
MPO-ANCA
PR3-ANCA
*
*
**

Figure 4.1 – Cytokine production from peripheral blood monocytes. Monocytes from 3 donors were incubated with polyclonal control IgG (n=10), MPO-ANCA (n=11) or PR3-ANCA (n=9). All monocyte samples were stimulated with LPS except the NA group (non-activated). Plots in A show IL10, IL6 and TNFα levels whilst the plots in B show IL1β, IL8 and MIP1α levels in the supernatants. Data were analysed using a one way ANOVA with Dunnett's post test (* = $p < 0.05$, ** = $p < 0.01$, *** = $p < 0.001$).

As depicted, both IL6 and IL10 were consistently and significantly decreased by MPO-ANCA across all three donors, with the most profound effect seen for IL10. We did not observe an effect of MPO-ANCA on IL8 and MIP1α production by monocytes, and its effects on TNFα and IL1β production were variable among donors, Addition of PR3-ANCAs only had a consistent down-modulatory effect on IL10, which was less marked than that of MPO-ANCA.

Previously described effects of ANCA on neutrophils have been reported to require Fc receptor binding and involve interaction with the β2 integrin CD11b/CD18 complex as discussed in chapter 1 [79, 110, 272]. We therefore examined if this was also the case for the observed effects of MPO-ANCA on monocytes. We generated $F(ab)_2$ fragments from 4 MPO-ANCAs and 2 control IgGs as described in section 2.4.3 and compared the responses of the $F(ab)_2$ fragments to that of whole IgG using monocytes from two healthy donors (see figure 4.2).

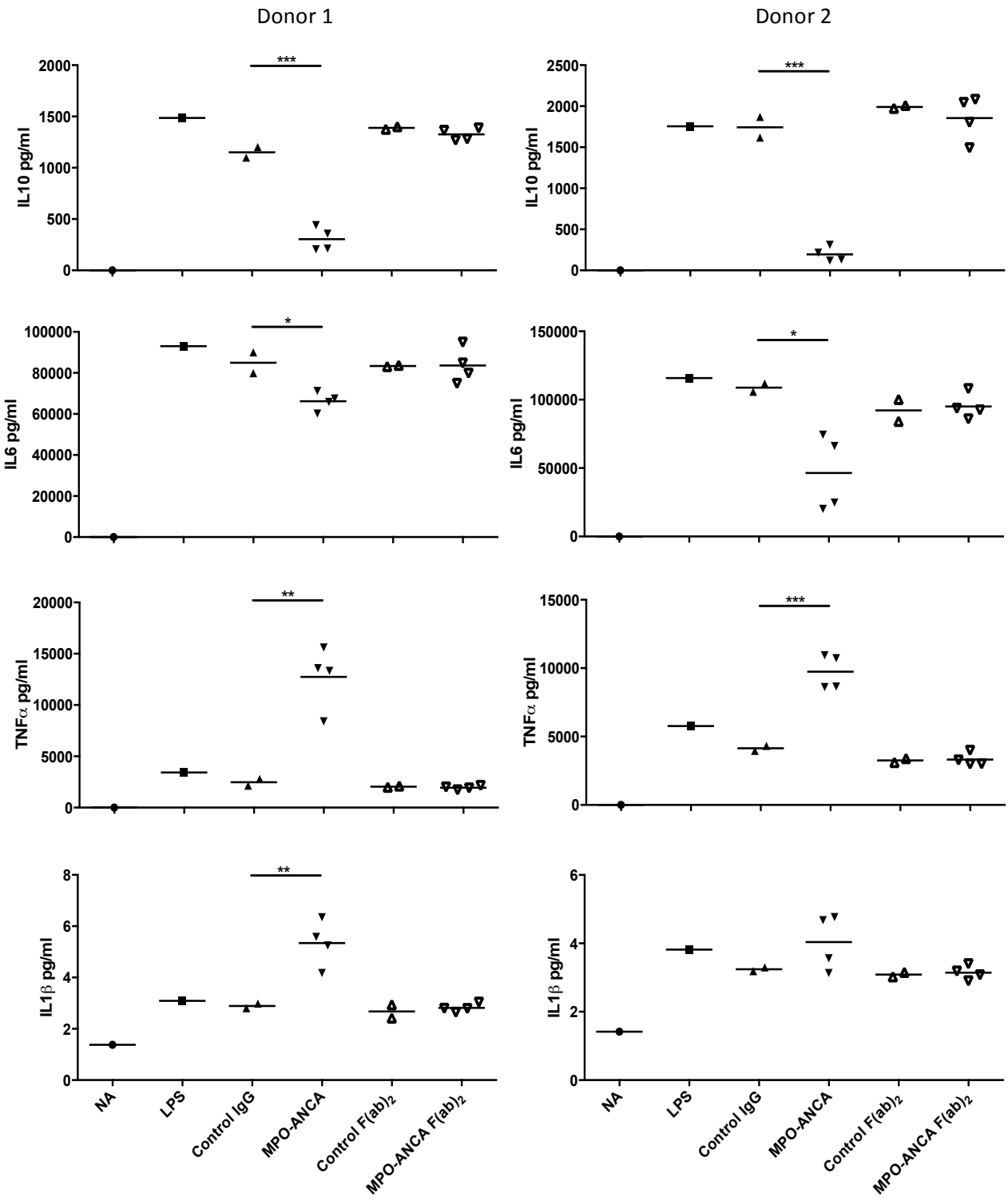

Figure 4.2 – Cytokine production from LPS stimulated monocytes incubated with whole IgG or F(ab)$_2$ fragments. Monocytes from 2 donors were incubated with whole control IgG (n=2), MPO-ANCA (n=4), control F(ab)$_2$ fragments (n=2) or MPO-ANCA F(ab)$_2$ fragments (n=4) for 16 hours. All monocyte samples were stimulated with LPS except the NA group (non-activated). Data were analysed using a one way ANOVA with Tukey's post test (* = $p < 0.05$, ** = $p < 0.01$, *** = $p < 0.001$).

While the MPO-ANCA whole IgG fraction elicited the expected reduction in IL6 and IL10, the MPO-ANCA $F(ab)_2$ failed to have the same effect, suggesting that co-engagement of the Fc receptors on the cell surface is also needed for ANCA effects on monocytes. Notably we saw a significant increase in TNFα levels following incubation with the selected MPO-ANCA IgG fractions in both donors, which is atypical (see figure 4.1).

We confirmed the importance of Fc receptor engagement in one monocyte donor, whereby monocytes were stimulated with MPO-ANCA with or without the use of Fc block, a purified recombinant Fc protein (figure 4.3).

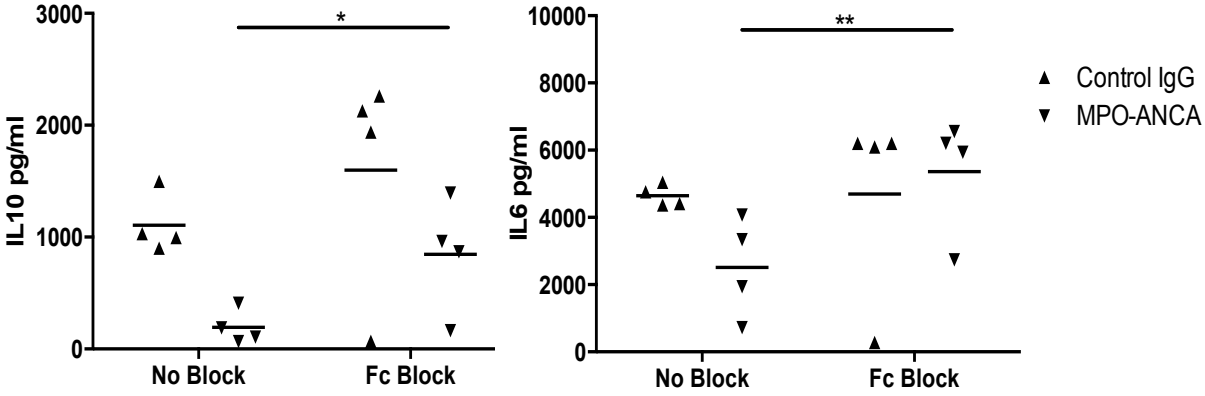

Figure 4.3 – Effect of Fc blockade on LPS stimulated monocytes incubated with MPO-ANCA. Monocytes from one donor were stimulated with LPS and incubated with polyclonal MPO-ANCA (n=4) or control IgG (n=4) with or without Fc block. Data was analysed using a student's t test (* = $p < 0.05$, ** = $p < 0.01$).

We also blocked CD11b, CD18 or both to deduce if the CD11b/CD18 complex has a role in the reduction of IL6 and IL10 associated with MPO-ANCA (see figure 4.4).

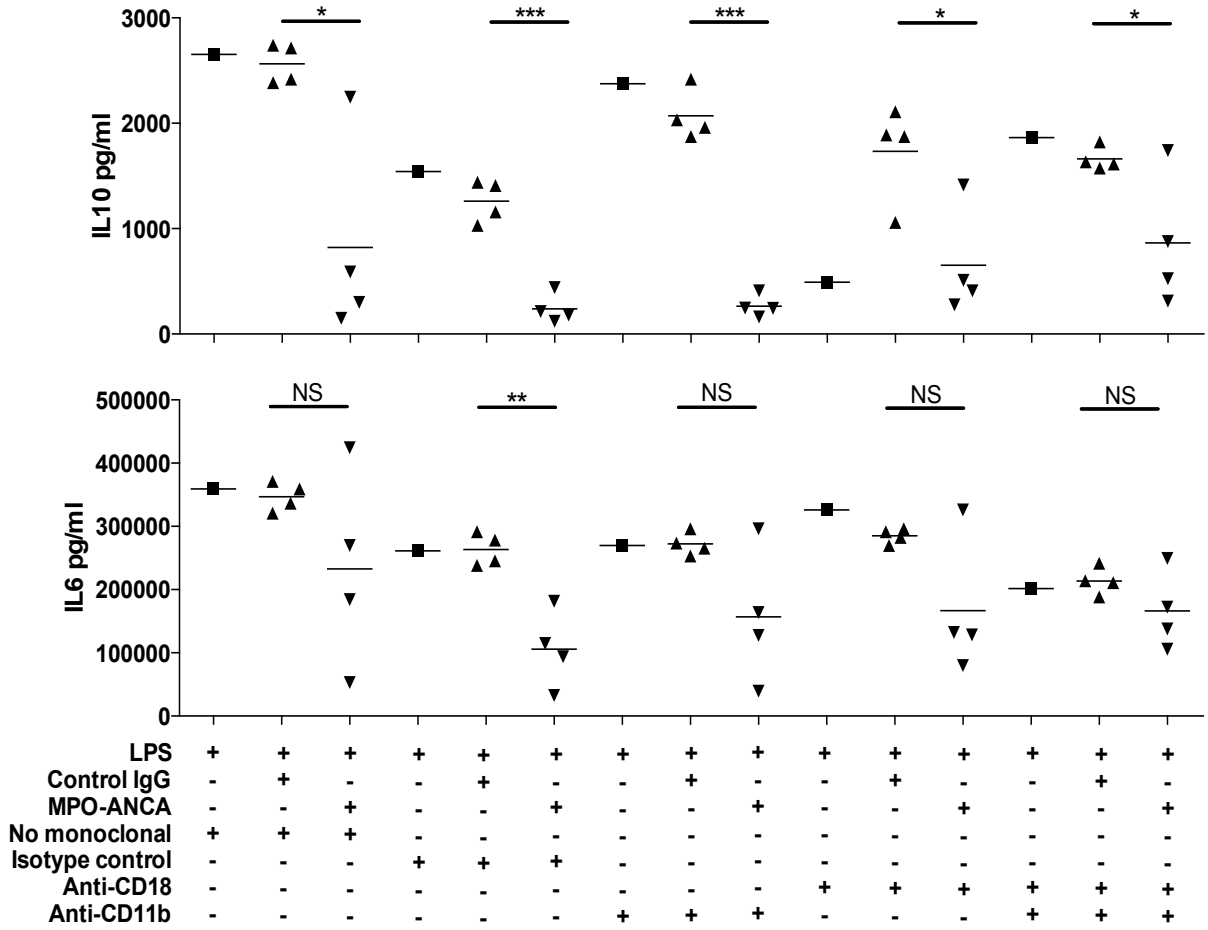

Figure 4.4 – Effect of CD11b/CD18 blockade on LPS stimulated monocytes incubated with MPO-ANCA. IL10 and IL6 production from peripheral blood monocytes incubated for 18 hours with LPS and MPO-ANCA (n=4) or control IgG (n=4) in the presence of monoclonal CD11b and/or CD18 blocking antibodies, no monoclonal antibodies or monoclonal isotype control antibody. Data was analysed using a student's t test (NS = non significant, * = $p < 0.05$, ** = $p < 0.01$, *** = $p < 0.001$).

Interestingly it appears that co-engagement of the CD11b/CD18 complex is not required for MPO-ANCA-induced reduction of IL6 and IL10, as blockade of CD11b, CD18 or both did not impact on altered cytokine production. This suggested that perhaps downstream signalling of Fc receptor engagement may not necessarily be involved in the effects noted. We hypothesised that perhaps MPO-ANCA tether MPO to the cell surface and MPO itself may cause the effects noted. To crudely test this hypothesis, we firstly added exogenous MPO to our monocyte cultures to ascertain if an effect on IL10 and IL6 could be found. We then added an enzymatic MPO inhibitor to assess whether this effect could be reversed and show that the noted effect was

indeed dependent on the enzymatic action of MPO. LPS stimulated monocytes were incubated with exogenously added MPO protein in the presence or absence of the specific MPO inhibitor AZD5904 at varying doses (see figure 4.5) [249].

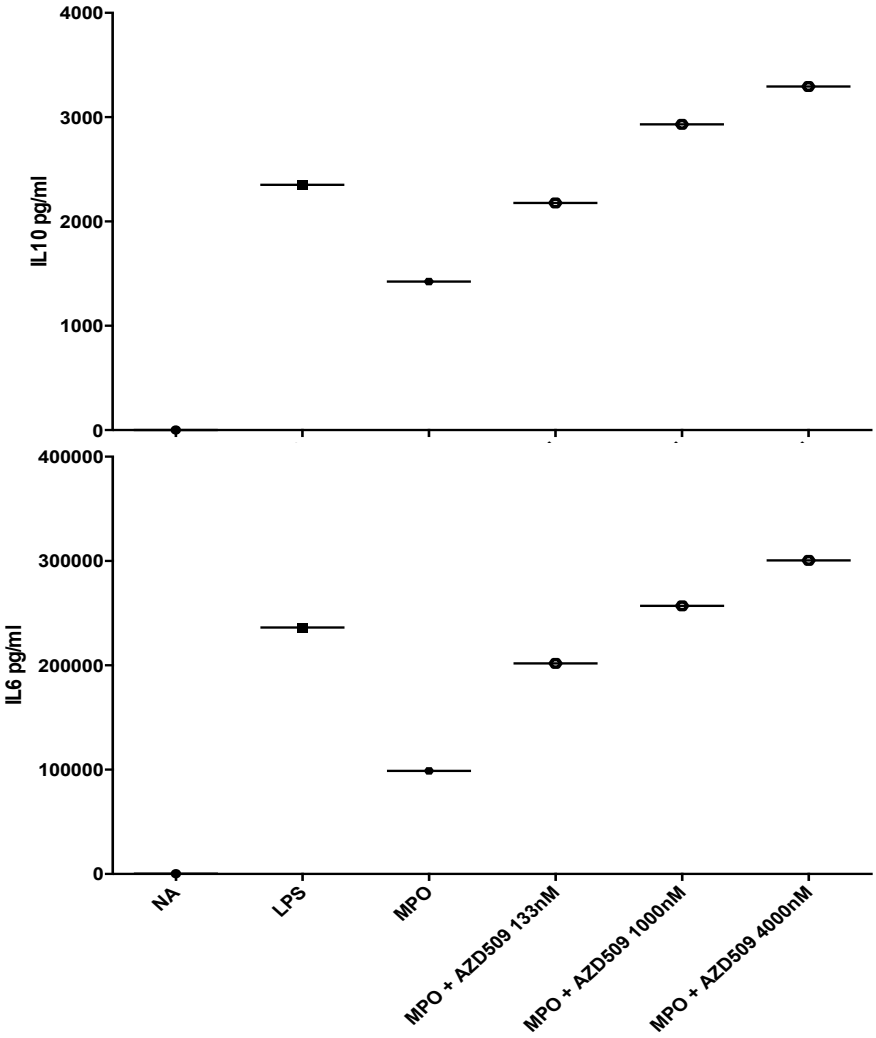

Figure 4.5 – The effect of MPO protein and MPO inhibitor on IL6 and IL10 production. Representative plot of the effects of exogenous MPO protein (2µg/ml) alone or in combination with the MPO inhibitor AZD5904 (in variable doses) on IL10 and IL6 production from LPS stimulated monocytes.

We found that exogenously added MPO mirrors the effect of MPO-ANCA and causes a reduction in IL6 and IL10 that is reversed by AZD5904 in a dose dependent manner. We then incubated monocytes (+/- LPS) with exogenously added MPO protein, MPO-ANCA or control IgG, in the presence or absence of AZD5904 (see figure 4.6).

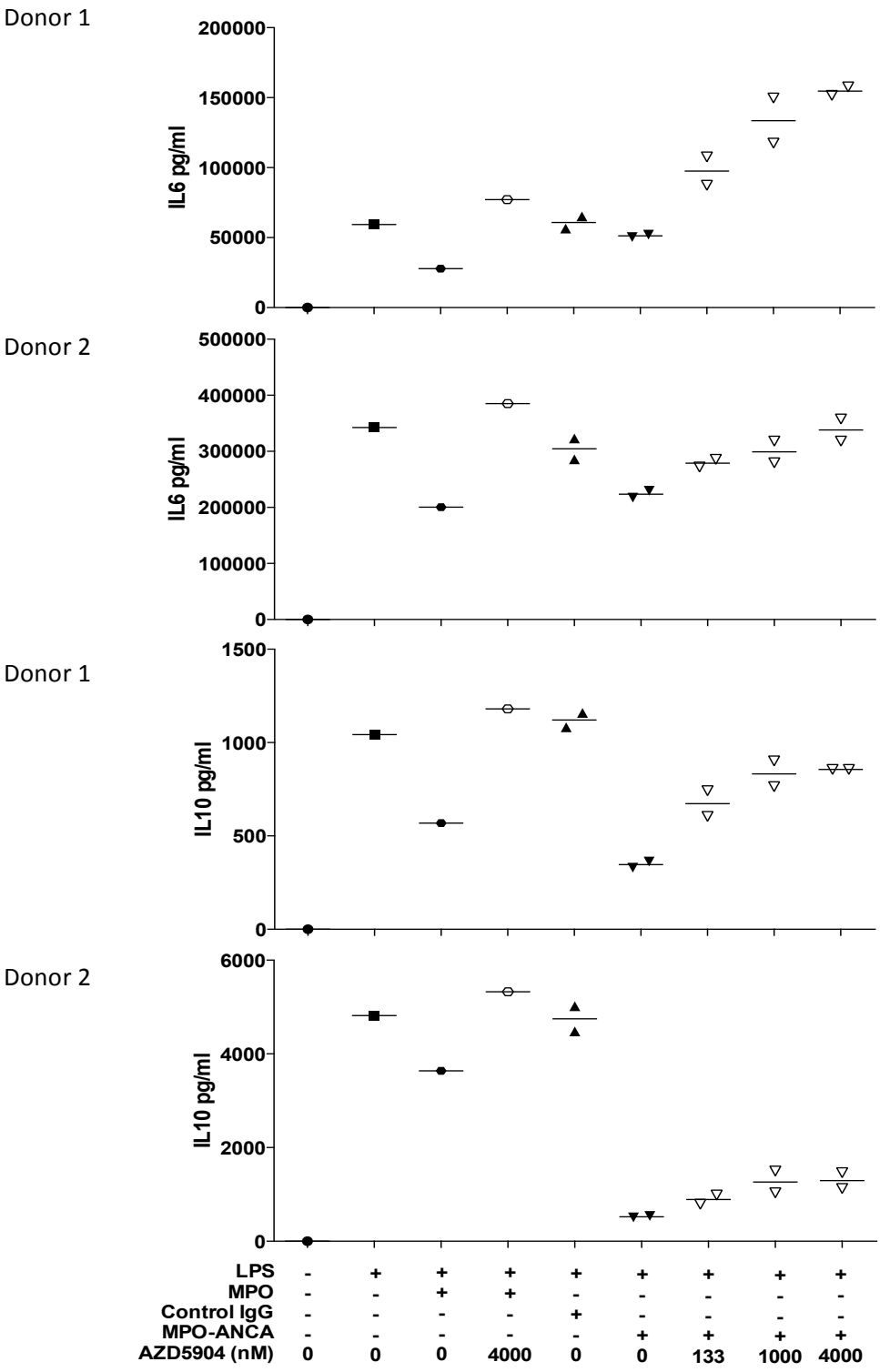

Figure 4.6 - Effect of varying doses of MPO inhibitor on IL6 and IL10 production from peripheral blood monocytes. Monocytes from two donors were incubated with LPS, MPO protein (2µg/ml), polyclonal control IgG (n=2) or MPO-ANCA (n=2), with or without the MPO inhibitor AZD5904 at varying concentrations.

AZD5904 partially reversed the reduction in IL6 and IL10 caused by MPO-ANCA in all donors tested in a dose dependent manner. These data suggest that MPO-ANCA is inhibiting IL6 and IL10 release in response to LPS by a mechanism that is partially dependent on the enzymatic activity of MPO.

We hypothesised that MPO-ANCA tether MPO released by activated monocytes to the cell surface. To test this we first showed that the concentration of MPO in the supernatant of MPO-ANCA activated monocytes was reduced whilst the corresponding monocyte surface expression of MPO was increased compared to control IgG treated cells (see figure 4.7).

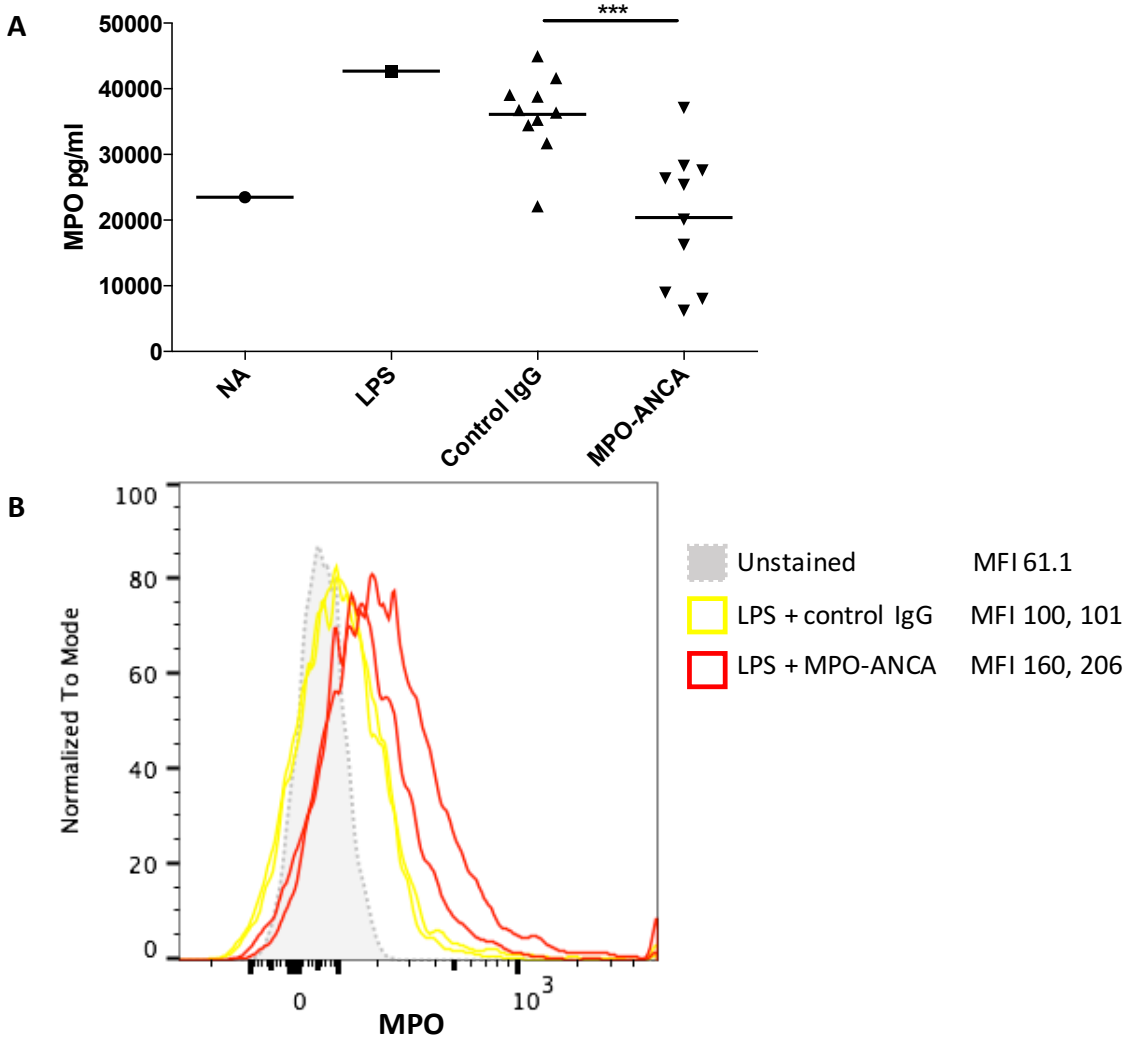

Figure 4.7 – MPO in the supernatant and cell surface of monocytes. (A) Graph showing the level of MPO in the supernatants of monocytes incubated with LPS and control IgG (n=10) or MPO-ANCA (n=10). NA depicts non activated cells. Data was analysed using a student's t test (*** = $p < 0.001$). (B) FACS histogram plots and MFI

showing the cell surface expression of MPO following incubation of LPS stimulated monocytes with control IgG (n=2) or MPO-ANCA (n=2).

Addition of MPO-ANCA to LPS stimulated monocytes led to a decrease in free MPO in the supernatant compared to control IgG. This was associated with a concomitant increase in cell surface MPO expression on monocytes incubated with MPO-ANCA.

IL6 has been shown to promote IL10 secretion in T cells [273] and we therefore assessed whether the reduction in IL10 production by monocytes upon ANCA-MPO addition was secondary to the reduction in IL6. Exogenous IL6 protein was added to monocytes incubated with either control IgG or MPO-ANCA (see figure 4.8).

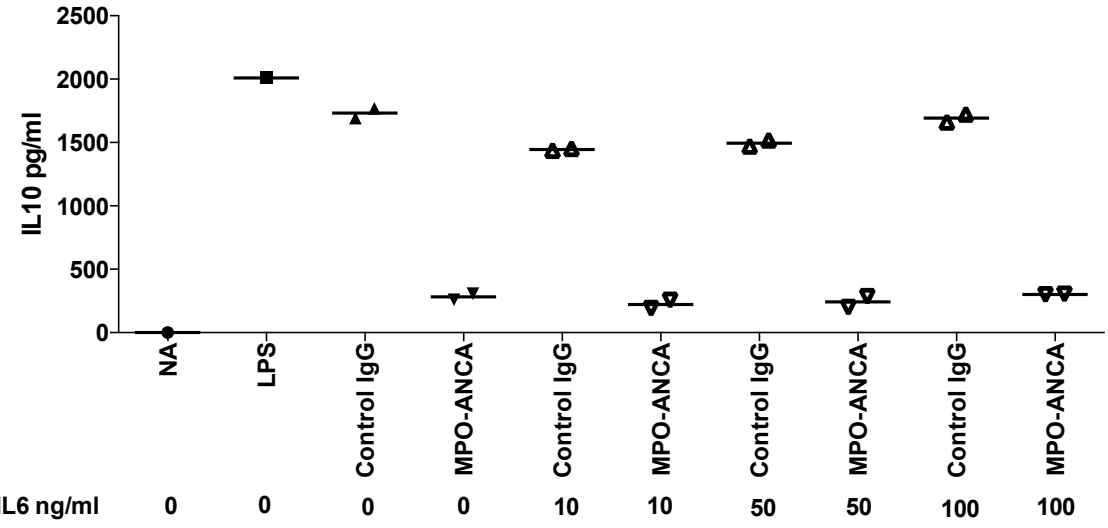

Figure 4.8 – Effect of addition of exogenous IL6 on IL10 production by LPS stimulated monocytes. Monocytes from one donor were incubated with varying concentrations of IL6 and control IgG or MPO-ANCA.

Unlike T cells, IL6 seems not to drive IL10 production in monocytes as addition of exogenous IL6 to monocyte cultures during activation failed to increase IL10 production.

4.4 MPO-ANCA affects TLR signalling pathways

To define the pathways driven by MPO-ANCA leading to altered cytokine production in monocytes, we performed gene expression microarrays on samples treated with LPS and MPO-ANCA (n=3) or control IgG (n=3) for six hours as described in section 2.5.13. We observed 566 genes differentially expressed between the groups, with a threshold of 1.75 in either direction (see figure 4.9 and appendix for list of genes).

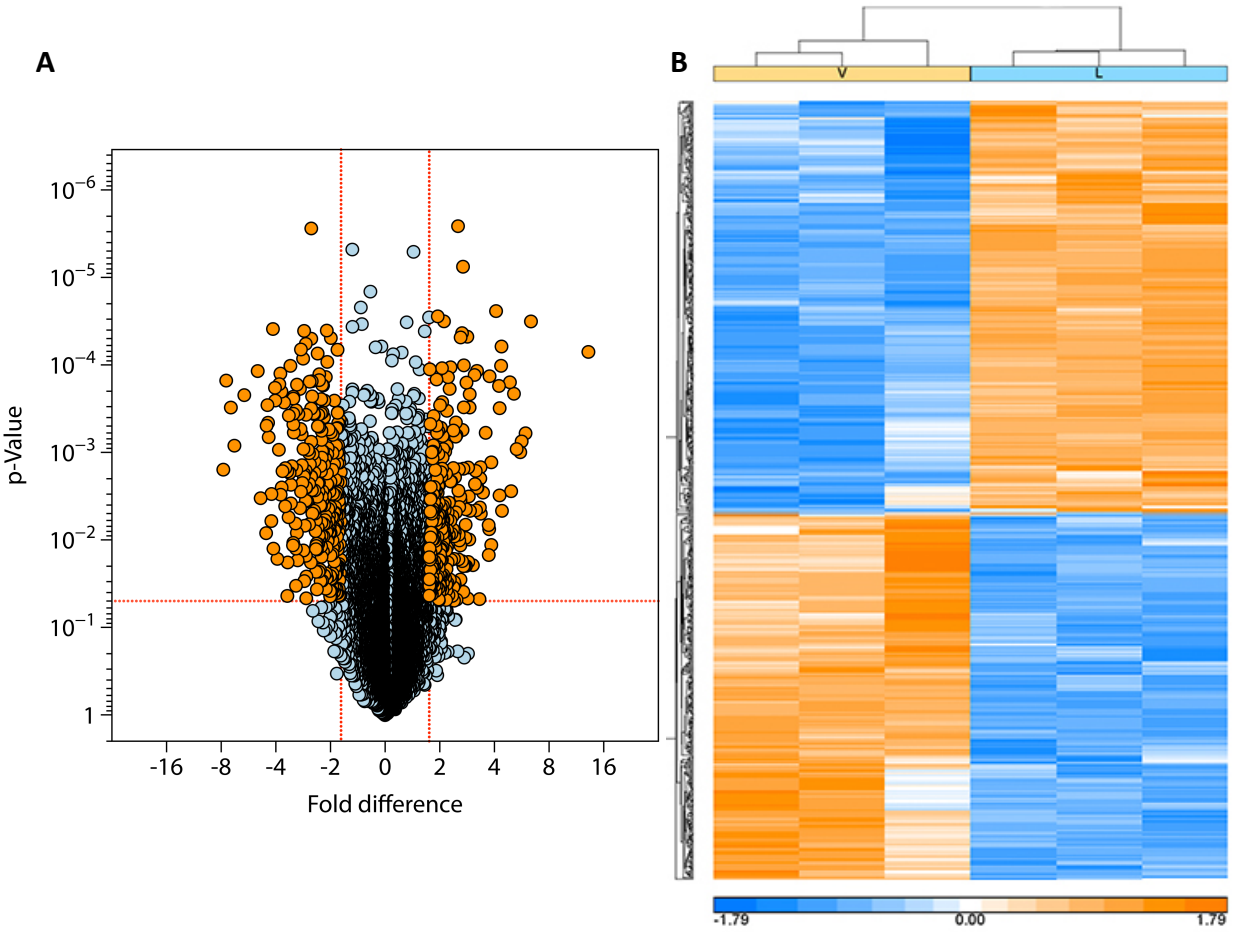

Figure 4.9 – Volcano plot and heatmap of gene expression data. (A) Volcano plot comparing monocytes activated for 6h with either MPO-ANCA (V, n=3) or IgG control (L, n=3) in the presence of LPS. Threshold for significance is 1.75 fold in either direction and p-value of <0.05. From this, 566 genes were differentially expressed. (B) Hierarchical clustering of these genes.

Subsequent pathway enrichment analyses revealed that the altered gene expression profile pertains overall to pathways involved in immune cell activation and inflammatory responses. These analyses demonstrated that one of the most prominently affected pathways is in genes regulated by TLR signalling (figure 4.10).

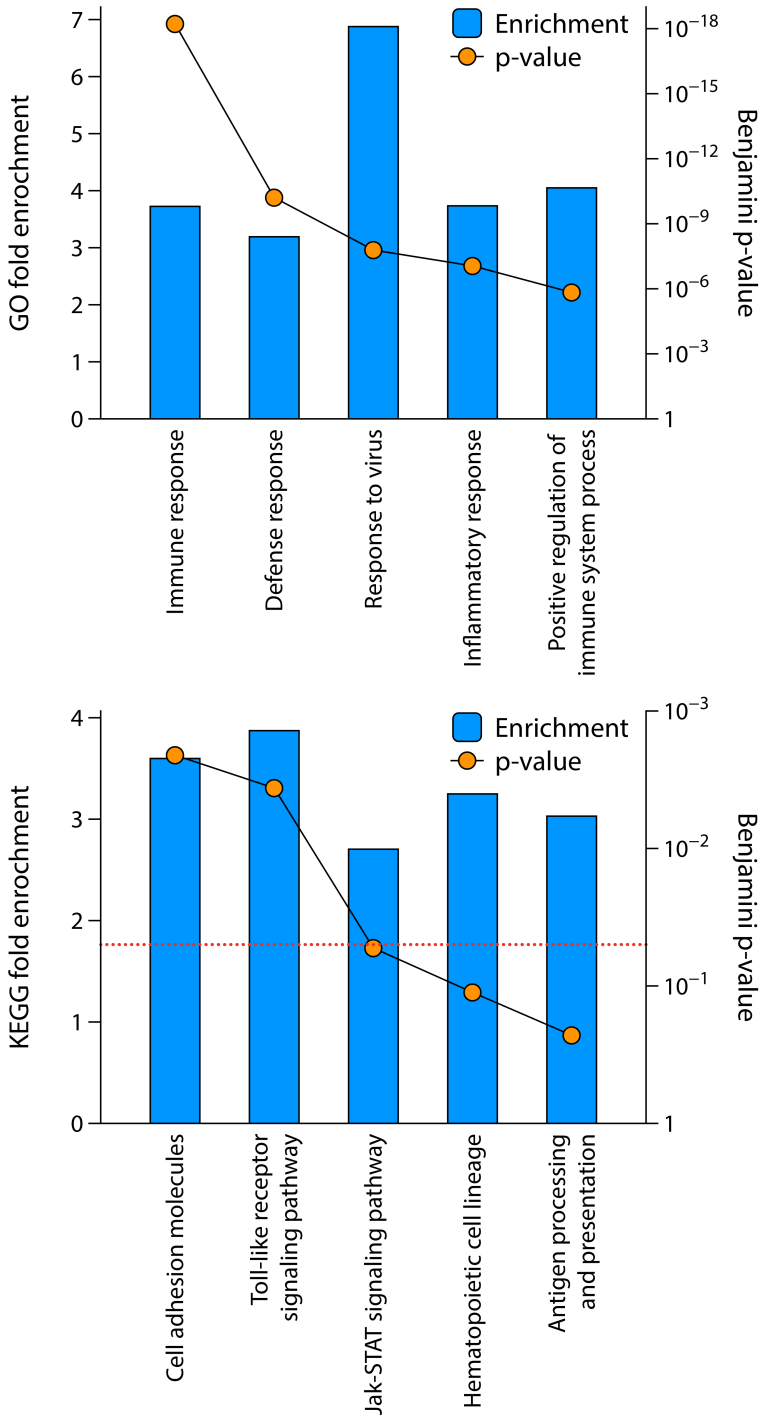

Figure 4.10 - Gene Ontology (GO) and KEGG enrichment analyses of genes.

Specific examination of the expression of genes known to be regulated by LPS or by the Myd88 pathways confirmed a profound inhibitory effect on these genes

engendered by the presence of MPO-ANCA (Z-scores -5.2 and -3.6 respectively). An unbiased gene set enrichment (GSEA) analysis was carried out, comparing expression of all genes expressed by MPO-ANCA and IgG-treated monocytes in our arrays for enrichment of genes in the KEGG TLR signaling pathway and found that these genes were preferentially inhibited in the ANCA-treated cells (figure 4.11)

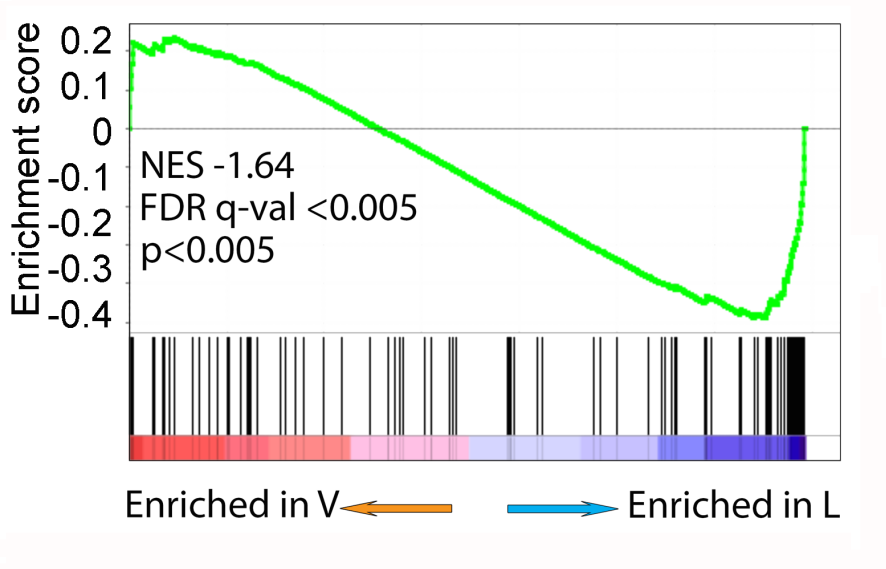

Figure 4.11 - Gene Set Enrichment Analysis of genes in the KEGG TLR signalling pathway.

The core genes inhibited in this gene set are shown in figure 4.12. In summary, MPO-ANCA caused a general reduction in normal LPS/TLR-triggered TLR-mediated pathways regulating monocyte activation.

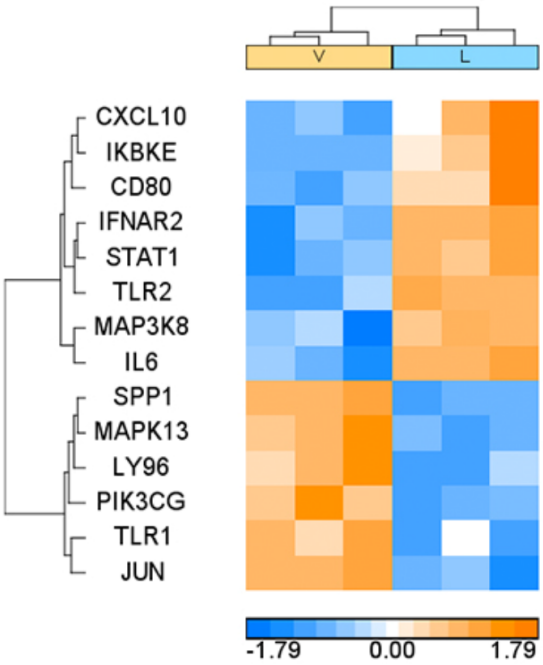

Ingenuity Pathway Analysis

	Z-score	Overlap p-Value	Effect direction
Myd88	-3.33	$1.56x10^{-9}$	Inhibited by MPO-ANCA relative to control IgG
LPS	-4.96	$1.87x10^{-58}$	Inhibited by MPO-ANCA relative to control IgG

Figure 4.12 – Heatmap of core genes altered in this gene set and ingenuity pathway analysis. The ingenuity pathway analysis illustrates the profound inhibition of both LPS and Myd88 mediated pathways, with Z-values and p-values shown.

4.5 MPO-ANCA generates oxidised phospholipids

MPO is a powerful oxidant and has the ability to oxidise glycerophospholipids, the building blocks of the cell membrane. Oxidation of these phospholipids can affect the integrity of the cell structure and also lead to the formation of oxidised phospholipids, which have biological functions. Oxidised phospholipids can be pro- or anti-inflammatory. There is increasing evidence that certain species of oxidised phospholipids are antagonists of LPS-induced TLR4 activation [274-276].

We hypothesized that MPO-ANCA anchor MPO protein on the cell surface, which in turn may lead to local production of oxidised phospholipids and block the effect of LPS noted in the microarray experiments (section 4.4).

We incubated peripheral blood monocytes with LPS and control IgG (n=3) or MPO-ANCA (n=3) for 18 hours and extracted phospholipids as detailed in section 2.5.14. Liquid chromatography mass spectrometry was used to assess the extracted phospholipids.

Treatment with MPO-ANCA did not affect the native phospholipid profile and a variety of chain-shortened oxidised phospholipids were observed in both control IgG and MPO-ANCA incubated monocytes (see figure 4.13). Table 4.1 provides the probable identities of native and oxidised phosphatidylcholine species detected in the lipid extracts of the treated monocytes.

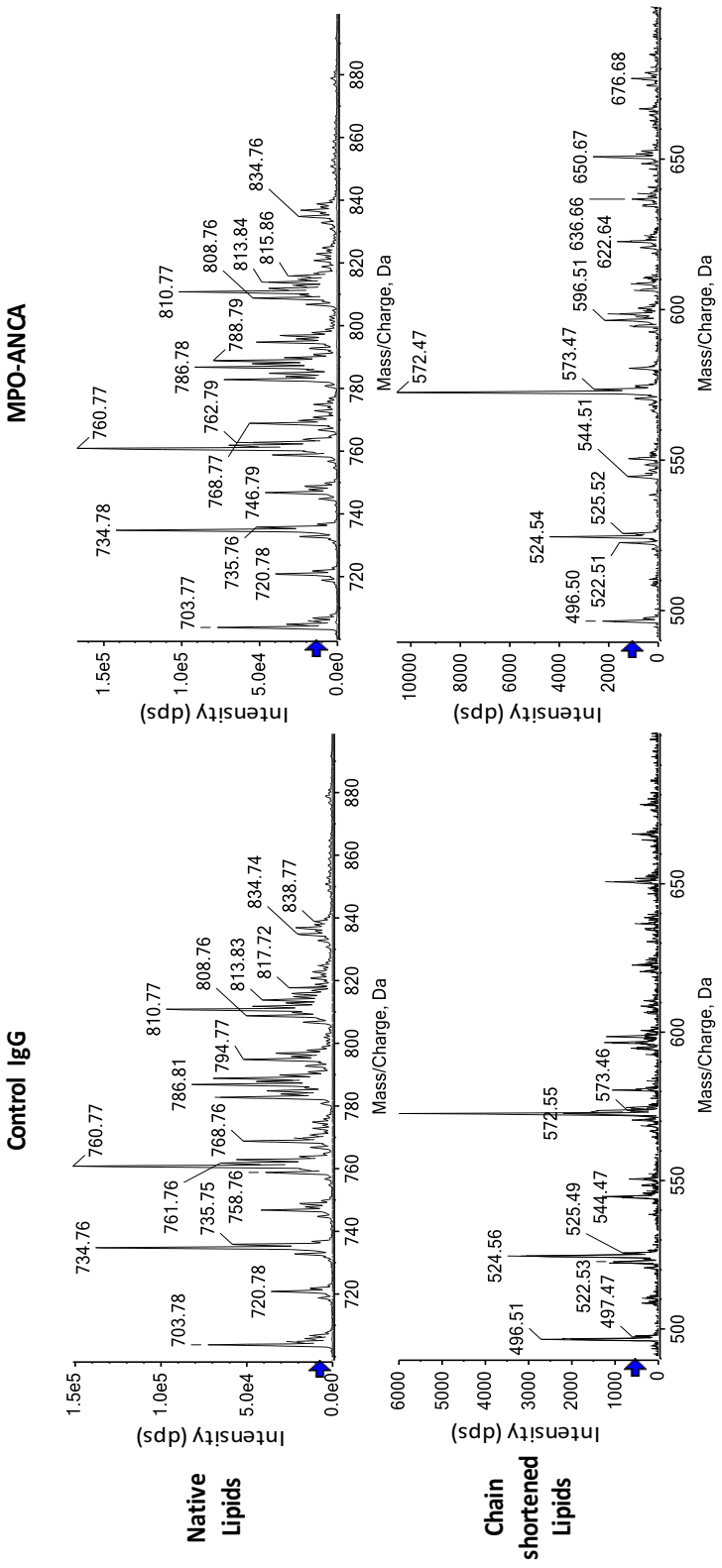

Figure 4.13 - Summed phospholipid spectra from treatments of monocytes with control IgG or MPO-ANCA. Sum of spectra in the region *m/z* 700-900 corresponding to unmodified phospholipids and sum of spectra in the region *m/z* 490-700 corresponding to chain-shortened and oxidised phospholipids from control IgG (n=3) and MPO-ANCA (n=3) treated monocytes.

m/z	Chemical formula	Identification
496.5	$C_{24}H_{51}NO_7P^+$	Lyso-PC 16:0
524.5	$C_{26}H_{55}NO_7P^+$	Lyso PC 18:0
544.5	$C_{28}H_{51}NO_7P^+$	Lyso-PC 20:4
572.5	-	Unidentified
596.5	$C_{28}H_{55}NO_{10}P^+$	1-Palmitoyl-2-Succinoyl-PC (16:0, 4-COOH) *SSPC*
622.5	$C_{31}H_{61}NO_9P^+$	1-Stearoyl-2-Oxovaleroyl-PC (18:0, 5-CHO) *SOVPC*
636.5	$C_{32}H_{63}NO_9P^+$	1-palmitoyl-2-8-oxo-octanoyl PC (16:0, 8-CHO)
650.5	$C_{32}H_{61}NO_{10}P^+$	HOOA-PC (1-palmitoyl-2-5-hydroxy-8-oxooct-6-enoyl-PC)
	$C_{33}H_{65}NO_9P^+$	1-Palmitoyl-2-Oxononanoyl-PC (16:0, 9-CHO) *PONPC*
666.5	$C_{33}H_{65}O_{10}NP^+$	1-Palmitoyl-2-Azelaoyl-PC (16:0, 9-COOH) *PAzPC*
720.8	$C_{39}H_{79}NO_8P^+$	PC (31:0)
720.8	$C_{40}H_{83}NO_7P^+$	PC (16:0,16:0) ether
734.8	$C_{40}H_{81}NO_8P^+$	PC (16:0,16:0) 1,2-Dialmitoyl-PC *DPPC*
746.8	$C_{42}H_{85}NO_7P^+$	PC (16:0, 18:1) Plasmenyl
758.8	$C_{42}H_{81}NO_8P^+$	PC (16:0/18:2)
760.8	$C_{42}H_{83}NO_8P^+$	PC (16:0,18:1)
762.8	$C_{42}H_{85}NO_8P^+$	PC (16:0, 18:0)
768.8	$C_{43}H_{79}NO_8P^+$	PC (16:0. 20:4) Plasmenyl
782.8	$C_{44}H_{81}NO_8P^+$	PC (16:0/20:4) *PAPC*
786.8	$C_{44}H_{85}NO_8P^+$	PC (18:0/18:2)
788.8	$C_{44}H_{87}NO_8P^+$	PC (18:0/18:1)
798.8	$C_{44}H_{81}NO_9P^+$	PC (16:0/20:4)-OH
806.8	$C_{46}H_{81}NO_8P^+$	PC (16:0/22:6)
810.8	$C_{46}H_{85}NO_8P^+$	PC (18:0/20:4)
828.8	$C_{44}H_{79}NO_{11}P^+$	1-palmitoyl-2-(5,6-epoxyisoprostane E_2)-PC *PEIPC*
834.8	$C_{48}H_{85}NO_8P^+$	PC (18:0/22:6)

Table 4.1 - Probable identities of native and oxidised phosphatidylcholine species detected in lipid extracts of monocytes by liquid chromatography mass spectrometry. Identities are based on retention time, *m/z* and previously published identifications. PC corresponds to sn-glycero-3-phosphocholine; plasmenyl corresponds to a vinyl ether linkage instead of an ester.

The relative intensities of 8 oxidatively modified and phosphatidylcholine species that were found to be most abundant are plotted in figure 4.14. The data are presented as a percentage of the signal of the saturated phospholipid dipalmitoyl phosphatidylcholine at *m/z* 734, as this is relatively resistant to oxidative damage. This approach allows correction for variability in the total phospholipid content of the samples and provides a better assessment of the levels of oxidised species within the total phospholipid pool.

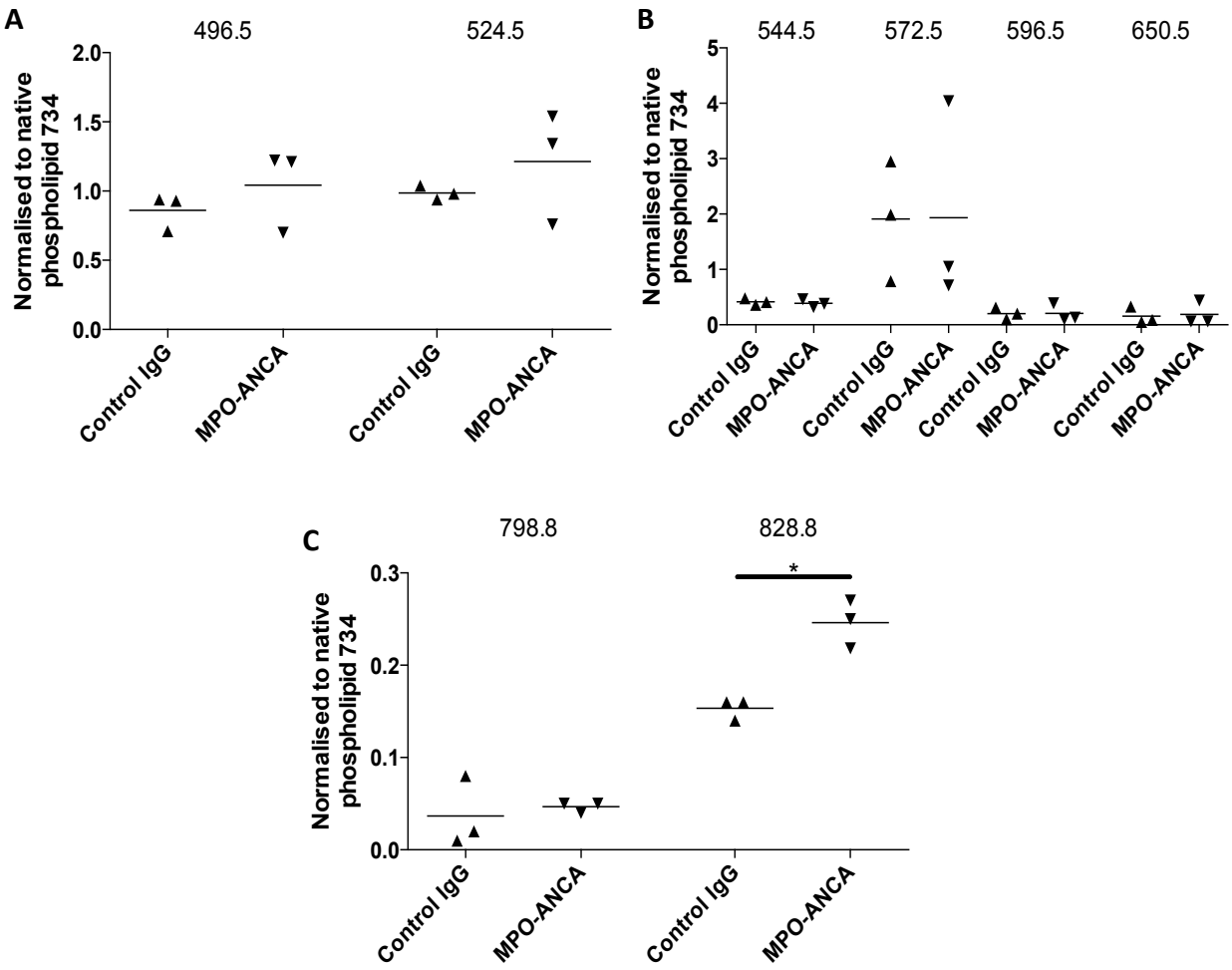

Figure 4.14 – Most abundant oxidised phospholipids extracted from the treated monocytes. (A) Lyso lipids (B) Short chained oxidised phospholipids (C) Long chained oxidised phospholipids and their corresponding *m/z* values for control IgG (n=3) and MPO-ANCA (n=3) treated LPS stimulated monocytes. Please refer to table 4.1 for identification of *m/z* values. Data was analysed using a student's t test (* = $p < 0.05$).

For most of the oxidatively modified phosphatidylcholine species, there was no significant difference in their relative abundance between control IgG and MPO-ANCA

treated monocytes, and the levels of some commonly observed chain-shortened oxidised phosphatidylcholines such as 1-palmitoyl-2-oxovaleroyl-PC (POVPC) and 1-palmitoyl-2-glutaroyl-PC (PGPC) were on the limit of detection. However, it was found that a phosphatidylcholine species at *m/z* 828.8 eluting in the range of long-chain oxidised phospholipids was significantly higher in MPO-ANCA treated monocytes.

Extracted ion chromatograms for *m/z* 828.8 for each of the 6 samples are shown in figure 4.15. This phospholipid was tentatively identified as 1-palmitoyl-2-(5,6-epoxyisoprostane E_2)- phosphatidylcholine (PEIPC).

Thus, we have found evidence of at least one oxidised phospholipid, which is increased in MPO-ANCA treated monocytes.

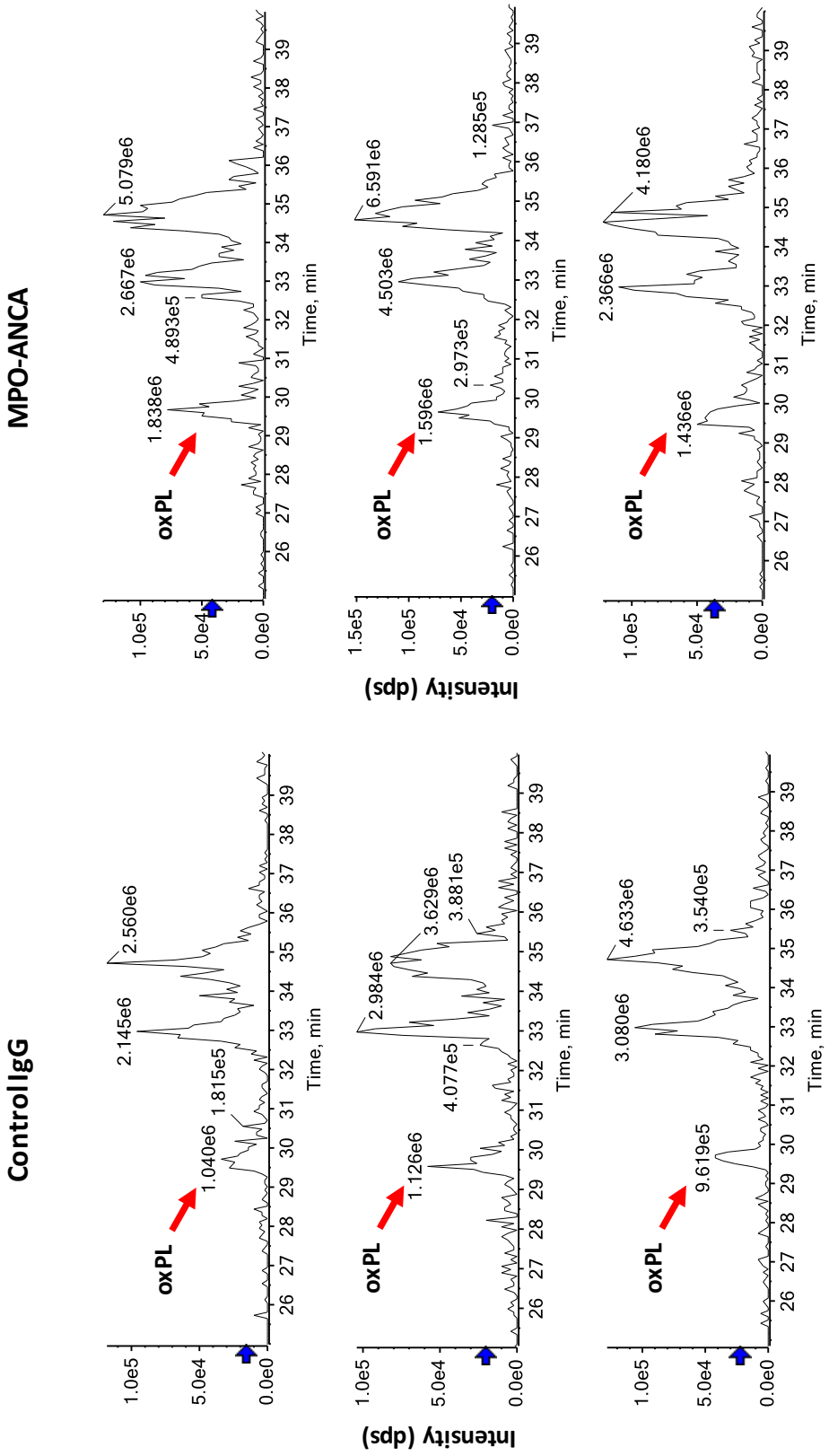

Figure 4.15 - Extracted ion chromatograms for the control IgG (n=3) and MPO-ANCA (n=3) treated samples. The chromatograms show the intensity of the long-chain oxidised phospholipid (oxPL) species at *m/z* 828.8 eluting at approximately 29.5 minutes.

4.6 MPO-ANCA increase monocyte survival and differentiation to macrophages

Whilst monitoring monocyte cultures over six days, we noticed that monocytes treated with MPO-ANCA were more abundant than those treated with control IgG. Based on these observations, we next explored the effect of MPO-ANCA on monocyte survival and differentiation in comparison to control IgG. To avoid the potential (M1 or M2) skewing effects of growth factor addition, we performed these experiments in the absence of LPS and in the presence of 10% AB serum as discussed in section 2.5.6.

Using the same 10 control IgG and 10 MPO-ANCA samples as in the previous experiments (see tables 3.1 and 3.2), we found that MPO-ANCA significantly increased cell survival after 6 days in culture using monocytes from 2 distinct donors (see figure 4.16).

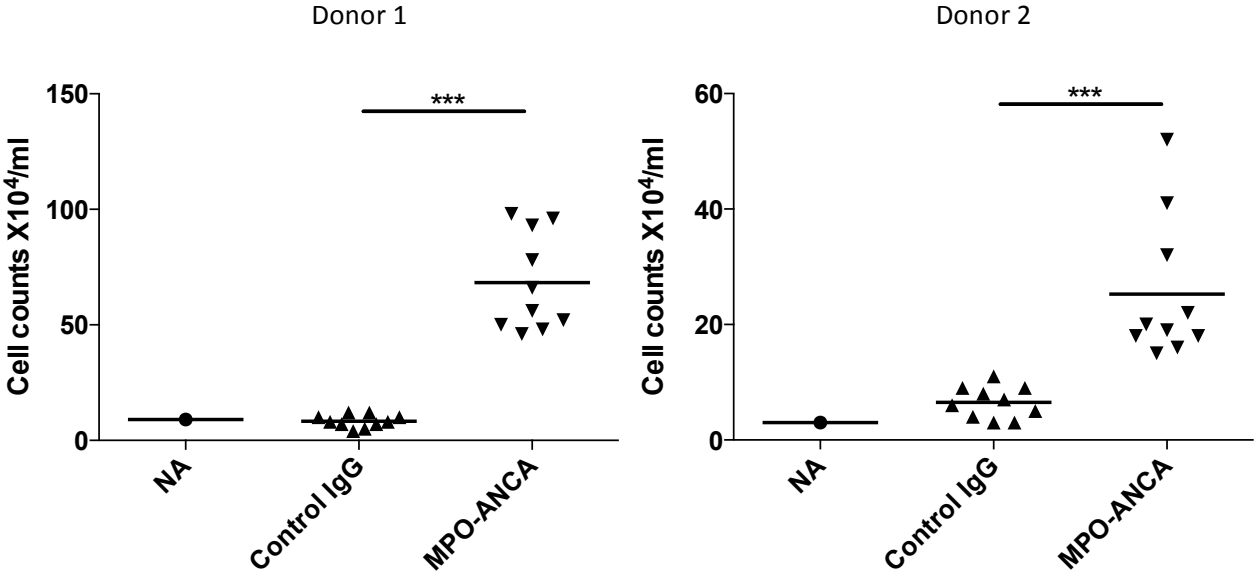

Figure 4.16 – Cell counts after culturing peripheral blood monocytes from 2 donors for 6 days. The number of cells remaining after culturing peripheral blood monocytes with 10% AB serum and MPO-ANCA (n=10) or control IgG for 6 days (n=10) are shown. Data were analysed using a student's t test (*** = $p < 0.001$).

Since CSF1 is a key survival and differentiation factor for monocytes and macrophages, we measured CSF1 production by monocytes using RT-qPCR as described in section 2.5.12. We found a marked increase in *CSF1* mRNA expression in the presence of MPO-ANCA compared with control IgG in two donors (figure 4.17).

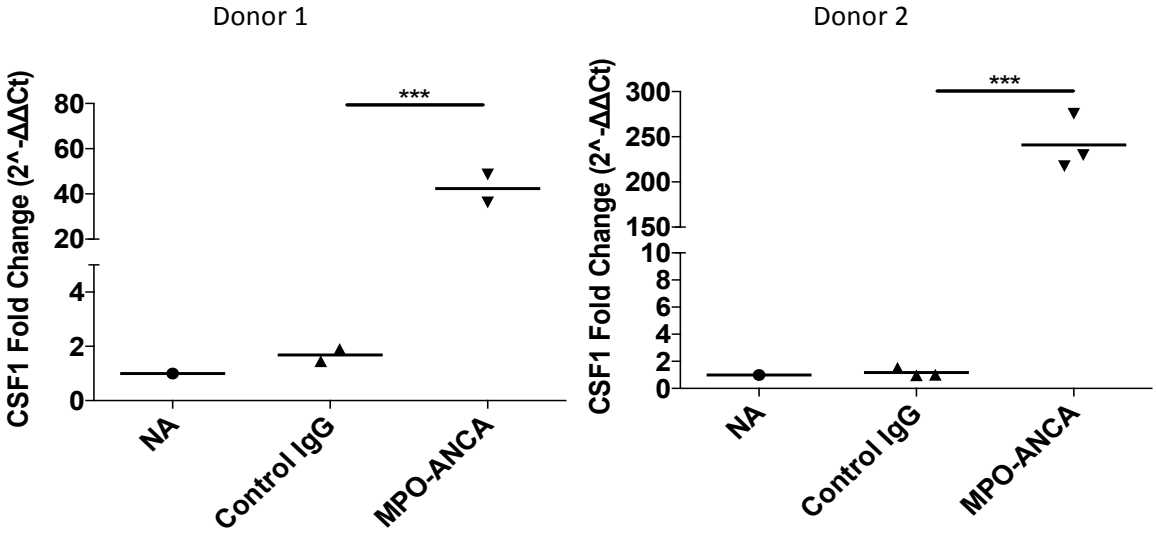

Figure 4.17 - CSF1 gene expression in peripheral blood monocytes after 18 hours in culture with control IgG or MPO-ANCA. Data are expressed as a fold change in mRNA expression compared to the non-activated cells. Data were analysed using a student's t test (*** = $p < 0.001$).

However, when CSF1 production was assessed at the protein level in the supernatants using an ELISA, we did not observe a consistent increase with MPO-ANCA treatment in both donors (figure 4.18). The discrepancy in gene expression and protein production is not clear as yet, but could be based on the fact that monocytes may consume CSF1 in an autocrine fashion to sustain proliferation.

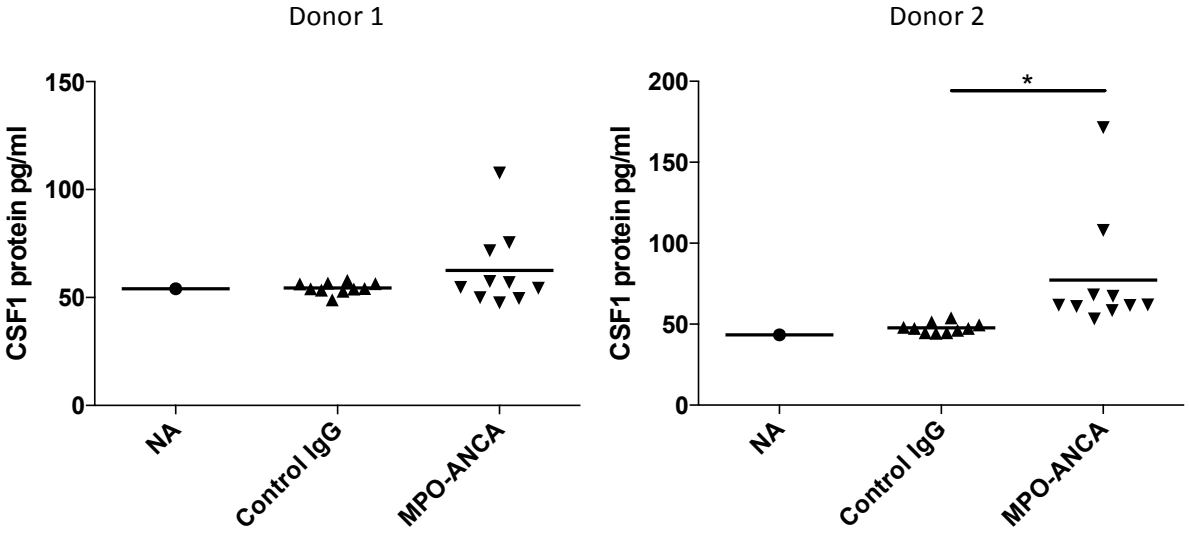

Figure 4.18 – CSF1 protein in the supernatants of peripheral blood monocytes after 18 hours in culture with control IgG or MPO-ANCA. Data were analysed using a student's t test (* = $p < 0.05$).

We analysed CSF1 receptor (CSF1R) mRNA expression in the presence of MPO-ANCA or control IgG to support this notion, however we found that the CSF1R mRNA expression was lower in the MPO-ANCA treated monocytes compared to the control IgG treated monocytes, although by a small margin (figure 4.19).

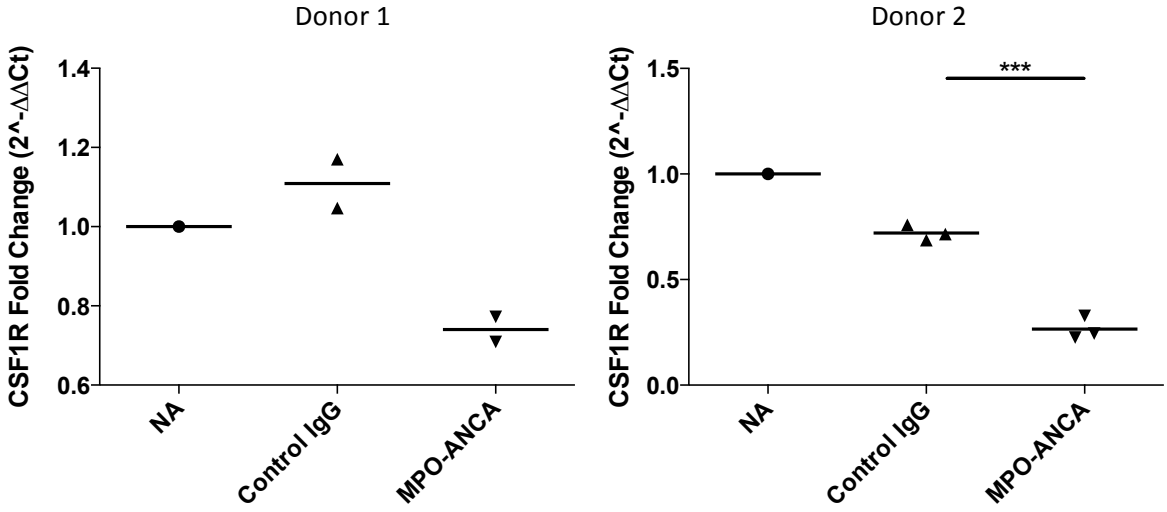

Figure 4.19 - CSF1R gene expression in peripheral blood monocytes after 18 hours in culture with control IgG or MPO-ANCA. Data are expressed as a fold change in mRNA expression compared to the non-activated cells. Data were analysed using a student's t test (*** = $p < 0.001$).

These results do not negate the hypothesis that CSF1 protein may be consumed by monocytes in an autocrine fashion. We used a CSF1R inhibitor GW2580 and found a dose-dependent reversal of the increase in cell survival at day 6 documented with MPO-ANCA. This confirms that the cell survival advantage seen with MPO-ANCA is CSF1 dependent (figure 4.20).

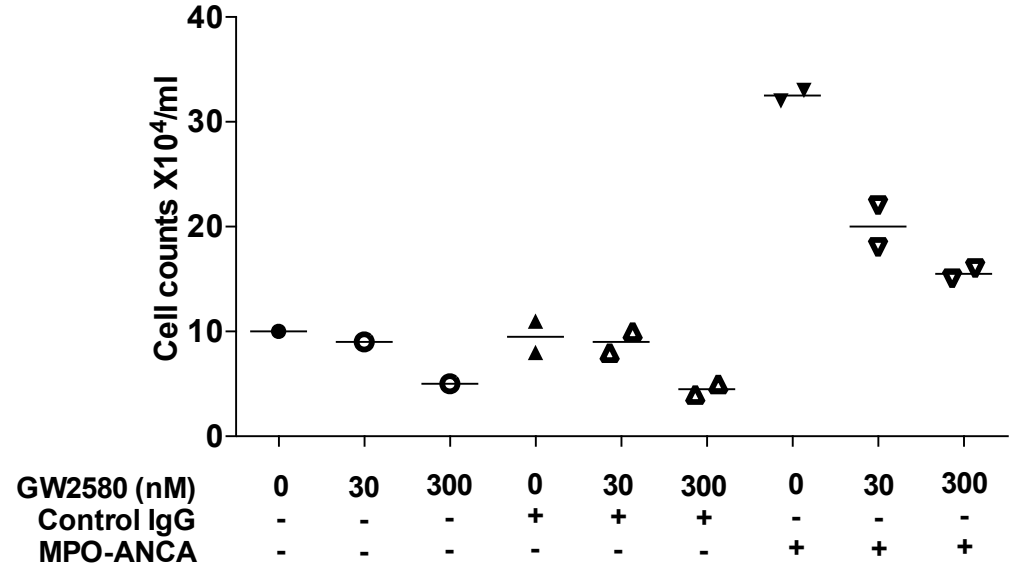

Figure 4.20 – Effect of a CSF1R inhibitor (GW2580) on cell counts after 6 days of peripheral blood monocyte culture. Monocytes from one donor were incubated with control IgG or MPO-ANCA with or without GW2580 at different doses.

We next assessed whether the MPO-ANCA/CSF1-driven effects on monocyte proliferation depended on enzymatic activity of MPO as we had found this to be the case for the reduction in IL10 and IL6 (see section 4.3). The MPO inhibitor AZD5904 did not prevent the increase in *CSF1* mRNA expression due to MPO-ANCA, in fact it led to a further increase in *CSF1* mRNA in the presence of MPO-ANCA (figure 4.21 A). The MPO inhibitor had no effect on CSF1 protein secretion into the supernatants of monocytes incubated with MPO-ANCA (figure 4.21 B). However, the MPO inhibitor did cause a partial reversal of the increase in macrophage numbers at day 6 associated with MPO-ANCA (figure 4.21 C).

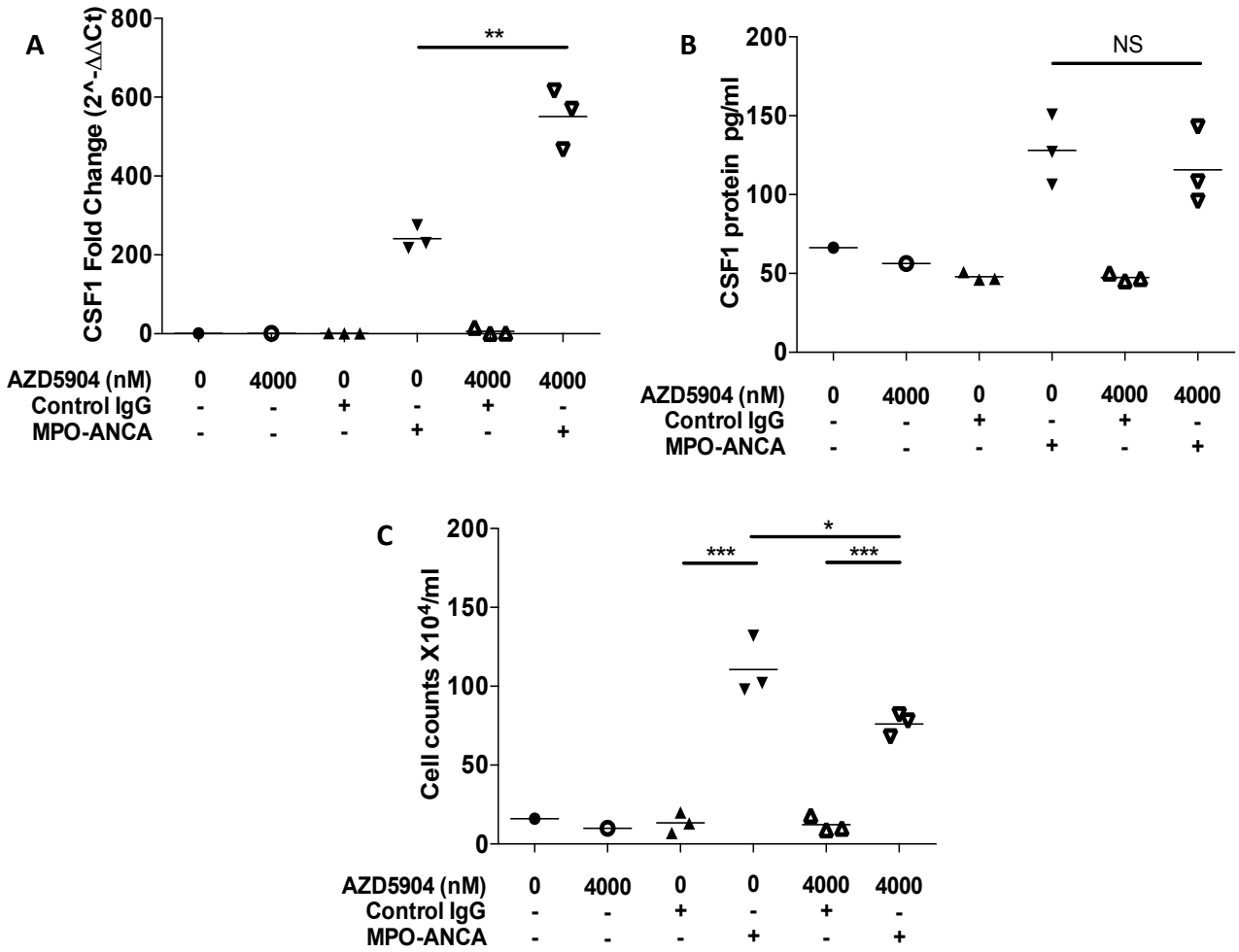

Figure 4.21 – Effect of MPO inhibitor AZD5904 on CSF1 gene expression, CSF1 protein secretion and cell counts. (A) The effect of AZD5904 on CSF1 gene expression 18 hours after monocyte culture with control IgG or MPO-ANCA. Data are expressed as a fold change in mRNA expression compared to the non-activated cells. Data were analysed using a student's t test (** = $p < 0.01$). (B) CSF1 protein in the supernatants of monocytes cultured with control IgG or MPO-ANCA with or without AZD9504. Data were analysed using a student's t test (NS = non significant). (C) The effect of AZD5904 on cell counts after 6 days of peripheral blood monocyte culture with control IgG or MPO-ANCA. Data were analysed using a one way ANOVA with Dunnett's post test (* = $p < 0.05$, *** = $p < 0.001$).

Since MPO-ANCA had been shown to interfere with TLR signalling pathways (section 4.4) and human serum contains endogenous ligands for TLR2 and TLR4, we assessed if the observed effect on differentiation and survival was the result of TLR4 antagonism.

Combined blockade of TLR2 and TLR4 with neutralising Abs had no effect on cell survival as shown in figure 4.22.

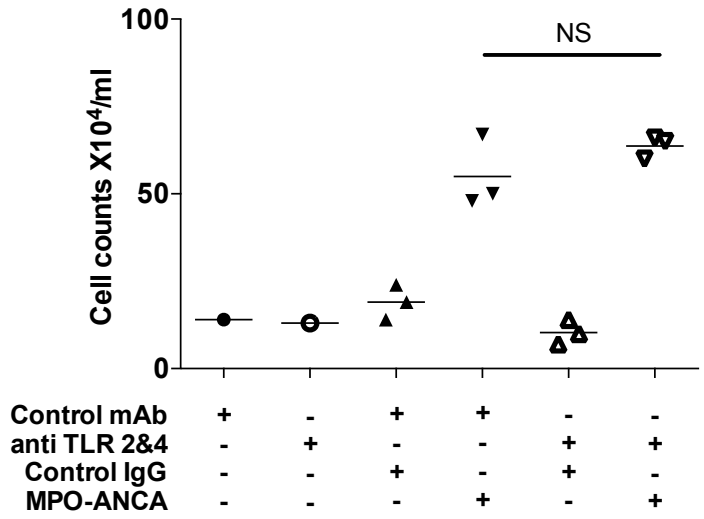

Figure 4.22 – Effect of TLR2/4 antagonists on cell counts after 6 days of peripheral blood monocyte culture. Monocytes from one donor were incubated with control IgG or MPO-ANCA with either control monoclonal antibodies or anti-TLR2 and TLR4 antagonists. Data were analysed using a student's t test (NS = non significant).

Overall these data show a marked increase in cell proliferation after peripheral blood monocytes are incubated for 6 days with MPO-ANCA compared to control IgG. The effect is largely due to an MPO-ANCA mediated increase in CSF1 production, which itself seems not to depend on MPO enzyme activity. However, through an unknown mechanism that is non-TLR2 and TLR4 dependent, the MPO enzyme activity also influences cell survival.

4.7 MPO-ANCA differentiated macrophages have an M2-like phenotype; they express increased CD206, secrete TGFβ and promote CD4 T cell production of IL10 and TGFβ

To explore the functional consequences of MPO-ANCA on macrophage maturation in human serum, we measured cytokines in the supernatant at day 6 in culture as described in sections 2.5.1 and 2.5.11. IL2, IL4, IL6, IL10, IFNγ, IL17A and TNFα were undetectable (data not shown). However, TGFβ was detected at levels above that found in the culture medium, and was specifically increased in the presence of MPO-ANCA in cultures (figure 4.23).

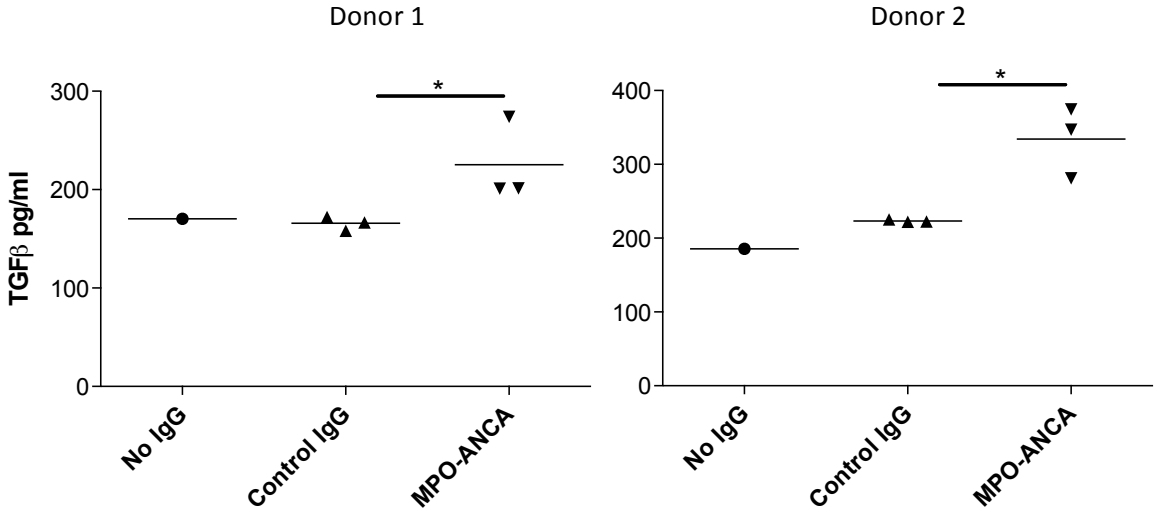

Figure 4.23 – TGFβ levels in the macrophage supernatants at day 6. Peripheral blood monocytes from two donors were cultured with 10% AB serum and no IgG, control IgG (n=3) or MPO-ANCA (n=3) for 6 days. TGFβ levels in supernatants were measured. Baseline whole medium TGFβ levels were subtracted from the supernatant TGFβ levels. Data were logarithmically transformed and analysed using a student's t test (* = $p < 0.05$).

Further, expression of the macrophage marker CD206, which is more readily expressed by M2 macrophages, was induced in both MPO-ANCA and control IgG treated cells at day 6 but was higher in the groups treated with MPO-ANCA (figure 4.24). This observation, together with the lower CD80 expression induction we observed in MPO-ANCA treated monocytes (figure 4.24) suggests that the macrophages maturing in the

presence of MPO-ANCA have an M2 phenotype in keeping with the role that we have shown for CSF1, which is known to favour M2 macrophage skewing.

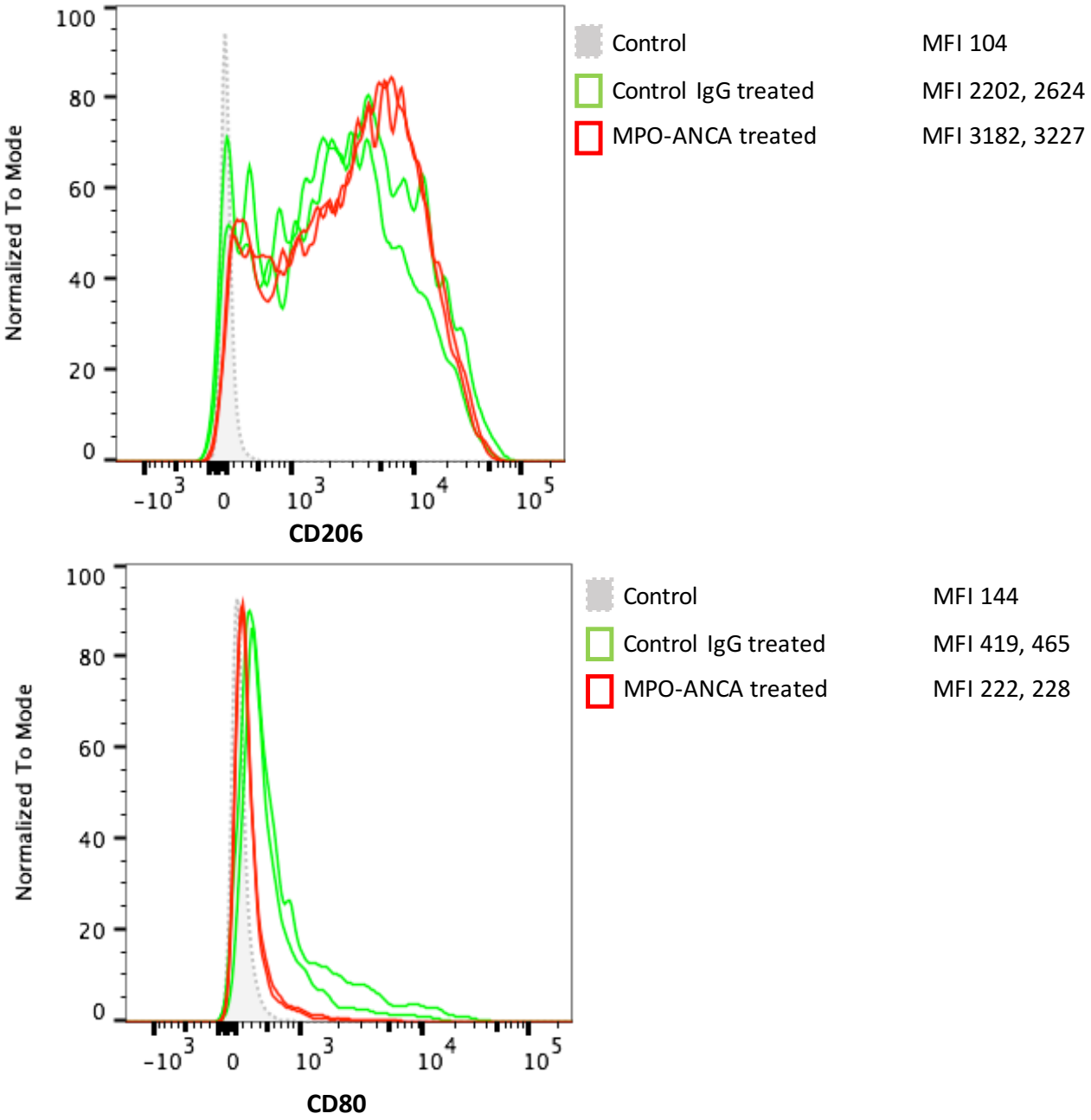

Figure 4.24 – Representative FACS histogram plots of CD206 and CD80 expression on macrophages. Monocytes from 2 donors were cultured for 6 days with 10% AB serum and control IgG (n=2) or MPO-ANCA (n=2). Histograms shown for one donor. CD206 MFIs were (donor 1) 3182, 3227 / (donor 2) 33466, 33287 for MPO-ANCA treated cells and (donor 1) 2202, 2624 / (donor 2) 20565, 8357 for control IgG treated cells. CD80 MFIs were (donor 1) 222, 228 / (donor 2) 1113, 1213 for MPO-ANCA treated cells and (donor 1) 419, 465 / (donor 2) 2413, 3806 control IgG treated cells respectively.

We next went on to assess the functional impact of the macrophage skewing observed on CD4 T cells. Patients with vasculitis have T cells within affected glomeruli and also changes in and persistence of local Th1 and Th2 responses [277]. Therefore, we transferred supernatants from antibody-treated macrophages onto anti-CD3 and anti-CD28 activated CD4 T cells as described in section 2.5.6 and measured the cytokine profile of the activated T cells. The CD4 T cells were not acquired from the same donors as the monocytes. Separate healthy donors were utilised.

TGFβ levels in the CD4 T cell supernatants were increased when the T cells were stimulated in the presence of supernatants from MPO-ANCA treated macrophages (figure 4.25). The TGFβ levels were higher than those found in the macrophage supernatants or the basal T cell medium and so they reflected production from CD4 T cells.

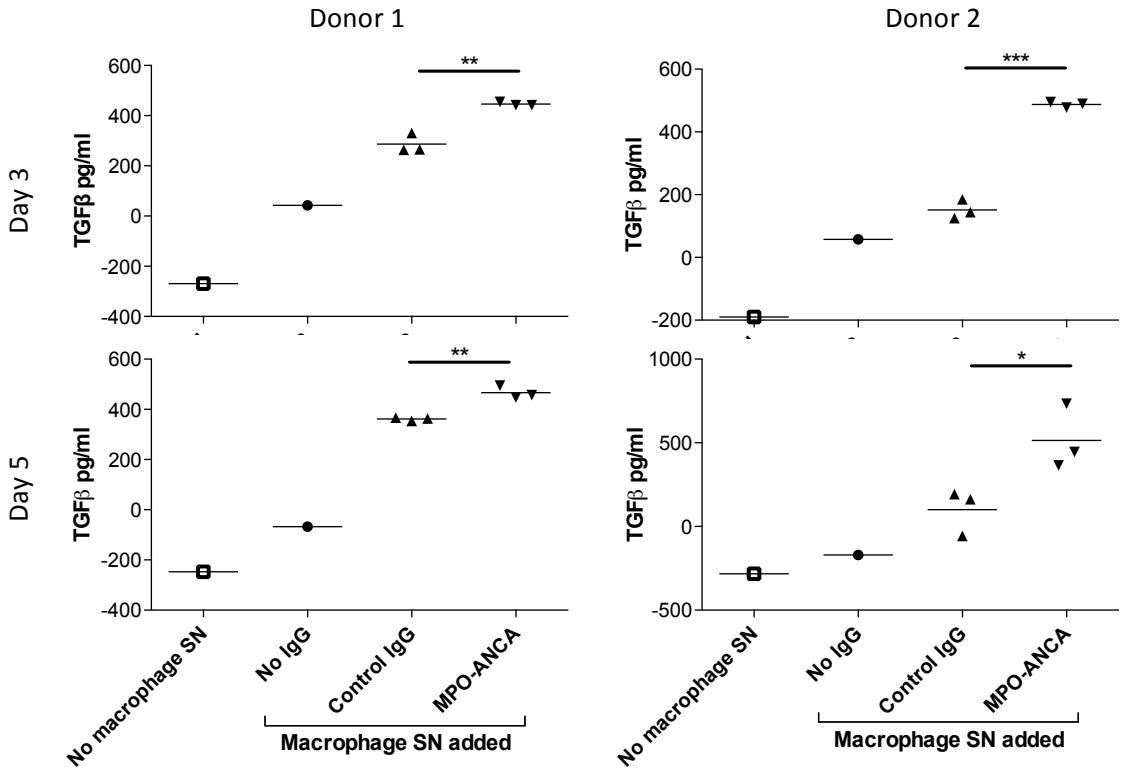

Figure 4.25 - TGFβ levels in anti-CD3 and anti-CD28 activated CD4 T cells supernatants at day 3 and day 5. The anti-CD3 and anti-CD28 activated CD4 T cells were incubated with supernatants from untreated macrophages; control IgG treated (n=3) or MPO-ANCA (n=3) treated macrophages. Baseline whole medium TGFβ levels were subtracted from the supernatant TGFβ levels. Data were analysed using a student's t test (* = $p < 0.05$, ** = $p < 0.01$, *** = $p < 0.001$).

To ensure that the ELISA data in figure 4.23 and figure 4.25 were comparable a standard sample was analysed on both ELISA sets (749.4 and 830.6 pg/ml respectively).

IL17A was not affected consistently by macrophage-derived factors and IL4 was not detected (data not shown), however, we observed a consistent decrease in IFNγ production accompanied with an increase in IL10 specifically in CD4 T cells activated in the presence of supernatants from MPO-ANCA treated macrophages with a statistically significant and persistent increase in the IL10 to IFNγ ratio on day 3 and day 5 of the CD4 T cell cultures (figure 4.26 A and B respectively).

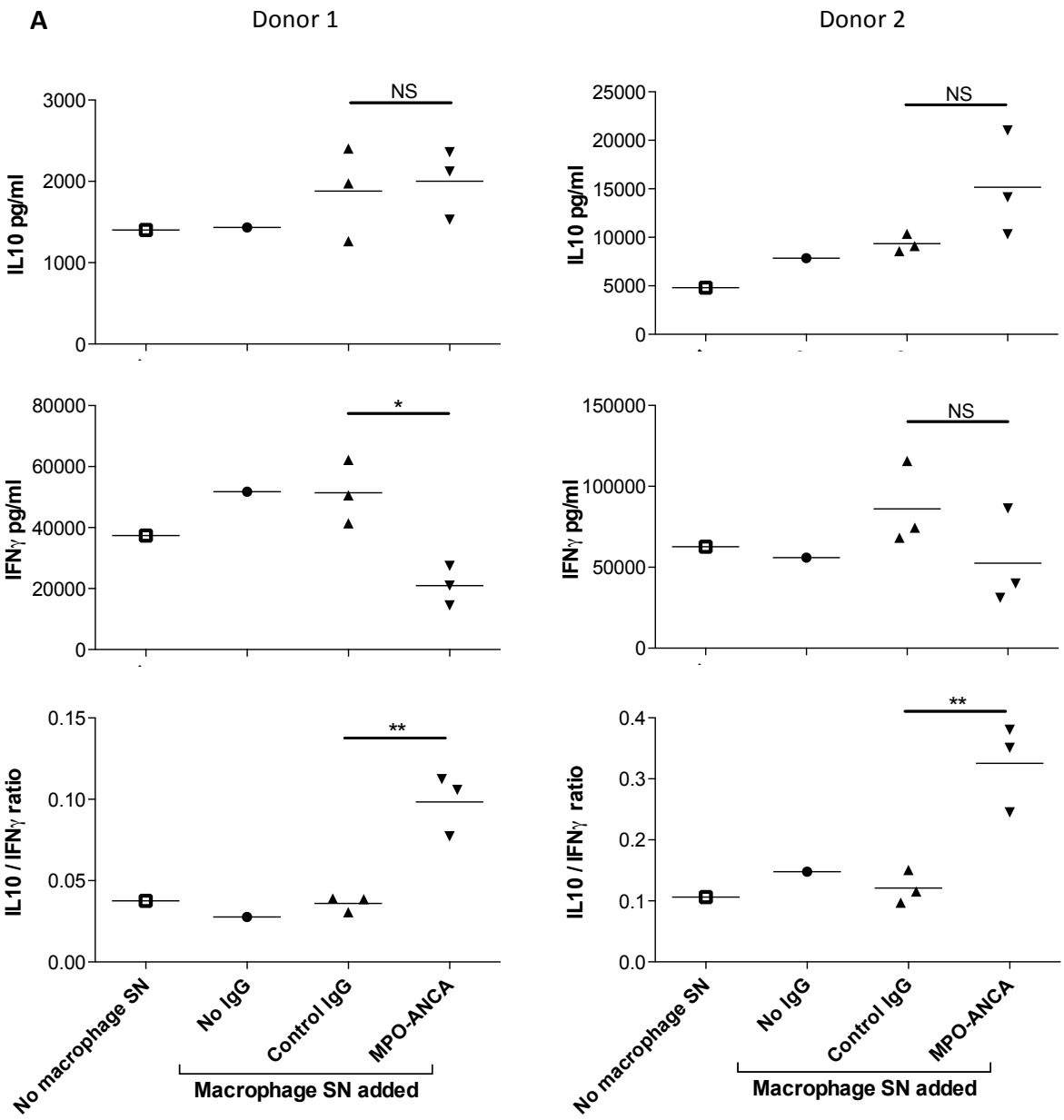
A
Donor 1
Donor 2
IL10 pg/ml
IFNγ pg/ml
IL10 / IFNγ ratio
NS
*
**
No macrophage SN
No IgG
Control IgG
MPO-ANCA
Macrophage SN added

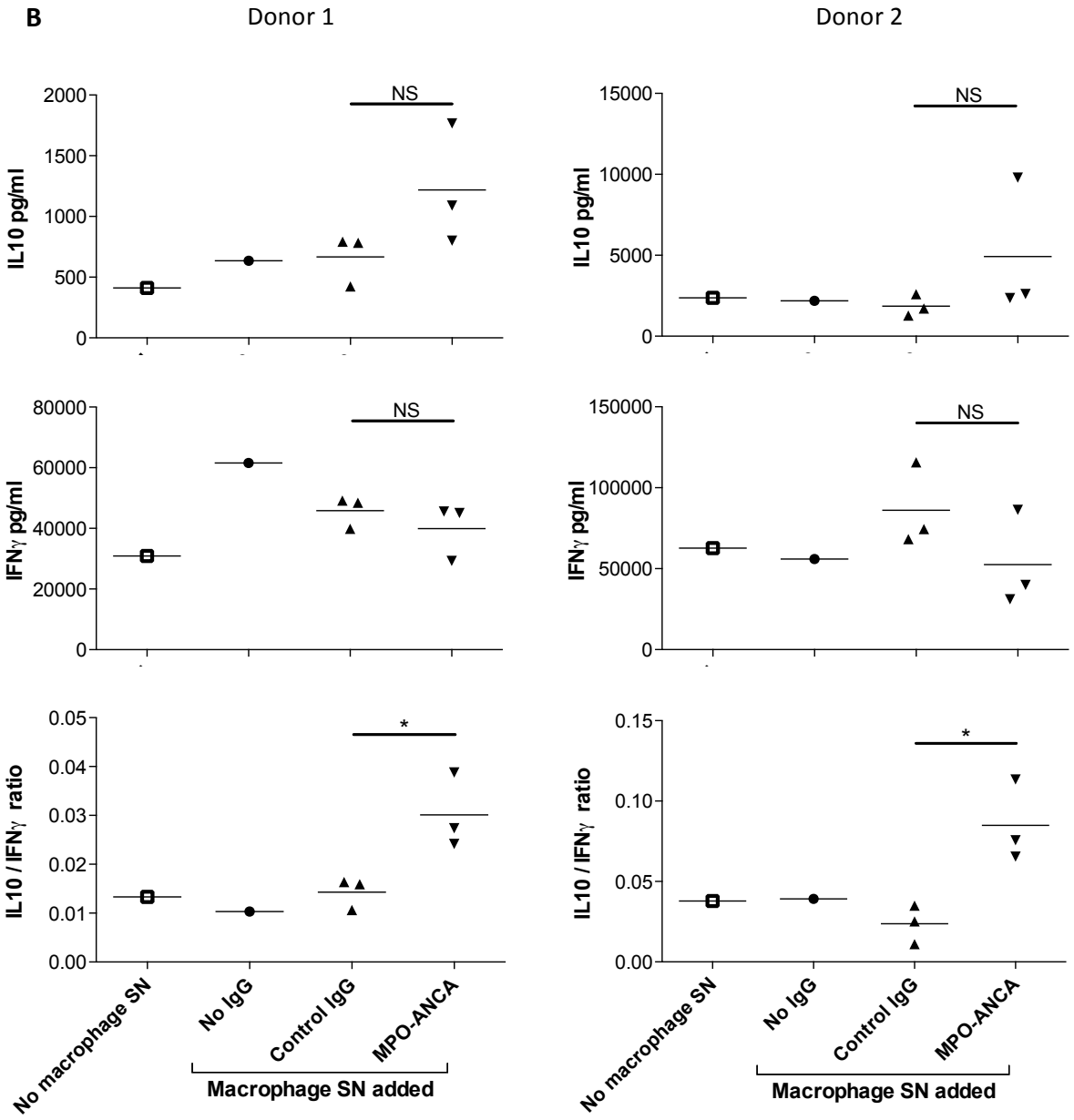

Figure 4.26 – Cytokine profile of CD4 T cells activated with anti-CD3 and anti-CD28 in the presence or absence of added supernatant from macrophages. Activated CD4 T cells from two donors cultured for 3 (A) or 5 (B) days with or without supernatants from macrophages incubated with control IgG (n=3) or MPO-ANCA (n=3). IL10, IFNγ and IL10 / IFNγ ratio in the supernatants of the CD4 T cells are depicted. Data were analysed using a student's t test (* = $p < 0.05$, ** = $p < 0.01$).

4.8 Discussion

We have discovered some novel effects of MPO-ANCA on human monocytes with potential implications for AAV pathogenesis. These include MPO-ANCA induced reduction in IL6 and IL10 production from monocytes in response to stimulation with LPS, which requires the Fc and MPO binding portion of ANCA. The effect seems to be dependent on MPO enzyme activity and is possibly mediated by MPO driven increase in oxidised phospholipids. The phosphatidylcholine species at m/z 828.8 that was increased in MPO-ANCA treated monocytes was tentatively identified as PEIPC, which has been reported previously to be generated in LPS-stimulated monocytes and neutrophils [59]. Oxidised phospholipids have been shown to have a wide variety of bioactivities, which can be both pro- and anti-inflammatory depending on the cell type and oxidised phospholipid species in question.

An important anti-inflammatory mechanism of oxidised phospholipids is through the inhibition of TLR2 and TLR4 signalling, in part by competitive interaction with LPS binding protein, CD14 and myeloid differentiation protein 2 [274-276]. There has been little work on the effects of PEIPC as an individual species, but it has been reported previously that it can induce IL8 production by endothelial cells and it can inhibit LPS-induced E-selectin expression at concentrations approximately 10-fold lower than those that induce IL8 production [276, 278, 279]. Currently, it is not clear why a significant increase was only observed for a single oxidised species, or whether the increase observed would be sufficient to cause inhibition of TLR signalling. However, PEIPC is indeed one of the most abundant esterified products produced during oxidation of PAPC *in vitro*, and has also been detected as a major product in various inflammatory lesions [280]. Furthermore, if MPO-ANCA is tethering MPO to the cell surface, this would cause localized oxidation that might not be readily apparent in extracts of total cellular phospholipids.

The effects of a reduction in IL6 are difficult to predict, as this cytokine has both pro- and anti-inflammatory effects mediated by classical membrane-bound receptor signalling and trans-signalling via a soluble receptor [281, 282]. For example IL6 regulates neutrophil recruitment to inflammatory sites by promoting granulopoeisis

[283], but following neutrophil recruitment and soluble IL6 receptor shedding, IL6 signalling limits neutrophil influx [284]. IL6 protein levels were consistently reduced in the supernatant of LPS stimulated monocytes treated with MPO-ANCA for 18 hours and in the microarray studies of MPO-ANCA treated monocytes at 6 hours of cell culture studies.

In contrast IL10 is an anti-inflammatory cytokine and moreover the reduction in response to MPO-ANCA was more pronounced than that seen for IL6 in our experiments. Many mechanisms are in place to prevent exaggerated inflammatory responses and IL10 has proved to be an essential factor in this protection [285]. For example, animals that are genetically deficient for IL10 or are treated with antibodies that neutralize IL10 die rapidly when infected with pathogens due to the overproduction of pro-inflammatory cytokines rather than a lack of control of infection [286, 287]. In the context of tissue inflammation in AAV, cells such as tissue macrophages, dendritic cells, epithelial cells and renal mesangial cells, do not contain MPO and will not be affected by MPO-ANCA directly. However, they will be influenced by cytokines released locally by monocytes. A reduction in monocyte IL10 production would therefore be expected to increase the responsiveness of these cells to stimulation by TLRs and other inflammatory stimuli and to lead to an exaggerated inflammatory response. This protective effect of IL10 is demonstrated in the context of renal inflammation in the unilateral ureteral obstruction (UUO) model. More severe inflammation develops in the kidney of mice lacking IL10 compared to wild type controls [288]. Overall, the dominant effect of MPO-ANCA on monocytes is a reduction in IL10 secretion, which would be expected to promote inflammation and disease in patients. Surprisingly we did not see a suppression of IL10 gene expression in the microarray studies of monocytes treated with MPO-ANCA. This may be due to the 6 hour time-point we selected to analyse the microarray data. It is possible that IL10 levels are suppressed at an earlier or later time-point.

We also showed that MPO-ANCA causes an increase in survival and differentiation of monocytes to M2-like macrophages in culture primarily through an increase in CSF1 production. Macrophages play an important role in wound healing as well as fibrosis. They stimulate and activate fibroblasts to produce extracellular matrix proteins [270,

289]. It is increasingly recognised that the phenotype of macrophages does not fall into a simple M1 or M2 category as discussed. However, the increased CD206 and reduced CD80 expression, together with higher TGFβ secretion on exposure to MPO-ANCA compared to control IgG, suggests that the macrophages fit most closely with an M2-like phenotype, consistent with their induction by an increased concentration of CSF1 [137, 138]. Ramirez *et al* have shown that patients with AAV have higher levels of CSF1 compared to healthy controls, this correlated with the BVAS score [290] supporting our data.

TGFβ has been established for over a decade as a key cytokine that promotes the induction of regulatory T cells [291]. In mice, macrophages polarised to secrete TGFβ have been shown to inhibit adriamycin-induced nephrosis by a mechanism that includes the induction of regulatory T cells [292]. A further report has also shown that human M2 macrophages can induce CD4 T cells with a regulatory phenotype [293]. In both of these examples, the mechanism of suppression was thought to require cell contact whereas we have shown the effect of a soluble factor in the supernatant. Nonetheless there are parallels with our data suggesting the M2 macrophages, generated from monocytes incubated with MPO-ANCA, limit T cell activation via TGFβ.

Our current data suggest that macrophages generated from MPO-ANCA stimulated monocytes act to limit the activation of IFNγ producing CD4 T cells and promote the switch to an IL10 producing phenotype. Over the past few years the life cycle of the Th1 cell as it changes from producing predominantly IFNγ to producing both IFNγ and IL10 and then to producing predominantly IL10 and acquiring suppressive capacity, has been described [186]. This represents a key pathway in the lifecycle of Th1 cells as they switch from an inflammatory to a regulatory phenotype. These IL10 secreting CD4 T cells may be similar to, if not the same as, those that have been called induced regulatory T cells [294]. It has been shown that CD46 activated CD4 T cells indeed express increased TGFβ (Kemper *et al* unpublished data). We now show that CD4 T cells activated in the presence of supernatants from MPO-ANCA stimulated monocytes/macrophages also produce TGFβ. T cells have been shown to be important in both pulmonary and renal fibrosis with several potential mechanisms that have not been fully defined [295, 296]. A direct effect of TGFβ produced by T cells is one

possibility and we have shown how this may be promoted by MPO-ANCA via its actions on monocytes. Effects of TGFβ include a direct stimulation of fibroblasts to cause differentiation into myofibroblasts with concomitant collagen secretion [268, 297]. The amount of fibrosis remaining in vital end organs such as the lung and kidney is a major prognostic factor for patients with AAV [267].

In summary we have shown two novel effects of MPO-ANCA on monocytes with implications for disease in patients. These are firstly, a reduction in IL10 in response to LPS stimulation, potentially due to inhibition of TLR signalling by oxidised phospholipids, which are known to be TLR4 antagonists. Secondly MPO-ANCA promotes monocyte survival and differentiation to macrophages, which instruct the generation of regulatory T cells that produce IL10 and TGFβ and may promote fibrosis. These two effects and the mechanisms involved are illustrated in figure 4.27.

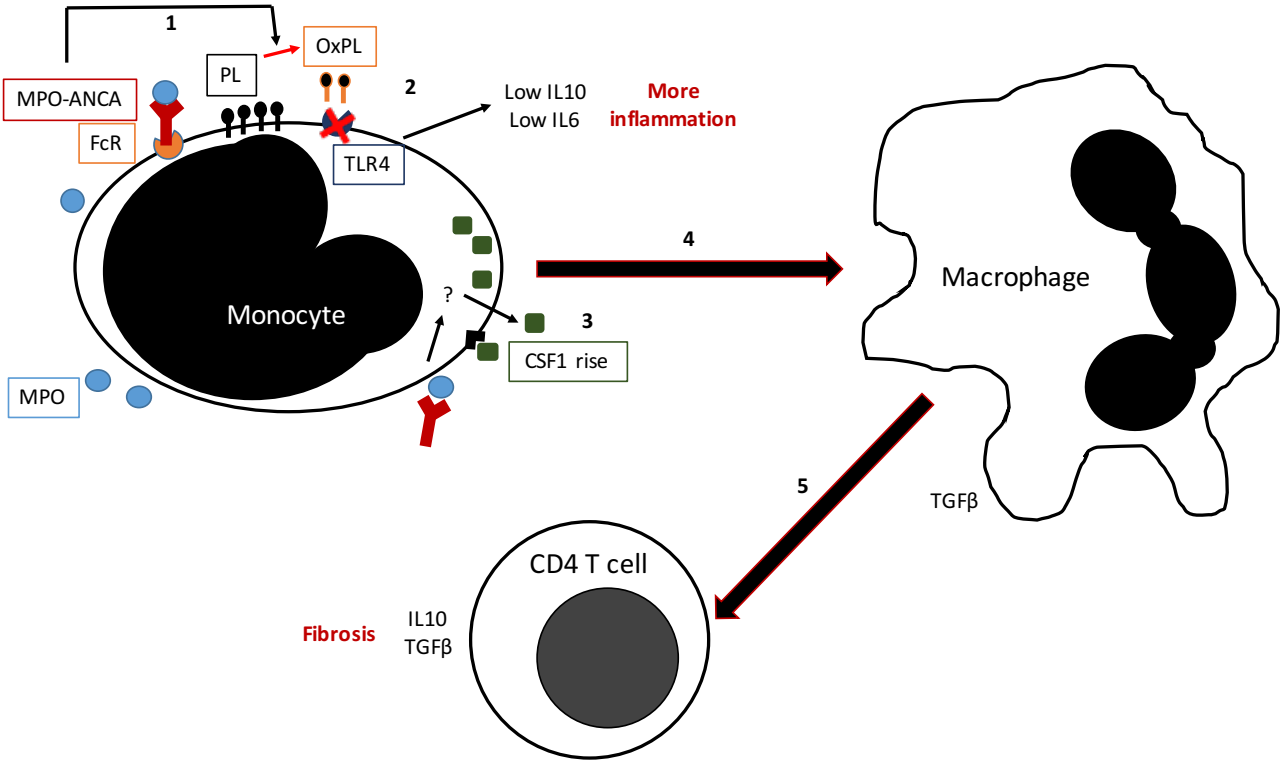

Figure 4.27 – Summary of proposed actions of MPO-ANCA on monocytes and the subsequent downstream effects. 1. MPO-ANCA tether MPO via the Fc receptors (FcR) onto the monocyte surface and generates local oxidised phospholipids (OxPL) from native cell phospholipids (PL). 2. The oxidised phospholipids inhibit LPS induced TLR4 activation, which culminates in a reduction in IL10 and IL6, promoting inflammation in

the acute phase of the disease. 3. MPO-ANCA also increase CSF1 production from monocytes through an unknown mechanism. 4. These set of events increase the survival and generation of M2-like macrophages that generate TGFβ. 5. The macrophages create a milieu that leads to the generation of regulatory CD4 T cells that produce IL10 and TGFβ, which is thought in turn to promote fibrosis and possibly an attempt at resolution of the on-going chronic inflammation.

Chapter 5 – The role of complement in AAV

5.1 Introduction

The various animal models of AAV have been discussed in section 1.11. We recently published a modification of the passive transfer model using GCSF to exacerbate disease [119]. The passive transfer model was first established by Xiao *et al* [100]. The disease severity in the passive transfer model was exacerbated by the use of systemic bacterial LPS [32]. The model, which needed minor modifications, has been established in our laboratory. The methodology is summarised below in figure 5.1. Please refer to section 2.3.5 for precise protocols of LPS and GCSF administration used for each *in vivo* experiment.

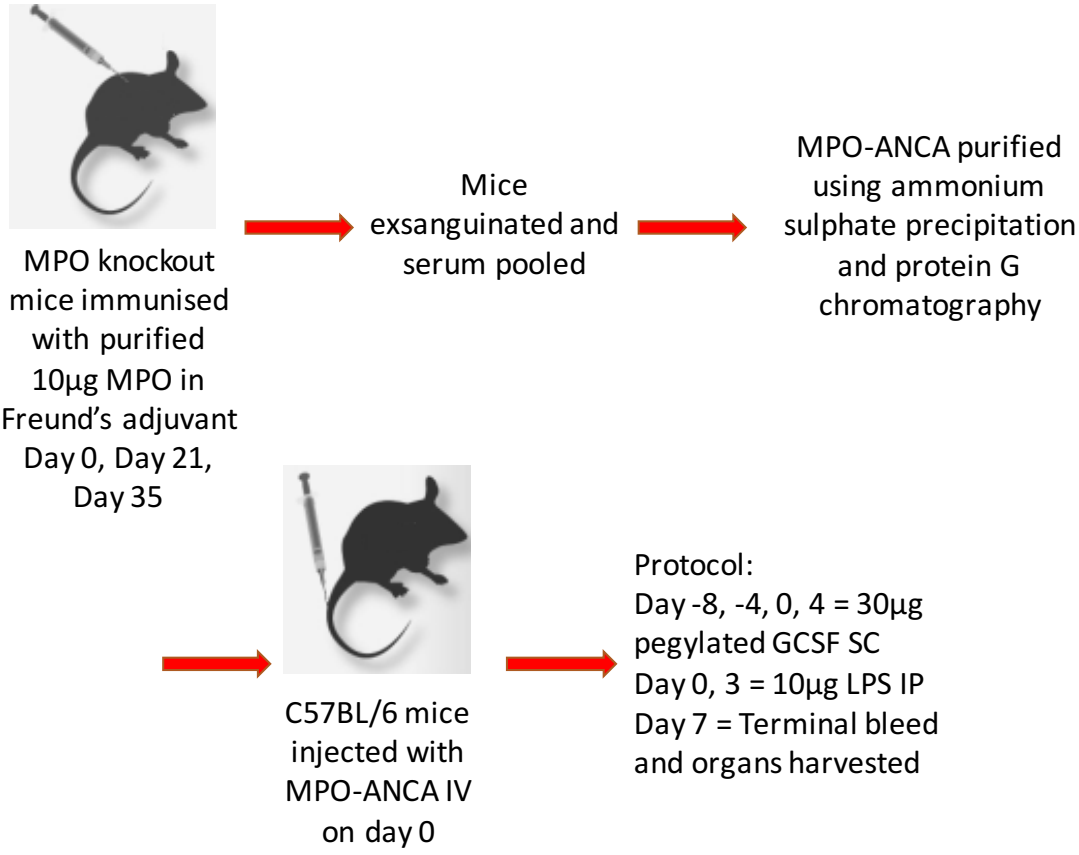

Figure 5.1 – The overall passive transfer model protocol of AAV used for this PhD.

The histological features of glomerulonephritis induced with the passive transfer model closely mirror the situation in patients presenting with AAV. The crescentic glomerulonephritis is focal and segmental, with a lack of immune deposits. These

features recapitulate characteristics of the histology seen in clinical renal biopsy samples. Furthermore, the proteinuria observed is in the non-nephrotic range, as is the case for patients with AAV. These features make this a good model of MPO-ANCA disease.

Several pathogen associated molecular pattern molecules including LPS activate TLR. LPS is a structural component of the outer membrane of gram-negative bacteria. LPS induced activation occurs through a series of interactions with LPS binding protein, CD14, myeloid differentiation protein 2 and TLR4 [298]. The LPS binding protein facilitates binding of LPS and CD14 which in turn transfers LPS to the TLR4 / myeloid differentiation protein 2 complex. Upon LPS binding, TLR4 undergoes oligomerisation [298]. TLR4 activation in this manner leads to further interaction with Toll-interleukin-1 receptor domains (namely MyD88, MAL, TRIF, TRAM and SARM), which recruit downstream signalling cascades generally separated into MyD88 dependent and independent pathways that lead to the production of pro-inflammatory cytokines and type 1 interferons respectively [299].

Huugen *et al* showed that in C57BL/6 mice administration of LPS led to a transient increase in systemic TNFα levels as well as circulating MPO levels [32]. The rise in TNFα levels was thought to prime neutrophils exposing more of the antigens to the MPO-ANCA administered, worsening disease in the passive transfer model.

GCSF as discussed in section 1.6 acts via a transmembrane protein to mobilise, proliferate, differentiate and maintain the survival of myeloid cells. We showed that GCSF also primes neutrophils to induce respiratory burst on exposure to monoclonal MPO-ANCA [119]. Together these functions lead to more antigen containing cells that propagate further inflammation.

As a result it is comprehensible that both LPS and GCSF exacerbate disease in the passive transfer model. However, it is not known whether GCSF alone can exacerbate disease without LPS.

In section 1.10 we discussed the role of complement in AAV. Previous published work using the passive transfer model implicates the alternative pathway of complement in

pathogenesis. The administration of cobra venom factor to mice offered protection against the development of MPO-ANCA disease, furthermore, mice deficient in factor B but not C4 were protected from disease [207]. C5 deficient mice are also protected and treatment with an anti-C5 monoclonal antibody inhibited disease induction [208]. MPO deficient mice immunised with MPO and transplanted with bone marrow from C5aR1 deficient mice were protected from disease when compared with mice that received wild type bone marrow, suggesting that the anaphylatoxin C5a is a key mediator [209]. This work was extended with evidence of therapeutic efficacy for the CCX168, a C5aR1 antagonist, in human C5aR1 knock in mice [211].

The trigger that leads to the activation of the alternative pathway has not been elucidated. We showed data in section 3.5 to suggest that neutrophils are capable of expressing C3 and C5. Furthermore, we suggested that PR3 could cleave C3 into different components. This may have a role to play in the generation of C3a and C3b. We discussed that neutrophils are capable of releasing the machinery for the formation of a C5 convertase, which may propagate the downstream events of the complement pathway [187, 210]. There are other potential initiators of the alternative pathway.

Properdin is established as a key stabiliser of the alternative pathway but it also binds to various cell surfaces including apoptotic cells and serves as a platform for C3bBb assembly, leading to C3 cleavage and complement activation [151-153]. Hence, properdin itself may serve as a PRM for alternative pathway activation. However, previous work in our laboratory done by Freeley *et al* (The role of complement and GCSF in ANCA associated vasculitis, PhD Thesis 2013, King's College London) showed that properdin knockout mice were not protected from disease in the passive transfer model. The percentage of glomerular crescents between the groups was similar (mean of 27.5±6.9% and 27.8±8.2% for the wild type and properdin deficient mice respectively), as was the glomerular macrophage count, albuminuria, haematuria and serum creatinine. This makes properdin an unlikely candidate for initiating and propagating the alternative pathway.

Another candidate for initiating activation of the alternative pathway is possibly the lectin pathway. Recent work has shown that C4 is not required for lectin pathway

activation, so it is possible that the lectin pathway in a C4-independent manner may be important in initiating complement activation, with subsequent amplification by the alternative pathway [245]. Interestingly work in our laboratory (Simon Freeley, The role of complement and GCSF in ANCA associated vasculitis, PhD Thesis 2013, King's College London) showed that MASP2 deficiency led to a significant exacerbation of renal disease when compared to controls in the context of the passive transfer model. MASP2 knockout mice had significantly more glomerular crescents (mean of 30.9±4% and 17.1±2.8% respectively), higher albumin creatinine ratios and more haematuria as well as raised serum creatinine than wild type mice. This result was surprising; we anticipated as in the ischaemia reperfusion model, MASP2 deficiency would lead to an attenuation of disease [245]. This data suggested that in the context of the passive transfer model, MASP2 has a protective effect. The exact mechanisms responsible for this effect were unclear. MBL binds and clears modified immunoglobulins and immune complexes. MBL deficiency has been shown in a mouse model of vaccination to increase antibody responses. As a result the MPO-ANCA levels were measured at day 7 in the MASP2 deficient mice and wild type mice serum but no significant difference in titres were found. The possibility of whether this effect on disease severity is mediated through the alternative pathway was not determined at the time.

The other interesting aspect of complement activation, which to our knowledge has not been previously addressed in AAV, is the differential role of systemic and local complement production in pathogenesis. As discussed in section 1.10.7, intracellular derived complement and intracellular complement receptors may have distinct functions compared to their extracellular counterparts.

5.2 Aims

In this chapter we aimed to assess whether LPS and GCSF were both required for the generation of robust disease in the passive transfer model. We also set out to explore the possible mechanism for the attenuation in disease noted in MASP2 knockout mice and in doing so confirming a role for complement in pathogenesis. Lastly we explored the role of leucocyte local C5 production in comparison to systemic complement component C5 in the pathogenesis of AAV.

5.3 LPS and GCSF have a synergistic effect in the passive transfer model

MPO-ANCA was generated from a group of MPO-deficient mice that had been immunised with 10µg MPO (RZ=0.44) as described in section 2.3.2 and 2.4.1.

The passive transfer model was set up as described in section 2.3.5 with four groups of wild type mice (C57BL/6); group 1 received PBS and dextrose (in place of LPS and GCSF respectively) n = 5, group 2 received LPS and dextrose (in place of GCSF) n = 6, group 3 received PBS (in place of LPS) and GCSF n = 6, group 4 received LPS and GCSF n = 5 on the respective days highlighted in figure 5.1. Urine, blood and tissue was harvested and processed as detailed in sections 2.3.6 to 2.3.11.

As shown in figure 5.2, at day 7, the glomerular crescent counts were significantly higher in the group of mice that had both LPS and GCSF administered compared to the other three groups (mean group 1 0±0%, group 2 0.33±0.33%, group 3 0.17±0.17% and group 4 31.6±5.2%). Similarly and as expected, the glomerular macrophage infiltration was significantly higher in the group receiving both LPS and GCSF together compared to the other three experimental groups as depicted in figure 5.3 (mean group 1 0.47±0.09 cells, group 2 2.2±0.28 cells, group 3 4.14±0.81 and group 4 15.34±1.25 cells).

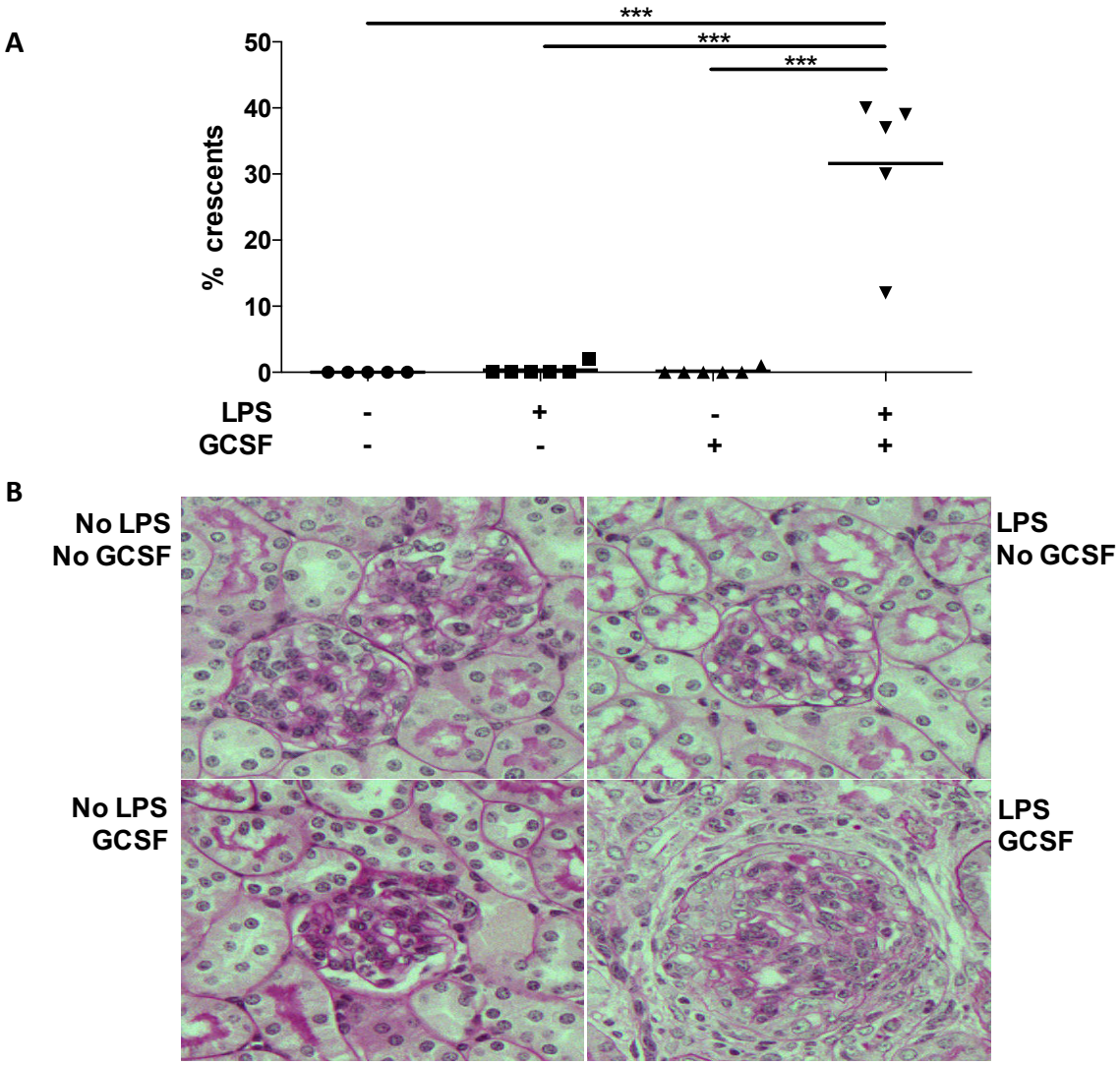

Figure 5.2 - Glomerular crescent formation following disease induction. A) Graph depicting day 7 glomerular crescent counts in the four experimental groups of mice. Each symbol is data from a separate mouse. Data were analysed using one way ANOVA and a Tukey's multiple comparison post test (*** = $p < 0.001$). B) Representative periodic acid schiff stain slides of glomerular sections on day 7 of the passive transfer model in each experimental group (light microscopy x400 magnification).

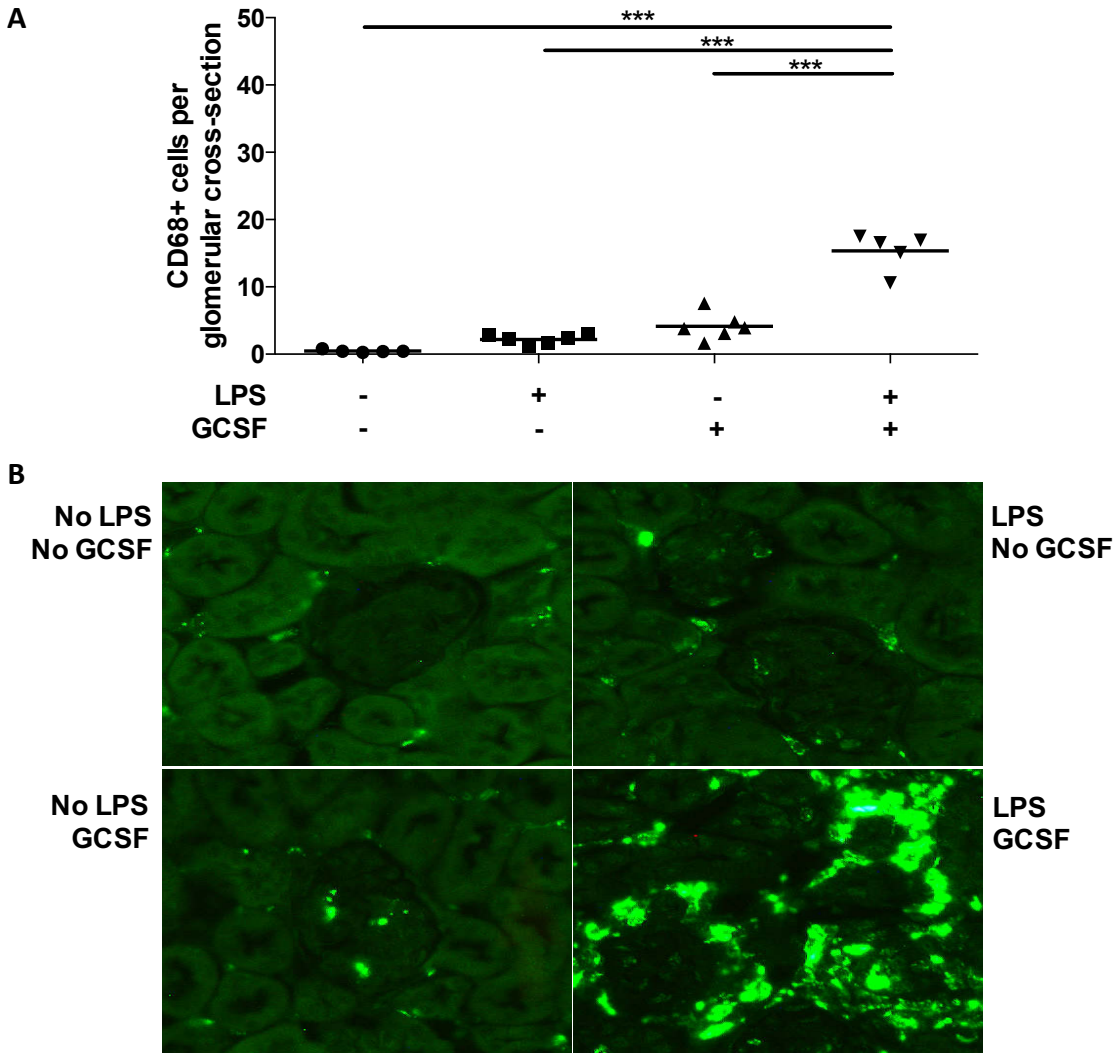

Figure 5.3 – Glomerular macrophage infiltration following disease induction in the passive transfer model. A) Day 7 CD68 positive macrophage infiltration counts. Data were analysed using a one way ANOVA and a Tukey's multiple comparison post test (*** = $p < 0.001$). B) Representative immunofluorescence staining of CD68 positive macrophages in the four experimental groups (x400 magnification).

We measured pre- and post-disease induction 24 hour albuminuria (day -4 and day 7 respectively) as described in section 2.3.6. As shown in figure 5.4A, at baseline, prior to MPO-ANCA IV injection the four groups had low grade albuminuria which was not significantly different among the groups. At day 7, the mice that received both LPS and GCSF had significantly higher levels of albuminuria than the other three groups (figure 5.4B).

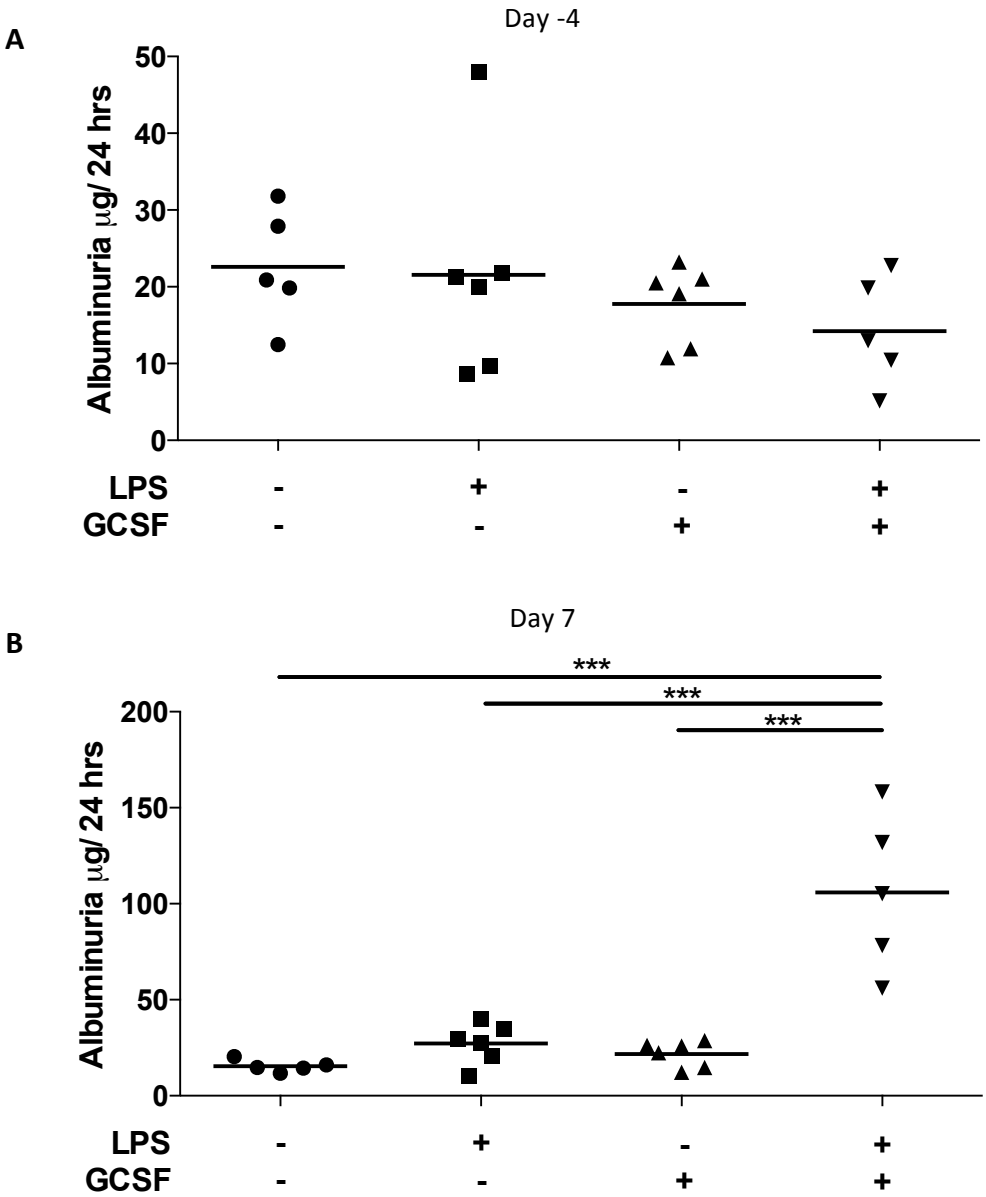

Figure 5.4 – Albuminuria levels prior to and after disease induction. Albuminuria measurements in the four experimental groups of mice prior to disease induction on day -4 (A) and after disease induction on day 7 (B). Data were analysed by a one way ANOVA and a Tukey's multiple comparison post test (*** = $p < 0.001$).

Haematuria was assessed as described in section 2.3.7 and there was no significant difference in haematuria severity between groups on day 7 (data not shown). Measurements of serum creatinine on day -1 revealed no significant differences between groups, however on day 7 the group, which received both LPS and GCSF had significantly higher serum Cr levels than the other 3 groups (figure 5.5).

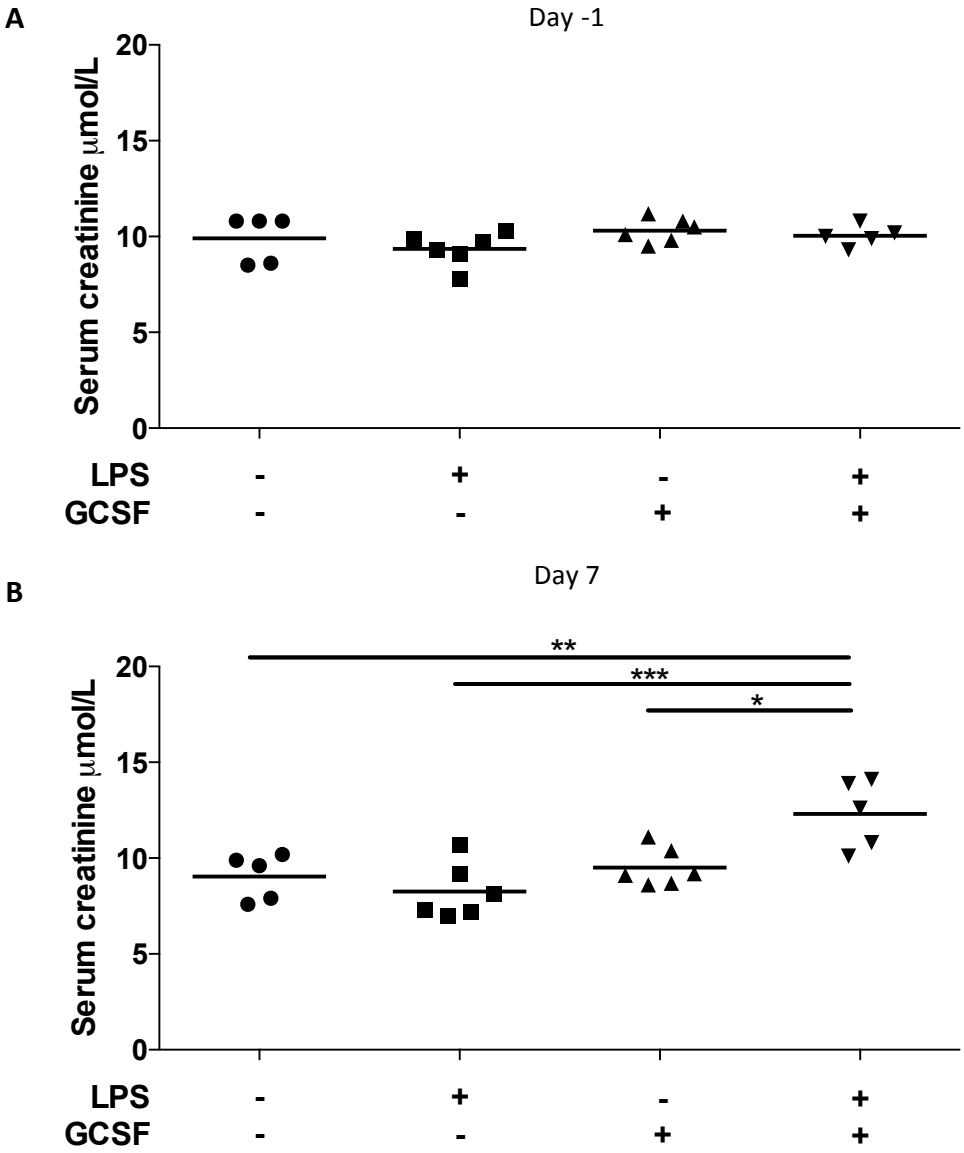

Figure 5.5 – Serum creatinine levels prior to and after disease induction. Serum creatinine measures at day -1 (A) and day 7 (B) in the four groups of mice. Data were analysed using a one way ANOVA and a Tukey's multiple comparison post test (* = $p < 0.05$, ** = $p < 0.01$, *** = $p < 0.001$).

So it appears that both LPS and GCSF are required to produce a robust disease model.

5.4 MASP2/C3 deficient and C3 deficient mice are protected from disease

We sought to examine if the increased disease in MASP2 knockout mice depended on complement activation. We compared disease in wild type mice, mice deficient in both C3 and MASP2 with mice deficient in C3.

MPO-ANCA was generated from a group of MPO-deficient mice that had been immunised with 10µg MPO (RZ=0.69) as described in section 2.3.2 and 2.4.1.

There was no significant difference in the neutrophil counts on day -1 in peripheral blood between mice in the three groups (mean neutrophil counts $X10^7$/ml in wild type mice 0.68±0.04, MASP2/C3 knockout 0.65±0.1 and C3 knockout mice 0.68±0.08).

As shown in figure 5.6, compared to wild type mice, there was very mild disease in both MASP2/C3 double deficient and C3 deficient mice (glomerular crescent counts mean for wild type mice 20.4±5.8%, MASP2/C3 double knockout mice 1.5±0.86% and C3 knockout mice 2.8±0.98%). Similarly the glomerular macrophage infiltration count was low in the MASP2/C3 double deficient and C3 deficient mice compared to wild type mice as demonstrated in figure 5.7 (CD68 positive cell count mean for wild type mice 6.2±0.5 cells, MASP2/C3 double knockout mice 2.8±0.28 cells and C3 knockout mice 2.6±0.18 cells per glomerular cross-section).

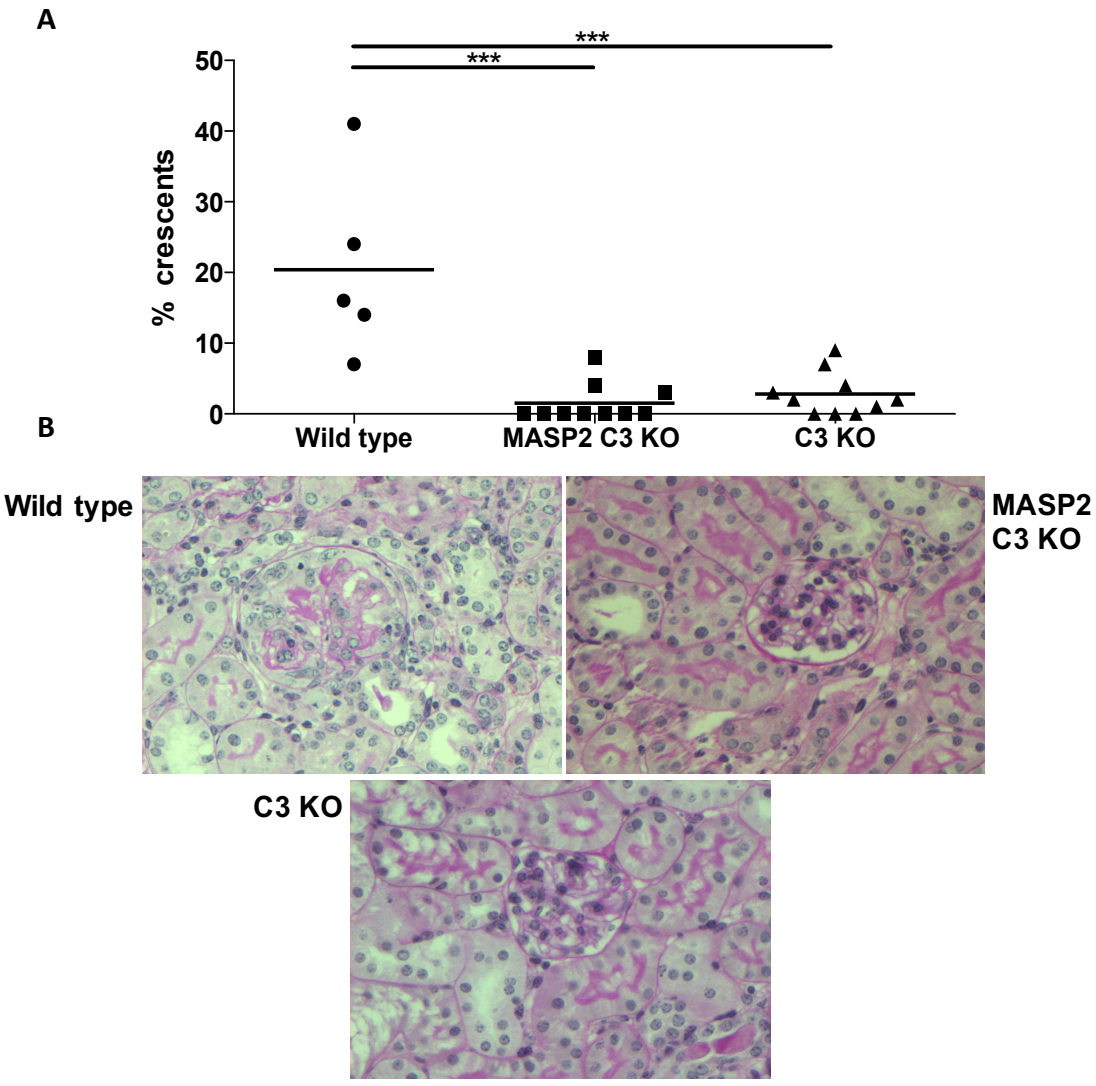

Figure 5.6 – Glomerular crescents in wild type, MASP2/C3 double knockout and C3 knockout mice. A) Graph depicting day 7 glomerular crescent counts in the three experimental groups of mice. Each symbol is data from a separate mouse. Data were analysed using one way ANOVA and a Tukey's multiple comparison post test (*** = $p < 0.001$). B) Representative periodic acid schiff stain slides of glomerular sections on day 7 of the passive transfer model in each experimental group (light microscopy x400 magnification).

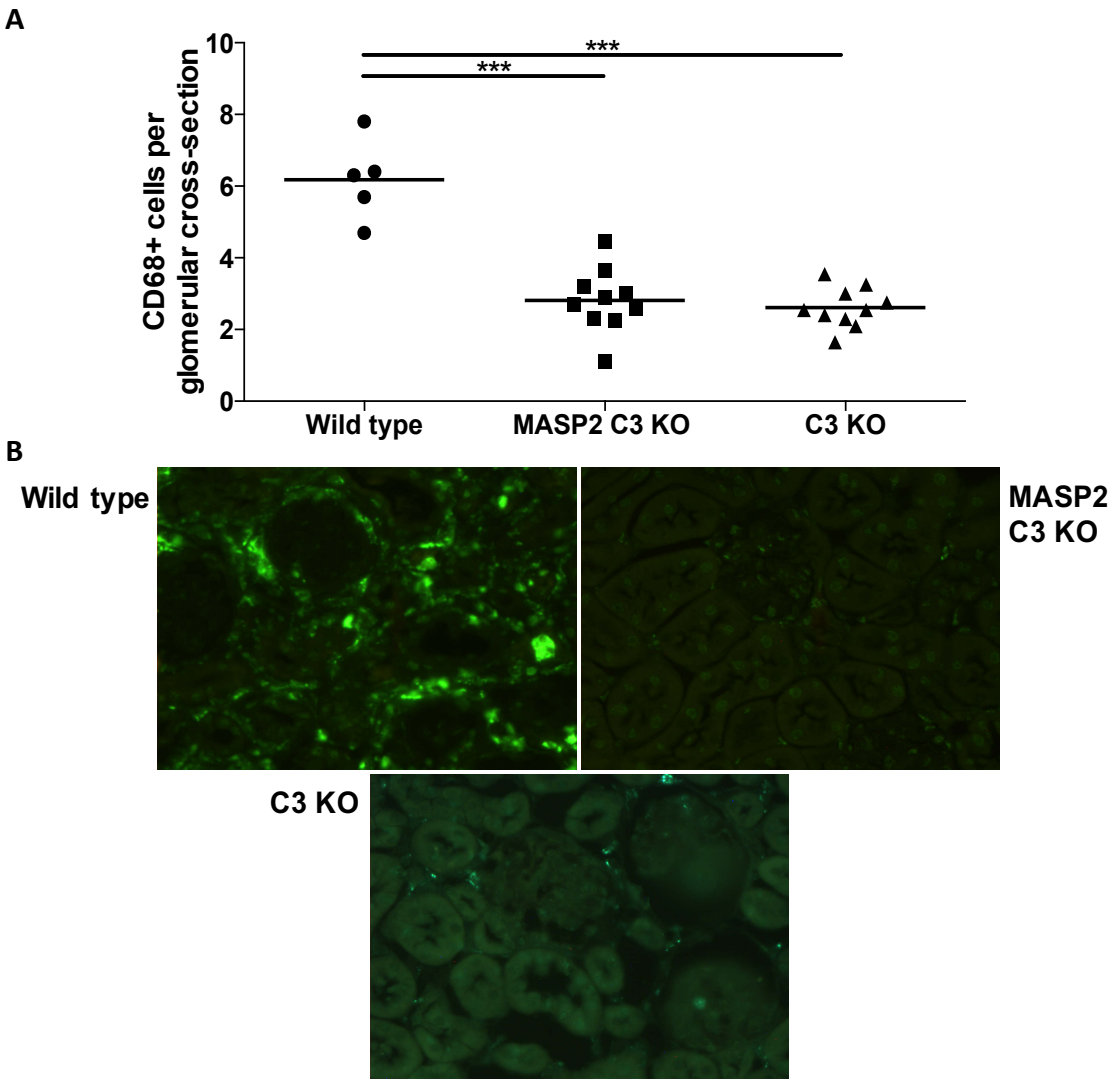

Figure 5.7 – Glomerular macrophage infiltration in wild type, MASP2/C3 double knockout and C3 knockout mice. A) Day 7 CD68 positive macrophage infiltration counts. Data were analysed using a one way ANOVA and a Tukey's multiple comparison post test (*** = $p < 0.001$). B) Representative immunofluorescence staining of CD68 positive macrophages in the three experimental groups (x400 magnification).

Similarly, when assessing the functional parameters, there was no difference between MASP2/C3 knockout and C3 knockout mice. We measured pre- and post-disease albumin creatinine ratios and serum creatinine levels as shown in figures 5.8 and 5.9 respectively. Haematuria was also assessed as shown in figure 5.10.

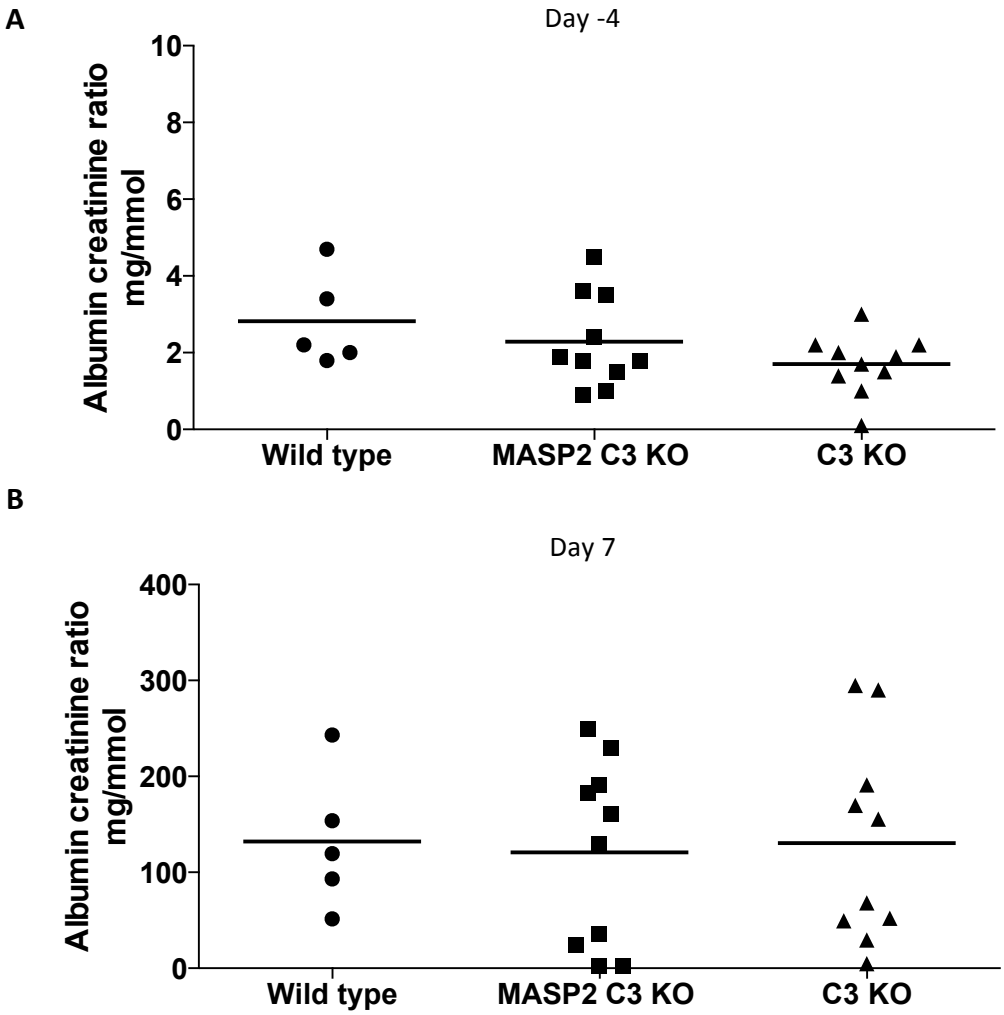

Figure 5.8 – Albumin creatinine ratio levels prior to and after disease induction. Albumin creatinine ratio measurements in the experimental groups of mice prior to disease induction on day -4 (A) and after disease induction on day 7 (B). Data were analysed by a one way ANOVA and a Tukey's multiple comparison post test.

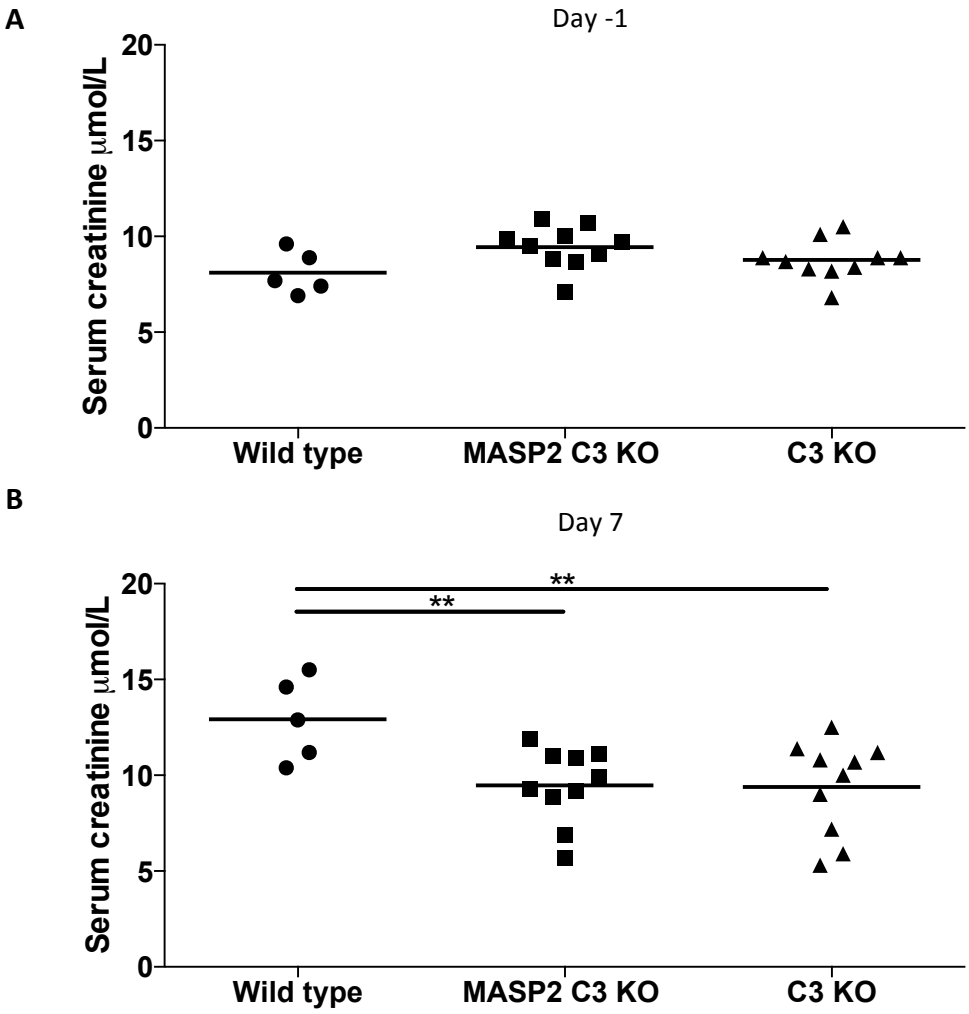

Figure 5.9 – Serum creatinine levels prior to and after disease induction. Serum creatinine measures at day -1 (A) and day 7 (B) in the three groups of mice. Data were analysed using a one way ANOVA and a Tukey's multiple comparison post test (** $p < 0.01$).

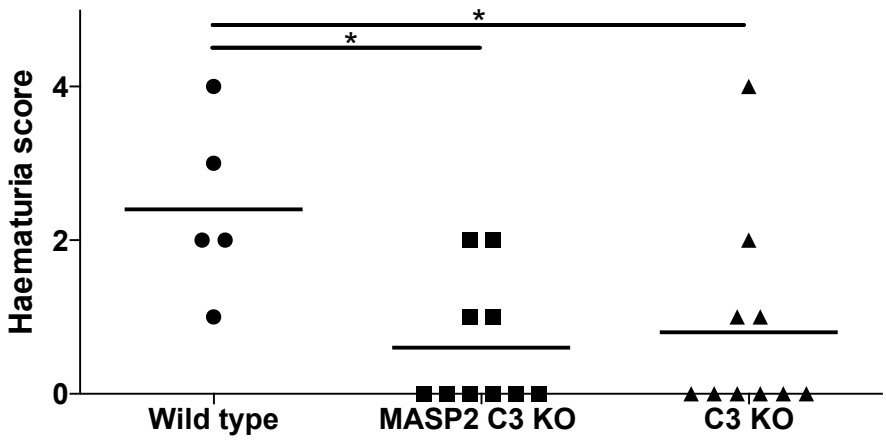

Figure 5.10 – Haematuria score at day 7 following disease induction in the three experimental groups. Haematuria was scored 0-4 on day 7. Data were analysed using a one way ANOVA and a Tukey's multiple comparison post test (* $p < 0.05$).

There was no difference between MASP2/C3 knockout mice and C3 knockout mice in any of the histological or functional parameters examined, and both had significantly less disease than wild type mice. This meant that we were unable to determine if the increase in disease in MASP2 deficient mice (compared to wild type mice) depended on C3 activation with this experiment. However, we found no difference in circulating C3 levels in untreated MASP2 deficient mice compared to wild type mice nor did we find a difference in glomerular C3 deposition in diseased MASP2 deficient mice compared to diseased wild type mice (figure 5.11). This suggested that there was no major deregulation of the alternative pathway of complement in MASP2 deficient mice.

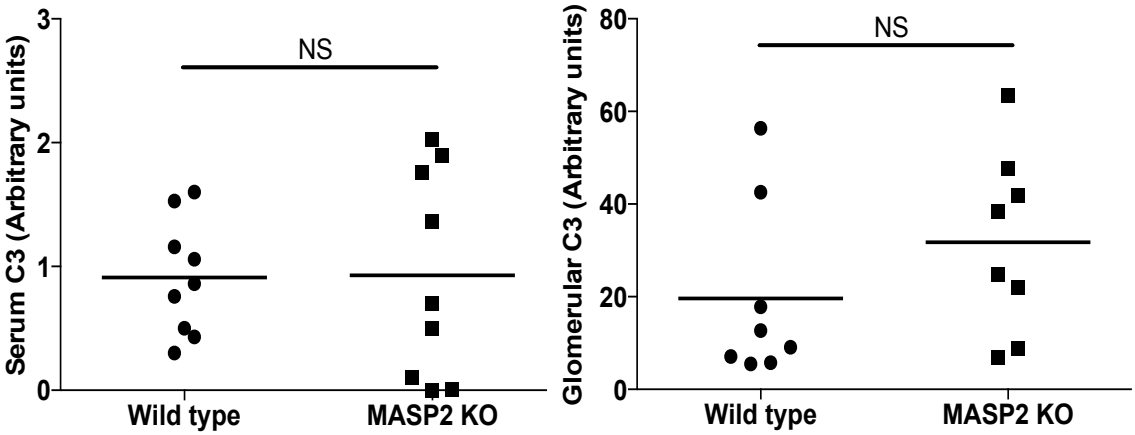

Figure 5.11 – Serum C3 and glomerular C3 deposition in wild type mice and MASP2 deficient mice. Serum C3 was measured in non-diseased animals. Data were analysed using a student's t test (NS = non significant).

We also demonstrated the presence of MBL in diseased glomeruli in both wild type mice and MASP2 deficient mice (figure 5.12 for representative immunofluorescence staining).

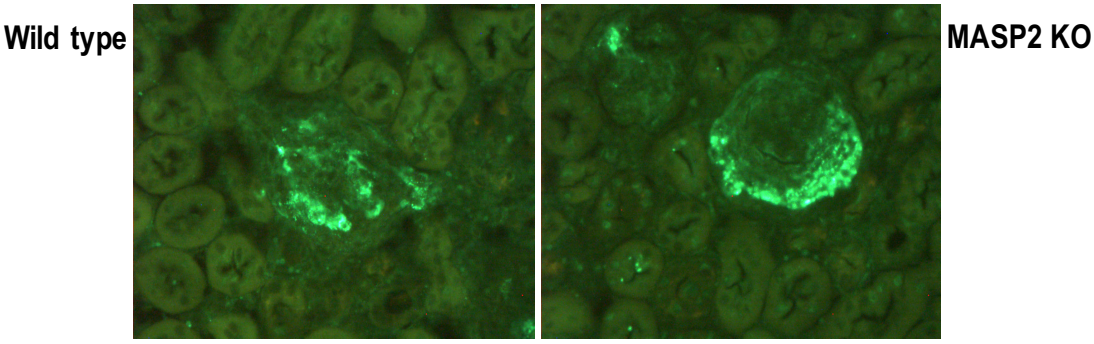

Figure 5.12 – Glomerular MBL deposition in wild type and MASP2 deficient mice. Day 7 representative immunofluorescence staining of MBL (x400 magnification).

5.5 Evidence for increased prothrombin activation in MASP2 deficient mice

Cross-talk between the complement and coagulation cascade has been well described in the literature (see section 1.10.8). MASP2 is able to cleave prothrombin to thrombin at the same site as factor Xa, though it is far less efficient, cleaving approximately 20% of prothrombin in comparison to factor Xa [197]. So under normal circumstances MASP2 may limit factor Xa mediated cleavage of prothrombin. In the absence of MASP2 there may be more factor Xa activity leading to increased thrombin generation and consumption with increased fibrin generation. Since fibrin generation is an essential feature of glomerular crescent formation, we wondered if the increased disease in MASP2 deficient mice might be explained by over-activation of the coagulation cascade. We measured prothrombin fragment 1.2, which is a breakdown product of prothrombin activation in the plasma of untreated MASP2 mice and wild type mice (figure 5.13).

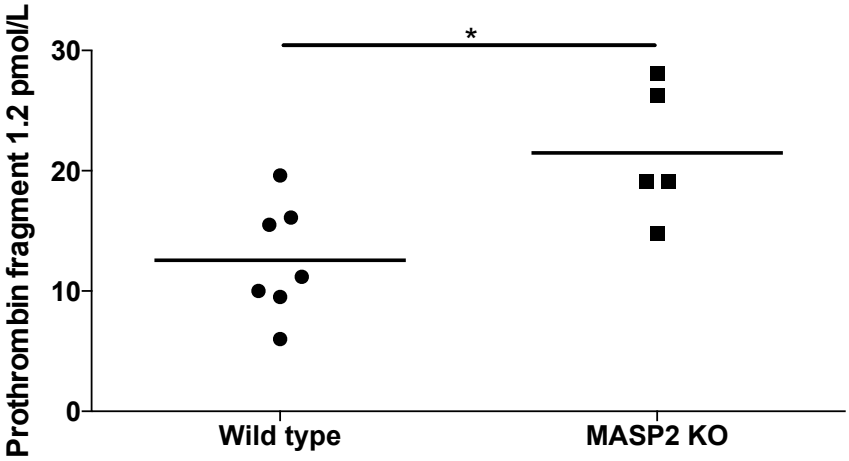

Figure 5.13 – Prothrombin fragment 1.2 levels in plasma of wild type and MASP2 knockout mice. Data were analysed using a student's t test (* = $p < 0.05$).

The prothrombin fragment 1.2 levels were elevated in MASP2 deficient mice compared to wild type mice suggesting increased prothrombin activation.

We then measured residual thrombin generation in the plasma of MASP2 deficient mice compared to wild type mice and figure 5.14 shows a typical trace (thrombogram) of thrombin generation over time in a wild type and MASP2 deficient mouse.

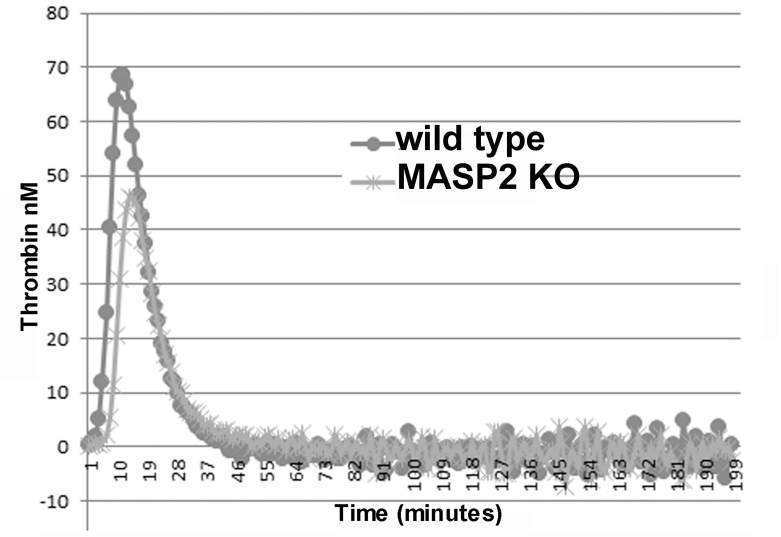

Figure 5.14 – Representative thrombin generation thrombogram from a wild type mouse and MASP2 knockout mouse over time.

The parameters when analysing thrombin generation include the lag time (time taken for thrombin concentration to reach 5nM), the endogenous thrombin potential (ETP, area under the curve of the thrombin generation curve), the time to peak thrombin generation and the ETP peak.

MASP2 deficient mice had an increase in the lag time and a decrease in the overall ETP as shown in figure 5.15. No significant difference in time to peak, peak thrombin generation (ETP peak) or fibrinogen concentration was seen, but these are crude tests compared to the sensitivity of prothrombin fragment 1.2.

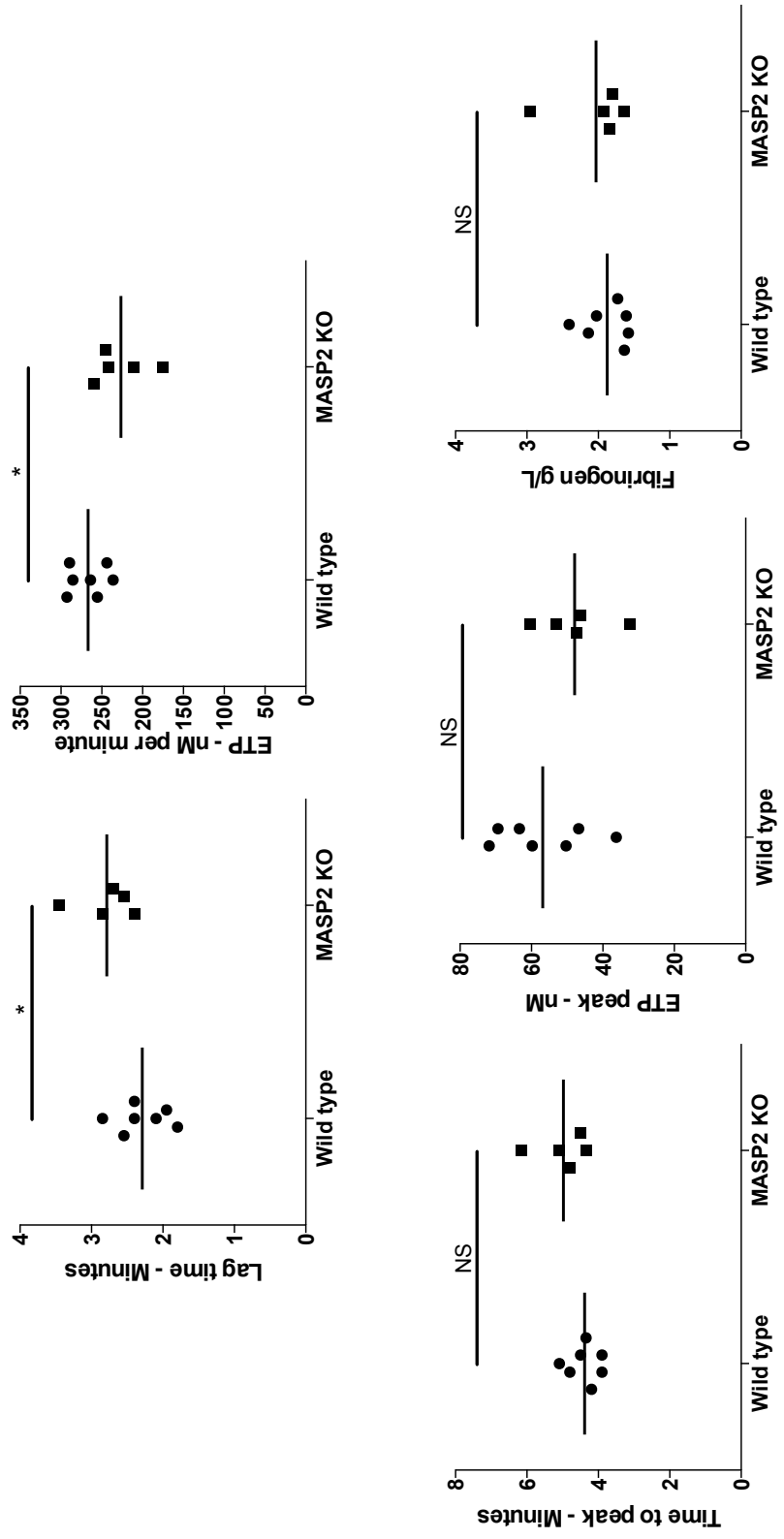

Figure 5.15 - Coagulation parameters in plasma from wild type or MASP2 deficient mice. Each graph represents the parameter indicated and each symbol represents plasma from a separate mouse. Data was analysed using a student's t test (* = $p < 0.05$, NS = non significant).

The decrease in ETP suggested a reduction in residual thrombin generation in plasma, due to consumption of prothrombin.

5.6 Factor B and C4 deficient mice are not protected in the passive transfer model

We had confirmed that complement was essential for disease in the passive transfer model as evidenced by our results in C3 deficient mice (section 5.4), but had also shown that the lectin pathway was not essential for this complement activation, nor was properdin, as surprisingly properdin knockout mice were not protected. In view of this, we revisited the role of the alternative pathway and classical pathway in this model by studying factor B deficient and C4 deficient mice. The experiments on factor B mice were performed with Dr Simon Freeley.

MPO-ANCA was generated from a group of MPO-deficient mice that had been immunised with 10µg MPO (RZ=0.55) as described in section 2.3.2 and 2.4.1.

There was no significant difference in the neutrophil counts on day -1 in peripheral blood between wild type and factor B deficient mice (mean neutrophil counts $X10^7$/ml in wild type mice 1.69±0.19, factor B deficient mice 1.79±0.17).

As shown in figure 5.16, the histological parameters of wild type and factor B deficient mice were not significantly different. Similarly, the functional parameters in terms of albumin creatinine ratio, haematuria and serum creatinine were not significantly different between the two groups (figure 5.17).

We used genomic DNA from the kidney tissue and re-confirmed that the factor B deficient mice were indeed factor B knockout mice. The genotyping experiments were performed by Dr Simon Freeley.

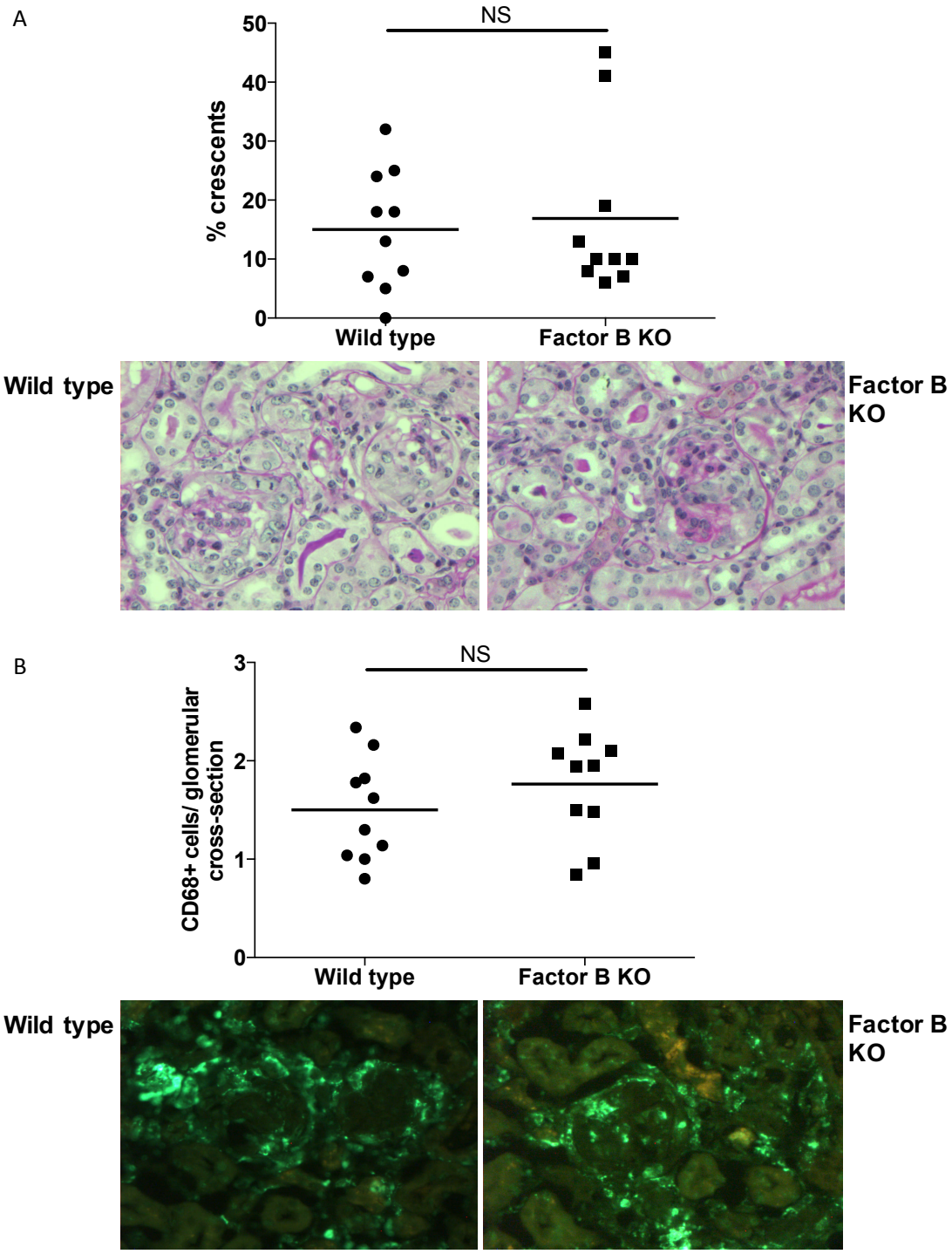

Figure 5.16 - Glomerular crescents (A) and macrophage infiltration (B) in wild type and factor B deficient mice. Graphical presentation of data with representative periodic acid schiff stain slides and CD68 immunofluorescence stains of glomerular sections in the two groups (x400 magnification). Data were analysed using a student's t test (NS = non significant).

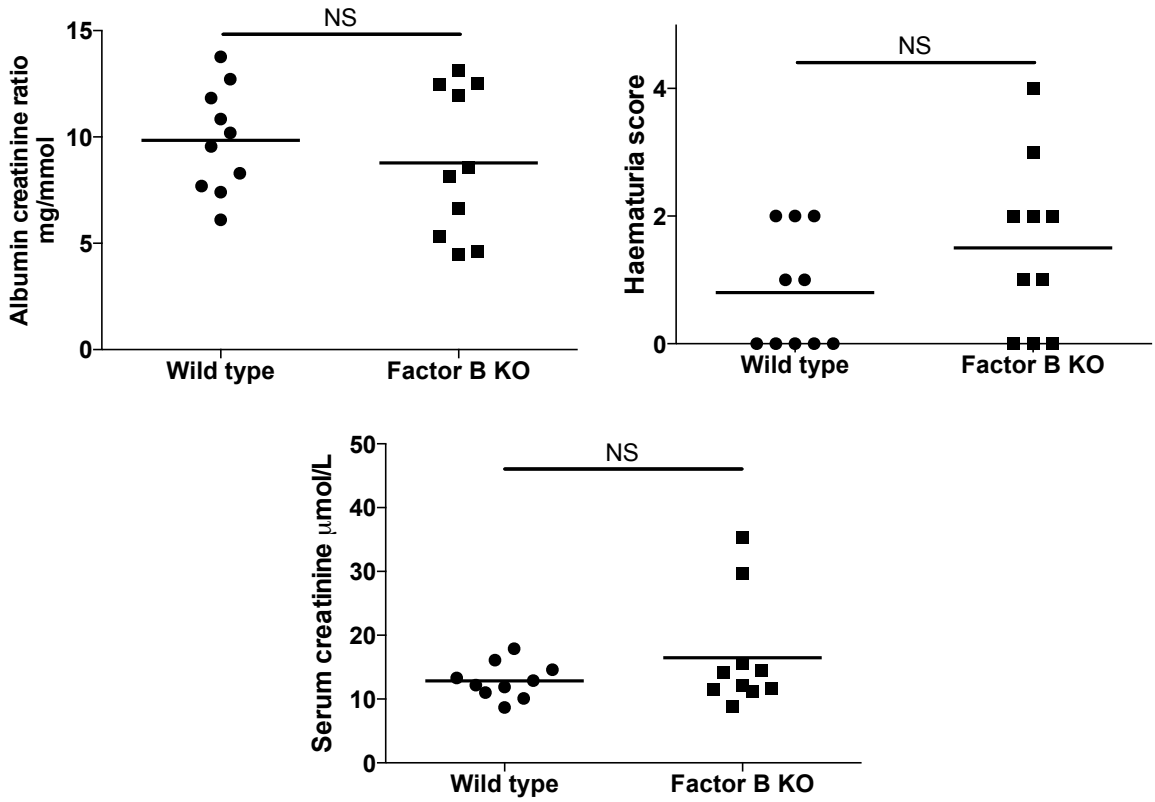

Figure 5.17 – Albumin creatinine ratio, haematuria score and serum creatinine in wild type and factor B deficient mice. Data were analysed using a student's t test (NS = non significant).

Our data in both properdin and factor B deficient mice therefore suggested that the alternative pathway was not essential for disease induction, in contrast to previous reports [207]. Since we had not shown a requirement for the alternative pathway, we decided to revisit the role of the classical pathway and compared wild type mice with C4 deficient mice.

There was no significant difference in the neutrophil counts on day -1 in peripheral blood between wild type and C4 deficient mice (mean neutrophil counts $X10^7$/ml in wild type mice 0.45±0.07, C4 deficient mice 0.46±0.05). As shown in figure 5.18, there was no significant difference in crescent counts or glomerular macrophage infiltration in C4 deficient mice and wild type mice. Similarly, there was no difference in the albumin creatinine ratio, haematuria score or serum creatinine between groups at day 7 (figure 5.19).

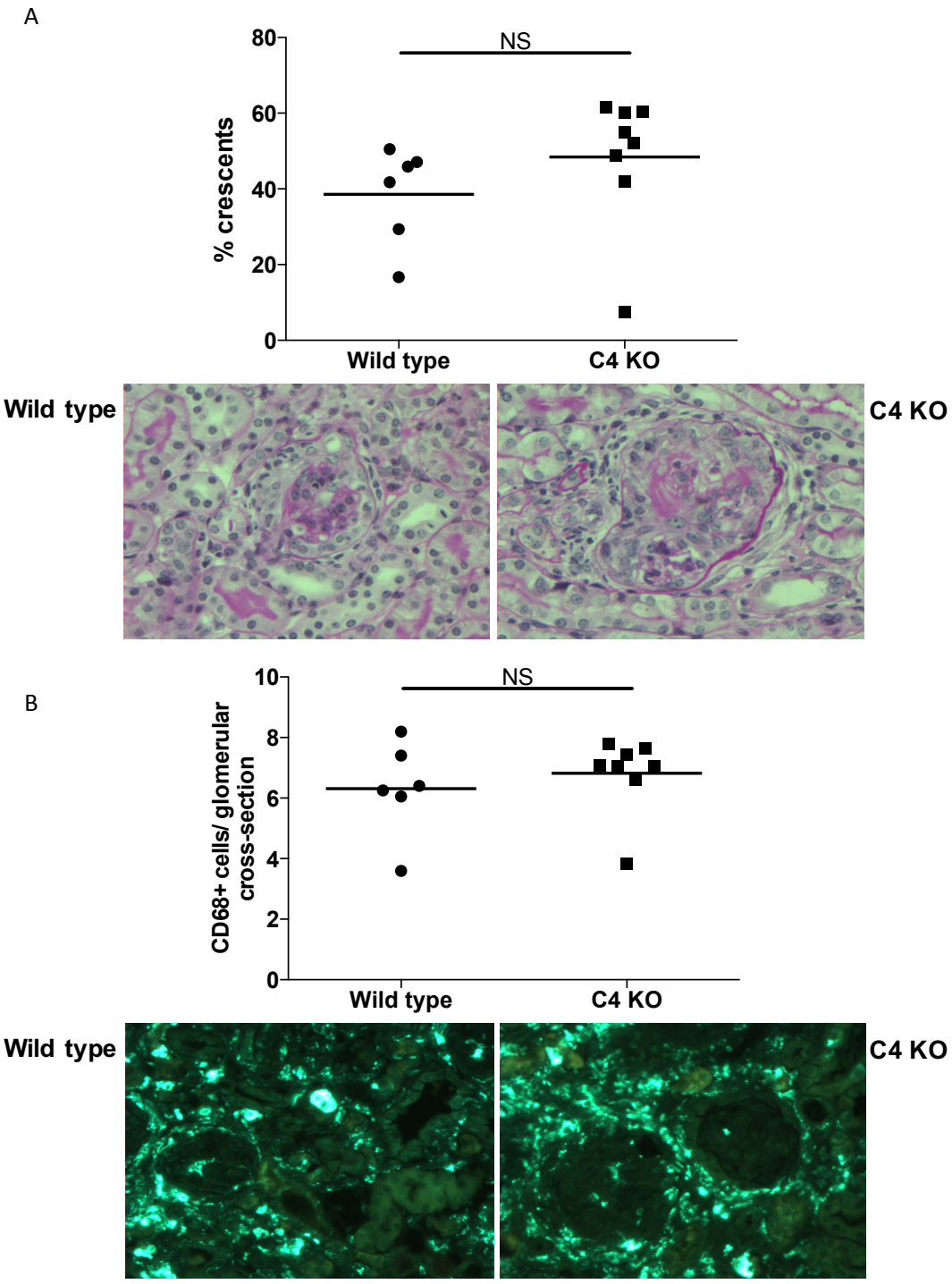

Figure 5.18 - Glomerular crescents (A) and macrophage infiltration (B) in wild type and C4 deficient mice. Graphical presentation of data with representative periodic acid schiff stain slides and CD68 immunofluorescence stains of glomerular sections in the two groups (x400 magnification). Data were analysed using a student's t test (NS = non significant).

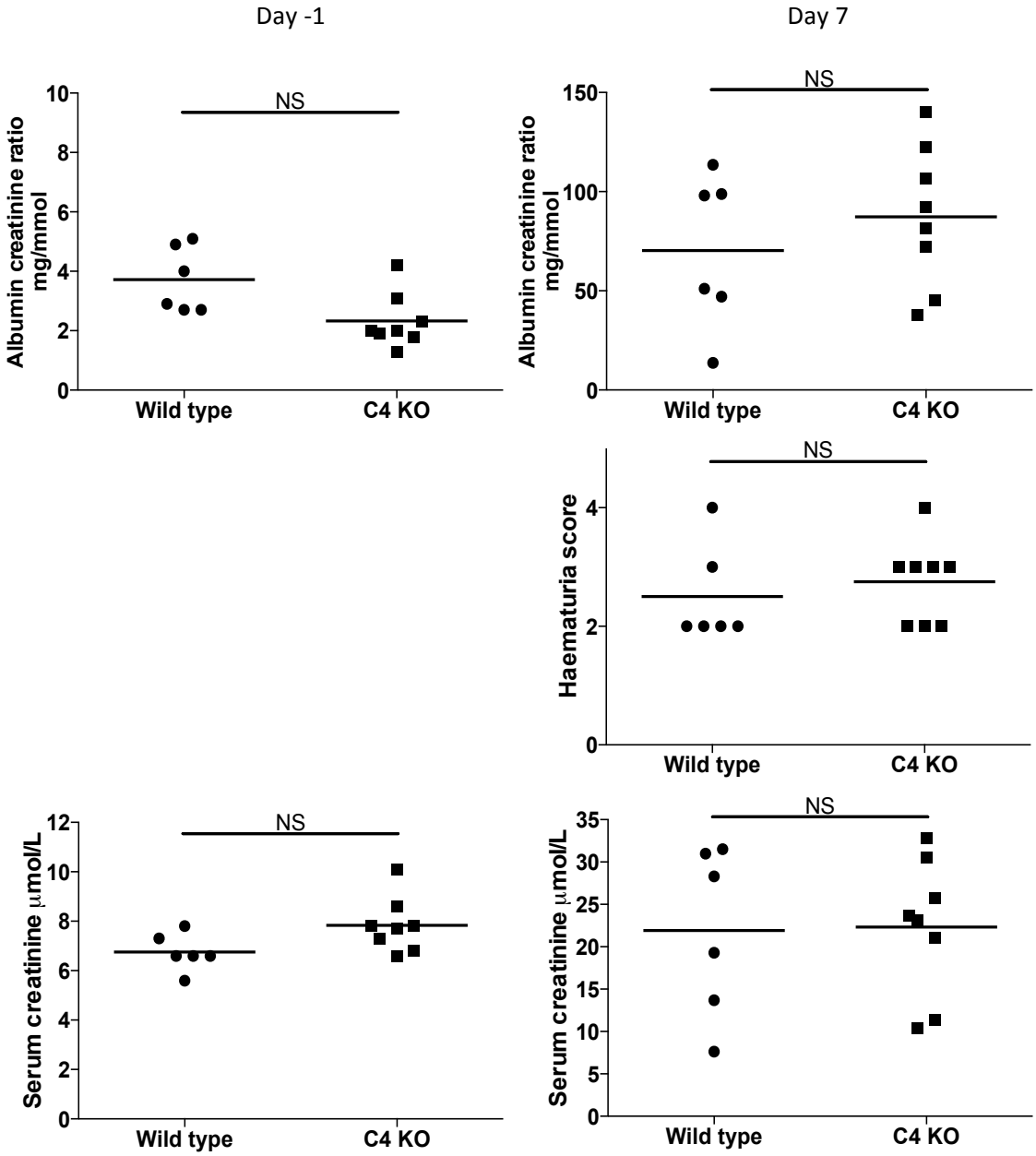

Figure 5.19 - Albumin creatinine ratio, haematuria score and serum creatinine in wild type and C4 deficient mice. The albumin creatinine ratio and serum creatinine were measured at baseline (day -1) and day 7. Data were analysed using a student's t test (NS = non significant).

Overall, we have shown that despite a requirement for C3 (section 5.4), there was no absolute requirement for properdin (previous work), factor B or C4 (section 5.6) in the passive transfer model of MPO-ANCA vasculitis. This suggests a possible redundancy in the complement pathway when utilising knockout mice.

5.7 Circulating and not bone marrow derived C5 mediates disease

We had shown in section 3.5 that neutrophils are capable of expressing C3 and C5 as well as the respective anaphylatoxins. Other leucocytes including T cells, B cells, monocytes and macrophages have also been shown to express C3 and C5 [187]. As discussed, locally derived complement may have distinct functions compared to systemically generated complement and this has not been explored in the context of AAV. We next examined if leucocyte derived complement was important in pathogenesis and constructed four groups of bone marrow chimeric mice from wild type or C5 deficient donors and recipients as described in section 2.3.3, and induced MPO-ANCA vasculitis using the passive transfer model (see section 2.3.5). MPO-ANCA was generated from a group of MPO-deficient mice that had been immunised with 10μg MPO (RZ=0.69) as described in section 2.3.2 and 2.4.1.

A parallel cohort of chimeras were also made between wild type C57BL/6 mice and C57BL/6 mice congenic for CD45.1 (B6.SJL-*Ptprc*^{a} *Pepc*^{b}/BoyJ). Chimerism was determined by flow cytometry for CD45.2 and was >90% in all cases (n=7).

There was no significant difference in the neutrophil counts on day -1 in peripheral blood between mice in the four groups (mean neutrophil counts X10^{7}/ml in wild type recipients with wild type donor bone marrow 1.62±0.11, wild type recipients with C5 deficient donor bone marrow 1.75±0.07, C5 deficient recipients with wild type donor bone marrow 1.86±0.06 and C5 deficient recipients with C5 deficient donor bone marrow 1.96±0.1).

Histological measures of disease showed crescentic glomerulonephritis was more severe in both groups of C5 sufficient recipients compared to both groups of C5 deficient recipients, as indicated by more crescents and CD68+ macrophage infiltration within glomeruli (figures 5.20 and 5.21).

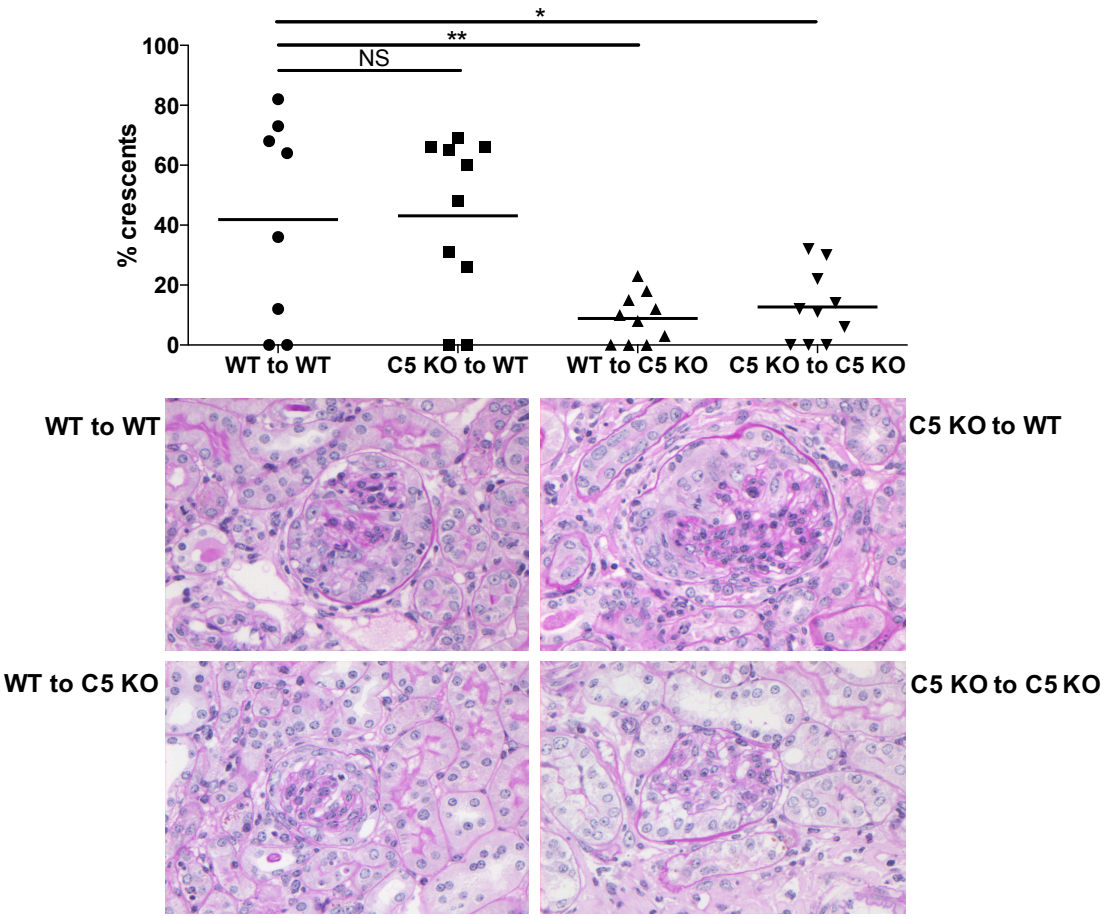

Figure 5.20 - Glomerular crescent formation following passive transfer of MPO-ANCA in the bone marrow chmeric mice. Graph depicting day 7 glomerular crescent counts in the four experimental groups of mice. C5 KO to WT depicts wild type mice that received C5 deficient bone marrow; WT to C5 KO depicts C5 deficient mice that received wild type bone marrow. Each symbol is data from a separate mouse. Data were analysed using one way ANOVA and a Tukey's multiple comparison post test (** = $p < 0.01$, * = $p < 0.05$, NS = non significant). Associated representative periodic acid schiff stain slides of glomerular sections on day 7 of the passive transfer model in each experimental group (light microscopy x400 magnification).

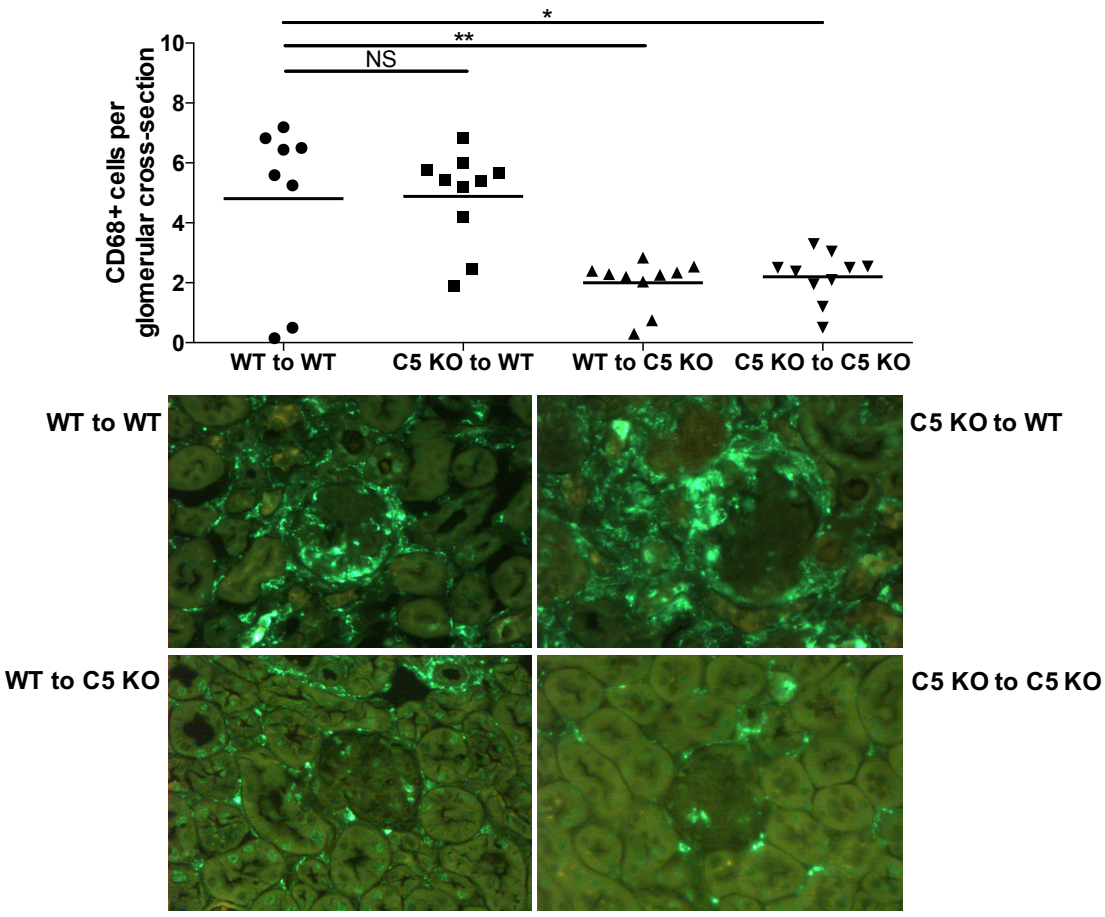

Figure 5.21 - Glomerular macrophage infiltration following passive transfer of MPO-ANCA in the bone marrow chmeric mice. Graph depicting day 7 glomerular CD68+ cell infiltration in the four experimental groups of mice. C5 KO to WT depicts wild type mice that received C5 deficient bone marrow; WT to C5 KO depicts C5 deficient mice that received wild type bone marrow. Each symbol is data from a separate mouse. Data were analysed using a one way ANOVA and a Tukey's multiple comparison post test (** = $p < 0.01$, * = $p < 0.05$, NS = non significant). Associated representative CD68 immunofluorescence stains of glomerular sections on day 7 of the passive transfer model in each experimental group (x400 magnification).

There were no differences in baseline urine albumin creatinine ratio (figure 5.22) or serum creatinine (figure 5.23). At day 7, serum creatinine was higher in both groups of C5 sufficient recipients, compared to both groups of C5 deficient recipients. The presence or absence of C5 in the bone marrow compartment again had no effect (figure 5.23). Wild type mice receiving C5 deficient bone marrow had more haematuria and a higher albumin creatinine ratio than both C5 deficient recipient groups (figure 5.22).

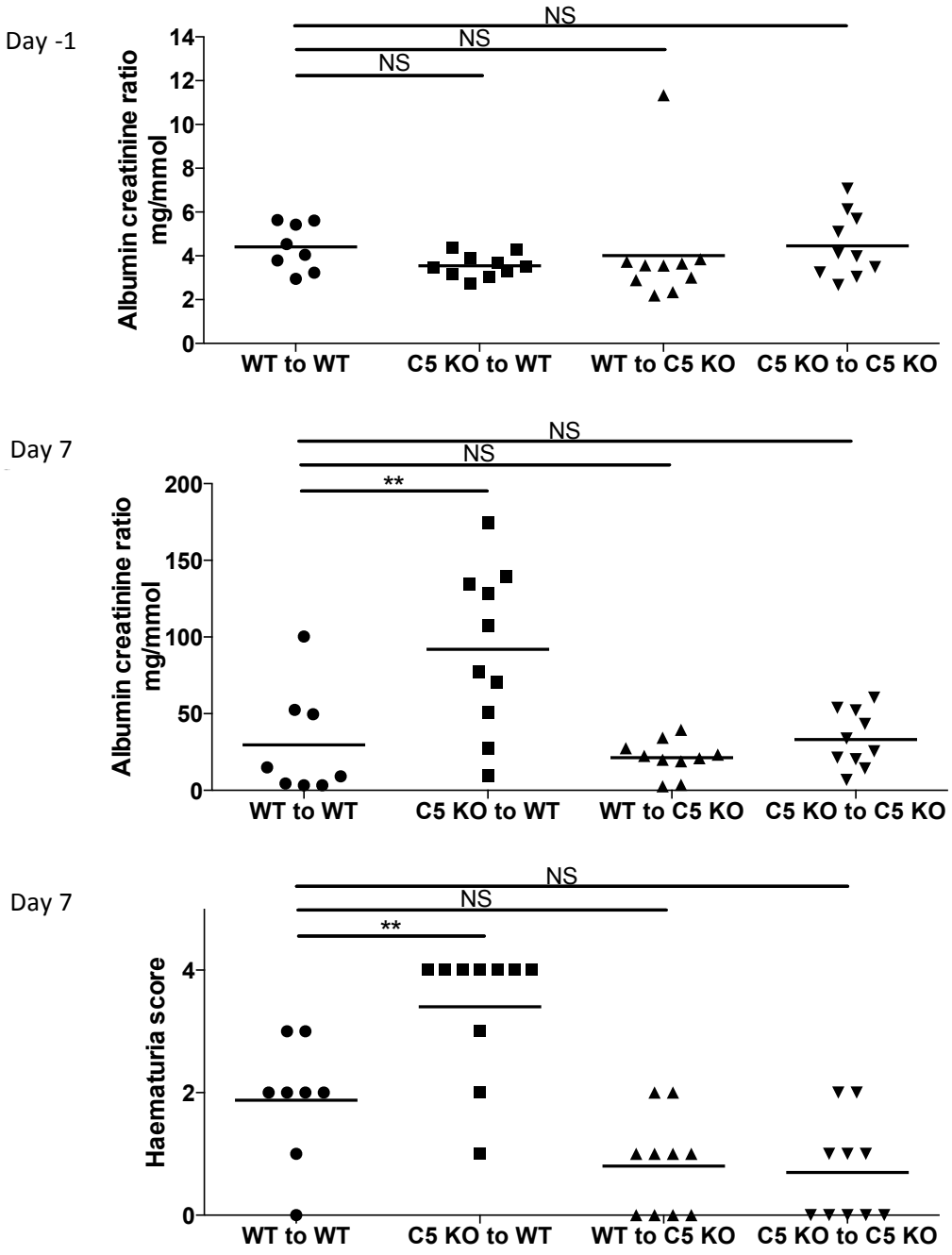

Figure 5.22 - Albumin creatinine ratio and haematuria score in the bone marrow chimeric mice. The albumin creatinine ratio was measured at baseline (day -1) and day 7, whilst the haematuria score for day 7 is shown. Data were analysed using a one way ANOVA and a Tukey's multiple comparison post test (** = $p < 0.01$, NS = non significant).

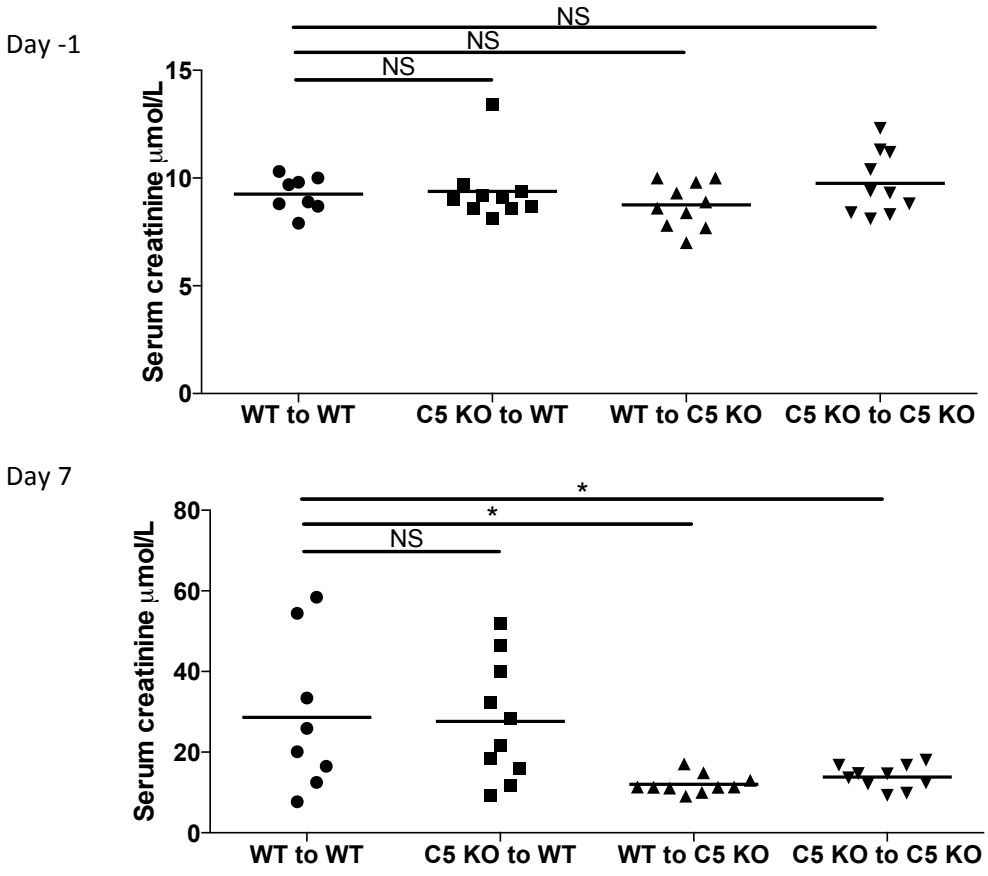

Figure 5.23 – Baseline and day 7 serum creatinine measures in the bone marrow chimeric mice. Data were analysed using a one way ANOVA and a Tukey's multiple comparison post test (* = $p < 0.05$, NS = non significant).

These results show that C5 within the bone marrow-derived cells is not important in pathogenesis and that systemic C5 from the liver or other cells is required for disease.

5.8 Discussion

We had previously shown that GCSF levels were raised in serum samples of patients with active AAV compared to healthy age matched controls. GCSF was also shown to prime human neutrophils to the response of MPO-ANCA. *In vivo*, GCSF in the presence of LPS administration exacerbated disease in the passive transfer model and interestingly led to an increase in serum creatinine, few studies have shown a difference in serum creatinine [119]. This suggested the importance of the role of GCSF in pathogenesis. As part of the current thesis we tested the effect of GCSF alone in the absence of concurrent LPS administration. We showed that both LPS and GCSF are

required to exacerbate disease in the passive transfer model of vasculitis, suggesting GCSF acts synergistically with LPS. We also show that GCSF is necessary together with LPS to produce a robust model of disease.

We have made a number of observations in this model that are of clinical relevance, given the current interest in targeting complement in patients with AAV. Of note, none of our results were influenced by differences between mouse strains or circulating neutrophil counts in responses to GCSF. Firstly, the protective role of C3 deficiency has not previously been reported in this model. Here we have shown for the first time that C3 deficient mice are protected. It is important to note that we have confirmed that complement is important in this model in our laboratory, given the lack of protection we have previously seen in properdin deficient and MASP2 deficient mice (Simon Freeley, The role of complement and GCSF in ANCA associated vasculitis, PhD Thesis 2013, King's College London).

Disease in MASP2 deficient mice was increased compared to wild type mice in previous studies performed within our laboratory (Simon Freeley, The role of complement and GCSF in ANCA associated vasculitis, PhD Thesis 2013, King's College London). We wondered if the increased disease required complement activation. MASP1 has been shown to activate factor D and MASP3 can activate both factor B and factor D [300, 301]. Therefore the absence of MASP2 could result in an increase in circulating MASP1 and MASP3, which could potentially enhance alternative pathway activation and lead to worsening disease. Our results in mice deficient in both MASP2 and C3 were not conclusive. However, the similarity in levels of circulating and deposited C3 in wild type and MASP2 deficient mice suggested that the increased disease in MASP2 deficient mice was not due to increased complement activation.

We therefore sought an alternative explanation for the increased crescent formation in MASP2 deficient mice, and wondered if cross talk with the coagulation pathway could be involved. A link between coagulation and crescentic glomerulonephritis is well established. Fibrin deposition, initiated physiologically by tissue factor, promotes disease [302]. We confirmed that MBL is deposited in glomeruli of mice with crescentic glomerulonephritis due to MPO-ANCA as this would be a requirement for an effect on glomerular fibrin formation.

Activation of either the intrinsic or extrinsic pathways of the coagulation cascade leads to the formation of a prothrombinase complex composed of factors Va and Xa, which cleave prothrombin to thrombin. Thrombin then activates fibrinogen leading to the deposition of cross-linked fibrin. As discussed, cleavage of prothrombin by MASP2 has been shown to occur at the same molecular site as a factor Xa but in a far less efficient manner [197]. Our data show evidence of increased prothrombin activation in MASP2 deficient mice compared to wild type mice. Therefore a plausible explanation for the increase in crescentic glomerulonephritis seen in MASP2 deficient mice is their tendency to enhanced fibrin generation. The molecular basis for the increased prothrombin activation we observed is unclear.

We have also shown that there was no absolute requirement for properdin (previous work), factor B or C4 in the passive transfer model of MPO-ANCA vasculitis. The most plausible explanation may be that both the alternative and the classical pathway are required, but the absence of either pathway on its own may offer only insufficient protection due to their redundancy. The presence of an intact classical or alternative pathway alone may be sufficient to cause C3 activation. An alternative explanation is that both C3 and C5 are activated independently of C4 or factor B.

It is not clear why our data differ from a previous report showing a requirement for factor B in the development of MPO-ANCA vasculitis using the passive transfer model [207]. The factor B knockout mice used in our data and the published data are from the same group (Colten *et al*). Our model has some differences to the other published passive transfer models, including the use of LPS and GCSF and this is a possible factor. Another variable to consider is the nature of the MPO-ANCA IgG used to induce disease. As discussed above, both the alternative and classical pathway may be involved with neither alone being essential for disease. If this was the case, then the relative ability of specific MPO-ANCA IgG preparations to activate the classical pathway may be important. If an antibody preparation activates the classical pathway weakly, then disease may be more strongly reliant on the alternative pathway activation and as a result factor B deficient mice may be protected. One way of addressing this may be to compare disease in factor B C4 double deficient mice compared to factor B knockout mice.

Circulating complement components are derived primarily from the liver, but it has recently become clear that complement proteins are found not only in serum and plasma but also within leukocytes [187, 210]. More recent data has shown that resting human CD4 T cells contain intracellular stores of C3 and that the protease cathepsin L cleaves C3 into C3a and C3b with important roles described for T cell function and homeostasis [188, 191]. However, despite these developments highlighting the role of complement components within leukocytes, our data show that activation of C5 from other sources is important in AAV. Since synthesis of C5 from murine or human renal cells has not been described, our results most likely reflect a role for circulating C5. Based on our data, an alternative therapeutic approach to C5a receptor blockade would be to prevent C5 secretion by the liver. This would not interfere with the important homeostatic interactions between leukocyte-derived C5a and C5a receptors that may be affected by generic C5a receptor blockade. Such an approach has been developed using N-acetylgalactosamine-conjugated siRNA to target the hepatocyte asialoglycoprotein receptor. A phase 1/2 clinical trial in patients with paroxysmal nocturnal haemaglobinuria is underway (NCT02352493).

Chapter 6 – Conclusion

6.1 Summary of results

Chapter 3

We set up various methods of assessing neutrophil activation in our laboratory including two readouts of respiratory burst (DHR123 assay and the luminometer assay) and four readouts of degranulation (lactoferrin ELISA, MPO assay, CD66b and CD11b expression).

This chapter was divided into two sections. Firstly, using randomly selected twenty polyclonal patient samples (11 MPO-ANCA and 9 PR3-ANCA) and ten control IgG fractions from healthy donors, we found no significant difference in respiratory burst output or degranulation of TNFα primed human neutrophils from two separate donors. Polyclonal mouse MPO-ANCA did not consistently cause a significant rise in ROS production either as measured by the luminometer assay in comparison to polyclonal control IgG.

As detailed in section 3.6, there are various studies using limited numbers of patient derived ANCA and control IgG from healthy donors that show ANCA activate neutrophils *in vitro*. Where large selections of ANCA and control IgG samples were used in multiple donors there are inconsistencies in the ability of ANCA to stimulate TNFα primed neutrophils to undergo respiratory burst or degranulation, validating our results [95, 256].

As discussed in section 3.6, various other factors may also compound the inconsistent data. The use of non-affinity purified ANCA means the precise concentration of MPO-ANCA and PR3-ANCA in each antibody preparation is unknown. The subclass of IgG in the polyclonal samples are also variable. Furthermore, the expression of MPO and PR3 on the neutrophil surface in response to TNFα priming in different donors (not assessed in our studies) may vary and hence the exposure of ANCA to the antigen will vary. Lastly the ANCA samples vary in epitope specificity and affinity. These variable factors may explain the differential response noted in studies.

It is also important to note that the simplified *in vitro* studies carried out do not accurately reflect *in vivo* mechanisms. Isolating neutrophils from peripheral blood and treating them with TNFα and polyclonal ANCA in isolation, without the neighbouring cells they interact with nor the systemic / local milieu of proteins such as cytokines, chemokines and complement components does not reflect the accurate events *in vivo*.

The second part of this chapter suggests that neutrophils are capable of expressing C3 and C5 as well as their respective anaphylatoxins as shown by FACS studies. The expression of these complement components was not altered by polyclonal or monoclonal ANCA nor fMLP induced activation either within the intracellular compartment or on the cell surface. However, we showed that TNFα primed neutrophils when stimulated by ANCA had higher concentrations of C5a in the supernatant than TNFα primed neutrophils incubated with control IgG. The results for C3a generation were not consistent between two donors. It is a possibility that ANCA alter the processing of C5 into its anaphylatoxin in neutrophils. This may occur through conventional convertases or local proteases within the neutrophils themselves. However, we need to assess these findings further using other techniques including RT-qPCR and confocal microscopy.

Chapter 4

In chapter 4 we set up and used various *in vitro* techniques to assess the impact of ANCA on monocyte function and macrophage development. We used the same ANCA and control IgG isolated in chapter 3 to show consistent effects. We showed that polyclonal MPO-ANCA consistently reduced IL6 and IL10 production from monocytes isolated from three healthy donors in response to LPS. This effect was dependent on the Fc portion of MPO-ANCA and it appears the enzymatic activity of MPO itself. Using gene expression microarrays we showed that MPO-ANCA profoundly inhibits TLR4 mediated signalling. A possible mechanism for the TLR4 inhibition was identified using mass spectrometry. Analysis of phospholipids extracted from LPS stimulated monocytes that had been incubated with MPO-ANCA showed a significantly increased abundance of a phosphatidylcholine species at m/z 828.8 that was tentatively identified as PEIPC, which has been shown to inhibit LPS induced pro-inflammatory effects [279].

Interestingly, we demonstrated that MPO-ANCA increases survival and differentiation of monocytes into macrophages with an M2-like phenotype in culture as well as increasing CSF1 production. The monocytes incubated with MPO-ANCA developed macrophages with increased CD206 and reduced CD80 expression and secreted higher levels of TGFβ than those incubated with control IgG in keeping with an M2-like macrophage phenotype. Functionally the supernatant of the macrophages acquired from exposure to MPO-ANCA promote CD4 T cells to develop a more regulatory phenotype by inducing a higher IL10 / IFNγ ratio and more TGFβ production compared to controls. These results suggest that MPO-ANCA may well promote the development of a milieu that could potentially promote fibrosis and chronicity in AAV possibly in an attempt to dampen down inflammation.

However, as discussed earlier, interpreting and correlating data from *in vitro* studies into *in vivo* events should be done with the knowledge that there are many confounding factors that are not taken into account whilst performing the *in vitro* studies.

Chapter 5

The final results chapter confirmed the fact that GCSF acts synergistically with LPS to produce a robust model of disease using the passive antibody transfer technique. Both GCSF and LPS are required to induce sufficient disease that would allow comparison across different mouse genotypes as well as identify any potential differences using therapeutic agents. Of note our passive transfer model varies from the published literature as we find that the use of GCSF and LPS (rather than LPS alone) with MPO-ANCA is necessary to induce robust disease. This difference in disease model induction may account for some of the key differences we present compared to the published literature.

In this chapter, we confirmed that complement is crucial to pathogenesis as we showed that C3 knockout mice were protected from disease development.

We had previously shown that MASP2 deficiency surprisingly exacerbated disease and we sought to define possible explanations for this observation. We compared disease

in mice deficient in both MASP2 and C3 with C3 deficient mice to ascertain if this effect was complement dependent, but we were unable to draw any conclusions as in both groups there was very mild disease. However, in MASP2 deficient mice serum C3 levels and glomerular C3 deposition was similar to that in wild type mice suggesting that the exacerbation in disease was not necessarily complement dependent. We showed evidence of cross talk between the complement pathway and coagulation pathway with increased prothrombin activation in MASP2 deficient mice compared to wild type mice. This may be a contributing factor to disease in MASP2 deficient mice.

In this chapter we also suggest that there is a redundancy between the initiating pathways of complement activation as properdin (previous work), factor B or C4 deficient mice are not protected from disease in the passive transfer model. Lastly we show that circulating complement component C5 as opposed to leucocyte derived C5 is important in AAV pathogenesis. This suggests that more directed therapy targeting C5 secretion from the liver may be more beneficial and would limit the effect on local homeostatic functions of C5.

6.2 Limitations

Our data does not necessarily suggest that ANCA are not pathogenic nor does it undermine the role of neutrophils in pathogenesis, but it does highlight the inconsistencies of using limited numbers of samples and the need for more robust *in vitro* measures of the effect of ANCA. Extrapolating data from *in vitro* studies have to be done so with caution, as they may not necessarily convey the mechanisms that occur *in vivo*. Neutrophils *in vivo* will interact with various other cells including endothelial cells, which may be crucial to pathogenesis. Another factor that must be considered is the use of whole non-affinity purified IgG fractions in these assays means that the percentage of MPO-ANCA or PR3-ANCA in the samples is unknown. Hence, it is possible that strong neutrophil responses were not achieved with the ANCA samples simply because they are composed of low proportions of PR3-ANCA or MPO-ANCA IgG versus other contaminating IgG. The ANCA present within samples will also vary in epitope specificity and affinity, which may account for differences in neutrophil activation as suggested by Roth *et al* [94]. Another possibility is that ANCA's role in

AAV pathogenesis is not mediated through neutrophil respiratory burst or degranulation, but through differing mechanisms including a possible role on processing of complement components as well as the effects on monocyte and macrophage function.

The *in vitro* studies of the impact of ANCA on monocytes need further characterisation with *in vivo* work in murine models. This will clarify the potential clinical importance of the effects noted.

6.3 Future work

We have reported various important and novel discoveries in the last three chapters of this thesis. Results arising from this work provide other avenues of research that need to be pursued.

As discussed the use of affinity purified ANCA in neutrophil and monocyte assays would provide more controlled conditions, as we would have ANCA of known concentration and specificity. To mimic *in vivo* conditions activation conditions, endothelial cell and neutrophil co-cultures could be used.

We have shown that MPO-ANCA increase TGFβ secretion from macrophages as well as CD4 T cells and this may promote fibrosis. A wound healing assay can be utilised to demonstrate this. The migration of cells such as fibroblasts can be monitored using time lapse imaging in the presence of treated macrophage or CD4 T cell supernatants.

To ascertain a role for monocytes and macrophages in AAV pathogenesis, various methods of blocking monocyte recruitment and depleting macrophages can be used *in vivo*. A CCR2 (MCP-1 receptor) inhibitor or CCR2 deficient mice can be utilised [269]. Liposomal clodronate can be administered systemically or locally. Liposomal clodronate is ingested by and accumulates in macrophages, resulting in cell apoptosis thereby depleting macrophages in various tissues [303]. Another technique involves the use of conditional macrophage ablation transgenic mice, based upon CD11b promoter mediated expression of the human diphtheria toxin receptor [304]. A CSF1

receptor inhibitor can also be utilised to demonstrate the role of ANCA on monocytes and macrophages *in vivo*.

These experiments would further enhance our understanding of AAV pathogenesis.

References

1. Jennette, J.C., *Overview of the 2012 revised International Chapel Hill Consensus Conference nomenclature of vasculitides.* Clin Exp Nephrol, 2013. **17**(5): p. 603-6.
2. Haas, M. and J.A. Eustace, *Immune complex deposits in ANCA-associated crescentic glomerulonephritis: a study of 126 cases.* Kidney Int, 2004. **65**(6): p. 2145-52.
3. Weidner, S., et al., *Histologic analysis of renal leukocyte infiltration in antineutrophil cytoplasmic antibody-associated vasculitis: importance of monocyte and neutrophil infiltration in tissue damage.* Arthritis Rheum, 2004. **50**(11): p. 3651-7.
4. Mukhtyar, C., et al., *Modification and validation of the Birmingham Vasculitis Activity Score (version 3).* Ann Rheum Dis, 2009. **68**(12): p. 1827-32.
5. Seo, P., et al., *The future of damage assessment in vasculitis.* J Rheumatol, 2007. **34**(6): p. 1357-71.
6. Watts, R.A., et al., *The contrasting epidemiology of granulomatosis with polyangiitis (Wegener's) and microscopic polyangiitis.* Rheumatology (Oxford), 2012. **51**(5): p. 926-31.
7. Fujimoto, S., et al., *Comparison of the epidemiology of anti-neutrophil cytoplasmic antibody-associated vasculitis between Japan and the U.K.* Rheumatology (Oxford), 2011. **50**(10): p. 1916-20.
8. Hagen, E.C., et al., *Diagnostic value of standardized assays for anti-neutrophil cytoplasmic antibodies in idiopathic systemic vasculitis. EC/BCR Project for ANCA Assay Standardization.* Kidney Int, 1998. **53**(3): p. 743-53.
9. Walton EW, *Giant-cell granuloma of the respiratory tract (Wegener's granulomatosis).* Br Med J, 1958. **5091**: p. 265-70.
10. Mukhtyar, C., et al., *Outcomes from studies of antineutrophil cytoplasm antibody associated vasculitis: a systematic review by the European League Against Rheumatism systemic vasculitis task force.* Ann Rheum Dis, 2008. **67**(7): p. 1004-10.
11. Sriskandarajah, S., et al., *Improved prognosis in Norwegian patients with glomerulonephritis associated with anti-neutrophil cytoplasmic antibodies.* Nephrol Dial Transplant, 2015. **30 Suppl 1**: p. i67-75.
12. Lai, Q.Y., et al., *Predictors for mortality in patients with antineutrophil cytoplasmic autoantibody-associated vasculitis: a study of 398 Chinese patients.* J Rheumatol, 2014. **41**(9): p. 1849-55.
13. Lee, T., et al., *Predictors of treatment outcomes in ANCA-associated vasculitis with severe kidney failure.* Clin J Am Soc Nephrol, 2014. **9**(5): p. 905-13.
14. de Joode, A.A., J.S. Sanders, and C.A. Stegeman, *Renal survival in proteinase 3 and myeloperoxidase ANCA-associated systemic vasculitis.* Clin J Am Soc Nephrol, 2013. **8**(10): p. 1709-17.
15. Flossmann, O., et al., *Long-term patient survival in ANCA-associated vasculitis.* Ann Rheum Dis, 2011. **70**(3): p. 488-94.
16. Hilhorst, M., et al., *Improved outcome in anti-neutrophil cytoplasmic antibody (ANCA)-associated glomerulonephritis: a 30-year follow-up study.* Nephrol Dial Transplant, 2013. **28**(2): p. 373-9.
17. Little, M.A., et al., *Early mortality in systemic vasculitis: relative contribution of adverse events and active vasculitis.* Ann Rheum Dis, 2010. **69**(6): p. 1036-43.
18. Nuyts, G.D., et al., *Wegener granulomatosis is associated to exposure to silicon compounds: a case-control study.* Nephrol Dial Transplant, 1995. **10**(7): p. 1162-5.
19. Beaudreuil, S., et al., *Occupational exposure in ANCA-positive patients: a case-control study.* Kidney Int, 2005. **67**(5): p. 1961-6.
20. Leigh, J., et al., *Silica-induced apoptosis in alveolar and granulomatous cells in vivo.* Environ Health Perspect, 1997. **105 Suppl 5**: p. 1241-5.

21. Slot, M.C., et al., *Occurrence of antineutrophil cytoplasmic antibodies and associated vasculitis in patients with hyperthyroidism treated with antithyroid drugs: A long-term followup study.* Arthritis Rheum, 2005. **53**(1): p. 108-13.
22. Keasberry, J., et al., *Hydralazine-induced anti-neutrophil cytoplasmic antibody-positive renal vasculitis presenting with a vasculitic syndrome, acute nephritis and a puzzling skin rash: a case report.* J Med Case Rep, 2013. **7**: p. 20.
23. Sethi, S., M. Sahani, and L.S. Oei, *ANCA-positive crescentic glomerulonephritis associated with minocycline therapy.* Am J Kidney Dis, 2003. **42**(2): p. E27-31.
24. McGrath, M.M., et al., *Contaminated cocaine and antineutrophil cytoplasmic antibody-associated disease.* Clin J Am Soc Nephrol, 2011. **6**(12): p. 2799-805.
25. Stegeman, C.A., et al., *Association of chronic nasal carriage of Staphylococcus aureus and higher relapse rates in Wegener granulomatosis.* Ann Intern Med, 1994. **120**(1): p. 12-7.
26. Zycinska, K., et al., *Chronic crusting, nasal carriage of Staphylococcus aureus and relapse rate in pulmonary Wegener's granulomatosis.* J Physiol Pharmacol, 2008. **59 Suppl 6**: p. 825-31.
27. Stegeman, C.A., et al., *Trimethoprim-sulfamethoxazole (co-trimoxazole) for the prevention of relapses of Wegener's granulomatosis. Dutch Co-Trimoxazole Wegener Study Group.* N Engl J Med, 1996. **335**(1): p. 16-20.
28. Pendergraft, W.F., 3rd, et al., *Autoimmunity is triggered by cPR-3(105-201), a protein complementary to human autoantigen proteinase-3.* Nat Med, 2004. **10**(1): p. 72-9.
29. Tadema, H., et al., *Reactivity against complementary proteinase-3 is not increased in patients with PR3-ANCA-associated vasculitis.* PLoS One, 2011. **6**(3): p. e17972.
30. Kain, R., et al., *A novel class of autoantigens of anti-neutrophil cytoplasmic antibodies in necrotizing and crescentic glomerulonephritis: the lysosomal membrane glycoprotein h-lamp-2 in neutrophil granulocytes and a related membrane protein in glomerular endothelial cells.* J Exp Med, 1995. **181**(2): p. 585-97.
31. Kain, R., et al., *Molecular mimicry in pauci-immune focal necrotizing glomerulonephritis.* Nat Med, 2008. **14**(10): p. 1088-96.
32. Huugen, D., et al., *Aggravation of anti-myeloperoxidase antibody-induced glomerulonephritis by bacterial lipopolysaccharide: role of tumor necrosis factor-alpha.* Am J Pathol, 2005. **167**(1): p. 47-58.
33. Kuligowski, M.P., et al., *Antimyeloperoxidase antibodies rapidly induce alpha-4-integrin-dependent glomerular neutrophil adhesion.* Blood, 2009. **113**(25): p. 6485-94.
34. Summers, S.A., et al., *Intrinsic renal cell and leukocyte-derived TLR4 aggravate experimental anti-MPO glomerulonephritis.* Kidney Int, 2010. **78**(12): p. 1263-74.
35. Knight, A., S. Sandin, and J. Askling, *Risks and relative risks of Wegener's granulomatosis among close relatives of patients with the disease.* Arthritis Rheum, 2008. **58**(1): p. 302-7.
36. Heckmann, M., et al., *The Wegener's granulomatosis quantitative trait locus on chromosome 6p21.3 as characterised by tagSNP genotyping.* Ann Rheum Dis, 2008. **67**(7): p. 972-9.
37. Stassen, P.M., et al., *HLA-DR4, DR13(6) and the ancestral haplotype A1B8DR3 are associated with ANCA-associated vasculitis and Wegener's granulomatosis.* Rheumatology (Oxford), 2009. **48**(6): p. 622-5.
38. Schreiber, A., et al., *Membrane expression of proteinase 3 is genetically determined.* J Am Soc Nephrol, 2003. **14**(1): p. 68-75.
39. Rarok, A.A., et al., *Neutrophil membrane expression of proteinase 3 (PR3) is related to relapse in PR3-ANCA-associated vasculitis.* J Am Soc Nephrol, 2002. **13**(9): p. 2232-8.
40. Mahr, A.D., et al., *Alpha(1)-antitrypsin deficiency-related alleles Z and S and the risk of Wegener's granulomatosis.* Arthritis Rheum, 2010. **62**(12): p. 3760-7.
41. Zhou, Y., et al., *An analysis of CTLA-4 and proinflammatory cytokine genes in Wegener's granulomatosis.* Arthritis Rheum, 2004. **50**(8): p. 2645-50.

42. Lyons, P.A., et al., *Genetically Distinct Subsets within ANCA-Associated Vasculitis.* New England Journal of Medicine, 2012. **367**(3): p. 214-223.
43. Davies, D.J., et al., *Segmental necrotising glomerulonephritis with antineutrophil antibody: possible arbovirus aetiology?* Br Med J (Clin Res Ed), 1982. **285**(6342): p. 606.
44. Hall, J.B., et al., *Vasculitis and glomerulonephritis: a subgroup with an antineutrophil cytoplasmic antibody.* Aust N Z J Med, 1984. **14**(3): p. 277-8.
45. van der Woude, F.J., et al., *Autoantibodies against neutrophils and monocytes: tool for diagnosis and marker of disease activity in Wegener's granulomatosis.* Lancet, 1985. **1**(8426): p. 425-9.
46. Ludemann, J., B. Utecht, and W.L. Gross, *Anti-neutrophil cytoplasm antibodies in Wegener's granulomatosis recognize an elastinolytic enzyme.* J Exp Med, 1990. **171**(1): p. 357-62.
47. Falk, R.J. and J.C. Jennette, *Anti-neutrophil cytoplasmic autoantibodies with specificity for myeloperoxidase in patients with systemic vasculitis and idiopathic necrotizing and crescentic glomerulonephritis.* N Engl J Med, 1988. **318**(25): p. 1651-7.
48. Niles, J.L., et al., *Wegener's granulomatosis autoantigen is a novel neutrophil serine proteinase.* Blood, 1989. **74**(6): p. 1888-93.
49. Agner, K., *Detoxicating effect of verdoperoxidase on toxins.* Nature, 1947. **159**(4034): p. 271.
50. Inazawa, J., et al., *Assignment of the Human Myeloperoxidase Gene (Mpo) to Bands Q21.3-]Q23 of Chromosome-17.* Cytogenetics and Cell Genetics, 1989. **50**(2-3): p. 135-136.
51. Nauseef, W.M., *Myeloperoxidase Biosynthesis by a Human Promyelocytic Leukemia-Cell Line - Insight into Myeloperoxidase Deficiency.* Blood, 1986. **67**(4): p. 865-872.
52. Nauseef, W.M., S.J. McCormick, and M. Goedken, *Coordinated participation of calreticulin and calnexin in the biosynthesis of myeloperoxidase.* J Biol Chem, 1998. **273**(12): p. 7107-11.
53. Nauseef, W.M., S. McCormick, and H. Yi, *Roles of heme insertion and the mannose-6-phosphate receptor in processing of the human myeloid lysosomal enzyme, myeloperoxidase.* Blood, 1992. **80**(10): p. 2622-33.
54. Andrews, P.C. and N.I. Krinsky, *The reductive cleavage of myeloperoxidase in half, producing enzymically active hemi-myeloperoxidase.* J Biol Chem, 1981. **256**(9): p. 4211-8.
55. Olsen, R.L. and C. Little, *Studies on the subunits of human myeloperoxidase.* Biochem J, 1984. **222**(3): p. 701-9.
56. Hurst, J.K., *What really happens in the neutrophil phagosome?* Free Radic Biol Med, 2012. **53**(3): p. 508-20.
57. Leichert, L.I., et al., *Quantifying changes in the thiol redox proteome upon oxidative stress in vivo.* Proc Natl Acad Sci U S A, 2008. **105**(24): p. 8197-202.
58. Rosen, H., et al., *Methionine oxidation contributes to bacterial killing by the myeloperoxidase system of neutrophils.* Proc Natl Acad Sci U S A, 2009. **106**(44): p. 18686-91.
59. Jerlich, A., et al., *The formation of phosphatidylcholine oxidation products by stimulated phagocytes.* Free Radical Research, 2003. **37**(6): p. 645-653.
60. Klinke, A., et al., *Myeloperoxidase attracts neutrophils by physical forces.* Blood, 2011. **117**(4): p. 1350-8.
61. Falk, R.J., et al., *Anti-neutrophil cytoplasmic autoantibodies induce neutrophils to degranulate and produce oxygen radicals in vitro.* Proc Natl Acad Sci U S A, 1990. **87**(11): p. 4115-9.
62. Kettritz, R., et al., *Role of mitogen-activated protein kinases in activation of human neutrophils by antineutrophil cytoplasmic antibodies.* J Am Soc Nephrol, 2001. **12**(1): p. 37-46.

63. Minota, S., et al., *Circulating myeloperoxidase and anti-myeloperoxidase antibody in patients with vasculitis.* Scand J Rheumatol, 1999. **28**(2): p. 94-9.
64. Hess, C., S. Sadallah, and J.A. Schifferli, *Induction of neutrophil responsiveness to myeloperoxidase antibodies by their exposure to supernatant of degranulated autologous neutrophils.* Blood, 2000. **96**(8): p. 2822-7.
65. Lau, D., et al., *Myeloperoxidase mediates neutrophil activation by association with CD11b/CD18 integrins.* Proc Natl Acad Sci U S A, 2005. **102**(2): p. 431-6.
66. Rao, N.V., et al., *Characterization of proteinase-3 (PR-3), a neutrophil serine proteinase. Structural and functional properties.* J Biol Chem, 1991. **266**(15): p. 9540-8.
67. Sturrock, A.B., et al., *Localization of the gene encoding proteinase-3 (the Wegener's granulomatosis autoantigen) to human chromosome band 19p13.3.* Cytogenet Cell Genet, 1993. **64**(1): p. 33-4.
68. Rao, N.V., et al., *Biosynthesis and processing of proteinase 3 in U937 cells. Processing pathways are distinct from those of cathepsin G.* J Biol Chem, 1996. **271**(6): p. 2972-8.
69. Sorensen, O.E., et al., *Human cathelicidin, hCAP-18, is processed to the antimicrobial peptide LL-37 by extracellular cleavage with proteinase 3.* Blood, 2001. **97**(12): p. 3951-9.
70. Coeshott, C., et al., *Converting enzyme-independent release of tumor necrosis factor alpha and IL-1beta from a stimulated human monocytic cell line in the presence of activated neutrophils or purified proteinase 3.* Proc Natl Acad Sci U S A, 1999. **96**(11): p. 6261-6.
71. Padrines, M., et al., *Interleukin-8 processing by neutrophil elastase, cathepsin G and proteinase-3.* FEBS Lett, 1994. **352**(2): p. 231-5.
72. Uehara, A., et al., *Activation of human oral epithelial cells by neutrophil proteinase 3 through protease-activated receptor-2.* J Immunol, 2002. **169**(8): p. 4594-603.
73. Yang, J.J., et al., *Internalization of proteinase 3 is concomitant with endothelial cell apoptosis and internalization of myeloperoxidase with generation of intracellular oxidants.* Am J Pathol, 2001. **158**(2): p. 581-92.
74. Pendergraft, W.F., 3rd, et al., *Proteinase 3 sidesteps caspases and cleaves p21(Waf1/Cip1/Sdi1) to induce endothelial cell apoptosis.* Kidney Int, 2004. **65**(1): p. 75-84.
75. Witko-Sarsat, V., et al., *A large subset of neutrophils expressing membrane proteinase 3 is a risk factor for vasculitis and rheumatoid arthritis.* J Am Soc Nephrol, 1999. **10**(6): p. 1224-33.
76. Csernok, E., et al., *Activated neutrophils express proteinase 3 on their plasma membrane in vitro and in vivo.* Clin Exp Immunol, 1994. **95**(2): p. 244-50.
77. Kantari, C., et al., *Molecular analysis of the membrane insertion domain of proteinase 3, the Wegener's autoantigen, in RBL cells: implication for its pathogenic activity.* J Leukoc Biol, 2011. **90**(5): p. 941-50.
78. Bauer, S., et al., *Proteinase 3 and CD177 are expressed on the plasma membrane of the same subset of neutrophils.* J Leukoc Biol, 2007. **81**(2): p. 458-64.
79. Jerke, U., et al., *Complement receptor Mac-1 is an adaptor for NB1 (CD177)-mediated PR3-ANCA neutrophil activation.* J Biol Chem, 2011. **286**(9): p. 7070-81.
80. Schreiber, A., et al., *Neutrophil serine proteases promote IL-1beta generation and injury in necrotizing crescentic glomerulonephritis.* J Am Soc Nephrol, 2012. **23**(3): p. 470-82.
81. Carlsson, S.R., et al., *Isolation and characterization of human lysosomal membrane glycoproteins, h-lamp-1 and h-lamp-2. Major sialoglycoproteins carrying polylactosaminoglycan.* J Biol Chem, 1988. **263**(35): p. 18911-9.
82. Tanaka, Y., et al., *Accumulation of autophagic vacuoles and cardiomyopathy in LAMP-2-deficient mice.* Nature, 2000. **406**(6798): p. 902-6.

83. Beertsen, W., et al., *Impaired phagosomal maturation in neutrophils leads to periodontitis in lysosomal-associated membrane protein-2 knockout mice.* J Immunol, 2008. **180**(1): p. 475-82.
84. Zhou, D., et al., *Lamp-2a facilitates MHC class II presentation of cytoplasmic antigens.* Immunity, 2005. **22**(5): p. 571-81.
85. Kain, R., et al., *High prevalence of autoantibodies to hLAMP-2 in anti-neutrophil cytoplasmic antibody-associated vasculitis.* J Am Soc Nephrol, 2012. **23**(3): p. 556-66.
86. Roth, A.J., et al., *Anti-LAMP-2 antibodies are not prevalent in patients with antineutrophil cytoplasmic autoantibody glomerulonephritis.* J Am Soc Nephrol, 2012. **23**(3): p. 545-55.
87. Schlieben, D.J., et al., *Pulmonary-renal syndrome in a newborn with placental transmission of ANCAs.* Am J Kidney Dis, 2005. **45**(4): p. 758-61.
88. Silva, F., et al., *Successful pregnancy and delivery of a healthy newborn despite transplacental transfer of antimyeloperoxidase antibodies from a mother with microscopic polyangiitis.* Am J Kidney Dis, 2009. **54**(3): p. 542-5.
89. Boomsma, M.M., et al., *Prediction of relapses in Wegener's granulomatosis by measurement of antineutrophil cytoplasmic antibody levels: a prospective study.* Arthritis Rheum, 2000. **43**(9): p. 2025-33.
90. Jayne, D.R., et al., *Randomized trial of plasma exchange or high-dosage methylprednisolone as adjunctive therapy for severe renal vasculitis.* J Am Soc Nephrol, 2007. **18**(7): p. 2180-8.
91. Cui, Z., et al., *Natural autoantibodies to myeloperoxidase, proteinase 3, and the glomerular basement membrane are present in normal individuals.* Kidney Int, 2010. **78**(6): p. 590-7.
92. Xu, P.C., et al., *Comparison of characteristics of natural autoantibodies against myeloperoxidase and anti-myeloperoxidase autoantibodies from patients with microscopic polyangiitis.* Rheumatology (Oxford), 2011. **50**(7): p. 1236-43.
93. Pankhurst, T., et al., *Immunoglobulin subclass determines ability of immunoglobulin (Ig)G to capture and activate neutrophils presented as normal human IgG or disease-associated anti-neutrophil cytoplasm antibody (ANCA)-IgG.* Clin Exp Immunol, 2011. **164**(2): p. 218-26.
94. Roth, A.J., et al., *Epitope specificity determines pathogenicity and detectability in ANCA-associated vasculitis.* J Clin Invest, 2013. **123**(4): p. 1773-83.
95. Franssen, C.F., et al., *In vitro neutrophil activation by antibodies to proteinase 3 and myeloperoxidase from patients with crescentic glomerulonephritis.* J Am Soc Nephrol, 1999. **10**(7): p. 1506-15.
96. Savage, C.O., et al., *Autoantibodies developing to myeloperoxidase and proteinase 3 in systemic vasculitis stimulate neutrophil cytotoxicity toward cultured endothelial cells.* Am J Pathol, 1992. **141**(2): p. 335-42.
97. Kessenbrock, K., et al., *Netting neutrophils in autoimmune small-vessel vasculitis.* Nat Med, 2009. **15**(6): p. 623-5.
98. Ciavatta, D.J., et al., *Epigenetic basis for aberrant upregulation of autoantigen genes in humans with ANCA vasculitis.* J Clin Invest, 2010. **120**(9): p. 3209-19.
99. Wegener's Granulomatosis Etanercept Trial Research, G., *Etanercept plus standard therapy for Wegener's granulomatosis.* N Engl J Med, 2005. **352**(4): p. 351-61.
100. Xiao, H., et al., *Antineutrophil cytoplasmic autoantibodies specific for myeloperoxidase cause glomerulonephritis and vasculitis in mice.* J Clin Invest, 2002. **110**(7): p. 955-63.
101. Nimmerjahn, F. and J.V. Ravetch, *Fcgamma receptors as regulators of immune responses.* Nat Rev Immunol, 2008. **8**(1): p. 34-47.
102. Kettritz, R., J.C. Jennette, and R.J. Falk, *Crosslinking of ANCA-antigens stimulates superoxide release by human neutrophils.* J Am Soc Nephrol, 1997. **8**(3): p. 386-94.
103. Keogan, M.T., et al., *Activation of normal neutrophils by anti-neutrophil cytoplasm antibodies.* Clin Exp Immunol, 1992. **90**(2): p. 228-34.

104. Porges, A.J., et al., *Anti-neutrophil cytoplasmic antibodies engage and activate human neutrophils via Fc gamma RIIa.* J Immunol, 1994. **153**(3): p. 1271-80.
105. Mulder, A.H., et al., *Activation of granulocytes by anti-neutrophil cytoplasmic antibodies (ANCA): a Fc gamma RII-dependent process.* Clin Exp Immunol, 1994. **98**(2): p. 270-8.
106. Williams, J.M., et al., *Activation of the G(i) heterotrimeric G protein by ANCA IgG F(ab')2 fragments is necessary but not sufficient to stimulate the recruitment of those downstream mediators used by intact ANCA IgG.* J Am Soc Nephrol, 2003. **14**(3): p. 661-9.
107. Nolan, S.L., et al., *Mechanisms of ANCA-mediated leukocyte-endothelial cell interactions in vivo.* J Am Soc Nephrol, 2008. **19**(5): p. 973-84.
108. van Timmeren, M.M., et al., *IgG glycan hydrolysis attenuates ANCA-mediated glomerulonephritis.* J Am Soc Nephrol, 2010. **21**(7): p. 1103-14.
109. Radford, D.J., J.M. Lord, and C.O. Savage, *The activation of the neutrophil respiratory burst by anti-neutrophil cytoplasm autoantibody (ANCA) from patients with systemic vasculitis requires tyrosine kinases and protein kinase C activation.* Clin Exp Immunol, 1999. **118**(1): p. 171-9.
110. Hewins, P., et al., *Activation of Syk in neutrophils by antineutrophil cytoplasm antibodies occurs via Fcgamma receptors and CD18.* J Am Soc Nephrol, 2004. **15**(3): p. 796-808.
111. Ben-Smith, A., et al., *Antineutrophil cytoplasm autoantibodies from patients with systemic vasculitis activate neutrophils through distinct signaling cascades: comparison with conventional Fcgamma receptor ligation.* Blood, 2001. **98**(5): p. 1448-55.
112. Schreiber, A., et al., *Phosphoinositol 3-kinase-gamma mediates antineutrophil cytoplasmic autoantibody-induced glomerulonephritis.* Kidney Int, 2010. **77**(2): p. 118-28.
113. Wright, H.L., et al., *Neutrophil function in inflammation and inflammatory diseases.* Rheumatology (Oxford), 2010. **49**(9): p. 1618-31.
114. Lieschke, G.J., et al., *Mice lacking granulocyte colony-stimulating factor have chronic neutropenia, granulocyte and macrophage progenitor cell deficiency, and impaired neutrophil mobilization.* Blood, 1994. **84**(6): p. 1737-46.
115. Carulli, G., *Effects of recombinant human granulocyte colony-stimulating factor administration on neutrophil phenotype and functions.* Haematologica, 1997. **82**(5): p. 606-16.
116. Christopher, M.J., et al., *Suppression of CXCL12 production by bone marrow osteoblasts is a common and critical pathway for cytokine-induced mobilization.* Blood, 2009. **114**(7): p. 1331-9.
117. Brouwer, E., et al., *Neutrophil activation in vitro and in vivo in Wegener's granulomatosis.* Kidney Int, 1994. **45**(4): p. 1120-31.
118. Xiao, H., et al., *The role of neutrophils in the induction of glomerulonephritis by anti-myeloperoxidase antibodies.* Am J Pathol, 2005. **167**(1): p. 39-45.
119. Freeley, S.J., et al., *Granulocyte colony stimulating factor exacerbates antineutrophil cytoplasmic antibody vasculitis.* Ann Rheum Dis, 2012.
120. Sanders, J.S., et al., *Plasma levels of soluble interleukin 2 receptor, soluble CD30, interleukin 10 and B cell activator of the tumour necrosis factor family during follow-up in vasculitis associated with proteinase 3-antineutrophil cytoplasmic antibodies: associations with disease activity and relapse.* Ann Rheum Dis, 2006. **65**(11): p. 1484-9.
121. King, W.J., et al., *T lymphocyte responses to anti-neutrophil cytoplasmic autoantibody (ANCA) antigens are present in patients with ANCA-associated systemic vasculitis and persist during disease remission.* Clin Exp Immunol, 1998. **112**(3): p. 539-46.
122. Schmitt, W.H., et al., *Treatment of refractory Wegener's granulomatosis with antithymocyte globulin (ATG): an open study in 15 patients.* Kidney Int, 2004. **65**(4): p. 1440-8.

123. Ruth, A.J., et al., *Anti-neutrophil cytoplasmic antibodies and effector CD4+ cells play nonredundant roles in anti-myeloperoxidase crescentic glomerulonephritis.* J Am Soc Nephrol, 2006. **17**(7): p. 1940-9.
124. Ooi, J.D., et al., *The immunodominant myeloperoxidase T-cell epitope induces local cell-mediated injury in antimyeloperoxidase glomerulonephritis.* Proc Natl Acad Sci U S A, 2012. **109**(39): p. E2615-24.
125. Wang, G., et al., *High plasma levels of the soluble form of CD30 activation molecule reflect disease activity in patients with Wegener's granulomatosis.* Am J Med, 1997. **102**(6): p. 517-23.
126. Csernok, E., et al., *Cytokine profiles in Wegener's granulomatosis: predominance of type 1 (Th1) in the granulomatous inflammation.* Arthritis Rheum, 1999. **42**(4): p. 742-50.
127. Hoshino, A., et al., *MPO-ANCA induces IL-17 production by activated neutrophils in vitro via classical complement pathway-dependent manner.* J Autoimmun, 2008. **31**(1): p. 79-89.
128. Gan, P.Y., et al., *Th17 cells promote autoimmune anti-myeloperoxidase glomerulonephritis.* J Am Soc Nephrol, 2010. **21**(6): p. 925-31.
129. Abdulahad, W.H., et al., *Functional defect of circulating regulatory CD4+ T cells in patients with Wegener's granulomatosis in remission.* Arthritis Rheum, 2007. **56**(6): p. 2080-91.
130. Abdulahad, W.H., et al., *Persistent expansion of CD4+ effector memory T cells in Wegener's granulomatosis.* Kidney Int, 2006. **70**(5): p. 938-47.
131. Abdulahad, W.H., et al., *Urinary CD4+ effector memory T cells reflect renal disease activity in antineutrophil cytoplasmic antibody-associated vasculitis.* Arthritis Rheum, 2009. **60**(9): p. 2830-8.
132. Iking-Konert, C., et al., *T lymphocytes in patients with primary vasculitis: expansion of CD8+ T cells with the propensity to activate polymorphonuclear neutrophils.* Rheumatology (Oxford), 2008. **47**(5): p. 609-16.
133. McKinney, E.F., et al., *A CD8+ T cell transcription signature predicts prognosis in autoimmune disease.* Nat Med, 2010. **16**(5): p. 586-91, 1p following 591.
134. Steinmetz, O.M., et al., *Analysis and classification of B-cell infiltrates in lupus and ANCA-associated nephritis.* Kidney Int, 2008. **74**(4): p. 448-57.
135. Bunch, D.O., et al., *Decreased CD5(+) B cells in active ANCA vasculitis and relapse after rituximab.* Clin J Am Soc Nephrol, 2013. **8**(3): p. 382-91.
136. Monach, P.A., et al., *Serum proteins reflecting inflammation, injury and repair as biomarkers of disease activity in ANCA-associated vasculitis.* Ann Rheum Dis, 2013. **72**(8): p. 1342-50.
137. Lenda, D.M., E.R. Stanley, and V.R. Kelley, *Negative role of colony-stimulating factor-1 in macrophage, T cell, and B cell mediated autoimmune disease in MRL-Fas(lpr) mice.* J Immunol, 2004. **173**(7): p. 4744-54.
138. Mills, C.D. and K. Ley, *M1 and M2 macrophages: the chicken and the egg of immunity.* J Innate Immun, 2014. **6**(6): p. 716-26.
139. Charles, L.A., R.J. Falk, and J.C. Jennette, *Reactivity of antineutrophil cytoplasmic autoantibodies with mononuclear phagocytes.* J Leukoc Biol, 1992. **51**(1): p. 65-8.
140. Casselman, B.L., et al., *Antibodies to neutrophil cytoplasmic antigens induce monocyte chemoattractant protein-1 secretion from human monocytes.* J Lab Clin Med, 1995. **126**(5): p. 495-502.
141. Ralston, D.R., et al., *Antineutrophil cytoplasmic antibodies induce monocyte IL-8 release. Role of surface proteinase-3, alpha1-antitrypsin, and Fcgamma receptors.* J Clin Invest, 1997. **100**(6): p. 1416-24.
142. Wikman, A., et al., *Monocyte activation and relationship to anti-proteinase 3 in acute vasculitis.* Nephrol Dial Transplant, 2003. **18**(9): p. 1792-9.

143. Weidner, S., et al., *Antineutrophil cytoplasmic antibodies induce human monocytes to produce oxygen radicals in vitro.* Arthritis Rheum, 2001. **44**(7): p. 1698-706.
144. Nowack, R., et al., *Upregulation of CD14 and CD18 on monocytes In vitro by antineutrophil cytoplasmic autoantibodies.* J Am Soc Nephrol, 2000. **11**(9): p. 1639-46.
145. O'Brien, E.C., et al., *Intermediate monocytes in ANCA vasculitis: increased surface expression of ANCA autoantigens and IL-1beta secretion in response to anti-MPO antibodies.* Sci Rep, 2015. **5**: p. 11888.
146. Zhao, L., et al., *M2 macrophage infiltrates in the early stages of ANCA-associated pauci-immune necrotizing GN.* Clin J Am Soc Nephrol, 2015. **10**(1): p. 54-62.
147. Ohlsson, S.M., et al., *Serum from patients with systemic vasculitis induces alternatively activated macrophage M2c polarization.* Clin Immunol, 2014. **152**(1-2): p. 10-9.
148. Ehrnthaller, C., et al., *New insights of an old defense system: structure, function, and clinical relevance of the complement system.* Mol Med, 2011. **17**(3-4): p. 317-29.
149. Kaplan, M.H. and J.E. Volanakis, *Interaction of C-reactive protein complexes with the complement system. I. Consumption of human complement associated with the reaction of C-reactive protein with pneumococcal C-polysaccharide and with the choline phosphatides, lecithin and sphingomyelin.* J Immunol, 1974. **112**(6): p. 2135-47.
150. Chen, C.B. and R. Wallis, *Two mechanisms for mannose-binding protein modulation of the activity of its associated serine proteases.* J Biol Chem, 2004. **279**(25): p. 26058-65.
151. Kemper, C., J.P. Atkinson, and D.E. Hourcade, *Properdin: emerging roles of a pattern-recognition molecule.* Annu Rev Immunol, 2010. **28**: p. 131-55.
152. Kemper, C., et al., *The complement protein properdin binds apoptotic T cells and promotes complement activation and phagocytosis.* Proc Natl Acad Sci U S A, 2008. **105**(26): p. 9023-8.
153. Xu, W., et al., *Properdin binds to late apoptotic and necrotic cells independently of C3b and regulates alternative pathway complement activation.* J Immunol, 2008. **180**(11): p. 7613-21.
154. Zipfel, P.F. and C. Skerka, *Complement regulators and inhibitory proteins.* Nat Rev Immunol, 2009. **9**(10): p. 729-40.
155. Gronski, P., et al., *The functional inhibition of activated C1 inhibitor in normal human serum causes spontaneous consumption of the complement components C2, C3, C4, and factor B.* Immunobiology, 1986. **171**(3): p. 252-62.
156. Parej, K., et al., *The control of the complement lectin pathway activation revisited: both C1-inhibitor and antithrombin are likely physiological inhibitors, while alpha2-macroglobulin is not.* Mol Immunol, 2013. **54**(3-4): p. 415-22.
157. Fukui, A., et al., *Mapping of the sites responsible for factor I-cofactor activity for cleavage of C3b and C4b on human C4b-binding protein (C4bp) by deletion mutagenesis.* J Biochem, 2002. **132**(5): p. 719-28.
158. Weiler, J.M., et al., *Control of the amplification convertase of complement by the plasma protein beta1H.* Proc Natl Acad Sci U S A, 1976. **73**(9): p. 3268-72.
159. Whaley, K. and S. Ruddy, *Modulation of C3b hemolytic activity by a plasma protein distinct from C3b inactivator.* Science, 1976. **193**(4257): p. 1011-3.
160. Bokisch, V.A. and H.J. Muller-Eberhard, *Anaphylatoxin inactivator of human plasma: its isolation and characterization as a carboxypeptidase.* J Clin Invest, 1970. **49**(12): p. 2427-36.
161. Iida, K. and V. Nussenzweig, *Complement receptor is an inhibitor of the complement cascade.* J Exp Med, 1981. **153**(5): p. 1138-50.
162. Ross, G.D., et al., *Generation of three different fragments of bound C3 with purified factor I or serum. I. Requirements for factor H vs CR1 cofactor activity.* J Immunol, 1982. **129**(5): p. 2051-60.
163. Seya, T. and J.P. Atkinson, *Functional properties of membrane cofactor protein of complement.* Biochem J, 1989. **264**(2): p. 581-8.

164. Nicholson-Weller, A., et al., *Isolation of a human erythrocyte membrane glycoprotein with decay-accelerating activity for C3 convertases of the complement system.* J Immunol, 1982. **129**(1): p. 184-9.
165. Hugli, T.E., *Structure and function of the anaphylatoxins.* Springer Semin Immunopathol, 1984. **7**(2-3): p. 193-219.
166. Ehrengruber, M.U., T. Geiser, and D.A. Deranleau, *Activation of human neutrophils by C3a and C5A. Comparison of the effects on shape changes, chemotaxis, secretion, and respiratory burst.* FEBS Lett, 1994. **346**(2-3): p. 181-4.
167. Scola, A.M., et al., *The human complement fragment receptor, C5L2, is a recycling decoy receptor.* Mol Immunol, 2009. **46**(6): p. 1149-62.
168. Bamberg, C.E., et al., *The C5a receptor (C5aR) C5L2 is a modulator of C5aR-mediated signal transduction.* J Biol Chem, 2010. **285**(10): p. 7633-44.
169. Krych-Goldberg, M. and J.P. Atkinson, *Structure-function relationships of complement receptor type 1.* Immunol Rev, 2001. **180**: p. 112-22.
170. Helmy, K.Y., et al., *CRIg: a macrophage complement receptor required for phagocytosis of circulating pathogens.* Cell, 2006. **124**(5): p. 915-27.
171. Dashiell, S.M., H. Rus, and C.L. Koski, *Terminal complement complexes concomitantly stimulate proliferation and rescue of Schwann cells from apoptosis.* Glia, 2000. **30**(2): p. 187-98.
172. David, S., et al., *Alternative pathway complement activation induces proinflammatory activity in human proximal tubular epithelial cells.* Nephrol Dial Transplant, 1997. **12**(1): p. 51-6.
173. Pepys, M.B., *Role of complement in induction of the allergic response.* Nat New Biol, 1972. **237**(74): p. 157-9.
174. Matsumoto, A.K., et al., *Functional dissection of the CD21/CD19/TAPA-1/Leu-13 complex of B lymphocytes.* J Exp Med, 1993. **178**(4): p. 1407-17.
175. Dempsey, P.W., et al., *C3d of complement as a molecular adjuvant: bridging innate and acquired immunity.* Science, 1996. **271**(5247): p. 348-50.
176. Fischer, W.H. and T.E. Hugli, *Regulation of B cell functions by C3a and C3a(desArg): suppression of TNF-alpha, IL-6, and the polyclonal immune response.* J Immunol, 1997. **159**(9): p. 4279-86.
177. Kemper, C. and J.P. Atkinson, *T-cell regulation: with complements from innate immunity.* Nat Rev Immunol, 2007. **7**(1): p. 9-18.
178. Kopf, M., et al., *Complement component C3 promotes T-cell priming and lung migration to control acute influenza virus infection.* Nat Med, 2002. **8**(4): p. 373-8.
179. Marsh, J.E., et al., *The allogeneic T and B cell response is strongly dependent on complement components C3 and C4.* Transplantation, 2001. **72**(7): p. 1310-8.
180. Zhou, W., et al., *Macrophages from C3-deficient mice have impaired potency to stimulate alloreactive T cells.* Blood, 2006. **107**(6): p. 2461-9.
181. Li, K., et al., *Cyclic AMP plays a critical role in C3a-receptor-mediated regulation of dendritic cells in antigen uptake and T-cell stimulation.* Blood, 2008. **112**(13): p. 5084-94.
182. Heeger, P.S., et al., *Decay-accelerating factor modulates induction of T cell immunity.* J Exp Med, 2005. **201**(10): p. 1523-30.
183. Strainic, M.G., et al., *Locally produced complement fragments C5a and C3a provide both costimulatory and survival signals to naive CD4+ T cells.* Immunity, 2008. **28**(3): p. 425-35.
184. Zaffran, Y., et al., *CD46/CD3 costimulation induces morphological changes of human T cells and activation of Vav, Rac, and extracellular signal-regulated kinase mitogen-activated protein kinase.* J Immunol, 2001. **167**(12): p. 6780-5.
185. Le Friec, G., et al., *The CD46-Jagged1 interaction is critical for human TH1 immunity.* Nat Immunol, 2012. **13**(12): p. 1213-21.

186. Cardone, J., et al., *Complement regulator CD46 temporally regulates cytokine production by conventional and unconventional T cells.* Nat Immunol, 2010. **11**(9): p. 862-71.
187. Morgan, B.P. and P. Gasque, *Extrahepatic complement biosynthesis: where, when and why?* Clin Exp Immunol, 1997. **107**(1): p. 1-7.
188. Kolev, M., G. Le Friec, and C. Kemper, *Complement--tapping into new sites and effector systems.* Nat Rev Immunol, 2014. **14**(12): p. 811-20.
189. Sheerin, N.S., et al., *Synthesis of complement protein C3 in the kidney is an important mediator of local tissue injury.* FASEB J, 2008. **22**(4): p. 1065-72.
190. Pratt, J.R., S.A. Basheer, and S.H. Sacks, *Local synthesis of complement component C3 regulates acute renal transplant rejection.* Nat Med, 2002. **8**(6): p. 582-7.
191. Liszewski, M.K., et al., *Intracellular complement activation sustains T cell homeostasis and mediates effector differentiation.* Immunity, 2013. **39**(6): p. 1143-57.
192. Adams, R.L. and R.J. Bird, *Review article: Coagulation cascade and therapeutics update: relevance to nephrology. Part 1: Overview of coagulation, thrombophilias and history of anticoagulants.* Nephrology (Carlton), 2009. **14**(5): p. 462-70.
193. Oikonomopoulou, K., et al., *Interactions between coagulation and complement--their role in inflammation.* Semin Immunopathol, 2012. **34**(1): p. 151-65.
194. Ghebrehiwet, B., M. Silverberg, and A.P. Kaplan, *Activation of the classical pathway of complement by Hageman factor fragment.* J Exp Med, 1981. **153**(3): p. 665-76.
195. Huber-Lang, M., et al., *Generation of C5a in the absence of C3: a new complement activation pathway.* Nat Med, 2006. **12**(6): p. 682-7.
196. Amara, U., et al., *Molecular intercommunication between the complement and coagulation systems.* J Immunol, 2010. **185**(9): p. 5628-36.
197. Krarup, A., et al., *Simultaneous activation of complement and coagulation by MBL-associated serine protease 2.* PLoS One, 2007. **2**(7): p. e623.
198. Krarup, A., et al., *The action of MBL-associated serine protease 1 (MASP1) on factor XIII and fibrinogen.* Biochim Biophys Acta, 2008. **1784**(9): p. 1294-300.
199. Polley, M.J. and R.L. Nachman, *Human platelet activation by C3a and C3a des-arg.* J Exp Med, 1983. **158**(2): p. 603-15.
200. Platt, J.L., et al., *The role of C5a and antibody in the release of heparan sulfate from endothelial cells.* Eur J Immunol, 1991. **21**(11): p. 2887-90.
201. Ikeda, K., et al., *C5a induces tissue factor activity on endothelial cells.* Thromb Haemost, 1997. **77**(2): p. 394-8.
202. Tedesco, F., et al., *The cytolytically inactive terminal complement complex activates endothelial cells to express adhesion molecules and tissue factor procoagulant activity.* J Exp Med, 1997. **185**(9): p. 1619-27.
203. Xing, G.Q., et al., *Complement activation is involved in renal damage in human antineutrophil cytoplasmic autoantibody associated pauci-immune vasculitis.* J Clin Immunol, 2009. **29**(3): p. 282-91.
204. Gou, S.J., et al., *Circulating complement activation in patients with anti-neutrophil cytoplasmic antibody-associated vasculitis.* Kidney Int, 2013. **83**(1): p. 129-37.
205. Xing, G.Q., et al., *Differential deposition of C4d and MBL in glomeruli of patients with ANCA-negative pauci-immune crescentic glomerulonephritis.* J Clin Immunol, 2010. **30**(1): p. 144-56.
206. Hilhorst, M., et al., *Complement in ANCA-associated glomerulonephritis.* Nephrol Dial Transplant, 2015.
207. Xiao, H., et al., *Alternative complement pathway in the pathogenesis of disease mediated by anti-neutrophil cytoplasmic autoantibodies.* Am J Pathol, 2007. **170**(1): p. 52-64.
208. Huugen, D., et al., *Inhibition of complement factor C5 protects against anti-myeloperoxidase antibody-mediated glomerulonephritis in mice.* Kidney Int, 2007. **71**(7): p. 646-54.

209. Schreiber, A., et al., *C5a receptor mediates neutrophil activation and ANCA-induced glomerulonephritis.* J Am Soc Nephrol, 2009. **20**(2): p. 289-98.
210. Botto, M., et al., *Biosynthesis and secretion of complement component (C3) by activated human polymorphonuclear leukocytes.* J Immunol, 1992. **149**(4): p. 1348-55.
211. Xiao, H., et al., *C5a receptor (CD88) blockade protects against MPO-ANCA GN.* J Am Soc Nephrol, 2014. **25**(2): p. 225-31.
212. Esnault, V.L., et al., *Autoantibodies to myeloperoxidase in brown Norway rats treated with mercuric chloride.* Lab Invest, 1992. **67**(1): p. 114-20.
213. Mathieson, P.W., S. Thiru, and D.B. Oliveira, *Mercuric chloride-treated brown Norway rats develop widespread tissue injury including necrotizing vasculitis.* Lab Invest, 1992. **67**(1): p. 121-9.
214. Kinjoh, K., M. Kyogoku, and R.A. Good, *Genetic selection for crescent formation yields mouse strain with rapidly progressive glomerulonephritis and small vessel vasculitis.* Proc Natl Acad Sci U S A, 1993. **90**(8): p. 3413-7.
215. Brouwer, E., et al., *Antimyeloperoxidase-associated proliferative glomerulonephritis: an animal model.* J Exp Med, 1993. **177**(4): p. 905-14.
216. Kobayashi, K., T. Shibata, and T. Sugisaki, *Aggravation of rat nephrotoxic serum nephritis by anti-myeloperoxidase antibodies.* Kidney Int, 1995. **47**(2): p. 454-63.
217. Heeringa, P., et al., *Autoantibodies to myeloperoxidase aggravate mild anti-glomerular-basement-membrane-mediated glomerular injury in the rat.* Am J Pathol, 1996. **149**(5): p. 1695-706.
218. Xiao, H., et al., *Genetically determined severity of anti-myeloperoxidase glomerulonephritis.* Am J Pathol, 2013. **182**(4): p. 1219-26.
219. Schreiber, A., et al., *Bone marrow-derived cells are sufficient and necessary targets to mediate glomerulonephritis and vasculitis induced by anti-myeloperoxidase antibodies.* J Am Soc Nephrol, 2006. **17**(12): p. 3355-64.
220. Little, M.A., et al., *Antineutrophil cytoplasm antibodies directed against myeloperoxidase augment leukocyte-microvascular interactions in vivo.* Blood, 2005. **106**(6): p. 2050-8.
221. Little, M.A., et al., *Experimental autoimmune vasculitis: an animal model of anti-neutrophil cytoplasmic autoantibody-associated systemic vasculitis.* Am J Pathol, 2009. **174**(4): p. 1212-20.
222. Pfister, H., et al., *Antineutrophil cytoplasmic autoantibodies against the murine homolog of proteinase 3 (Wegener autoantigen) are pathogenic in vivo.* Blood, 2004. **104**(5): p. 1411-8.
223. van der Geld, Y.M., et al., *Rats and mice immunised with chimeric human/mouse proteinase 3 produce autoantibodies to mouse Pr3 and rat granulocytes.* Ann Rheum Dis, 2007. **66**(12): p. 1679-82.
224. Primo, V.C., et al., *Anti-PR3 immune responses induce segmental and necrotizing glomerulonephritis.* Clin Exp Immunol, 2010. **159**(3): p. 327-37.
225. Little, M.A., et al., *Anti-proteinase 3 anti-neutrophil cytoplasm autoantibodies recapitulate systemic vasculitis in mice with a humanized immune system.* PLoS One, 2012. **7**(1): p. e28626.
226. Cochrane, C.G., E.R. Unanue, and F.J. Dixon, *A Role of Polymorphonuclear Leukocytes and Complement in Nephrotoxic Nephritis.* J Exp Med, 1965. **122**: p. 99-116.
227. Cochrane, C.G., *Mediating systems in inflammatory disease.* J Invest Dermatol, 1978. **71**(1): p. 40-8.
228. Tomosugi, N.I., et al., *Modulation of antibody-mediated glomerular injury in vivo by bacterial lipopolysaccharide, tumor necrosis factor, and IL-1.* J Immunol, 1989. **142**(9): p. 3083-90.
229. Brown, H.J., et al., *Toll-like receptor 4 ligation on intrinsic renal cells contributes to the induction of antibody-mediated glomerulonephritis via CXCL1 and CXCL2.* Journal of the American Society of Nephrology, 2007. **18**(6): p. 1732-1739.

230. Brown, H.J., et al., *TLR2 stimulation of intrinsic renal cells in the induction of immune-mediated glomerulonephritis.* J Immunol, 2006. **177**(3): p. 1925-31.
231. Unanue, E.R. and F.J. Dixon, *Experimental Glomerulonephritis. V. Studies on the Interaction of Nephrotoxic Antibodies with Tissue of the Rat.* J Exp Med, 1965. **121**: p. 697-714.
232. Park, S.Y., et al., *Resistance of Fc receptor- deficient mice to fatal glomerulonephritis.* J Clin Invest, 1998. **102**(6): p. 1229-38.
233. Otten, M.A., et al., *Both complement and IgG fc receptors are required for development of attenuated antiglomerular basement membrane nephritis in mice.* J Immunol, 2009. **183**(6): p. 3980-8.
234. Tarzi, R.M., et al., *Nephrotoxic nephritis is mediated by Fcgamma receptors on circulating leukocytes and not intrinsic renal cells.* Kidney Int, 2002. **62**(6): p. 2087-96.
235. Li, S., S.R. Holdsworth, and P.G. Tipping, *Antibody independent crescentic glomerulonephritis in mu chain deficient mice.* Kidney Int, 1997. **51**(3): p. 672-8.
236. Huang, X.R., et al., *Mechanisms of T cell-induced glomerular injury in anti-glomerular basement membrane (GBM) glomerulonephritis in rats.* Clin Exp Immunol, 1997. **109**(1): p. 134-42.
237. Iskandar, S.S., et al., *Interstrain variations in nephritogenicity of heterologous protein in mice.* Lab Invest, 1982. **46**(3): p. 344-51.
238. Farquhar, M.G., et al., *The Heymann nephritis antigenic complex: megalin (gp330) and RAP.* J Am Soc Nephrol, 1995. **6**(1): p. 35-47.
239. Kerjaschki, D. and M.G. Farquhar, *The pathogenic antigen of Heymann nephritis is a membrane glycoprotein of the renal proximal tubule brush border.* Proc Natl Acad Sci U S A, 1982. **79**(18): p. 5557-61.
240. Perry, D., et al., *Murine models of systemic lupus erythematosus.* J Biomed Biotechnol, 2011. **2011**: p. 271694.
241. Lawson, N.D., D.S. Krause, and N. Berliner, *Normal neutrophil differentiation and secondary granule gene expression in the EML and MPRO cell lines.* Exp Hematol, 1998. **26**(12): p. 1178-85.
242. Hope, H.R., et al., *Large-scale purification of myeloperoxidase from HL60 promyelocytic cells: characterization and comparison to human neutrophil myeloperoxidase.* Protein Expr Purif, 2000. **18**(3): p. 269-76.
243. Brennan, M.L., et al., *Increased atherosclerosis in myeloperoxidase-deficient mice.* J Clin Invest, 2001. **107**(4): p. 419-30.
244. Wessels, M.R., et al., *Studies of group B streptococcal infection in mice deficient in complement component C3 or C4 demonstrate an essential role for complement in both innate and acquired immunity.* Proc Natl Acad Sci U S A, 1995. **92**(25): p. 11490-4.
245. Schwaeble, W.J., et al., *Targeting of mannan-binding lectin-associated serine protease-2 confers protection from myocardial and gastrointestinal ischemia/reperfusion injury.* Proc Natl Acad Sci U S A, 2011. **108**(18): p. 7523-8.
246. Matsumoto, M., et al., *Abrogation of the alternative complement pathway by targeted deletion of murine factor B.* Proc Natl Acad Sci U S A, 1997. **94**(16): p. 8720-5.
247. Wetsel, R.A., D.T. Fleischer, and D.L. Haviland, *Deficiency of the murine fifth complement component (C5). A 2-base pair gene deletion in a 5'-exon.* J Biol Chem, 1990. **265**(5): p. 2435-40.
248. Tchaikovski, S.N., et al., *Development of a calibrated automated thrombography based thrombin generation test in mouse plasma.* J Thromb Haemost, 2007. **5**(10): p. 2079-86.
249. Tiden, A.K., et al., *2-thioxanthines are mechanism-based inactivators of myeloperoxidase that block oxidative stress during inflammation.* J Biol Chem, 2011. **286**(43): p. 37578-89.
250. Schmittgen, T.D. and K.J. Livak, *Analyzing real-time PCR data by the comparative C(T) method.* Nat Protoc, 2008. **3**(6): p. 1101-8.

251. Kettritz, R., et al., *Phosphatidylinositol 3-kinase controls antineutrophil cytoplasmic antibodies-induced respiratory burst in human neutrophils.* J Am Soc Nephrol, 2002. **13**(7): p. 1740-9.
252. Clark, R.A., *Activation of the neutrophil respiratory burst oxidase.* J Infect Dis, 1999. **179 Suppl 2**: p. S309-17.
253. Lundqvist, H. and C. Dahlgren, *Isoluminol-enhanced chemiluminescence: a sensitive method to study the release of superoxide anion from human neutrophils.* Free Radic Biol Med, 1996. **20**(6): p. 785-92.
254. Faurschou, M. and N. Borregaard, *Neutrophil granules and secretory vesicles in inflammation.* Microbes Infect, 2003. **5**(14): p. 1317-27.
255. Camous, L., et al., *Complement alternative pathway acts as a positive feedback amplification of neutrophil activation.* Blood, 2011. **117**(4): p. 1340-9.
256. Harper, L., et al., *IgG from myeloperoxidase-antineutrophil cytoplasmic antibody-positive patients stimulates greater activation of primed neutrophils than IgG from proteinase 3-antineutrophil cytosplasmic antibody-positive patients.* Arthritis Rheum, 2001. **44**(4): p. 921-30.
257. Mulder, A.H., C.A. Stegeman, and C.G. Kallenberg, *Activation of granulocytes by anti-neutrophil cytoplasmic antibodies (ANCA) in Wegener's granulomatosis: a predominant role for the IgG3 subclass of ANCA.* Clin Exp Immunol, 1995. **101**(2): p. 227-32.
258. Schreiber, A., F.C. Luft, and R. Kettritz, *Phagocyte NADPH oxidase restrains the inflammasome in ANCA-induced GN.* J Am Soc Nephrol, 2015. **26**(2): p. 411-24.
259. Hao, J., et al., *p38MAPK, ERK and PI3K signaling pathways are involved in C5a-primed neutrophils for ANCA-mediated activation.* PLoS One, 2012. **7**(5): p. e38317.
260. Cros, J., et al., *Human CD14dim monocytes patrol and sense nucleic acids and viruses via TLR7 and TLR8 receptors.* Immunity, 2010. **33**(3): p. 375-86.
261. Wong, K.L., et al., *Gene expression profiling reveals the defining features of the classical, intermediate, and nonclassical human monocyte subsets.* Blood, 2011. **118**(5): p. e16-31.
262. Hashimoto, D., et al., *Tissue-resident macrophages self-maintain locally throughout adult life with minimal contribution from circulating monocytes.* Immunity, 2013. **38**(4): p. 792-804.
263. Ricardo, S.D., H. van Goor, and A.A. Eddy, *Macrophage diversity in renal injury and repair.* J Clin Invest, 2008. **118**(11): p. 3522-30.
264. Verreck, F.A., et al., *Human IL-23-producing type 1 macrophages promote but IL-10-producing type 2 macrophages subvert immunity to (myco)bacteria.* Proc Natl Acad Sci U S A, 2004. **101**(13): p. 4560-5.
265. Hao, N.B., et al., *Macrophages in tumor microenvironments and the progression of tumors.* Clin Dev Immunol, 2012. **2012**: p. 948098.
266. Mills, C.D., et al., *M-1/M-2 macrophages and the Th1/Th2 paradigm.* J Immunol, 2000. **164**(12): p. 6166-73.
267. Berden, A.E., et al., *Histopathologic Classification of ANCA-Associated Glomerulonephritis.* J Am Soc Nephrol, 2010.
268. Yang, J. and Y. Liu, *Dissection of key events in tubular epithelial to myofibroblast transition and its implications in renal interstitial fibrosis.* Am J Pathol, 2001. **159**(4): p. 1465-75.
269. Kitagawa, K., et al., *Blockade of CCR2 ameliorates progressive fibrosis in kidney.* Am J Pathol, 2004. **165**(1): p. 237-46.
270. Pan, B., et al., *Regulation of renal fibrosis by macrophage polarization.* Cell Physiol Biochem, 2015. **35**(3): p. 1062-9.
271. Lloyd, C.M., et al., *RANTES and monocyte chemoattractant protein-1 (MCP-1) play an important role in the inflammatory phase of crescentic nephritis, but only MCP-1 is involved in crescent formation and interstitial fibrosis.* J Exp Med, 1997. **185**(7): p. 1371-80.

272. Reumaux, D., et al., *Effect of tumor necrosis factor-induced integrin activation on Fc gamma receptor II-mediated signal transduction: relevance for activation of neutrophils by anti-proteinase 3 or anti-myeloperoxidase antibodies.* Blood, 1995. **86**(8): p. 3189-95.
273. McGeachy, M.J., et al., *TGF-beta and IL-6 drive the production of IL-17 and IL-10 by T cells and restrain T(H)-17 cell-mediated pathology.* Nat Immunol, 2007. **8**(12): p. 1390-7.
274. Erridge, C., et al., *Oxidized phospholipid inhibition of toll-like receptor (TLR) signaling is restricted to TLR2 and TLR4: roles for CD14, LPS-binding protein, and MD2 as targets for specificity of inhibition.* J Biol Chem, 2008. **283**(36): p. 24748-59.
275. Bochkov, V.N., et al., *Protective role of phospholipid oxidation products in endotoxin-induced tissue damage.* Nature, 2002. **419**(6902): p. 77-81.
276. von Schlieffen, E., et al., *Multi-hit inhibition of circulating and cell-associated components of the toll-like receptor 4 pathway by oxidized phospholipids.* Arterioscler Thromb Vasc Biol, 2009. **29**(3): p. 356-62.
277. Abdulahad, W.H., P. Lamprecht, and C.G. Kallenberg, *T-helper cells as new players in ANCA-associated vasculitides.* Arthritis Res Ther, 2011. **13**(4): p. 236.
278. Subbanagounder, G., et al., *Epoxyisoprostane and epoxycyclopentenone phospholipids regulate monocyte chemotactic protein-1 and interleukin-8 synthesis. Formation of these oxidized phospholipids in response to interleukin-1beta.* J Biol Chem, 2002. **277**(9): p. 7271-81.
279. Oskolkova, O.V., et al., *Oxidized phospholipids are more potent antagonists of lipopolysaccharide than inducers of inflammation.* J Immunol, 2010. **185**(12): p. 7706-12.
280. Bochkov, V.N., et al., *Generation and biological activities of oxidized phospholipids.* Antioxid Redox Signal, 2010. **12**(8): p. 1009-59.
281. Scheller, J., et al., *The pro- and anti-inflammatory properties of the cytokine interleukin-6.* Biochim Biophys Acta, 2011. **1813**(5): p. 878-88.
282. Hunter, C.A. and S.A. Jones, *IL-6 as a keystone cytokine in health and disease.* Nat Immunol, 2015. **16**(5): p. 448-57.
283. Liu, F., et al., *Interleukin-6 and the granulocyte colony-stimulating factor receptor are major independent regulators of granulopoiesis in vivo but are not required for lineage commitment or terminal differentiation.* Blood, 1997. **90**(7): p. 2583-90.
284. Hurst, S.M., et al., *Il-6 and its soluble receptor orchestrate a temporal switch in the pattern of leukocyte recruitment seen during acute inflammation.* Immunity, 2001. **14**(6): p. 705-14.
285. Moore, K.W., et al., *Interleukin-10 and the interleukin-10 receptor.* Annu Rev Immunol, 2001. **19**: p. 683-765.
286. Hunter, C.A., et al., *IL-10 is required to prevent immune hyperactivity during infection with Trypanosoma cruzi.* J Immunol, 1997. **158**(7): p. 3311-6.
287. Gazzinelli, R.T., et al., *In the absence of endogenous IL-10, mice acutely infected with Toxoplasma gondii succumb to a lethal immune response dependent on CD4+ T cells and accompanied by overproduction of IL-12, IFN-gamma and TNF-alpha.* J Immunol, 1996. **157**(2): p. 798-805.
288. Jin, Y., et al., *Interleukin-10 deficiency aggravates kidney inflammation and fibrosis in the unilateral ureteral obstruction mouse model.* Lab Invest, 2013. **93**(7): p. 801-11.
289. Wermuth, P.J. and S.A. Jimenez, *The significance of macrophage polarization subtypes for animal models of tissue fibrosis and human fibrotic diseases.* Clin Transl Med, 2015. **4**: p. 2.
290. Ramirez, G.A., et al., *Plasma levels of M-CSF are increased in ANCA-associated vasculitides with active nephritis.* Results Immunol, 2015. **5**: p. 33-6.

291. Chen, W., et al., *Conversion of peripheral CD4+CD25- naive T cells to CD4+CD25+ regulatory T cells by TGF-beta induction of transcription factor Foxp3.* J Exp Med, 2003. **198**(12): p. 1875-86.
292. Cao, Q., et al., *IL-10/TGF-beta-modified macrophages induce regulatory T cells and protect against adriamycin nephrosis.* J Am Soc Nephrol, 2010. **21**(6): p. 933-42.
293. Savage, N.D., et al., *Human anti-inflammatory macrophages induce Foxp3+ GITR+ CD25+ regulatory T cells, which suppress via membrane-bound TGFbeta-1.* J Immunol, 2008. **181**(3): p. 2220-6.
294. Cope, A., et al., *The Th1 life cycle: molecular control of IFN-gamma to IL-10 switching.* Trends Immunol, 2011. **32**(6): p. 278-86.
295. Luzina, I.G., et al., *Roles of T lymphocytes in pulmonary fibrosis.* J Leukoc Biol, 2008. **83**(2): p. 237-44.
296. Tapmeier, T.T., et al., *Pivotal role of CD4+ T cells in renal fibrosis following ureteric obstruction.* Kidney Int, 2010. **78**(4): p. 351-62.
297. Wynn, T.A. and L. Barron, *Macrophages: master regulators of inflammation and fibrosis.* Semin Liver Dis, 2010. **30**(3): p. 245-57.
298. Miyake, K., *Innate immune sensing of pathogens and danger signals by cell surface Toll-like receptors.* Semin Immunol, 2007. **19**(1): p. 3-10.
299. O'Neill, L.A. and A.G. Bowie, *The family of five: TIR-domain-containing adaptors in Toll-like receptor signalling.* Nat Rev Immunol, 2007. **7**(5): p. 353-64.
300. Iwaki, D., et al., *The role of mannose-binding lectin-associated serine protease-3 in activation of the alternative complement pathway.* J Immunol, 2011. **187**(7): p. 3751-8.
301. Takahashi, M., et al., *Essential role of mannose-binding lectin-associated serine protease-1 in activation of the complement factor D.* J Exp Med, 2010. **207**(1): p. 29-37.
302. Erlich, J.H., S.R. Holdsworth, and P.G. Tipping, *Tissue factor initiates glomerular fibrin deposition and promotes major histocompatibility complex class II expression in crescentic glomerulonephritis.* Am J Pathol, 1997. **150**(3): p. 873-80.
303. van Rooijen, N. and A. Sanders, *Elimination, blocking, and activation of macrophages: three of a kind?* J Leukoc Biol, 1997. **62**(6): p. 702-9.
304. Cailhier, J.F., et al., *Conditional macrophage ablation demonstrates that resident macrophages initiate acute peritoneal inflammation.* J Immunol, 2005. **174**(4): p. 2336-42.

Appendix

Probeset ID	Symbol	p-value (V vs. L)	Fold-Change (V vs. L)	
SPRY2	SPRY2	0.000071	13.186	V up vs L
FOSB	FOSB	0.000032	6.366	V up vs L
EDN1	EDN1	0.000603	5.944	V up vs L
HSPA7	HSPA7	0.000747	5.655	V up vs L
TM4SF1	TM4SF1	0.000993	5.560	V up vs L
RDH13	RDH13	0.000915	5.311	V up vs L
HSPA6	HSPA6	0.000213	5.130	V up vs L
SCG5	SCG5	0.002770	4.951	V up vs L
SPINK1	SPINK1	0.000158	4.873	V up vs L
TMEM158	TMEM158	0.004643	4.407	V up vs L
TFPI2	TFPI2	0.000062	4.381	V up vs L
PLCXD1	PLCXD1	0.000102	4.358	V up vs L
SPP1	SPP1	0.000312	4.279	V up vs L
MMP1	MMP1	0.003097	4.274	V up vs L
KBTBD8	KBTBD8	0.000174	4.244	V up vs L
TIMM8A	TIMM8A	0.000024	4.087	V up vs L
TM4SF19	TM4SF19	0.001296	3.849	V up vs L
ADCY3	ADCY3	0.011415	3.847	V up vs L
HS.578401		0.000134	3.766	V up vs L
ACRC	ACRC	0.007537	3.747	V up vs L
ANKRD57	ANKRD57	0.014863	3.726	V up vs L
CCND1	CCND1	0.006761	3.721	V up vs L
C10ORF54	C10orf54	0.000596	3.583	V up vs L
DHRS9	DHRS9	0.002876	3.465	V up vs L
MYADM	MYADM	0.005008	3.367	V up vs L
GEM	GEM	0.001474	3.356	V up vs L
MAPK13	MAPK13	0.001982	3.346	V up vs L
YARS	YARS	0.004247	3.331	V up vs L
SGK1	SGK1	0.047400	3.312	V up vs L
BAG3	BAG3	0.002524	3.230	V up vs L
BHLHB2	BHLHB2	0.000117	3.209	V up vs L
KLF5	KLF5	0.002543	3.207	V up vs L
MOAP1	MOAP1	0.004579	3.173	V up vs L
SGMS2	SGMS2	0.001623	3.160	V up vs L
RGS2	RGS2	0.002297	3.131	V up vs L
GNPDA1	GNPDA1	0.000130	3.114	V up vs L
CD300LF	CD300LF	0.019427	3.047	V up vs L
RNASET2	RNASET2	0.004643	2.939	V up vs L
CRTAM	CRTAM	0.000216	2.926	V up vs L
HLA-DMA	HLA-DMA	0.000306	2.924	V up vs L

C10ORF128	C10orf128	0.009899	2.912	V up vs L
TCTEX1D2	TCTEX1D2	0.003180	2.893	V up vs L
C14ORF109	C14orf109	0.017840	2.875	V up vs L
HS.519750		0.001485	2.870	V up vs L
MATK	MATK	0.046663	2.856	V up vs L
TRAPPC6A	TRAPPC6A	0.000048	2.840	V up vs L
HBEGF	HBEGF	0.000159	2.810	V up vs L
DNAJB1	DNAJB1	0.019811	2.792	V up vs L
HLA-DMB	HLA-DMB	0.004464	2.788	V up vs L
LY96	LY96	0.006694	2.779	V up vs L
LTA4H	LTA4H	0.009489	2.773	V up vs L
EGR1	EGR1	0.019702	2.743	V up vs L
LOC401588	LOC401588	0.000101	2.717	V up vs L
HS.499716		0.000305	2.715	V up vs L
CLEC7A	CLEC7A	0.001533	2.704	V up vs L
LOC650803	LOC650803	0.019936	2.702	V up vs L
ZFR2	ZFR2	0.039214	2.701	V up vs L
RP5-1022P6.2	RP5-1022P6.2	0.000008	2.689	V up vs L
RRAGD	RRAGD	0.000554	2.674	V up vs L
C20ORF20	C20orf20	0.017479	2.659	V up vs L
GMFG	GMFG	0.000043	2.656	V up vs L
S1PR3	S1PR3	0.000048	2.608	V up vs L
NR4A2	NR4A2	0.003510	2.606	V up vs L
EPS8	EPS8	0.028303	2.604	V up vs L
BLVRB	BLVRB	0.011541	2.598	V up vs L
TKTL1	TKTL1	0.003197	2.597	V up vs L
SGK	SGK	0.010119	2.566	V up vs L
EVI2B	EVI2B	0.004196	2.563	V up vs L
JUN	JUN	0.001560	2.553	V up vs L
CD163	CD163	0.008699	2.548	V up vs L
AMICA1	AMICA1	0.016664	2.539	V up vs L
ZFAND2A	ZFAND2A	0.002735	2.536	V up vs L
NP	NP	0.000003	2.524	V up vs L
ITGAM	ITGAM	0.047991	2.478	V up vs L
SLC20A1	SLC20A1	0.000636	2.474	V up vs L
ZNF165	ZNF165	0.004834	2.456	V up vs L
LAT2	LAT2	0.000454	2.456	V up vs L
WBP5	WBP5	0.000660	2.452	V up vs L
LOC606724	LOC606724	0.001915	2.431	V up vs L
HCST	HCST	0.032321	2.424	V up vs L
KLF10	KLF10	0.008145	2.424	V up vs L
HEXB	HEXB	0.009101	2.404	V up vs L
CAT	CAT	0.030306	2.404	V up vs L

FLJ22662	FLJ22662	0.049372	2.400	V up vs L
PRCP	PRCP	0.016426	2.398	V up vs L
ADRB2	ADRB2	0.034683	2.382	V up vs L
HSPA1A	HSPA1A	0.000561	2.380	V up vs L
CXCR4	CXCR4	0.001505	2.377	V up vs L
RRN3P2	RRN3P2	0.007610	2.370	V up vs L
ZNF622	ZNF622	0.005351	2.355	V up vs L
TMEM91	TMEM91	0.043597	2.346	V up vs L
RRP12	RRP12	0.008489	2.324	V up vs L
LOC653340	LOC653340	0.016887	2.315	V up vs L
DLL1	DLL1	0.002146	2.313	V up vs L
ITGB2	ITGB2	0.000106	2.296	V up vs L
LIPN	LIPN	0.006026	2.291	V up vs L
LOC649555	LOC649555	0.002140	2.290	V up vs L
CIRH1A	CIRH1A	0.028322	2.275	V up vs L
HPSE	HPSE	0.000187	2.268	V up vs L
KLF2	KLF2	0.008723	2.250	V up vs L
LPCAT2	LPCAT2	0.003737	2.250	V up vs L
GARS	GARS	0.042652	2.237	V up vs L
LOC100131693	LOC100131693	0.000138	2.223	V up vs L
CSF3R	CSF3R	0.004808	2.216	V up vs L
MGC61598	MGC61598	0.017988	2.214	V up vs L
WAS	WAS	0.031084	2.211	V up vs L
ARHGDIB	ARHGDIB	0.005862	2.205	V up vs L
HAVCR2	HAVCR2	0.007684	2.198	V up vs L
KLHL6	KLHL6	0.012178	2.192	V up vs L
HSPA1L	HSPA1L	0.000334	2.190	V up vs L
SDSL	SDSL	0.000841	2.189	V up vs L
CSF1	CSF1	0.037481	2.182	V up vs L
SELL	SELL	0.021519	2.181	V up vs L
MAPKAPK3	MAPKAPK3	0.032212	2.176	V up vs L
CD36	CD36	0.048588	2.172	V up vs L
NFE2	NFE2	0.009396	2.171	V up vs L
C13ORF15	C13orf15	0.001744	2.170	V up vs L
ANXA1	ANXA1	0.013141	2.168	V up vs L
BEX1	BEX1	0.008838	2.153	V up vs L
FCN1	FCN1	0.000976	2.145	V up vs L
MOGAT1	MOGAT1	0.027321	2.142	V up vs L
ITGA5	ITGA5	0.009433	2.139	V up vs L
FCGR2C	FCGR2C	0.004543	2.134	V up vs L
FRG1	FRG1	0.003810	2.134	V up vs L
LY86	LY86	0.007807	2.115	V up vs L
C14ORF169	C14orf169	0.000032	2.112	V up vs L

LOC341784	LOC341784	0.008479	2.108	V up vs L
EGR3	EGR3	0.005902	2.100	V up vs L
LOC100130264	LOC100130264	0.010399	2.098	V up vs L
FGL2	FGL2	0.025072	2.093	V up vs L
ABL2	ABL2	0.000913	2.093	V up vs L
TXNIP	TXNIP	0.006734	2.092	V up vs L
HSPA9	HSPA9	0.030929	2.086	V up vs L
ITPRIP	ITPRIP	0.004080	2.084	V up vs L
ST3GAL6	ST3GAL6	0.000648	2.078	V up vs L
SLC7A5	SLC7A5	0.008462	2.076	V up vs L
IRF8	IRF8	0.006033	2.075	V up vs L
NPC1	NPC1	0.001141	2.075	V up vs L
CCND2	CCND2	0.012223	2.075	V up vs L
DPEP2	DPEP2	0.037195	2.073	V up vs L
LOC651524	LOC651524	0.001530	2.065	V up vs L
ADNP2	ADNP2	0.012049	2.063	V up vs L
WDSOF1	WDSOF1	0.000265	2.063	V up vs L
RNMTL1	RNMTL1	0.016817	2.060	V up vs L
TMEM38B	TMEM38B	0.000109	2.060	V up vs L
GLIPR1	GLIPR1	0.026192	2.057	V up vs L
GSTK1	GSTK1	0.005044	2.051	V up vs L
FCGRT	FCGRT	0.006694	2.050	V up vs L
ICAM3	ICAM3	0.007482	2.049	V up vs L
NRIP3	NRIP3	0.001887	2.047	V up vs L
BEX2	BEX2	0.012564	2.032	V up vs L
SPRED1	SPRED1	0.004196	2.032	V up vs L
PPARG	PPARG	0.000522	2.031	V up vs L
CKS2	CKS2	0.017299	2.030	V up vs L
MIR221	MIR221	0.001681	2.029	V up vs L
ZMIZ1	ZMIZ1	0.005859	2.023	V up vs L
LOC100129186	LOC100129186	0.005218	2.023	V up vs L
LOC646626	LOC646626	0.035687	2.020	V up vs L
LOC728653	LOC728653	0.025872	2.019	V up vs L
NME1	NME1	0.012915	2.017	V up vs L
CFD	CFD	0.014690	2.011	V up vs L
CD4	CD4	0.000288	2.009	V up vs L
LOC732415	LOC732415	0.031567	2.006	V up vs L
HS.575725		0.032917	2.005	V up vs L
DEDD2	DEDD2	0.005377	2.004	V up vs L
RUSC2	RUSC2	0.024516	2.004	V up vs L
ZSCAN5A	ZSCAN5A	0.017001	1.995	V up vs L
C5AR1	C5AR1	0.006303	1.992	V up vs L
RNF130	RNF130	0.039708	1.991	V up vs L

DUSP6	DUSP6	0.005137	1.987	V up vs L
TRIB1	TRIB1	0.002358	1.987	V up vs L
HDDC2	HDDC2	0.049152	1.982	V up vs L
B3GNT5	B3GNT5	0.003763	1.978	V up vs L
LOC100132918	LOC100132918	0.020961	1.977	V up vs L
PPT1	PPT1	0.047816	1.976	V up vs L
LOC728247	LOC728247	0.005937	1.975	V up vs L
CCR1	CCR1	0.002324	1.975	V up vs L
TDRD9	TDRD9	0.000570	1.967	V up vs L
VGF	VGF	0.001039	1.967	V up vs L
OBFC2A	OBFC2A	0.035676	1.966	V up vs L
TMEM49	TMEM49	0.002417	1.966	V up vs L
LOC100131565	LOC100131565	0.026087	1.957	V up vs L
CHSY1	CHSY1	0.000028	1.951	V up vs L
CKLF	CKLF	0.002881	1.949	V up vs L
AVPI1	AVPI1	0.005331	1.949	V up vs L
NOP58	NOP58	0.009265	1.946	V up vs L
RGS16	RGS16	0.002011	1.939	V up vs L
FOSL1	FOSL1	0.000599	1.932	V up vs L
PLIN2	PLIN2	0.034011	1.923	V up vs L
ZNF185	ZNF185	0.000493	1.923	V up vs L
HEBP2	HEBP2	0.004207	1.923	V up vs L
VPS37B	VPS37B	0.000146	1.922	V up vs L
FKBP15	FKBP15	0.027567	1.921	V up vs L
BCAP31	BCAP31	0.019058	1.921	V up vs L
ACTN1	ACTN1	0.027083	1.919	V up vs L
SERTAD1	SERTAD1	0.006594	1.912	V up vs L
SAAL1	SAAL1	0.005925	1.911	V up vs L
LOC730050	LOC730050	0.002782	1.909	V up vs L
CRY1	CRY1	0.012246	1.903	V up vs L
SMCR7L	SMCR7L	0.038361	1.902	V up vs L
SLC2A3	SLC2A3	0.012256	1.894	V up vs L
CHD1	CHD1	0.000904	1.891	V up vs L
C9ORF47	C9orf47	0.001586	1.890	V up vs L
LOC338758	LOC338758	0.004420	1.888	V up vs L
LOC729608	LOC729608	0.010290	1.881	V up vs L
COL15A1	COL15A1	0.033273	1.876	V up vs L
LONRF3	LONRF3	0.002545	1.875	V up vs L
PRNP	PRNP	0.003144	1.874	V up vs L
HS.79881		0.003345	1.873	V up vs L
PI3	PI3	0.009117	1.872	V up vs L
EFHD2	EFHD2	0.017430	1.868	V up vs L
TLR1	TLR1	0.020650	1.867	V up vs L

RPF2	RPF2	0.003689	1.865	V up vs L
S100A8	S100A8	0.002476	1.863	V up vs L
TNFSF14	TNFSF14	0.004482	1.855	V up vs L
C12ORF23	C12orf23	0.022393	1.853	V up vs L
TSC22D2	TSC22D2	0.000383	1.851	V up vs L
MRPS17	MRPS17	0.009786	1.848	V up vs L
RRP15	RRP15	0.000830	1.846	V up vs L
RBM15	RBM15	0.003013	1.840	V up vs L
HS.415576		0.030609	1.837	V up vs L
LOC441505	LOC441505	0.005516	1.835	V up vs L
LOC389137	LOC389137	0.000977	1.832	V up vs L
DNTTIP2	DNTTIP2	0.001168	1.830	V up vs L
ZNF593	ZNF593	0.020556	1.828	V up vs L
PIK3CG	PIK3CG	0.004381	1.827	V up vs L
NIP7	NIP7	0.020361	1.827	V up vs L
CD93	CD93	0.026750	1.825	V up vs L
UAP1	UAP1	0.004718	1.824	V up vs L
ADAM15	ADAM15	0.008174	1.819	V up vs L
RPS23	RPS23	0.029799	1.816	V up vs L
DENND2D	DENND2D	0.020310	1.815	V up vs L
PSCD4	PSCD4	0.009933	1.815	V up vs L
CPVL	CPVL	0.006055	1.814	V up vs L
RRAD	RRAD	0.006110	1.813	V up vs L
NOLC1	NOLC1	0.041637	1.813	V up vs L
TMC6	TMC6	0.018023	1.813	V up vs L
JOSD1	JOSD1	0.020662	1.812	V up vs L
ACSL3	ACSL3	0.000996	1.808	V up vs L
UTP11L	UTP11L	0.005009	1.805	V up vs L
LOC651745	LOC651745	0.015966	1.802	V up vs L
UBL3	UBL3	0.032190	1.798	V up vs L
HS.578899		0.038429	1.795	V up vs L
NAAA	NAAA	0.032335	1.795	V up vs L
LOC730081	LOC730081	0.008237	1.793	V up vs L
ERCC1	ERCC1	0.003349	1.789	V up vs L
TBC1D2	TBC1D2	0.002472	1.786	V up vs L
NEU1	NEU1	0.035552	1.783	V up vs L
ARHGAP4	ARHGAP4	0.013796	1.781	V up vs L
TRMT5	TRMT5	0.009340	1.780	V up vs L
IARS	IARS	0.003439	1.780	V up vs L
LOC645430	LOC645430	0.033480	1.779	V up vs L
KIFC2	KIFC2	0.021975	1.777	V up vs L
TSPO	TSPO	0.004738	1.776	V up vs L
EIF3E	EIF3E	0.000473	1.775	V up vs L

UPP1	UPP1	0.031380	1.773	V up vs L
EIF1AD	EIF1AD	0.016551	1.769	V up vs L
USPL1	USPL1	0.016812	1.766	V up vs L
SNORD10	SNORD10	0.040630	1.766	V up vs L
NFIL3	NFIL3	0.041685	1.765	V up vs L
KIAA2018	KIAA2018	0.000112	1.764	V up vs L
BIN2	BIN2	0.012503	1.760	V up vs L
CXORF15	CXorf15	0.033288	1.755	V up vs L
CD244	CD244	0.028158	1.754	V up vs L
SETDB2	SETDB2	0.015730	1.752	V up vs L
PPP1R15A	PPP1R15A	0.043244	1.751	V up vs L
IL10RA	IL10RA	0.006155	-1.752	V down vs L
RASSF4	RASSF4	0.001676	-1.754	V down vs L
LOC648927	LOC648927	0.042133	-1.756	V down vs L
TAP2	TAP2	0.016799	-1.757	V down vs L
TLR2	TLR2	0.002189	-1.760	V down vs L
EZH2	EZH2	0.023912	-1.771	V down vs L
RNF145	RNF145	0.042431	-1.772	V down vs L
RAP2C	RAP2C	0.000423	-1.774	V down vs L
GTF2E2	GTF2E2	0.043590	-1.776	V down vs L
LOC100132184	LOC100132184	0.011217	-1.776	V down vs L
ZC3H5	ZC3H5	0.007776	-1.778	V down vs L
GORASP1	GORASP1	0.004667	-1.784	V down vs L
USP41	USP41	0.001310	-1.784	V down vs L
ANXA7	ANXA7	0.000476	-1.784	V down vs L
FLJ45340	FLJ45340	0.028706	-1.785	V down vs L
EXT1	EXT1	0.003088	-1.789	V down vs L
SLC30A1	SLC30A1	0.018869	-1.789	V down vs L
LCOR	LCOR	0.004382	-1.791	V down vs L
IL6	IL6	0.003732	-1.792	V down vs L
HS.543261		0.004053	-1.792	V down vs L
CNKSR3	CNKSR3	0.042870	-1.794	V down vs L
ETV6	ETV6	0.036272	-1.795	V down vs L
CHMP5	CHMP5	0.003562	-1.797	V down vs L
AGRN	AGRN	0.005148	-1.797	V down vs L
CAB39	CAB39	0.001094	-1.801	V down vs L
GK	GK	0.019992	-1.803	V down vs L
PI4K2B	PI4K2B	0.001144	-1.803	V down vs L
ICAM1	ICAM1	0.008132	-1.804	V down vs L
PRF1	PRF1	0.000462	-1.813	V down vs L
VRK2	VRK2	0.000826	-1.814	V down vs L
BRD7	BRD7	0.002933	-1.817	V down vs L
CYTIP	CYTIP	0.000348	-1.817	V down vs L

LAIR2	LAIR2	0.012794	-1.823	V down vs L
DRAM1	DRAM1	0.000352	-1.825	V down vs L
LOC641851	LOC641851	0.002178	-1.826	V down vs L
OASL	OASL	0.002776	-1.827	V down vs L
TSC22D1	TSC22D1	0.000523	-1.827	V down vs L
CCL22	CCL22	0.000067	-1.827	V down vs L
VDAC1	VDAC1	0.040363	-1.828	V down vs L
PSCD1	PSCD1	0.001322	-1.829	V down vs L
RAP2A	RAP2A	0.020076	-1.831	V down vs L
FBXL11	FBXL11	0.006427	-1.832	V down vs L
NBN	NBN	0.001004	-1.834	V down vs L
CDKN2B	CDKN2B	0.011664	-1.838	V down vs L
DCAF7	DCAF7	0.009156	-1.838	V down vs L
CD99	CD99	0.023569	-1.842	V down vs L
CLIC4	CLIC4	0.000534	-1.845	V down vs L
KANK1	KANK1	0.004983	-1.847	V down vs L
CDC42SE2	CDC42SE2	0.006919	-1.847	V down vs L
LOC440280	LOC440280	0.036112	-1.849	V down vs L
XRN1	XRN1	0.000533	-1.849	V down vs L
LMO2	LMO2	0.002904	-1.852	V down vs L
PSCDBP	PSCDBP	0.006825	-1.855	V down vs L
MYST3	MYST3	0.024113	-1.855	V down vs L
AGPAT4	AGPAT4	0.005280	-1.856	V down vs L
HS.548433		0.040660	-1.857	V down vs L
IKBKE	IKBKE	0.019386	-1.859	V down vs L
TMEM165	TMEM165	0.000838	-1.861	V down vs L
AKR1B1	AKR1B1	0.006632	-1.865	V down vs L
LYSMD2	LYSMD2	0.018688	-1.868	V down vs L
HCK	HCK	0.022712	-1.873	V down vs L
TRIM8	TRIM8	0.024887	-1.874	V down vs L
CYTH1	CYTH1	0.002072	-1.878	V down vs L
MLLT6	MLLT6	0.002042	-1.879	V down vs L
LOC283767	LOC283767	0.019117	-1.880	V down vs L
GCH1	GCH1	0.003080	-1.886	V down vs L
MTSS1	MTSS1	0.004211	-1.886	V down vs L
HSH2D	HSH2D	0.035475	-1.890	V down vs L
VPS29	VPS29	0.004843	-1.893	V down vs L
PHF11	PHF11	0.007358	-1.897	V down vs L
PNRC1	PNRC1	0.007441	-1.898	V down vs L
PCID2	PCID2	0.007797	-1.901	V down vs L
BRWD2	BRWD2	0.000255	-1.901	V down vs L
HIP1	HIP1	0.020669	-1.902	V down vs L
CALR	CALR	0.017602	-1.902	V down vs L

TDRD6	TDRD6	0.004910	-1.904	V down vs L
PLA2G4A	PLA2G4A	0.001367	-1.907	V down vs L
NIPA1	NIPA1	0.039318	-1.910	V down vs L
HS.24119		0.011730	-1.912	V down vs L
FLNB	FLNB	0.005577	-1.923	V down vs L
PML	PML	0.002966	-1.933	V down vs L
C13ORF31	C13orf31	0.012436	-1.938	V down vs L
NCOA3	NCOA3	0.000629	-1.942	V down vs L
RNF19B	RNF19B	0.001010	-1.943	V down vs L
SRD5A1	SRD5A1	0.014419	-1.946	V down vs L
DNAJB6	DNAJB6	0.024329	-1.947	V down vs L
GATAD2B	GATAD2B	0.036649	-1.948	V down vs L
AIDA	AIDA	0.010117	-1.948	V down vs L
HS.373429		0.001578	-1.950	V down vs L
IFITM3	IFITM3	0.033823	-1.952	V down vs L
MRPS24	MRPS24	0.027574	-1.955	V down vs L
LOC392635	LOC392635	0.005505	-1.960	V down vs L
LYN	LYN	0.028292	-1.963	V down vs L
CYBA	CYBA	0.043477	-1.976	V down vs L
FMNL3	FMNL3	0.037915	-1.985	V down vs L
STAT5A	STAT5A	0.027632	-1.987	V down vs L
CUL4A	CUL4A	0.000588	-1.988	V down vs L
LOC100130308	LOC100130308	0.000049	-1.989	V down vs L
HS.444683		0.008296	-1.993	V down vs L
SSB	SSB	0.014954	-1.996	V down vs L
MAMLD1	MAMLD1	0.002156	-1.996	V down vs L
ATXN1	ATXN1	0.004187	-2.002	V down vs L
LOC100130199	LOC100130199	0.025688	-2.002	V down vs L
IFI6	IFI6	0.044171	-2.007	V down vs L
TRIM56	TRIM56	0.038358	-2.011	V down vs L
FAM60A	FAM60A	0.007010	-2.014	V down vs L
LOC731881	LOC731881	0.006499	-2.017	V down vs L
MIR155HG	MIR155HG	0.002796	-2.021	V down vs L
GCKR	GCKR	0.008260	-2.022	V down vs L
LOC730818	LOC730818	0.005311	-2.035	V down vs L
SMPDL3A	SMPDL3A	0.007234	-2.042	V down vs L
LRIG1	LRIG1	0.000544	-2.043	V down vs L
DDX60	DDX60	0.006053	-2.045	V down vs L
CEP350	CEP350	0.004395	-2.052	V down vs L
MARCKSL1	MARCKSL1	0.010032	-2.066	V down vs L
TNFSF13B	TNFSF13B	0.000891	-2.068	V down vs L
CXCL1	CXCL1	0.002353	-2.071	V down vs L
LY6E	LY6E	0.010107	-2.071	V down vs L

CD226	CD226	0.010346	-2.071	V down vs L
FAM49A	FAM49A	0.007740	-2.074	V down vs L
IFNAR2	IFNAR2	0.001052	-2.079	V down vs L
CD274	CD274	0.000092	-2.081	V down vs L
RNF144B	RNF144B	0.002292	-2.083	V down vs L
PPP3CC	PPP3CC	0.007673	-2.083	V down vs L
TDRD7	TDRD7	0.027315	-2.085	V down vs L
PARP4	PARP4	0.001739	-2.088	V down vs L
LMNA	LMNA	0.000040	-2.094	V down vs L
CD80	CD80	0.027499	-2.097	V down vs L
RAB13	RAB13	0.012171	-2.098	V down vs L
KIAA0020	KIAA0020	0.008083	-2.100	V down vs L
KYNU	KYNU	0.006476	-2.114	V down vs L
SEMA4A	SEMA4A	0.024022	-2.117	V down vs L
MX1	MX1	0.036117	-2.118	V down vs L
HS.4988		0.000137	-2.120	V down vs L
EPS15	EPS15	0.005330	-2.121	V down vs L
CD38	CD38	0.003121	-2.131	V down vs L
PGD	PGD	0.001177	-2.133	V down vs L
GRAMD1A	GRAMD1A	0.005924	-2.147	V down vs L
C3ORF59	C3orf59	0.004025	-2.159	V down vs L
SLC41A2	SLC41A2	0.000255	-2.159	V down vs L
PIM2	PIM2	0.025429	-2.161	V down vs L
CCDC56	CCDC56	0.001368	-2.163	V down vs L
TNFAIP2	TNFAIP2	0.000395	-2.167	V down vs L
FTSJD2	FTSJD2	0.006566	-2.175	V down vs L
TRAFD1	TRAFD1	0.009058	-2.180	V down vs L
TBC1D9	TBC1D9	0.000171	-2.194	V down vs L
DDX58	DDX58	0.000969	-2.195	V down vs L
TRIM25	TRIM25	0.013563	-2.198	V down vs L
USP18	USP18	0.002771	-2.209	V down vs L
ITGAV	ITGAV	0.000348	-2.211	V down vs L
PSTPIP2	PSTPIP2	0.003578	-2.214	V down vs L
SAMHD1	SAMHD1	0.029193	-2.219	V down vs L
LOC647886	LOC647886	0.000966	-2.221	V down vs L
BST2	BST2	0.000169	-2.221	V down vs L
EIF1B	EIF1B	0.003191	-2.230	V down vs L
HS3ST3B1	HS3ST3B1	0.001144	-2.231	V down vs L
HS.10862		0.008978	-2.234	V down vs L
ZNRF2	ZNRF2	0.000718	-2.236	V down vs L
LHFPL2	LHFPL2	0.015588	-2.236	V down vs L
CEP135	CEP135	0.000565	-2.237	V down vs L
LOC650369	LOC650369	0.006389	-2.239	V down vs L

LOC728772	LOC728772	0.000246	-2.246	V down vs L
AKR1C3	AKR1C3	0.011845	-2.248	V down vs L
LOC389465	LOC389465	0.004077	-2.252	V down vs L
TMEM123	TMEM123	0.000359	-2.253	V down vs L
DYNLT1	DYNLT1	0.001640	-2.255	V down vs L
KIAA1033	KIAA1033	0.029452	-2.264	V down vs L
RSAD2	RSAD2	0.001430	-2.269	V down vs L
NUB1	NUB1	0.004017	-2.273	V down vs L
LOC654192	LOC654192	0.021931	-2.284	V down vs L
ALCAM	ALCAM	0.000510	-2.301	V down vs L
GBP5	GBP5	0.009783	-2.301	V down vs L
LILRB2	LILRB2	0.000127	-2.302	V down vs L
GPR68	GPR68	0.000149	-2.307	V down vs L
IFI44	IFI44	0.002226	-2.312	V down vs L
SDHAP2	SDHAP2	0.008859	-2.313	V down vs L
IFIT2	IFIT2	0.023064	-2.318	V down vs L
PTPRJ	PTPRJ	0.002800	-2.322	V down vs L
GJB2	GJB2	0.000372	-2.328	V down vs L
C20ORF103	C20orf103	0.011135	-2.332	V down vs L
LOC100132891	LOC100132891	0.000501	-2.346	V down vs L
IFIH1	IFIH1	0.002245	-2.347	V down vs L
MCOLN2	MCOLN2	0.007147	-2.348	V down vs L
TNFAIP6	TNFAIP6	0.000074	-2.352	V down vs L
EPB41L3	EPB41L3	0.003210	-2.364	V down vs L
DLD	DLD	0.012856	-2.370	V down vs L
SLC25A28	SLC25A28	0.011804	-2.370	V down vs L
GBP4	GBP4	0.036738	-2.373	V down vs L
VCAN	VCAN	0.011008	-2.381	V down vs L
MTF1	MTF1	0.011708	-2.396	V down vs L
TNFRSF9	TNFRSF9	0.005947	-2.397	V down vs L
CXCL10	CXCL10	0.023142	-2.398	V down vs L
NECAP2	NECAP2	0.012718	-2.402	V down vs L
ADORA2A	ADORA2A	0.007940	-2.415	V down vs L
IFI35	IFI35	0.004997	-2.438	V down vs L
UBE2L6	UBE2L6	0.002716	-2.444	V down vs L
NCK2	NCK2	0.001706	-2.446	V down vs L
IL19	IL19	0.001256	-2.449	V down vs L
CALM1	CALM1	0.000365	-2.453	V down vs L
C1ORF24	C1orf24	0.004627	-2.462	V down vs L
EREG	EREG	0.000357	-2.468	V down vs L
G0S2	G0S2	0.001042	-2.501	V down vs L
PCMTD1	PCMTD1	0.004991	-2.513	V down vs L
FAM129A	FAM129A	0.000228	-2.522	V down vs L

TAP1	TAP1	0.002696	-2.526	V down vs L
STAT4	STAT4	0.000153	-2.532	V down vs L
SP110	SP110	0.000050	-2.549	V down vs L
MST4	MST4	0.000003	-2.549	V down vs L
SLFN5	SLFN5	0.001878	-2.551	V down vs L
LOC400759	LOC400759	0.000754	-2.552	V down vs L
DHX58	DHX58	0.000315	-2.553	V down vs L
DTX3L	DTX3L	0.001896	-2.554	V down vs L
TNFSF10	TNFSF10	0.018134	-2.562	V down vs L
DNCL1	DNCL1	0.001365	-2.593	V down vs L
LOC54103	LOC54103	0.000155	-2.602	V down vs L
PID1	PID1	0.002281	-2.616	V down vs L
CD47	CD47	0.006623	-2.619	V down vs L
PPPDE2	PPPDE2	0.001020	-2.621	V down vs L
LOC645116	LOC645116	0.000934	-2.656	V down vs L
ATF7IP	ATF7IP	0.003593	-2.681	V down vs L
RFTN1	RFTN1	0.026179	-2.711	V down vs L
CCL8	CCL8	0.002528	-2.715	V down vs L
DFNA5	DFNA5	0.046430	-2.717	V down vs L
FAM46A	FAM46A	0.002502	-2.723	V down vs L
PARP12	PARP12	0.000371	-2.723	V down vs L
MAP3K8	MAP3K8	0.015186	-2.729	V down vs L
MAP3K4	MAP3K4	0.003555	-2.730	V down vs L
THBS1	THBS1	0.000057	-2.733	V down vs L
CRIM1	CRIM1	0.001606	-2.736	V down vs L
MAFB	MAFB	0.006871	-2.766	V down vs L
PTEN	PTEN	0.029513	-2.784	V down vs L
CCL23	CCL23	0.001763	-2.789	V down vs L
AKR1C4	AKR1C4	0.000041	-2.792	V down vs L
RHOU	RHOU	0.001879	-2.802	V down vs L
DYNLL1	DYNLL1	0.000913	-2.815	V down vs L
C21ORF71	C21orf71	0.013196	-2.817	V down vs L
HS.125087		0.000085	-2.827	V down vs L
ANPEP	ANPEP	0.002234	-2.853	V down vs L
LAP3	LAP3	0.001399	-2.868	V down vs L
APOL3	APOL3	0.000621	-2.881	V down vs L
STAT1	STAT1	0.002806	-2.903	V down vs L
EMR1	EMR1	0.000067	-2.906	V down vs L
SPATS2L	SPATS2L	0.000539	-2.921	V down vs L
INSIG2	INSIG2	0.004336	-2.938	V down vs L
PARP14	PARP14	0.000187	-2.945	V down vs L
GBP1	GBP1	0.000364	-3.001	V down vs L
HS.580229		0.017107	-3.030	V down vs L

TRIM22	TRIM22	0.000168	-3.056	V down vs L
PARP9	PARP9	0.008289	-3.059	V down vs L
ABTB2	ABTB2	0.001586	-3.081	V down vs L
MTE	MTE	0.000330	-3.092	V down vs L
KIAA1618	KIAA1618	0.033384	-3.095	V down vs L
PLSCR1	PLSCR1	0.012568	-3.096	V down vs L
RASGRP1	RASGRP1	0.006485	-3.113	V down vs L
SAMD9	SAMD9	0.000592	-3.181	V down vs L
MOV10	MOV10	0.000478	-3.198	V down vs L
PLA2G7	PLA2G7	0.000361	-3.201	V down vs L
KCNJ2	KCNJ2	0.000230	-3.201	V down vs L
SLC39A8	SLC39A8	0.000242	-3.201	V down vs L
EBI3	EBI3	0.010783	-3.203	V down vs L
SIGLEC1	SIGLEC1	0.011522	-3.215	V down vs L
NT5C3	NT5C3	0.001436	-3.258	V down vs L
NDP	NDP	0.002337	-3.298	V down vs L
C17ORF96	C17orf96	0.003819	-3.300	V down vs L
C7ORF60	C7orf60	0.000102	-3.322	V down vs L
IRG1	IRG1	0.001713	-3.351	V down vs L
LOC730249	LOC730249	0.000379	-3.387	V down vs L
LOC441019	LOC441019	0.005500	-3.398	V down vs L
HERC5	HERC5	0.018064	-3.438	V down vs L
EHF	EHF	0.043619	-3.454	V down vs L
EPSTI1	EPSTI1	0.001649	-3.455	V down vs L
SAMD9L	SAMD9L	0.001510	-3.541	V down vs L
EIF2AK2	EIF2AK2	0.004127	-3.550	V down vs L
MN1	MN1	0.000269	-3.593	V down vs L
MX2	MX2	0.001635	-3.670	V down vs L
OAS2	OAS2	0.002514	-3.711	V down vs L
ITGB8	ITGB8	0.000202	-3.721	V down vs L
C3ORF1	C3orf1	0.003038	-3.757	V down vs L
CMPK2	CMPK2	0.000125	-3.772	V down vs L
STAT2	STAT2	0.000166	-3.824	V down vs L
MSC	MSC	0.000931	-3.845	V down vs L
ADA	ADA	0.016461	-3.919	V down vs L
RGL1	RGL1	0.000255	-4.024	V down vs L
IFIT3	IFIT3	0.000182	-4.039	V down vs L
IFI44L	IFI44L	0.012556	-4.121	V down vs L
PLAC8	PLAC8	0.000039	-4.145	V down vs L
TMOD1	TMOD1	0.002983	-4.224	V down vs L
IL7R	IL7R	0.006079	-4.231	V down vs L
OAS3	OAS3	0.000669	-4.376	V down vs L
APOBEC3A	APOBEC3A	0.000457	-4.409	V down vs L

RIN2	RIN2	0.000288	-4.444	V down vs L
OAS1	OAS1	0.000494	-4.493	V down vs L
HERC6	HERC6	0.008357	-4.520	V down vs L
ISG15	ISG15	0.003331	-4.846	V down vs L
MT1A	MT1A	0.000117	-5.029	V down vs L
IFIT1	IFIT1	0.000221	-5.964	V down vs L
INDO	INDO	0.000836	-6.760	V down vs L
MT2A	MT2A	0.000307	-7.072	V down vs L
IDO1	IDO1	0.000151	-7.500	V down vs L
CFB	CFB	0.001571	-7.781	V down vs L

Supplementary table 1 - List of the 566 genes depicted in the volcano plot shown In figure 4.9, comparing monocytes activated for 6 hours with either MPO-ANCA (V, n=3) or control IgG (L, n=3) in the presence of LPS. Threshold for significance is 1.75 fold in both directions and p-value of <0.05.